# Modelling of surface water and groundwater exchange and denitrification process in the alluvial plain area at the catchment scale

Xiaoling Sun

Université de Toulouse

# THÈSE

**En vue de l'obtention du**

## DOCTORAT DE L'UNIVERSITÉ DE TOULOUSE

**Délivré par :**
Université Toulouse III Paul Sabatier (UT3 Paul Sabatier)

**Discipline ou spécialité :**

Hydrologie, Hydrochimie, Sol, Environnement

---

**Présentée et soutenue par :**
Xiaoling SUN

**le :** mardi 30 juin 2015

**Titre :**

Modélisation des échanges nappe-rivière et du processus de dénitrification dans les plaines alluviales à l'échelle du bassin versant

---

**Ecole doctorale :**
Sciences de l'Univers, de l'Environnement et de l'Espace (SDU2E)

**Unité de recherche :**
ECOLAB UMR 5245

**Directeur(s) de Thèse :**
José Miguel SANCHEZ-PEREZ, Directeur de Recherche au CNRS Directeur de thèse
Raghavan SRINIVASAN, Professeur à l'Université Texas A&M Co-directeur de thèse

**Rapporteurs :**
Iñaki ANTIGUEDAD, Professeur à Université du Pays Basque
Gilles BILLEN, Directeur de Recherche au CNRS
Philippe ACKERER, Directeur de Recherche au CNRS

**Membre(s) du jury :**

Magali GERINO, Professeur à l'Université Paul Sabatier
Sabine SAUVAGE, Ingénieur de recherche au CNRS
Mélanie BARDEAU, Ingénieur au BRGM

# Remerciements

Il y a presque trois ans que je suis à Toulouse et je sens que je suis déjà presque Toulousaine. Souvent quand je parle avec un inconnu, une des premiers questions est « Est-ce que ça vous plaît la France? » Et ma réponse est toujours « oui, j'ai beaucoup de chance d'habiter à Toulouse, avec le soleil », mais dans le même temps, j'ai une autre réponse que je me dis à moi-même « j'aime beaucoup Toulouse c'est surtout parce que les amis et les collègues ici, vous être mon soleil de Toulouse. »

Tout d'abord, je veux dire merci à mes chefs: José Miguel Sánchez-Pérez et Sabine Sauvage. Je peux imager la difficulté de communication avec une étudiante étrangère qui parle pas du tout le français et ne connait pas grand-chose sur le sujet au tout début. Merci pour leur patience et leurs encouragements.
Je remercie aussi Jean-Luc Probst de m'avoir accueilli au sein du laboratoire ECOLAB.

Un Grand merci à mes collègues Léonard, Youen et Cyril. Vous être les collègues parfaits. Léonard est mon 'troisième chef', il m'a beaucoup aidé sur le travail. Et Youen est comme un frère, qui donne un sens de famille. Cyril est mon premier prof de français ici, et grâce à lui, j'ai fait mon premier voyage à vélo.

Je tiens à remercie tous les mecs du bureau 204, Adrien, Antoine et Théo. Vous être une grande partie du soleil, la vie est beaucoup plus belle en votre compagnie.

Merci à Tiantian qui m'a accompagnée pendant ces trois ans à l'ENSAT. Jingmei, qui est la collègue et une aime intime. Julie, la petite et grande sœur Toulousaine.

Merci aux collègues de G-MOD, Laurie, Grégory, Samuel, Yi Hong, et à tous les participants du projet Attanagua. Merci à Annick, Marie-Jo et Virginie qui sont les mamans de labo.

Thanks to my co-supervisor Raghavan Srinivasan for his advices and teaching the SWAT model. Merci aux rapporteurs Gilles Billen, Iñaki Antiguedad et Philippe Ackerer, ainsi qu'aux membres de jury, Magalie Gerino et Mélanie Bardeau, d'avoir accepté d'évaluer ces travaux.

En plus, merci aux collègues et copines de l'ENSAT, Alicia, Allison, Christophe, Jianzhong, Laure, Pierre alexis, Ousama, Simon, Sophia.

Merci aux copains d’ailleurs, pour leur support et encouragement, Aihuan, Ane, Danielle, Haiyan, Le Han, Lin Zhu, Lu Wang, Luiz, Maite, Melissa, Mélodie, Qingna, Jianwei, Yang Liu, Yufeng, Yingzi, Yongwen, Tian Zhao.

Thanks to the SWAT work team in Texas for their help in the model modification, Jeff, Nancy, Georgie, Katrin, and all the others people helped me a lot when I was there, Bill, Jean-Claude, Joel and Paula.

很感谢家人一直以来的支持，尤其是我的爸爸。在过去的三年间只陪伴过他几天的时间，仅有的交流都只是通过无线电波。我们都是不会表达爱和想念的人，但我却知道浓浓的父爱和亲情一直在我的身边。

# Sommaire

# Résumé

La pollution par les nitrates des eaux de surface et des eaux souterraines a suscité une attention mondiale ces dernières années. La recharge des eaux souterraines via d'infiltraiton dans les zones cultivées est une source importante de la contamination des eaux de surfaces. Les plaines alluviales supportent une activité agricole intensive et subissent une pollution aux nitrates importante. Il a été démontré que les échanges entre les eaux de nappes et la rivière contribuent à la rétention et/ou transformation de l'azote dans le continuum eaux de surface-eaux souterrains. La compréhension et la quantification des processus d'atténuation des concentrations en nitrates se produisant à l'interface nappe-rivière permettraient d'améliorer la connaissance du cycle de l'azote à l'échelle du bassin versant. Les objectifs de cette thèse sont : 1) quantifier les volumes d'eau échangés entre la rivière et l'aquifère alluvial dans les zones de plaine alluviale à l'échelle du bassin versant et 2) quantifier les taux de dénitrification dans les nappes alluviales à l'échelle du bassin versant et évaluer leurs influences sur les flux de nitrates de la rivière. Un échantillonnage sur le terrain ainsi qu'un travail de modélisation ont été effectués pour atteindre ces objectifs. Les campagnes d'échantillonnages sur le terrain ont eu lieu d'avril 2013 à mars 2014 sur le site d'étude de Monbéqui dans la plaine alluviale de la Garonne. Le modèle Soil and Water Assessment Tool (SWAT) qui est largement utilisé à travers le monde a été choisi pour simuler les processus hydrologiques et le cycle de l'azote. Cependant, la simulation des échanges nappe-rivière qui se produisent dans la plaine alluviale n'est pas prise en compte dans la version originale de SWAT. Premièrement, l'équation de Darcy a été introduite pour simuler les échanges nappe-rivière à partir de la structure Landscape Unit (LU). L'influence des crues débordantes sur ces échanges a également été ajoutée dans le modèle. Le modèle modifié, SWAT-LUD, a d'abord été appliqué à un méandre de la plaine alluviale de la Garonne- Monbéqui (25 km²). Ensuite, un module supplémentaire représentant les processus de dénitrification dans les aquifères peu profonds des nappes alluviales a été développé et ajouté au modèle SWAT-LUD. Les flux de nitrates ainsi que les taux de dénitrification de l'aquifère alluvial de Monbéqui ont alors été quantifiés. Dans un deuxième temps, le modèle SWAT-LUD a été appliqué à l'échelle de la plaine alluviale de la Garonne dans son cours moyen (environ 4600 km²) et l'influence de la dénitrification de l'aquifère alluvial sur les flux de nitrates de la rivière a été quantifiée. Finalement, le modèle a été appliqué sur l'ensemble du bassin versant de la Garonne (environ 51 500 km²) et l'influence des échanges nappes-rivières sur le cycle hydrologique du bassin versant a été évaluée. Les résultats ont montré que le modèle SWAT-LUD pouvait représenter de façon réaliste les échanges nappe-rivière ainsi que les taux de dénitrification dans les aquifères alluviaux à différentes échelles. Les flux échangés vont majoritairement de l'aquifère vers la rivière et contribuent pour 65% du volume total échangé. À l'échelle du bassin versant de la Garonne, le volume annuel échangé entre la nappe et la rivière représente environ 5% du débit annuel de la Garonne. A l'échelle du méandre, le taux annuel de dénitrification dans la zone riparienne a été estimé à environ 130 $N\text{-}NO_3^-.ha^{-1}.an^{-1}$. Près de 40% des nitrates arrivant dans cette zone ont été dégradés via les processus de dénitrification. Dans le cours moyen de la Garonne, les taux de dénitrification annuels dans ces mêmes zones varient entre 55 et 120 kg $N\text{-}NO_3^- .ha^{-1}.an^{-1}$.

# Abstract

Nitrate pollution in surface water and groundwater systems has attracted worldwide attention in recent decades. Recharged groundwater infiltrating through cultivated fields is an important source of the nitrate contamination of surface water. As alluvial plains support intensive agricultural activities, they often suffer from groundwater nitrate pollution. The exchanges between surface water and groundwater (SW-GW) were proved contributing to nitrate retention and/or transformation in the land-surface water continuum. The understanding and quantifying of nitrate attenuation processes occurring at the surface-groundwater interface would enhance understanding of nitrogen cycling at the catchment scale. The objectives of this thesis were: 1) quantifying the exchanged SW-GW volume in the floodplain area at the catchment scale and 2) quantifying the shallow aquifer denitrification rate in the floodplain area at the catchment scale and evaluating its influence on the nitrate flux in the river. Field sampling and modelling study were conducted to achieve these objectives. Monthly field work campaigns were carried out from April 2013 to March 2014 at the Monbéqui site in the Garonne river floodplain. The Soil and Water Assessment Tool (SWAT) which has been successfully applied all over the world was chosen to simulate the hydrologic processes and nitrogen cycle. However, the simulation of the water exchange between river and groundwater occurring in the floodplain area was not simulated in the original SWAT model. Firstly, the Darcy's equation was implemented to simulate SW-GW exchanges based on the Landscape Unit (LU) structure in the floodplain area. The influence of flooding on the water exchange was also introduced to the model. The modified model was called SWAT-LUD and was applied to a meander of Garonne floodplain – Monbéqui (around 25 $km^2$). Then, another module representing the denitrification processes in the floodplain shallow aquifer was developed and added to the SWAT-LUD model. The nitrate flux and shallow aquifer denitrification rates in Monbéqui was then quantified. Afterwards, the SWAT-LUD model was applied to the middle floodplain section of the Garonne River (around 4 600 $km^2$) and the influence of shallow aquifer denitrification on the nitrate flux in the river was quantified. Lastly, the model was applied to the entire Garonne catchment (around 51 500 $km^2$) and the hydrologic influence of SW-GW exchanges was evaluated. The results showed that the SWAT-LUD model could satisfactorily represent the SW-GW exchanges and shallow aquifer denitrification rate at different spatial scales. The main water flow direction is from the shallow aquifer to the river, with water flowing in this direction accounted for around 65% of the total exchanged water volume. In the Garonne catchment, the annual total exchanged water volume represented around 5% of the total discharge volume of the Garonne river. For the Monbéqui site, the simulated annual denitrification rate in the riparian zone was around 130 kg $N\text{-}NO_3^- ha^{-1} y^{-1}$. Around 40% of the nitrate input in this zone was degraded through denitrification. In the middle floodplain section, the annual denitrification rate in the near bank zone ranges from 55 to 120 kg $N\text{-}NO_3^- ha^{-1} y^{-1}$.

## List of Figures

# List of Tables

# List of abbreviations

2SWEM: Surface-Subsurface Water Exchange Model
AFDM: Ash Free Dry Mass
A-HRU: Agricultural alluvial HRU
BDOC: Bioavailable Dissolved Organic Carbon
BMP: Best Management Practice
DNA: Deoxyribonucleic acid
DOC: Dissolved Organic Carbon
DOM: Dissolved Organic Matter
EC: Electrical conductivity
EPIC: Environmental Policy Integrated Climate
F-HRU: Forest alluvial HRU
HRU : Hydrologic Response Unit
HZ : Hyporheic Zone
LU: Landscape Unit
MOHID: Modelo Hidrodinâmico
OM: Organic Matter
OTIS: One-Dimensional Transport with Inflow and Storage
P-HRU: Pasture alluvial HRU
POC: Particulate Organic Carbon
REMM: Riparian Ecosystem Management Model
RNA: Ribonucleic acid
RNM: Riparian Nitrogen Model
SWAT: Soil and Water Assessment Tool
SWAT-LU: Soil and Water Assessment Tool-Landscape Unit
SWAT-LUD: Soil and Water Assessment Tool-Landscape Unit Darcy
SW-GW: Surface Water - Groundwater
SWIM: Soil and Water Integrated Model)
TN : Total nitrogen
TOC: Total Organic Carbon
USGS: U.S. Geological Survey
VFS: Vegetative Filter Strip
WASP: Water Quality Analysis Program

# 1.Introduction générale

La pollution par les nitrates des eaux souterraines et de surface a suscité une attention mondiale ces dernières années (Bijay-Singh et al., 1995; Carpenter et al., 1998; Jalali, 2011). Un excès de nitrate dans les masses d'eau peut être la cause d'eutrophisation et par suite impacter les écosystèmes aquatiques. Cela peut également engendrer des problèmes de santé publique tels que la Méthémoglobinémie ou certains cancers (McIsaac et al., 2001; Camargo and Alonso, 2006). L'Union Européenne et l'Organisation Mondiale de la Santé ont défini dans l'eau potable un standard de concentration en nitrate de 50 $mg.L^{-1}$. Les activités agricoles sont reconnues pour être des sources significatives de nitrate vers les eaux souterraines (Hamilton and Helsel, 1995; Almasri and Kaluarachchi, 2004; Liu et al., 2005b). Les activités agricoles intensives étant souvent localisées dans la plaine alluviale, cette dernière est donc un lieu majeur de pollution par les nitrates, particulièrement dans les eaux souterraines (Sánchez Pérez et al., 2003a; Liu et al., 2005; Arrate et al., 1997; Almasri and Kaluarachchi, 2007).

Les eaux de surface sont riches en oxygène et en matière organique, alors que les eaux souterraines sont riches en nutriments. Le mélange entre les deux systèmes a un impact significatif sur la qualité des eaux, sur les écosystèmes et les cycles biogéochimiques (Brunke and Gonser, 1997; Boulton et al., 1998; Sánchez-Pérez and Trémolières, 2003; Vervier et al., 2009; Krause et al., 2013; Marmonier et al., 2012). Le continuum hydrologique connecte la plaine alluviale et la rivière au sein d'un écosystème complexe. Des matières particulaires et dissoutes sont échangées entre ces deux systèmes, à la fois via l'écoulement de surface et les écoulements souterrains (Tockner et al., 1999).

La zone riparienne sert d'interface entre les écosystèmes terrestres et aquatiques, mais c'est également un outil efficace dans les processus de dénitrifications (Osborne and Kovacic, 1993; Lowrance et al., 1997; Dosskey et al., 2010). Le carbone organique est habituellement admis pour être le facteur limitant des réactions de dénitrification dans les systèmes aquifères alluviaux, une forte concentration en carbone organique dans la zone riparienne peut alors permettre au système de supporter un taux de dénitrification élevé. Il a été démontré que la concentration en nitrate est atténuée dans la zone saturée, même dans les zones ripariennes où

le niveau de l'eau souterraine n'atteint pas la zone racinaire. Dans ces conditions, l'eau qui alimente la rivière, riche en matière organique, est importante pour simuler la dénitrification. (Iribar, 2007; Sánchez-Pérez et al., 2003b).

Des modèles hydrologiques à grande échelle ont été développés pour simuler les processus hydrologiques à l'échelle du bassin versant ou de la région. SWIM (Krysanova et al., 1998), TOPMODEL (Franchini et al., 1996) et MODHYDROLOG (Chiew and McMahon, 1994) en sont des exemples. Cependant, l'interface nappe-rivière n'est généralement pas incluse dans ces modèles. D'autre part, la dénitrification peut être simulée par de nombreux modèles : Heinen (2006) a identifié plus de 50 modèles qui incluent les processus de dénitrification. Néanmoins, la plupart de ces modèles simulent la dénitrification seulement dans les sols, comme le modèle EPIC (Marchetti *et al.*, 1997), le modèle DAISY (Hansen *et al.*, 1991) et le modèle REMM (Lowrance *et al.*, 2000).

Le modèle *Soil and Water Assessment Tool* (SWAT) est un modèle déterministe, continu, semi-distribué, à l'échelle du bassin versant, qui permet la simulation d'un grand nombre de processus hydrologiques. Pour prendre en compte la connexion hydrologique entre l'amont et l'aval, une approche en chaine incluant des unités de paysages différents (*hillslope, divide et foodplain*) a été développée et incluse dans SWAT (Volk et al., 2007; Arnold et al., 2010, Rathjens et al., 2015). Un routage plus détaillé du ruissellement, des écoulements de subsurfaces et des eaux souterraines, peut alors être réalisé pour les parties à l'aval permettant l'évaluation des impacts de la gestion des zones amont sur les zones aval. (Arnold et al., 2010; Bosch et al., 2010). Le modèle modifié est appelé SWAT-LU (SWAT Landscape Unit). Cependant, les processus hydrologiques restent unidirectionnels au sein du SWAT-LU et aucune fonction intégrant les échanges nappe-rivière bidirectionnels n'est incluse. Pendant un évènement de crue, la distance de débordement est fixée à cinq fois la largeur de la surface du lit de la rivière, et l'influence des crues sur le niveau des nappes n'est pas prise en compte. Les fonctions simulant la dénitrification dans le SWAT-LU sont les mêmes que dans le modèle SWAT, et les processus se déroulant dans l'aquifère alluvial ne sont pas inclus. Par conséquent, les objectifs principaux de cette thèse sont alors : 1) de quantifier les volumes d'eau échangés entre la nappe et la rivière dans la plaine alluviale à l'échelle du bassin versant incluant le débordement et 2) de quantifier le taux de dénitrification de l'aquifère alluvial de la plaine, à l'échelle du bassin versant, et évaluer son influence sur les flux de nitrate dans la rivière.

**Structure de la thèse**

Chapitre 2 : revue de littérature des travaux existant sur le cycle de l'azote dans le système sol-plantes-atmosphère, la pollution aux nitrates dans les écosystèmes aquatiques, la caractérisation et les facteurs limitants des réactions de dénitrification, l'étude du système rivière-plaine d'inondation et les cycles biogéochimiques existant dans ce système. Les modèles permettant de simuler les processus biogéochimiques et hydrologiques à l'interface nappe-rivière sont introduits et les objectifs de la thèse sont décrits en détail.

Chapitre 3 : matériels et méthodes utilisés pour attendre les objectifs. La méthode inclut l'introduction et la description des processus hydrologiques ainsi que des cycles de l'azote et du carbone simulés dans le modèle SWAT. Cela inclut également la description du développement du nouveau module qui permet la simulation des échanges eaux de surface-eaux souterraines, l'influence des crues sur le niveau d'eau de surface et des nappes ainsi que la dénitrification se déroulant dans les aquifères alluviaux de la plaine. La partie matériels se concentre sur la description des sites d'études (le bassin versant de la Garonne, la moyenne section de la plaine alluviale de la Garonne et le site de Monbéqui) ainsi que sur les techniques d'échantillonnage et d'analyse de laboratoire pour la mesure des paramètres physico-chimiques.

Chapitre 4 : description et définition de la structure Lanscape Unit (LU) dans la plaine alluviale, développement du module hydrologique SWAT-LUD (SWAT Landscape Unit Darcy) et son application sur le site de Monbéqui. Des mesures du niveau des nappes sur la période 1999-2000 ont été utilisées pour calibrer le modèle. Des mesures du niveau des nappes sur une période se déroulant d'avril 2013 à mars 2014, les échanges d'eau simulés à l'aide d'un modèle 2D distribué (2SWEM), les concentrations mesurées d'un traceur conservatif (chlorure) ainsi que la simulation du même traceur par 2SWEM, ont été utilisés pour valider les résultats du modèle. Le volume des échanges nappe-rivière a été quantifié et l'influence des conditions hydrologiques de la rivière sur ces échanges a été analysée. Ce chapitre est basée sur un article en cours de révision pour le journal *Hydrological Processes*.

Chapitre 5 : description du nouveau module développé en ce qui concerne la simulation de la dénitrification dans l'aquifère alluvial et son application sur le site de Monbéqui. L'échange de nitrate entre l'aquifère alluvial et l'eau de la rivière à travers

l'infiltration latérale (rive) et verticale (surface) ainsi que l'influence des crues sur le lessivage des nitrates est prise en compte. L'influence du carbone organique dissout (COD) et du carbone organique particulaire (COP) sur la dénitrification est évaluée. La concentration en nitrates mesurée dans les eaux souterraines pendant les années 2005 et 2013 ainsi qu'une modélisation des flux d'eau et de nitrate avec le modèle STICS, sont utilisés pour calibrer le modèle modifié. Les flux de nitrate et le taux de dénitrification dans l'aquifère alluvial de Monbéqui sont également quantifiés. Ce chapitre a été écrit comme une publication soumise à Ecological Engineering.

Chapitre 6 : description des applications du modèle SWAT-LUD dans la moyenne section de la plaine alluviale de la Garonne et dans le bassin versant de la Garonne. Différents sous-bassins classiques et sous-bassin-LUs ont été inclus dans la modélisation de cette zone d'étude, et la connectivité entre les deux entités a été implémentée. La fonction de stockage de l'eau dans la plaine alluviale en cas de crues est présentée et l'influence de la dénitrification dans la nappe de la plaine alluviale sur les flux de nitrates de la rivière est quantifiée. Ce chapitre a été écrit comme une publication prévue pour être soumise au Journal Sustainability of water qaulity and Ecology.

Chapitre 7 : Conclusions générales reprenant les principaux résultats de cette étude ainsi que les perspectives basées sur ces recherches.

# 1. General introduction

Nitrate pollution in surface water and groundwater systems has attracted worldwide attention (Bijay-Singh et al., 1995; Carpenter et al., 1998; Jalali, 2011). Excess nitrate in water bodies can cause eutrophication and impact aquatic ecosystems. It also potentially causing public health problems such as methaemoglobinaemia and cancer (Camargo and Alonso, 2006; McIsaac et al., 2001). The European Union and the World Health Organization have set the standard for nitrate concentration at 50 $mg \cdot l^{-1}$ for drinking water. Agricultural activities are known to be a significant source of nitrate in groundwater (Almasri and Kaluarachchi, 2004; Hamilton and Helsel, 1995; Liu et al., 2005). As alluvial plains support intensive agricultural activities, they often suffer from groundwater nitrate pollution (Sánchez Pérez et al., 2003a; Liu et al., 2005; Arrate et al., 1997; Almasri and Kaluarachchi, 2007).

As surface water contains rich oxygen and organic matter and groundwater contains abundant nutriment elements, the water mix between those two systems has a significant impact on water quality, ecosystems and biogeochemistry cycling (Brunke and Gonser, 1997; Boulton et al., 1998; Sánchez-Pérez and Trémolières, 2003; Vervier et al., 2009; Krause et al., 2013; Marmonier et al., 2012). The hydrologic connectivity links floodplains and rivers into integrated ecosystems. Particulate and dissolved matter exchanged between those two systems via both surface flow and groundwater flow (Tockner et al., 1999)..

Riparian zones serve as interfaces between terrestrial and aquatic ecosystems and have proven to be efficient nitrate removal tools (Dosskey et al., 2010; Lowrance et al., 1997; Osborne and Kovacic, 1993). Since organic carbon usually identified as the major factor limiting denitrification rates in the shallow aquifers system, the rich content of organic carbon in riparian soil supported the high rate of denitrification. Denitrification has also been found efficient to attenuate nitrate in saturated zone of the riparian zones where groundwater levels are lower than soil root zones. In these conditions, the recharged river water, rich in organic matter, has allowed to stimulate the occurrence of denitrification (Iribar, 2007; Sánchez-Pérez et al., 2003b).

Large-scale hydrological models have been developed to simulate hydrologic processes at catchment or regional scale. Examples of such models include SWIM

(Krysanova et al., 1998), TOPMODEL (Franchini et al., 1996) and MODHYDROLOG (Chiew and McMahon, 1994). However the river/groundwater interface is mostly not included in these models. Denitrification is simulated in numerous models: Heinen (2006) has identified more than 50 models that include denitrification. Nevertheless most of the models only simulate the denitrification process in the soil profile, such as the EPIC model (Marchetti et al., 1997), the DAISY model (Hansen et al., 1991) and the REMM model (Lowrance et al., 2000).

The Soil and Water Assessment Tool (SWAT) model is a deterministic, continuous, semi-distributed, watershed-scale simulation model that allows a large number of different hydrologic processes to be simulated. To reflect the hydrologic connection between upslope and downslope parts of a landscape, a catena approach including:, hillslope, divide and floodplain landscape units has been developed and included in SWAT (Volk et al., 2007; Arnold et al., 2010, Rathjens et al., 2015). Thanks to this catena, a more detailed downslope routing of surface runoff, lateral flow and groundwater can be accomplished, and the impact of upslope management on downslope landscape can be assessed (Arnold et al., 2010; Bosch et al., 2010). The modified model was called SWAT-LU (SWAT Landscape Unit). However, the hydrologic processes are still single tracks in SWAT-LU and the function of SW-GW exchange in both directions is not included. During flooding events, the flooded distance is fixed at five times the bank full width of the channel and the influence of flooding on groundwater levels is not taken into account. The denitrification function in SWAT-LU is simulated as in SWAT model, the denitrifying process in the shallow aquifer is not included. Mains objectives of the thesis were: 1) quantifying the exchanged SW-GW volume in the floodplain area at the catchment scale and 2) quantifying the shallow aquifer denitrification rate in the floodplain area at the catchment scale and evaluate its influence on the river nitrate flux.

**Structure of the thesis**

Chapter 2 reviews studies about nitrogen cycling in the soil-plant-atmosphere system, the nitrate pollution in the aquatic ecosystem, the characterization and limit factors of denitrification function, the definition of river-floodplain system and the biogeochemical cycling occurs in this system. The models simulating the hydrologic and biogeochemical processes at the river-floodplain interface are introduced, and the objectives of the thesis are also described.

Chapter 3 describes materials and methods used to achieve the objectives. The methods include the introduction of hydrologic, nitrogen and organic carbon cycling processes simulated in SWAT model. It also include the description of the development of the new module that simulate surface water and groundwater exchanges, the influence of flooding on surface and groundwater levels and denitrification process in the shallow aquifer of floodplain. The materials part focus on the description of study sites (Garonne watershed, middle floodplain of the Garonne basin and Monbéqui study site), the field sampling and laboratory analyse technics of the measured physico-chemical elements.

Chapter 4 provides the description and definition of structure landscape unit (LU) in the floodplain area, the development of hydrologic module of SWAT-LUD (SWAT-Landscape Unit Darcy) and its application at Monbéqui site. Measured groundwater levels in period 1999-2000 are used to calibrate the model. Measured groundwater levels in period 2013, water exchange simulated with a 2D distributed model (2SWEM), measured concentrations of conservative tracer (chloride) and simulated concentrations of this same conservative tracer with 2SWEM are used to validate the simulated results. The SW-GW exchanged volume is quantified and the influence of river hydrologic conditions on SW-GW change is also analysed. This chapter presented the publication currently in a revising process of Hydrological processes.

Chapter 5 describes the new module developed as regard with the denitrification in the shallow aquifer of alluvial floodplains and its application at Monbéqui site. Nitrate exchanges between the shallow aquifer and the recharged river water through both lateral (river bank) and vertical (surface) infiltration as well as the influence of flooding on nitrate leaching is considered. The influences of both dissolved organic carbon (DOC) and particulate organic

carbon (POC) on denitrification is evaluated. Measured groundwater nitrate concentration in 2005 and 2013 as well as simulated infiltrated water and nitrate of STICS model are applied to calibrate the modified model. The nitrate flux and denitrification rate occurred in the shallow aquifer of Monbéqui site is quantified. This chapter has been written as the publication submitted to Ecological Engineering.

Chapter 6 describes the application of SWAT-LUD in the middle floodplain of the Garonne basin. Multiple classic subbasins and subbasin-LUs were included in the study area and the connection between both was implemented. The floodplain water storage function during flood event is presented and the influence of denitrification in the floodplain shallow aquifer on river nitrate flux is quantified. This chapter was written as the publication prepared to be submitted to Journal Sustainability of water qaulity and Ecology.

Chapter 7 present the general conclusion that reviewed the main results of this study and perspectives based on this research.

# Chapter 2. Nitrogen cycling, river-floodplain system, modelling approach.

This chapter reviews studies about nitrogen cycling in the soil-plant-atmosphere system, the nitrate pollution in the aquatic ecosystem, the characterization and limit factors of denitrification function, the definition of river-floodplain system and the biogeochemical cycling occurs in this system. The models simulating the hydrologic and biogeochemical processes at the river-floodplain interface are introduced, and the objectives of the thesis are described also.

### 2.1.1 Nitrogen

Nitrogen is a fundamental component in living organisms, is a component in all amino acids and is present in the bases that make up nucleic acids such as RNA (Ribonucleic Acid) and DNA (Deoxyribonucleic Acid). It is also a key element that controls the functioning of lots of terrestrial, freshwater and marine ecosystems (Vitousek et al., 1997). Nitrogen exists in both organic and mineral form in the environment. The inorganic forms of nitrogen are shown in Table 1.

Table 1 The oxidation state and the formula of inorganic nitrogen in the environment

| Formula | Oxidation state |
|---|---|
| $NO_3^-$ | +5 |
| $NO_2^-$ | +3 |
| NO | +2 |
| $N_2O$ | +1 |
| $N_2$ | 0 |
| $NH_3/NH_4^+$ | -3 |

Large numbers of transformation of nitrogen exist in the soil-plant-atmosphere system, both biological and physico-chemical process are included. The movement and transform of nitrogen in the soil-plant-atmosphere system is shown in Figure 1.

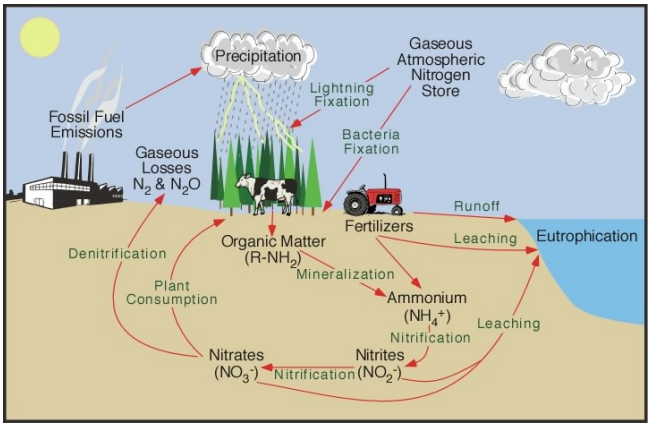


Figure 1. Nitrogen cycling in the soil-plant-atmosphere system (extracted from http://www.physicalgeography.net )

Nitrogen is the main component of atmosphere (78% by volume). The gaseous nitrogen in the atmosphere is very reactive and has limited availability for biological use.

Nitrogen enters into ecosystems main through biological fixation and artificial fertilization. Some free living or symbiotic bacteria could combine gaseous nitrogen with hydrogen to produce ammonia. The chemical fertilizers produced by industrial Haber-Bosch process which uses high temperature and pressure to convert nitrogen gas and a hydrogen source into ammonia is globally used in agricultural systems.

$NH_4^+$ and $NO_3^-$ could be uptake by plants and microorganisms and incorporate into organic forms, this process is called immobilization. Organic nitrogen is the main form of nitrogen in the soil, up to 90% of the nitrogen stored as organic form, either in living organisms or in humus originating from decomposition of organism residues. The organic nitrogen could be decomposed by microorganisms through mineralization and ammonium is produced by enzymatic degradation in this process. Fertilized and mineralized $NH_3$ would escape to atmosphere by volatilization or convert to $NO_3^-$ by nitrification. Nitrification is the biological process that converts $NH_3$ or $NH_4^+$ to $NO_2^-$ followed by the oxidation of $NO_2^-$ to $NO_3^-$, and $NH_4^+$ is rapidly converted to $NO_3^-$ in the majority of agriculture soil. $NH_4^+$ could also be converted into dinitrogen by anammox. Anammox is an important microbial process which was found in 1990s, $NO_2^-$ and $NH_4^+$ are converted directly into dinitrogen gas in this process in the anaerobic condition. $NO_3^-$ could convert to $N_2$ through the biological process called denitrification. The detail process of denitrification is described in 2.1.3.

Nitrogen is usually a limiting element for primary production, fertilizer produced by the industry process has sustained the global increased population over the past century (Gruber and Galloway, 2008). However, the excessive chemical N-fertilization during the past century caused environmental and health problems, like more greenhouse gases - nitrous oxide and ammonia released to the atmosphere, soil and water body acidification and eutrophication caused by the excessive inorganic nitrogen in aquatic ecosystem.

### 2.1.2 Nitrate pollution in the aquatic ecosystems

Nitrate pollution that enter aquatic ecosystems via point and nonpoint sources had drawn worldwide attention for a long time (Bijay-Singh et al., 1995; Carpenter et al., 1998; Jalali, 2011). The excess nitrate content in the water body could cause eutrophication, it could also cause health problems such as methaemoglobinaemic and cancer (Camargo and Alonso, 2006; McIsaac et al., 2001). European Union and World Health Organization had both set the standard for nitrate concentration at 50 $mg \cdot L^{-1}$ for drinking water.

Nitrate, as a negatively charged ion, is repelled by the negative charged clay mineral surfaces in soil. Nitrate is the primary form of nitrogen leached into groundwater and the most common contaminant of nitrogen in aquifer systems (Freeze and Cherry, 1979). The leaching of nitrate away from soil profile is a problem to both agricultural production and environment quality. The main two factors that impact the leaching of nitrate from the root zone to shallow groundwater are the amount of nitrate in the soil profile that above the amount required by plant and the vertical drainage volume. Crop system condition (crop type, rotation, irrigation and fertilization) and climate condition are regarded as have influence on nitrate leaching (Meisinger and Delgado, 2002; Simmelsgaard, 1998).

The climate impacts the water cycle directly. The soil water content and percolated water volume are significantly influenced by precipitation, temperate and humidity. The climate change may cause changes in temperature and precipitation, and will impact the agricultural nitrate cycling through changes in both soil processes and agricultural productivity (Stuart et al., 2011).

In the agriculture system, irrigation is a general action that provides water to crops during draught stress period. Irrigated water accounts for more than 60% of the freshwater use in southern Europe. After the irrigated water excess soil storage capacity, the nitrate would percolate to shallow groundwater along with soil water during heavy irrigation periods. Wang et al. (2010) found that the leached nitrate under heavy irrigation could arrive 60% of the accumulated N in the soil profile.

Fertilizers were widely applied in the agriculture system to stimulate the crop production, preferentially in regions where irrigation is available, and soil and climatic conditions are favorable for the growth of crop plants (Bijay-Singh et al., 1995). The massive fertilization could lead to nitrate accumulation in the soil profiles after successive cropping rotation (Westerman et al., 1994; Zhao et al., 2006). In agricultural region, especially in the irrigation areas, fertilizer is the main source of nitrate contamination of groundwater (Mishima et al., 2010).

Crop type has influence on the nitrate uptake, soil water drainage and soil microbial communities composition (Bending et al., 2002; Canter, 1996). The land cover and crop type in crop rotation have important influence on the leaching of nitrate (Beaudoin et al., 2005; Justes et al., 1999). Johnson et al. (2002) compared standard, intermediate and protective

systems, the leaching of nitrate were found significantly different in these three systems, the protective system was proved able to substantially decrease nitrate losses.

The characteristics and depths of soils have impact on the transfer of the water and the solute nitrate in the soil profile. The water storage capacity increased along with the rise of soil depth, and the clay soil has a greater water holding capacity than sandy soil. Beaudoin *et al.* (2005) found that the nitrate concentration in the shallow groundwater was lowest in deep loamy soils and greatest in shallow loamy sand soils in the agricultural area.

### 2.1.3 Denitrification

Denitrification is a biological process that transforms nitrate into $N_2$ gas in the anaerobic environment, microaerophilic, and occasionally aerobic conditions. In this process, N oxides rather than the general preferred oxygen are the terminal electron acceptors. It occurs in four steps, nitrate ($NO_3^-$) to nitrite ($NO_2^-$), $NO_2^-$ to nitric oxide (NO), NO to nitrous oxide ($N_2O$) and $N_2O$ to $N_2$, the process can be arrested at any of the intermediate stages. Each step is catalyzed by different enzymes, and not all the denitrifying bacterium have the capacity to be involved in the sequence of the four steps (Bothe et al., 2006; Zumft, 1997) (Figure 2).

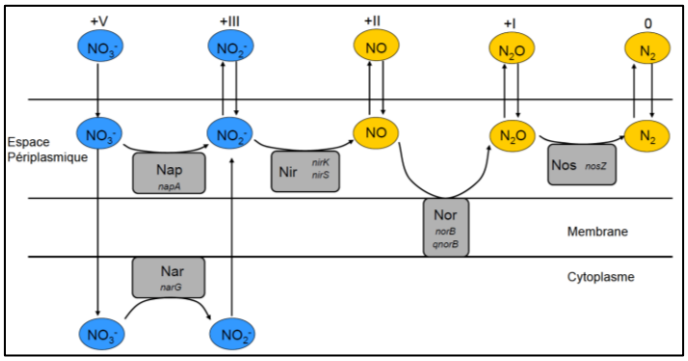


Figure 2. denitrification processes with different steps (extracted from Iribar, 2007)

The conditions required by denitrification are the presence of N oxides as the electron acceptors, and then the presence of organic carbon which is the electron donor, finally the anaerobic environment which controls the activity of denitrifying enzymes. Except the three conditions, pH and temperature are regularly identified as the limit factors also.

Denitrification usually occurs at low dissolved oxygen concentration condition, Körner and Zumft (1989) found that the dissolved oxygen concentration thresholds of nitrate reductase, nitrite reductase were 5 $mg \cdot L^{-1}$ and 2.5 $mg \cdot L^{-1}$ independently. Rivett et al. (2008) reviewed the studies of the dissolved oxygen concentration threshold in the groundwater (Table 2).

Table 2. Dissolved oxygen concentration threshold of denitrification in groundwater (extracted from Rivett et al. 2008)

| Dissolved oxygen concentration ($mg \cdot L^{-1}$) | Reference |
|---|---|
| 4 | Böhlke and Denver (1995) |
| 2 | Bates and Spalding (1998) |
| 2 | Gillham (1991) |
| 1.2 | Gallardo and Tase (2005) |
| 1 | Böhlke *et al.* (2002) |
| 1 | Christensen *et al.* (2000) |
| 1 | Vogel *et al.* (1981) |
| 1 | DeSimone and Howes (1998) |
| 1 | Starr and Gillham (1993) |
| 0.2 | Trudell *et al.* (1986) |

The relationship between pH and denitrification are complicate, both the rate of the process and the ratio of its gaseous products depend on pH. Studies found that the liberate of $N_2O$ and the ratio $N_2O$:$N_2$ increased along with the decrease of soil pH (ŠImek and Cooper, 2002). The optimum temperature range of denitrifying enzymes is between 25 and 35 °C, but denitrification could occur in the range 2–50 °C (Rivett et al., 2008).

Organic carbon as the 'energy' of denitrifying bacteria is necessary in the denitrifying process. The complexity compositions of organic carbon in the ecosystems makes it difficult to identify the effective carbon source (Dodla et al., 2008; Hume et al., 2002). Dissolved organic carbon (DOC) or Bioavailable dissolved organic carbon (BDOC) are taken for carbon sources of denitrification in most studies (Hill et al., 2000; Inwood et al., 2005; Peterson et al., 2013). Furthermore, particulate organic carbon (POC) could enhance denitrification rate in both aquatic and terrestrial ecosystems (Arango et al., 2007; Stelzer et al., 2014; Stevenson et al., 2011). The dominant limit factors of denitrification in terrestrial and aquatic systems are nitrate and organic carbon (McClain et al., 2003). The BDOC content is around 4-54 % of DOC in the surface water (Servais et al., 1989; Wickland et al., 2012; Wiegner et al., 2006) and only around 8 % in the groundwater (Shen et al., 2014). Compared with the surface water, the denitrification limitation caused by organic carbon availability in groundwater is more important.

Denitrification is an essential branch of the global N cycle, is also the main biological process in charge of emissions of nitrous oxide. The spatially distributed global models of denitrification applied by Seitzinger *et al.* (2006) propose that the largest portion occurs in continental shelf sediments, which account for around 44% of total global denitrification.

Freshwater systems (groundwater, lakes, rivers) taken about 20% and estuaries 1% of total global denitrification. The denitrification in terrestrial soils and oceanic oxygen minimum zones represented 22% and 14% respectively.

### 2.2 River-Floodplain system

Floodplain is the flat land area adjacent to a stream or river that experience flooding during high discharge period, is the result of both erosion and deposition (Brown, 1997). The size, form and vegetation type of floodplains are highly variable depend on the size, location and hydraulic condition of the rivers. Floodplain take a significant proportion of the earth's surface, around 2% of African, 3% of South America and a greater proportion of tropical Asia (Gerrard, 1992).

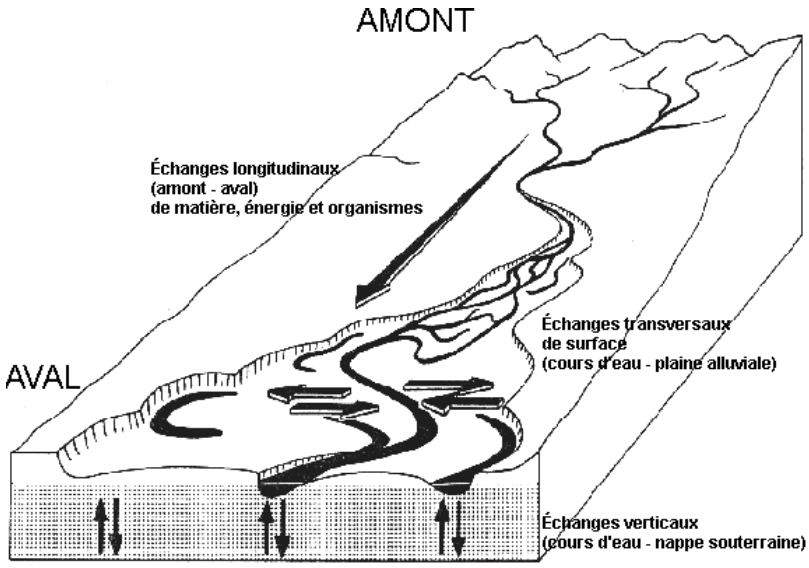


Figure 3. Floodplain (extracted from http://www.uved.fr ).

Alluvial soils are generally associated with floodplain, originated from ancient riverbeds and the deposited sediment taken by the river water during flooding periods. The soil materials and drainage condition are greatly influenced by the natural of alluviums, since alluviums vary in different sectors the basin, the characteristics of soils are different also. Except the origin alluvium, water dynamic, living organisms and time all have influence on local soil characteristics (Gerrard, 1992; Piégay et al., 2003).

The hydrologic connectivity links floodplains and rivers into integrated ecosystems. Particulate and dissolved matter exchanged between those two systems via both surface flow and groundwater flow (Tockner et al., 1999). The concept-flood pulse is developed and flood pulses are regarded as the principle drive force for the existence of the system (Junk, 1989).

The hydrologic connections have significant influence on the biotic communities and ecosystem process on both river and floodplain ecosystems (Bayley, 1995; Thomaz *et al.*, 2007). Large floodplains have an important role in the hydrologic cycle of watershed. In the flooding period, the water storage function of the floodplain could modify the river water and sediment transport (Frappart et al., 2005).

### 2.2.1 Hyporheic zone (HZ)

In the river-floodplain system, except flooding, the lateral flow also linked via beneath surface water and groundwater exchange also (Boulton et al., 2010). In recent decades, numerous studies indicated the importance of interactions between groundwater and surface water as they represent a substantial control on exchange of water, nutrients and organic matter in the connection area (Sophocleous, 2002). One of the most promising linkage concepts has been the development of what is known as the hyporheic zone (HZ) (Figure 4). It was first presented by Orghidan (1959) as a special underground ecosystem, but numerous different definitions by ecologists, hydrologists and biogeochemists have since been proposed. The HZ is viewed as a special benthic dynamic ecotone by ecologists and the zone of saturated sediment beneath and lateral to a stream or river channel that receive surface water input by hydrologists (Storey *et al.*, 2003; Sophocleous, 2002; Hancock *et al.*, 2005). The most important character of HZ is the mixture of surface water and subsurface water. Depends on the local hydrologic conditions, the HZs could be categorized into three broad typologies: 1) groundwater-dominated, 2) surface water-dominated and 3) sites exhibiting transient water table features (Malcolm et al., 2005).

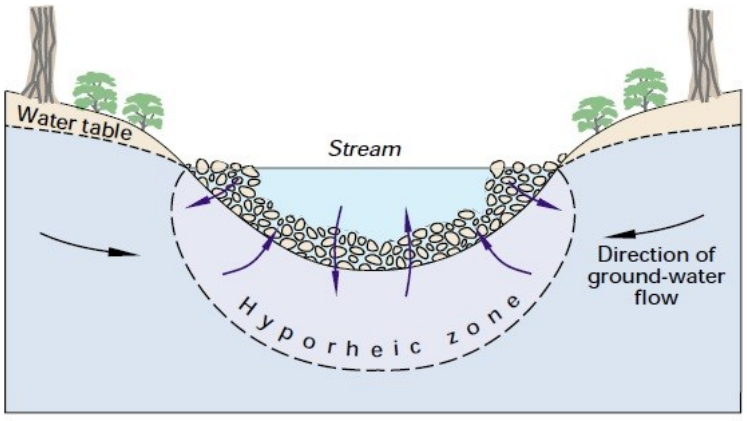


Figure 4. Hyporheic zone (extracted from: www.bgs.ac.uk)

The size and the flux of surface water groundwater (SW-GW) exchanges of the HZs vary both spatially and temporally according to the local conditions (Cardenas et al., 2004). The factors that regulatory SW-GW exchange in the hyporheic zone are different at different spatial scales. The key factors controlling HZ water exchange at riffle scale are found to be the hydraulic conductivity, the hydraulic gradient between upstream and downstream ends of the riffle and the flux of groundwater (Storey et al., 2003). Cardenas et al. (2004) found that streambed heterogeneity, stream curvature and bed form dynamically determined HZ geometry, fluxes, and residence time distributions. At the reach scale, the main factors are found to be the channel bed form, sediment permeability and particle size (Boano et al., 2007; Cardenas and Wilson, 2007a, 2007b). At the catchment scale, valley widths, depths of bedrock and aquifer properties are proved have influence on the HZ water flux (Bardini, 2013; Brunke and Gonser, 1997a; Malcolm et al., 2005).

The solute load capacity of HZs is highly dynamic, in the small channels, stream water is often completely exchanged with water storage in hyporheic zone within several kilometres (Jones and Mulholland, 1999). However, the ratio of HZ exchange flow compared with stream water discharge decreased as stream size increased (Wondzell, 2011).

### 2.2.2 Riparian zone

Riparian zones are known as the buffer zones that located between the terrestrial and the aquatic ecosystems (Gregory et al., 1991) (Figure 5). As ecotones, the ecosystem services values of riparian zones had been noticed for a long time. The relative function of riparian zones are different and depends on the size of the stream, the position of the stream within the drainage network, the hydrologic regime and the local geomorphology (Naiman and Decamps, 1997). Riparian zone as an efficient BMP (Best Management Practice) had been used all over the world (Ice, 2004; Lee et al., 2004; Matteo et al., 2006).

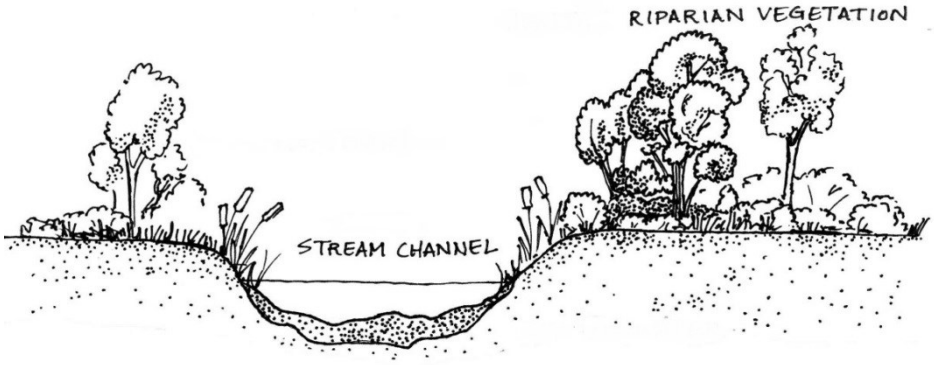


Figure 5. Riparian zone (extracted from www.mtwatercourse.org)

The environmental services of riparian zone main fall into three major categories:

1) Hydrology and sediment storage:

The high hydraulic roughness of riparian vegetation contribute to the decrease of both runoff from upland to river during no-flood period and the kinetic energy of flood from river to upland during flood period (Tabacchi et al., 2000). Since water flow through riparian zone before enters the channel, riparian zone is also known the area to trap sediment erosion from the agricultural land. The buffer width and slope of the riparian zone were proved have the most important factors on sediment trap (Cooper *et al.*, 1987; Liu *et al.*, 2008). The storage of water and sediment in the riparian zone could reduce damage from flood, stabilize river bank and reduce channel erosion also.

2) Biogeochemistry and nutrient cycling intercept, cycle and accumulate

The locations and the hydrologic conditions of riparian zones ensure their high biogeochemical activities. The saturate soil caused by inundation with river water and shallow confining layer make riparian zones are hot spots of anaerobic processes like denitrification (Hoffmann et al., 2009). The phosphorus attached on the sediment is trapped together with the sediment, however, the trapped phosphorus also could be release and enrich runoff waters in available soluble phosphorus (Surridge et al., 2007). Riparian vegetation could remove nutrients dissolved in the water and accumulate in the plants, lead to a short term accumulation of nutrients in non-woody tissues and a long term accumulation in woody tissues (Groffman *et al.*, 1992; Peterjohn and Correll, 1984). At the same time, litter of riparian vegetation is source of organic matters to aquatic organisms (Jardine et al., 2011).

3) Biodiversity maintenance

As ecotones, riparian zone could increase regional specie richness (Sabo et al., 2005). Variations of flood duration and frequency and the succession of riparian vegetation created complex and shifting habitats to support high biodiversity in the riparian system (Malanson, 1993).

### 2.2.3 Biogeochemistry cycling

#### 2.2.3.1 Flooding

Except the hydrologic impact, the connection in the floodplain-river systems also has great influence on the biogeochemistry process. Depend on the hydrograph and floodplain topography, the natural floodplains serve as sinks, sources, or transformers of dissolved and particulate organic matter, inorganic nutrients, and biota (Tockner et al., 1999).

The sedimentation and the buffer function of riparian zone in floodplain could lead to sediment and nutrients retention in floodplain. Noe and Hupp (2005) compared sediment and C, N, and P accumulation rates in floodplains with different watershed land use and hydrogeomorphology conditions, it is found that watershed land use types have significant impact on sediment and nutrient retention in floodplains. The hydrologic disconnections between river channels and floodplains minimize material retention by floodplains.

Floodplains usually are large pools of POC exist as litter or coarse woody debris (Robertson et al., 1999). The occurrence of flooding is proved increasing the turnover rates of organic matter and nutrients in the river-floodplain system (Bayley, 1995). The flooded water was found led to increasing nutrient mobilization (Banach et al., 2009). Flood, especially the duration of flood was proved can increase leaf decomposition rate in the floodplain (Langhans and Tockner, 2006).

Like the two pole water interaction, while sediment, nutrients and biota are transported from river channel to floodplain during flooding, the released DOC and nutrients during flooding and the POC storage in the floodplain tend to transported back into the river channel during flood recession. The study in the floodplain of Amazon river by Moreira-Turcq et al. (2013) illustrated that floodplains are important sources of organic carbon of the river main channels. Organic matter in the river is imported to floodplain during rising water period and the OM (organic materials) produced in the floodplain is exported to the river during high and falling water periods.

Baldwin and Mitchell (2000) illustrated the effects of the wetting-drying regime on nutrient cycles in floodplain system, four wetting-drying regimes were studied: partial drying sediment, complete desiccation of sediments, rewetting of desiccated soils and sediments and inundation of floodplain soils. It was proved that they all have different impact on nutrient cycling in floodplain.

#### 2.2.3.2 Denitrification in riparian soil

Floodplains support intensive agricultural activities, in Europe and North America, up to 90% of floodplains are cultivated (Tockner and Stanford, 2002). Floodplains are important source of nutrients like N, P, pesticides and sediment (Bainbridge et al., 2009). Since recharged groundwater in cultivated fields is a major source of the nitrate contamination of surface water, the nitrate level in groundwater can have a major influence on the quality of surface water (Cey et al., 1999).

Numerous studies proposed that denitrification in riparian areas is an important process that decreases the nitrate load of groundwater discharging into streams (Hill, 1996; Maître et al., 2003; Martin et al., 1999). Since organic carbon usually identified as the major factor limiting denitrification rates in the shallow aquifers system, the rich content of organic carbon in riparian soil supported the high rate of denitrification. The importance of riparian hydrology on denitrification was identified and it was suggested that the denitrification may be strongly influenced by the riparian zone hydrogeological setting which contains surface topography, soils and the composition, stratigraphy and hydraulic properties of the underlying geological deposits (Vidon and Hill, 2005). Groundwater table fluctuations are influenced by the size and seasonality hydrologic connection between the adjacent uplands and riparian zone, the depths of confining layers and the permeable of sediments overlying confining layer. The shallow groundwater depth of riparian zone increases the interaction of groundwater with organic rich surface soils that favor denitrification (Gold et al., 2001; Roulet, 1990). The topography and soil texture have influence on the groundwater residence time, the long residence time enhanced the development of anaerobic conditions which is necessary for the occurrence denitrifying process (Burt et al., 2002; Vidon and Hill, 2004).

#### 2.2.3.3 Denitrification in hyporheic zone

While the attenuate of nitrate in the riparian soil was widely investigated, the nitrate consummation processes in hyporheic zone (HZ) attracted interests also. HZ is regarded as a high biogeochemical activity zone, hyporheic sediments interact with nitrate contaminated groundwater before it enters the surface system (Boulton et al., 2010). The mixing of surface water which is rich in dissolved oxygen, nutrients and dissolved organic carbon and the groundwater that contains abundant nutriment elements enhance the biogeochemical activity and transformation rates (Boulton et al., 1998; Krause et al., 2009; Mulholland et al., 2008; Peyrard, 2008; Peyrard et al., 2011).

HZs were proven active nitrogen sink areas, the importance of the HZ on attenuating nitrate has been highlighted in a number of recent studies (Curie et al., 2009; Harvey et al., 2013). Triska *et al.* (1993) found that denitrification potential in HZ increased with distance from the channel. Zarnetske *et al.* (2011) illustrated that the main nitrate attenuate process in HZ is denitrification. Because of the complex hydrologic condition, the limit factors could be organic carbon, nitrate, oxygen and pH. Around all the elements, organic carbon is the main limit factor in most of the HZs. Since dissolved organic carbon (DOC) concentrations in most aquifers are relatively low, typically less than 5 $mg \cdot L^{-1}$ (Rivett et al., 2007). The recharged C

rich surface water could largely illustrate the occurrence of denitrification (Iribar, 2007; J. M. Sánchez-Pérez et al., 2003).

Schindler and Krabbenhoft (1998) found that the hyporheic zone acts as a source of DOC, however most of the other studies showed that HZ is the activity organic carbon sink zone. Findlay et al. (1993) found that almost half of stream water DOC disappeared from interstitial water moving along a hyporheic flow path below a gravel bar. Wong and Williams (2010) studied the seasonal dynamic of DOM (Dissolved Organic Matter) in HZ. The results illustrated that because of linkage with riparian zone and surface water, the sources of DOM in the hyporheic zone are seasonal variable. The allochthonous character of the DOM rise in the fall while the autochthonous character increased in spring and summer.

While most of the study focus on the effect of DOC, POC (Particulate Organic Carbon) in HZ was proved could stimulate denitrification also. Hill et al. (2000) found that denitrification "hotspots" occurred near interfaces between sands and buried river channel deposits. It was generally considered that POC could stimulate denitrification directly and indirectly and different quality and quantity of POC had different influence on nitrogen transformation. The decomposition of POC could release DOC and create the anaerobic environment that both in favor of the denitrifying process (Arango *et al.*, 2007; Stelzer *et al.*, 2011, 2014). In the hyporheic zone, the biofilm as an important composer of POC has great impacts on the metabolism of river system (Fischer et al., 1996). It is regarded as an important organic matter storage site and absorption site for DOM because of its large internal surface area (Koutný and Rulík, 2007).

### 2.3 Modelling approach of river-floodplain system

Different methods are proposed on the study of river-floodplain system: field sampling, chemical analyzing, mathematical statistics, modeling…., in which modeling is an economical and efficient method to quantify the continually occurred processes especially on the research at large spatial scale and long temporal scale. A model is the representation of simplified system that takes into account the important proprieties to represent the empirical objects, phenomena and physical processes of the studied system (Frigg and Hartmann, 2012). Mathematical models were generally classified into three types: empirical model, conceptual model and physical based model. The empirical models are models relate input to output through a very general relationship, with little or no attempt to identify the physical processes involved. Conceptual models are generally composed of interconnected conceptual elements, not fully physically based, but their developments are based on the understanding of

the physical processes. Physical based models are based on the mathematical representation of physical processes, have a logical structure similar to the real system (Maskey, 2004; Singh and Singh, 2001).

### 2.3.1 Models of river-floodplain system

Most of the models developed for the floodplain were aimed at predict flooding and simulate the hydrologic conditions of both the flooded stream and floodplain (Townsend and Walsh, 1998; Dutta *et al.*, 2000; Bates *et al.*, 2006; Yamazaki *et al.*, 2011; Jung *et al.*, 2012). Rare of them simulate the integrated biogeochemical cycling in the river floodplain system (Helton et al., 2012, 2010). Numerous models included the denitrifying process in the soil profiles, Heinen (2006) reviewed more than 50 models with simplified process for denitrification and the majority of these models are based on potential denitrification. Compared with the denitrification in the soil profile, denitrification occurred in aquifer and HZ were less studied (Bailey et al., 2013; Kinzelbach et al., 1991; Lee et al., 2009, 2006). Moreover, the simulation of denitrification process occurred in the floodplain region at the catchment scale has not been investigated.

#### 2.3.1.1 Hyporheic zone models and denitrification

As the hyporheic zone located at the interface between surface water and subsurface water system, models that simulate the hyporheic zone main consisting of three types of models: models developed for surface water, models developed for subsurface water and models that integrated the interface of the two domains.

The models developed to simulate surface water include QUAL2K (Park and Lee, 2002) , WASP (Water Quality Analysis Program) (Vuksanovic et al., 1996) and OTIS (One-Dimensional Transport with Inflow and Storage) model (Morrice et al., 1997). In these models the classical method is considers the hyporheic zone as a storage pool to keep water balance between upstream and downstream. This approach is easily to be applied in the large scale but most of them do not reflect the dynamic of hydrologic and biogeochemical process in the hyporheic zone.

The widely used subsurface water model is MODFLOW -- the USGS's three dimensional model, which has been successfully applied to simulate water flow through the hyporheic zone. Wroblicky et al. (1998) simulated the lateral SW-GW exchange through the HZ the lateral extent of the HZ along two first-order stream. Storey et al. (2003) simulated the

subsurface flow within a single riffle. Lautz and Siegel (2006) simulated the water movement in hyporheic zone around deribs dams and meanders along a semi-arid stream. As a physical based model, MODFLOW require detail topography input and long computation time, and it is difficult to be applied in large spatial scale. MOHID (Modelo Hidrodinâmico) Land is a three dimension physically-based, spatially distributed model designed to simulate water cycle in hydrographic basins and aquifer (Braunschweig et al., 2004; Trancoso et al., 2009). Bernard-Jannin et al (submitted) applied the model to simulate the SW-GW exchange in floodplain, the influence of flooding and biogeochemical cycling in the floodplain. As physical based models, the limitations of these models are long computation time and detail input information when apply to a large spatial scale.

Loague and VanderKwaak (2004) and Kollet and Maxwell (2006) reviewed the models that coupled surface and subsurface domains. Hussein and Schwartz (2003) developed FSTREAM model to simulate the water and contaminant transport between surface water and subsurface water systems. It coupled the aquifer model FTWORK with a 1D river water dynamic equation. A 2D model-2SWEM (Surface-Subsurface Water Exchange Model) model is developed by Peyrard et al. (2008) to simulate the water exchange between river and floodplain, horizontal 2D Saint-Venant equations for river flow and a 2D Dupuit equation for aquifer flow were coupled in the model to simulate the dynamic variation of HZ water level. Like the physically based model, the long computation time of this type of models prevent the application at large spatial and temporal scale.

Hydrologic process are simulated firstly, modules present biogeochemical processes are then coupled with the hydrologic part. Boano et al. (2010) simulated the hyporheic flow in the meander that induced by the river sinuosity, the main biogeochemical reactions of organic carbon degradation was included in the model. Gomez et al. (2012) simulated the biogeochemical zonation patterns with the concept of biogeochemical timescales. Denitrifying process in the hyporheic zones were simulated also. Zarnetske et al. (2012) integrated residence time model with a multiple Monod kinetics model that simulate the concentrations of oxygen ($O_2$), ammonium ($NH_4^+$), nitrate ($NO_3^-$) and dissolved organic carbon (DOC). Sheibley et al. (2003) simulated nitrification and denitrification process in sediment perfusion cores from the hyporheic zone. In 2SWEM model, the model NEMIS was coupled into the model to simulate the denitrification process in the floodplain hyporheic zone (Peyrard, 2008). Most of the denitrification models could only be applied at local scale, the

model that simulated the nitrate attenuation process in the hyporheic zone with few input data at catchment scale still does not exist.

#### 2.3.1.2 Riparian zone models and denitrification

The functions of riparian zone were simulated in many studies (Chen and MacQuarrie, 2004; Pinay and Decamps, 1988; Smart et al., 2001). The riparian ecosystem management model (REMM) is the model developed as a tool to help make decisions on management of riparian buffers to control nonpoint source pollution (Lowrance et al., 2000). In the REMM model, the riparian zone system consisting of three zones parallel to the stream: the forest zone located near to the stream, the woody vegetation zone adjacent to the forest zone, and the herbaceous zone located in the out layer of the buffer zone. The processes simulated in REMM model include surface and subsurface water movement and storage, sediment transport and deposition, nutrients (carbon, nitrogen, phosphorus) transport and cycling and vegetative growth, denitrification function is included in the model. In REMM model, the processes simulated are all in soil layers, the shallow groundwater processes are not included and the exchange between surface water and subsurface water is not taken into account.

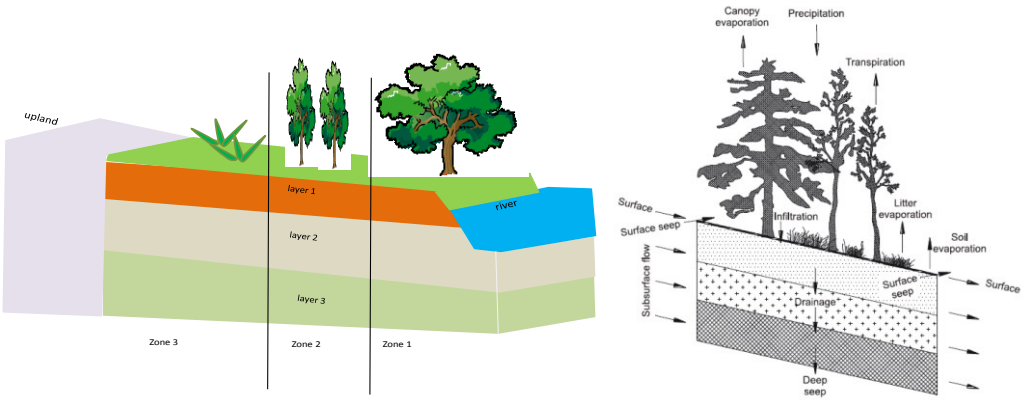


Figure 6. The main components and the main hydrologic processes of REMM model (extracted from Altier et al., (2005).

### 2.3.2 Catchment scale model and denitrification

The sedimentation function, and the material attached on the sediment (phosphorus, metals and pesticides) of floodplain at catchment scale were studied. However, the influence of floodplain on biogeochemical cycling at catchment scale was rarely quantified. The influences of riparian zones on biogeochemical cycling at catchment scale were considered by several model, like RNM (Riparian Nitrogen Model) model, SWIM (Soil and Water Integrated Model) model and SWAT model.

RNM model was developed to simulate nitrate removal from groundwater and surface water through denitrification as they interact with riparian zone soil at catchment scale. Based on stream order, the model operates at two conceptual levels: ephemeral low order streams and perennial middle order streams (Rassam et al., 2005, 2008). In RNM model, denitrification was assumed occur only in root zone. SWIM model is a watershed scale model that was developed for hydrological and water quality modelling in mesoscale watersheds (Krysanova et al., 1998). Hattermann et al. (2006) added the wetland function in SWIM model, in which the influence of plant uptake and denitrification in the riparian zone on nitrogen cycling were included into the model. In SWIM model, the denitrification occurs in the shallow aquifer was represented as a decay rate. SWAT model is a basin-scale, semi-distributed model that was applied successfully all over the world (Fohrer et al., 2013; Jayakrishnan et al., 2005; Romanowicz et al., 2005). The functions of vegetative filter strip (VFS) is simulated in SWAT model, however, like other catchment model, SW-GW exchange and denitrification occurred in the shallow aquifer are not included in the model. To represent the hydrologic role of riparian zone, Liu et al. (2008) developed a module to simulate the hydrologic and sediment storage function of the riparian zone in SWAT model. Nevertheless the transport of dissolved materials and denitrification occurred in the shallow aquifer were not included in the modified SWAT model. Nguyen et al. (2013) added a low slope strip to represent the riparian zone and integrated RNM model into the low slope zone to simulate the denitrification occurred in this region. To reflect the hydrologic connection between upslope and downslope parts of a landscape, a catena approach including divide, hillslope and floodplain landscape units has been developed and included in SWAT (Volk et al., 2007; Arnold et al., 2010, Rathjens et al., 2015). The catena approach in the modified model (SWAT-LU) represents an effort to impose a systematic upscaling from a topographic position to a watershed scale. Within the catena, a more detailed downslope routing of surface runoff, lateral flow and groundwater can be accomplished, and the impact of upslope management on downslope landscape positions can be assessed (Arnold et al., 2010; Bosch et al., 2010). However, the hydrologic processes are still single track in SWAT-LU and the function of two direction SW-GW exchange is not included and shallow aquifer denitrification function still is not represented.

## 2.4 Objective

Nitrate pollution is a critical issue in agricultural catchments, and groundwater was proved a main contributor of the pollution. Denitrification was found play an important role in nitrate

pollution control and the importance of denitrificaiotn occurred in both the river bank riparian zone and beneath HZ on nitrate attenuation has been highlighted. The influence of SW-GW exchange through both flooding and underneath lateral flow on the biogeochemical cycling in the river-floodplain systems was demonstrated in a lot of studies. However the contribution of connected floodplain area on river water nitrate control at the catchment scale has never been quantified. Hence, an understanding of the processes occurring in the surface-groundwater interface could offer considerable insight for the purposes of water management at catchment scale.

Modelling is an efficient role to study the hydrologic and biogeochemical cycling at large spatial and long temporal scale. However most of the models that simulate the hydrologic and denitrifying processes in the river-floodplain systems are physical based model, which would be difficult to be applied at large catchment. Moreover, rare of the models developed for large scale application considered the influence of SW-GW exchange on biogeochemical cycling. SWAT is a physically-based, deterministic, continuous, watershed-scale simulation model allowing a number of different physical processes to be simulated in a watershed. Studies have been carried out to simulate nitrate pollution on a catchment scale with SWAT (Boithias et al., 2014; Cerro et al., 2014; Ferrant et al., 2013, 2011). However, the simulation of the two-direction water exchange between river and groundwater occurring in the floodplain and the denitrification occurs in the floodplain shallow aquifer has not been simulated in the SWAT model.

The objectives of this thesis are: 1) quantifying the exchanged SW-GW volume in the floodplain area at the catchment scale with modified SWAT model and 2) quantifying the shallow aquifer denitrification rate in the floodplain area at the catchment scale and evaluate its influence on the river nitrate flux.

# Chapter 3. Material and methods.

This chapter describes materials and methods used to achieve the objectives. The methods include an overview of hydrologic, nitrogen and organic carbon cycling processes simulated in the initial SWAT model and the description of the development of the new modules that simulated surface water and groundwater exchange, the influence of flooding on surface and ground water levels and denitrification occurs in the shallow aquifer of floodplain. The materials main focus on the description of study sites (Garonne watershed, middle floodplain of the Garonne basin and Monbéqui study site) and the field sampling and laboratory analyse methods of the measured physico-chemical elements. These study sites are used to test the modules at different spatial and temporal scales.

## 3.1 Initial SWAT model

SWAT model is a basin-scale, physical based, semi-distributed, and continuous-time model that operates on a daily time step. SWAT is designed to predict the impact of management on water, sediment, and agricultural chemical yields in ungauged watersheds (Arnold et al., 1998). The model is computationally efficient, and capable of continuous simulation over long time periods. Major model components include weather, hydrology, soil temperature, plant growth, nutrients, pesticides, and land management. In SWAT, a watershed is divided into multiple subwatersheds, which are then further subdivided into Hydrologic Response Units (HRUs) that consists of homogeneous land use, management, and soil characteristics. The HRUs represent percentages of the subwatershed area and are not identified spatially within a SWAT simulation. Alternatively, a watershed can be subdivided into only subwatersheds that are characterized by dominant land use, soil type, and slope. Two main dominants in SWAT model were simulated: land (HRU) and channel, hydrologic elements and dissolved and particulate matters in the HRUs are summed and flow into the river channel (Neitsch et al., 2009).

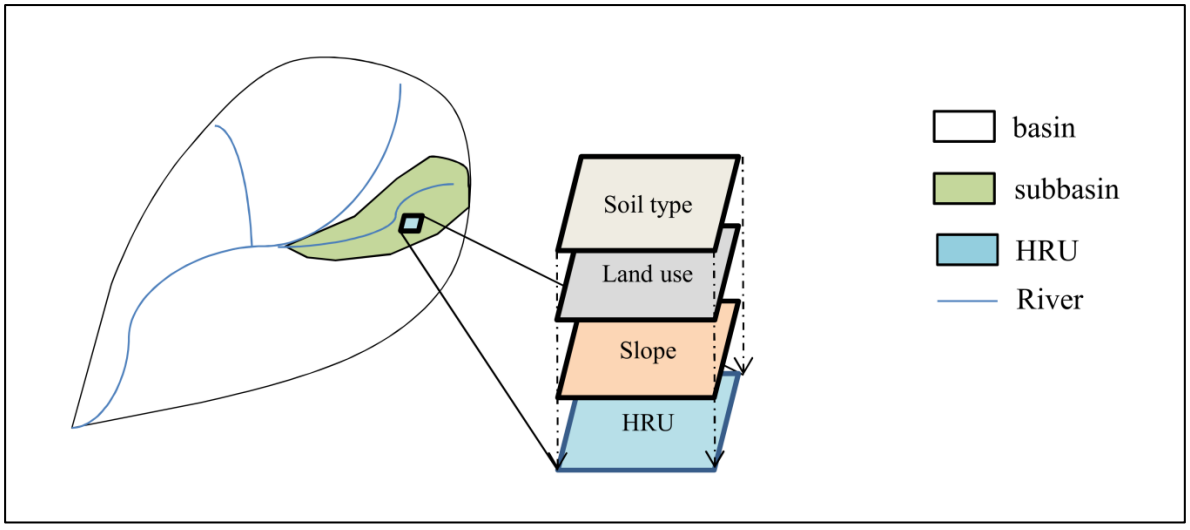


Figure 7. The structure of the SWAT model and the definition of HRU (Hydrologic Response Unit).

### 3.1.1 Hydrology in SWAT model

The simulated hydrologic processes in the two dominants (land (HRU) and channel) are as follows:

#### 3.1.1.1 The hydrologic processes in HRU

The hydrologic cycle in the soil phase is based on the water balance equation:

$$SW_t = SW_0 + \sum_{i=1}^{t}(R_{day} - Q_{surf} - E_A - w_{seep} - Q_{gw})$$

Where $SW_t$ is the final soil water content (mm $H_2O$), $SW_0$ is the initial soil water content (mm $H_2O$), t is the time (days), $R_{day}$ is the amount of precipitation on day i (mm $H_2O$), $Q_{surf}$ is the amount of surface water flow on day i (mm $H_2O$), $E_A$ is the amount of evaporation on day i (mm $H_2O$), $w_{seep}$ is the amount of percolation and bypass flow exiting the soil profile bottom on day i (mm $H_2O$), $Q_{gw}$ is the amount of return flow on day i (mm $H_2O$).

The hydrologic processes in the initial SWAT model are shown in Figure 8.

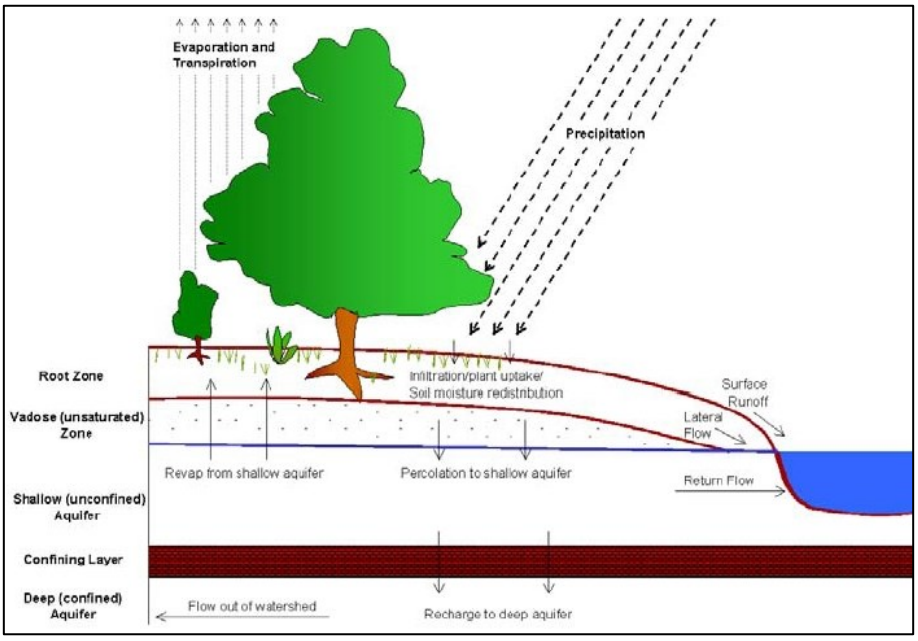


Figure 8. hydrologic processes in the initial SWAT model (extracted from Neitsch *et al.*, 2009)

In SWAT model, two methods were provided for estimating surface flow: SCS curve number procedure and the Green & Ampt infiltration method. For the estimation of potential evapotranspiration (PET), three methods have been incorporated into SWAT: the Penman-Monteith method, the Priestley-Taylor method and the Hargreaves method. For the lateral flow in the soil profile, SWAT incorporated a kinematic storage model developed by summarized by Sloan and Moore (1984). The detailed discripition about those methods could be found in Neitsch *et al.* (2009).

The groundwater flow in initial SWAT model is calculated as follows:

$$Q_{gw,i} = Q_{gw,i-1} \times exp[-\partial_{gw} \times \Delta t] + w_{rchrg,sh} \times (1 - exp[-\partial_{gw} \times \Delta t]) \qquad \text{If } aq_{sh} > aq_{shthr,q}$$

$Q_{gw,i} = 0$ If $aq_{sh} < aq_{shthr,q}$

Where $Q_{gw,i}$ is the groundwater flow into the main channel on day i (mm $H_2O$), $Q_{gw,i-1}$ is the groundwater flow into the main channel on day i-1 (mm $H_2O$), $\partial_{gw}$ is the base flow recession constant, $\Delta t$ is the time step (1 day), $w_{rchrg,sh}$ is the amount of recharge entering the shallow aquifer on day i (mm $H_2O$), $aq_{sh}$ is the amount of water stored in the shallow aquifer at the beginning of day i (mm $H_2O$), $aq_{shthr,q}$ is the threshold water level in the shallow aquifer for groundwater contribution to the main channel to occur (mm $H_2O$).

#### 3.1.1.2 The hydrologic processes in the channel

The water balance in the channel is as follows:

$$V_{stored,2} = V_{stored,1} + V_{in} - V_{out} - tloss - E_{ch} + div + V_{bnk}$$

Where $V_{stored,2}$ is the volume of water in the reach at the end of time step ($m^3$ $H_2O$), $V_{stored,1}$ is the volume of water in the reach at the beginning of time step ($m^3$ $H_2O$), $V_{in}$ is the volume of water flowing into the channel during the time step ($m^3$ $H_2O$), $V_{out}$ is the volume of water flowing out of the channel during the time step ($m^3$ $H_2O$), $tloss$ is the volume of water lost from the reach via transmission through the bed ($m^3$ $H_2O$), $E_{ch}$ is the evaporation form the reach for the day ($m^3$ $H_2O$), $div$ is the volume of water added or removed from the reach for the day through diversion ($m^3$ $H_2O$), $V_{bnk}$ is the volume of water added to the reach via return flow from bank storage ($m^3$ $H_2O$).

Manning's equation was used to define the rate and velocity of flow. Two methods are incorporated in the SWAT model to calculate the water flow process in the channel, the two methods are the variable storage routing method and Muskingum river routing method. The detailed description of the two methods could be found in Neitsch *et al.* (2009).

The water depth in the channel is calculated as follows:

$$ch_{dep} = \sqrt{\frac{A_{ch}}{z_{ch}} + \left(\frac{W_{btm}}{2 \times z_{ch}}\right)^2} - \frac{W_{btm}}{2 \times z_{ch}}$$

Where $ch_{dep}$ is the depth of water in the channel (m), $A_{ch}$ is the cross sectional area of flow in the channel ($m^2$), $W_{btm}$ is the bottom width of the channel (m), $z_{ch}$ is the inverse of the channel side slope.

Flood is also simulated in SWAT model. Flood occurs when the volume of water in the channel exceeds the maximum amount that can be held by the channel. During flooding, the bottom width of the floodplain is considered to be five times of the channel bank full width.

### 3.1.2 Nitrogen cycling in SWAT model

#### 3.1.2.1 The nitrogen cycling processes in HRU

SWAT separated soil nitrogen into two main pools: mineral N and organic N. The mineral nitrogen in the soil profile is separated into 2 pools, which are $NH_4^+$ and $NO_3^-$. For the organic N, two methods are applied in SWAT model to calculate the organic material cycling. The basic method considers organic nitrogen storage in 3 pools, which were fresh organic N, active humus and stable humus (Figure 9). While the new method considers that there is one pool for soil organic N and separate pools for residue and manure N. The pools are not separated into active and stable pools.

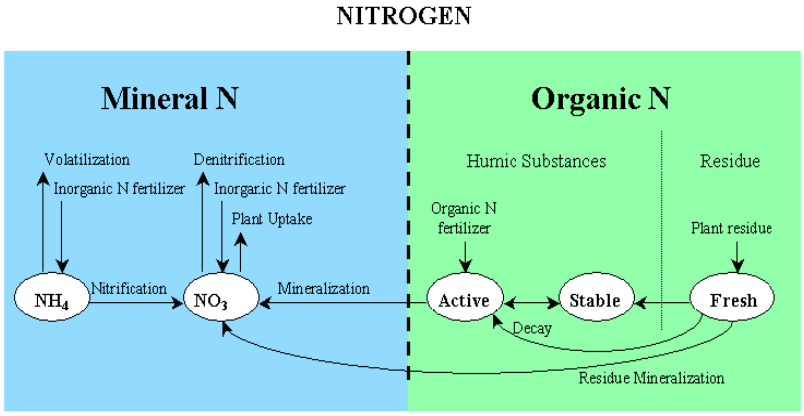


Figure 9. Simulated nitrogen cycling in the soil profile in the SWAT model (extracted from (Neitsch et al., 2009).

The growth cycles of plants were simulated, which was a simplified version of EPIC plant growth model. The management operations that control plant growth cycle like planting, harvest, tillage, fertilization application, pesticide application were applied in each HRU in SWAT model (Neitsch et al., 2009).

Nitrate cycling in the shallow aquifer was simulated in SWAT model. The main processes were uptake by plants, percolation from the soil profile, recharge to the deep aquifer, and flux into the main channel. A decay rate of nitrate in the shallow aquifer was also simulated (Neitsch et al., 2009). The recharge of nitrate from soil profile to aquifer layer was calculated as follow.

$$NO_{3_{rchrg,i}} = \left(1 - exp\left[-\frac{1}{\sigma_{gw}}\right]\right) \times NO_{3_{perc}} + exp\left[-\frac{1}{\sigma_{gw}}\right] \times NO_{3_{rchrg,i-1}}$$

Where $NO_{3_{rchrg,i}}$ is the amount of nitrate in recharge entering the aquifers on day i (kg N·ha$^{-1}$d$^{-1}$), $\sigma_{gw}$is the delay time or drainage time of the overlying geologic formations (days), $NO_{3_{perc}}$ is the total amount of nitrate exiting the bottom of the soil profile on day i (kg N·ha$^{-1}$d$^{-1}$), $NO_{3_{rchrg,i-1}}$ is the amount of nitrate in recharge entering the aquifers on day i-1 (kg N·ha$^{-1}$d$^{-1}$).

$$NO_{3_{sh,i}} = \frac{NO_{3_{sh,i-1}} + NO_{3_{rchrg,i}}}{aq_{sh,i} + Q_{gw} + w_{revap} + w_{rchrg,dp}} \times aq_{sh,i}$$

$$NO_{3_{gw}} = \frac{NO_{3_{sh,i-1}} + NO_{3_{rchrg,i}}}{aq_{sh,i} + Q_{gw} + w_{revap} + w_{rchrg,dp}} \times Q_{gw}$$

$$NO_{3_{revap}} = \frac{NO_{3_{sh,i-1}} + NO_{3_{rchrg,i}}}{aq_{sh,i} + Q_{gw} + w_{revap} + w_{rchrg,dp}} \times w_{revap}$$

$$NO_{3_{dp}} = \frac{NO_{3_{sh,i-1}} + NO_{3_{rchrg,i}}}{aq_{sh,i} + Q_{gw} + w_{revap} + w_{rchrg,dp}} \times w_{rchrg,dp}$$

Where $NO_{3_{sh,i}}$ is the amount of nitrate in the shallow aquifer on day i (kg N·ha$^{-1}$), $NO_{3_{sh,i-1}}$ is the amount of nitrate in the aquifer on day i-1 (kg N·ha$^{-1}$), $NO_{3_{gw}}$ is the amount of nitrate in groundwater flow from the shallow aquifer on day i (kg N·ha$^{-1}$), $NO_{3_{revap}}$ is the amount of nitrate in revap to the soil profile from the shallow aquifer on day i (kg N·ha$^{-1}$d$^{-1}$), $NO_{3_{dp}}$ is the amount of nitrate in recharge entering the deep aquifer on day i (kg N·ha$^{-1}$d$^{-1}$). $aq_{sh,i}$ is the amount of water stored in the aquifer on day i (kg N·ha$^{-1}$d$^{-1}$).

The nitrate decay in the shallow aquifer is calculated as follows:

$$NO_{3_{sh,t}} = NO_{3_{sh,o}} \times exp\left(-k_{NO_{3,sh}}\right)$$

Where $NO_{3_{sh,t}}$ is the amount of nitrate in the shallow aquifer at time t (kg N·ha$^{-1}$), $NO_{3_{sh,o}}$ is the initial amount of nitrate in the shallow aquifer (kg N·ha$^{-1}$), $k_{NO_{3,sh}}$ is the rate constant for removal of nitrate in the shallow aquifer (day$^{-1}$) and t is the time elapsed since the initial nitrate amount was determined (days).

The rate constant is related to half-life as follows:

$$t_{1/2,NO3,sh} = 0.693/k_{NO3,sh}$$

Where $t_{1/2,NO3,sh}$ is the half-life of nitrate in the shallow aquifer (days).

#### 3.1.2.2 The nitrogen cycling processes in the channel

The nitrogen cycling in the cycling is as follows:

$$\Delta NO_{3_{str}} = \left(\beta_{N,2} \times NO_{2_{str}} - \left(1 - fr_{NH_4} \times \alpha_1 \times \mu_a \times algae\right) \times TT\right)$$

Where $\Delta NO_{3_{str}}$ is the change in nitrate concentration (mg N·l$^{-1}$) on day i, $\beta_{N,2}$ is the rate constant for biological oxidation of nitrite to nitrate on day i-1 (day$^{-1}$), $NO_{2_{str}}$ is the nitrite concentration at the beginning of the day (mg N·l$^{-1}$), $fr_{NH_4}$ is the fraction of algal nitrogen uptake from ammonium pool, $\alpha_1$ is the fraction of algal biomass that is nitrogen (mg N·mg$^{-1}$ algae biomass), $\mu_a$ is the local growth rate of algae on day i-1 (day$^{-1}$), algae is the algal biomass concentration at the beginning of the day (mg algae·l$^{-1}$), TT is the flow travel time in the reach segment (day).

### 3.1.3 Organic Carbon in SWAT model

Like the organic N, two methods are applied in SWAT model to calculate the organic carbon content in the soil profile. The basic method is that the organic carbon in soil profile is read as input value. The new method is as follows:

There is one pool for soil organic C and separate pools for residue and manure C. The pools are not separated into active and stable pools.

$$\frac{dS_c}{dt} = h_R f_E k_R R_c + h_M f_E k_M M_c - k_S S_C$$

$$h_R = h_x \left(1 - (\frac{S_C}{S_{CC}})^{\alpha}\right)$$

$$h_x = 0.09(2 - e^{-5.5clay})$$

$$h_M = 1.6h_R$$

$$S_{CC} = S_{BD} Z_1 (0.021 + 0.038clay)$$

Where $S_C$ is the soil organic carbon content (kg·ha$^{-1}$), $R_c$ is the residue pool organic carbon content (kg·ha$^{-1}$), $M_c$ is the manure organic carbon content (kg·ha$^{-1}$), $h_R$ and $h_M$ are the residue and manure humification rates (kg·kg$^{-1}$), $k_S$ is the apparent organic matter decomposition rate (day$^{-1}$), $S_{CC}$ is the reference soil organic carbon content (kg·ha$^{-1}$), when $Sc = Scc$, the humification is 0, clay is the soil layer clay fraction (kg clay·kg$^{-1}$ dry soil), $S_{BD}$ is the soil layer

bulk density (kg·m$^{-3}$), $Z_1$ is the soil layer thickness (m), $\alpha$ is a constant value that modulates the response of the humification of the current $S_C$.

The organic carbon in shallow aquifer is not simulated in SWAT model.

### 3.1.4 Denitrification in SWAT model

Denitrification in the soil profiles is simulated in SWAT model:

$$N_{denit,ly} = NO_{3,ly} \times \left(1 - exp\left[-\beta_{denit} \times \gamma_{tmp,ly} \times orgC_{ly}\right]\right) \quad \text{If } \gamma_{sw,ly} \geq \gamma_{sw,thr}$$

$$N_{denit,ly} = 0 \quad \text{If } \gamma_{sw,ly} < \gamma_{sw,thr}$$

Where $N_{denit,ly}$ is the denitrification rate (kg N·ha$^{-1}$), $NO_{3,ly}$ is the amount of nitrate in layer $ly$ (kg N·ha$^{-1}$), $\beta_{denit}$ is the rate coefficient for denitrification, $\gamma_{tmp,ly}$ is the nutrient cycling temperature factor for layer $ly$, $\gamma_{sw,ly}$ is the nutrient cycling water factor for layer $ly$, $orgC_{ly}$ is the amount of organic carbon in the layer (%), $\gamma_{sw,thr}$ is the threshold value of nutrient cycling water factor for denitrification to occur.

$$\gamma_{tmp,ly} = 0.9 \times \frac{T_{soil,ly}}{T_{soil,ly} + exp\left[9.93 - 0.312 \times T_{soil,ly}\right]} + 0.1$$

Where $T_{soil,ly}$ is the temperature for layer $ly$ (°C). $\gamma_{tmp,ly}$ is never allow to fall below 0.1.

$$\gamma_{sw,ly} = \frac{SW_{ly}}{FC_{ly}}$$

Where $SW_{ly}$ is the water content of layer $ly$ on a given day (mm $H_2O$), $FC_{ly}$ is the water content of layer $ly$ at field capacity (mm $H_2O$). $\gamma_{sw,ly}$ is never allowed to fall below 0.05.

## 3.2 From SWAT to SWAT-LUD

In the HRU delineation method of the usual SWAT model, flow is summed at the subbasin scale and not routed across the landscape. To reflect the hydrologic connection between upslope and downslope parts of a landscape, a new structure called landscape unit (LU) was developed. LU represents additional unit that takes place between a subbasin and an HRU. The modified model called SWAT-LU. A catena approach including divide, hillslope and floodplain LUs has been developed and included in SWAT and multiple HRUs based on soil and land use are distributed across the different LUs (Volk *et al.*, 2007; Arnold *et al.*, 2010, Rathjens *et al.*, 2015). Processes in each HRU were still computed separately, but instead of being summed at the subbasin scale, they were summed at the LU scale (Figure

10). Surface runoff, lateral and groundwater flow from the divide were routed through the hillslope to the valley bottom and then entered the river.

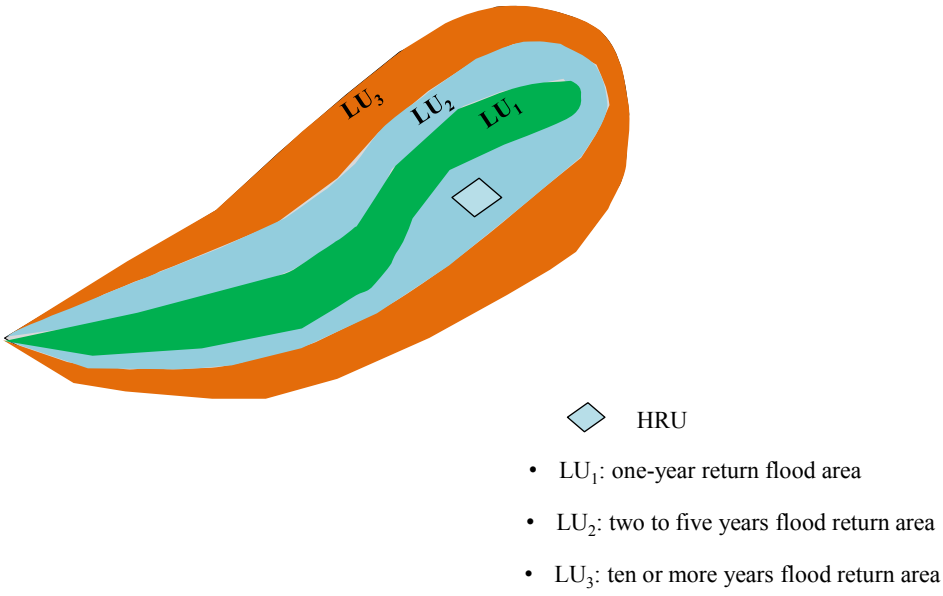


Figure 10. Distribution of LU and HRU in one subbasin

The hydrologic processes were still single tracks in SWAT-LU and the SW-GW exchanges function in both directions was not included. Furthermore, the flooded distance during flooding events was fixed at five times the width of the top channel and the influence of flooding on groundwater levels is not taken into account. To represent the SW-GW exchanges occurring in the alluvial plain, a new type of subbasin called subbasin-LU was developed. Subbasin-LU corresponds to the subbasin delimited by the floodplain and the LU structure was applied in subbasin-LU. Darcy's equation was applied to calculate the SW-GW exchange. Processes in the upland area of floodplain were calculated according to the original SWAT model. Processes were simulated for each HRU and aggregated to the river. Upland and subbasin-LU were connected through the river. The modified model was called SWAT-LUD. The evolution of SWAT model and the main modifications are shown in Figure 11.

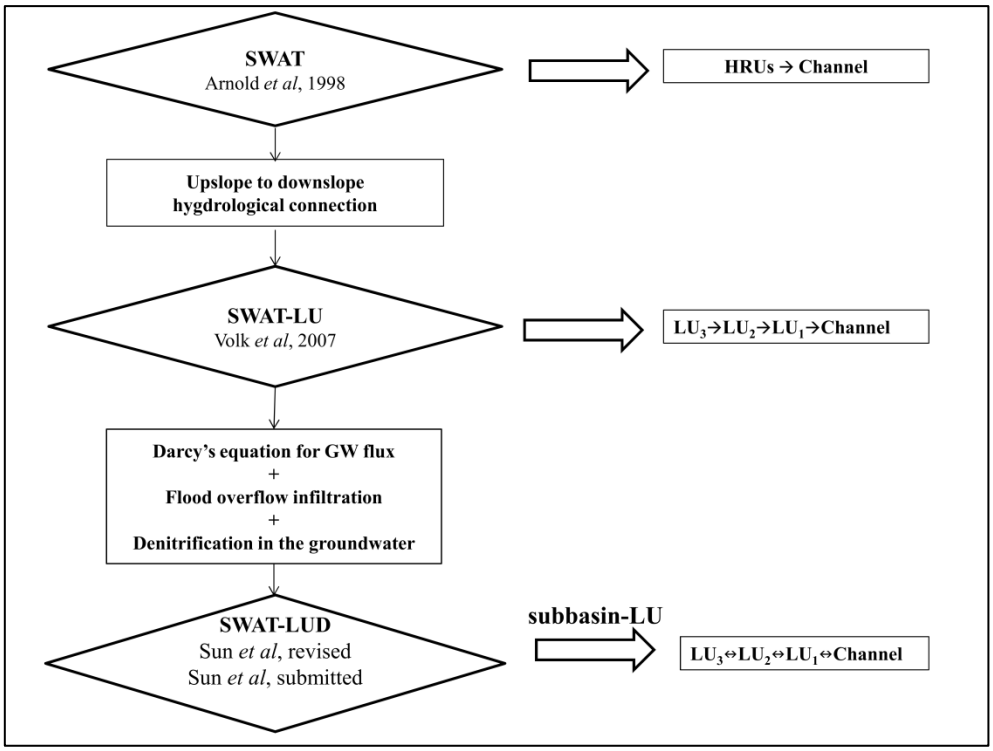


Figure 11. The evolution of SWAT model, from initial SWAT to SWAT-LUD.

### 3.2.1 SWAT-LU model

The catena approach in the SWAT-LU represents an effort to impose a systematic upscaling from a topographic position to a watershed scale. Within the catena, a more detailed downslope routing of surface runoff, lateral flow and groundwater can be accomplished, and the impact of upslope management on downslope landscape positions can be assessed (Arnold et al., 2010; Bosch et al., 2010). The hydrologic processes in SWAT-LU are shown in Figure 12.

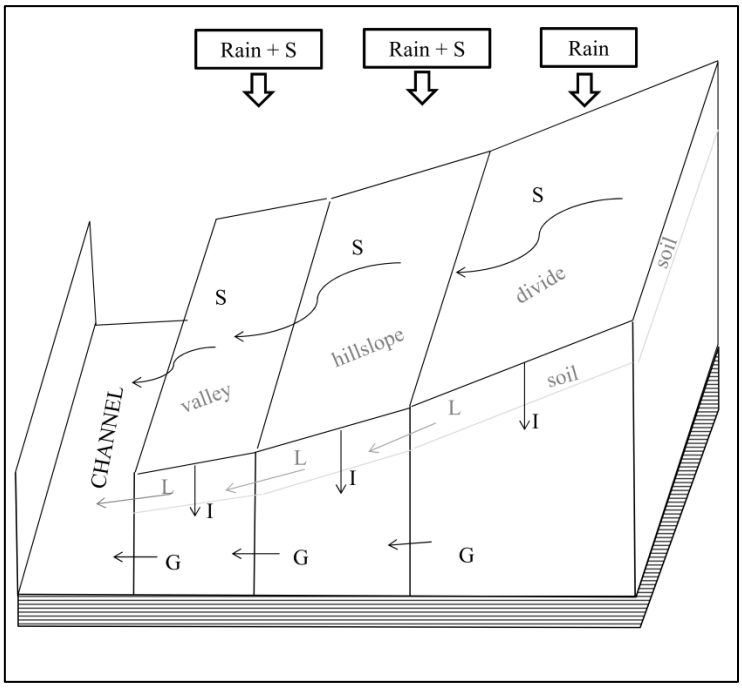


Figure 12. Hydrologic processes in the SWAT-LU model, where 'S' is surface flow, 'L' is lateral flow, 'I' is infiltration, 'G' is groundwater flow (adapted from Volk *et al.*, 2007 and Arnold *et al.*, 2010).

The calculation of hydrologic processes in HRU is kept as in SWAT model, but instead of summed at subbasin scale, the flows are summed at LU scale. For the surface runoff, it is accumulated in LU and then flow to the adjacent down slope LU. The surface runoff from the upward LU is calculated as the rainfall input, it would infiltrate into the unsaturated soil profile. The lateral runoff in the soil profile is simulated like the surface runoff, the lateral flow from the adjacent up slope LU would infiltrate into the unsaturated soil profile firstly before flow to the adjacent down slope LU. The shallow groundwater flow in SWAT-LU is simulated as routing through a series of linear storage elements. Infiltrated water from soil profile in each LU added to the groundwater storage pools. The accumulated surface, lateral and groundwater flow in the floodplain flow to the river channel. More detail description of SWAT-LU model could be found in Volk et al. (2007) and Arnold et al. (2010).

### 3.2.2 SWAT-LUD model

To represent the SW-GW exchange occurs in the floodplain, a new type of subbain, called subbasin-LU, was created and integrated into the original SWAT model. The LU structure was applied in the subbasin-LU. The surface runoff and lateral flow calculation were kept as in SWAT-LU model. Darcy's equation was applied to calculate groundwater flow between the LUs and water exchanges between the river and the aquifer. The algorithms of river water and groundwater levels during flooding events were modified. Moreover, the transfer of

dissolved parameters along with the SW-GW exchange and groundwater flow was introduced to the model and the denitrification function occurred in the shallow aquifer of floodplain was added to the model. The modified model was called SWAT-LUD and the detailed description could be found in the following sections.

#### 3.2.2.1 Subbasin-LU

The subbasin-LU was applied at floodplain area. Since alluvial soils are generally associated with floodplains, the distribution of floodplain was considered to be the same as the alluvial soil. The original subbasin that holds alluvial soil was separated into two subbasins: subbasin-LU and classic subbasin. Based on the soil types, the HRUs were divided into two groups: HRUs with the alluvial soil called alluvial HRU and HRUs without alluvial soil called no-alluvial HRU. The subbasin-LU was composed by the alluvial HRUs except alluvial HRUs with urban land cover, and the classic subbasin was composed by the no-alluvial HRUs and the urban alluvial HRU (Figure 13).

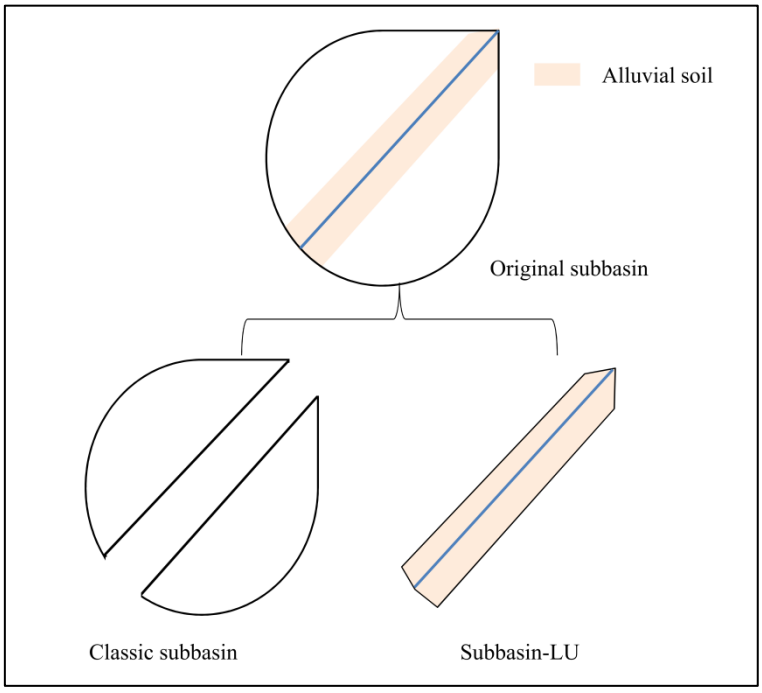


Figure 13. Locations of subbasin-LU and classic subbasin

#### 3.2.2.2 Landscape Unit in SWAT-LUD

In SWAT-LUD model, LUs were considered located parallel to the channel and were defined by their widths and slopes. As in SWAT-LU model, three LUs were applied in each subbasin-LU, which correspondence to the different flood return area. The definition of the widths of LUs was made according to the surface of floodplain covered by the flood return

period: $LU_1$ represented the one-year return flood area, $LU_2$ represented the two to five-year return flood area and $LU_3$ corresponded to the ten or more years return flood area. As LUs were located on both sides of the channel, the width of each side of LU was half its total width. All three LUs in one subbasin were considered as being of the same length, which was the length of the channel. The length was defined based on the river's hydromorphological structure. With the catena method, surface runoff and lateral flow from $LU_3$ (which was furthest from the channel) were routed through $LU_2$ to $LU_1$ (which was nearest to the channel) and then entered the channel (Figure 14). Groundwater flow was calculated with Darcy's equation which was introduced in 3.2.2.5. The location of LU and the hydrologic processes in SWAT-LUD are shown in Figure 13.

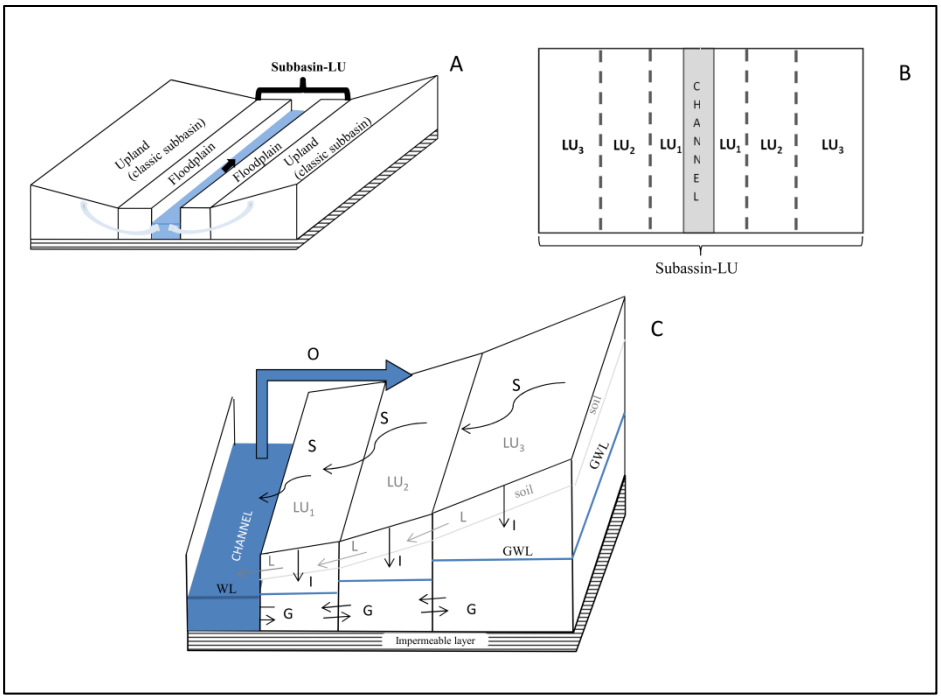


Figure 14. The locations of LUs in the subbasin-LU and the hydrologic processes of SWAT-LUD model. 'A' represents the location of subbasin-LU, 'B' represents subbasin-LU, and 'C' represents the hydrologic processes in the landscape units where 'S' is surface flow, 'L' is lateral flow, 'I' is infiltration, 'G' is groundwater flow, 'O' is overbank flow, 'GWL' is groundwater level and 'WL' is river water level.

#### 3.2.2.3 Distribution of HRUs in LUs

Alluvial HRUs (except urban alluvial HRUs) in the subbasin-LU were simplified into three groups based on their land use type: forest alluvial HRU (F-HRU), pasture alluvial HRU (P-HRU) and agricultural alluvial HRU (A-HRU). The alluvial HRUs with land cover of all types of forest were integrated to be an F-HRU. The characters of the F-HRU were considered to be the same as the largest forest alluvial HRU before the integration. The alluvial HRUs

with pasture land cover or land types similar to the characters of pasture (like orchard or vineyard) were integrated to be a P-HRU, and the alluvial HRUs with agriculture land use were integrated to be an A-HRU. The characters of these two HRUs were chosen with the same method for the F-HRU, taken the characters of the largest HRU before the integration.

Since the general natural distribution of land use in alluvial area is characterized by the succession of riparian forest, pasture and agriculture as the increase of the distance from the river. Based on this succession of land use, the distribution of HRUs into LUs was as follows: Firstly, F-HRU was assigned into $LU_1$. If the area of the F-HRU is larger than $LU_1$, the F-HRU was separated into two HRUs, one corresponding to the area of $LU_1$ and another to the remaining area. If the area of the F-HRU is smaller than $LU_1$, then all F-HRU was assigned into $LU_1$, and the empty area in $LU_1$ was completed by P-HRU. In this case, if the P-HRU area is bigger than the empty area in $LU_1$, the P-HRU was then separated into two HRUs, one corresponding to the area of the empty area in $LU_1$, another one to the remaining area. If P-HRU is smaller than the empty area in $LU_1$, then all the P-HRU was assigned into $LU_1$ and the empty area in $LU_1$ was completed by A-HRU. In this condition, A-HRU was divided into 2 HRUs. The same method was applied to distribute HRUs into $LU_2$ and $LU_3$. All the HRUs of the same type have the same characters.

#### 3.2.2.4 Create-LU tool

A Fortran subroutine called Create-LU was developed to separate classic subbaisn and subbasin-LU, the parameters of LUs in the subbasin-LUs and the distribution of alluvial HURs into LUs were done with this tool also. The algorithm includes different steps which are: 1) Reading output files from initial SWAT project; 2) Defining LUs according to flooded area for different return periods; 3) distributing alluvial HRUs into LUs based on their land use and slope.

#### 3.2.2.5 Hydrologic connection between classic subbasin, subbasin-LU and channel

The hydrologic connection between classic subbasin, subbasin-LU and channel is shown in Figure 15. In the classic subbasin, surface, lateral and groundwater flow calculated in the HRUs are then summed and flowed to the channel. In the subbasin-LU, surface and lateral flow from $LU_3$ routed through $LU_2$ to $LU_1$ and then enter the channel. The groundwater exchanged between LUs and between $LU_1$ and the channel.

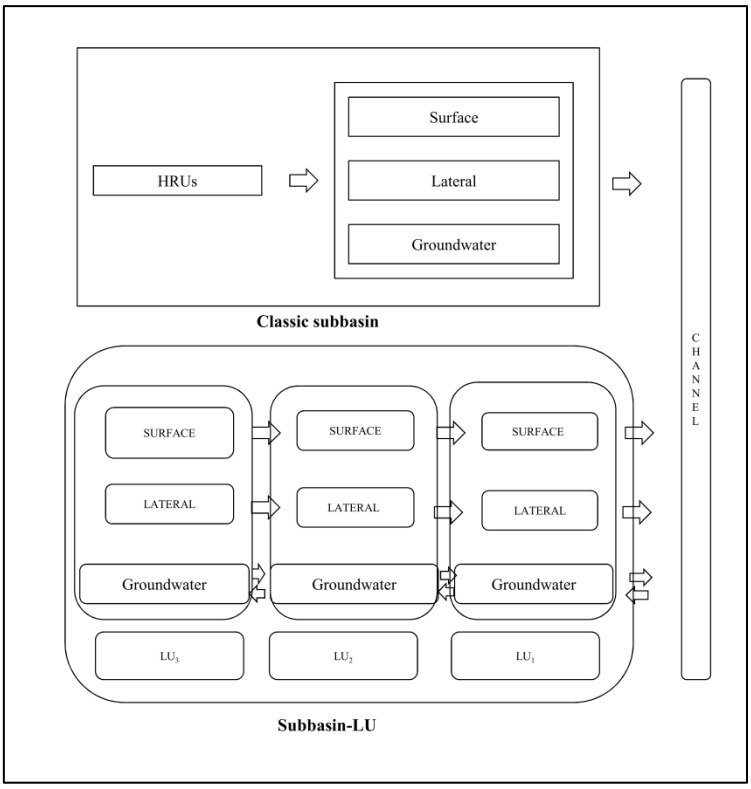


Figure 15. The hydrologic connection between classic subbasin and subbasin-LU

#### 3.2.2.6 SW-GW interaction with LU structure

Each LU was considered has a unique groundwater level, all the HRUs in the same LU have the same groundwater level. The groundwater levels in LUs were calculated as follows:

$$GH = GM \times p/LA$$

$$GM = GM + I - E - D$$

Where GH is the groundwater height in LU (m), GM is the groundwater volume in LU ($m^3$), $p$ is the porosity of shallow aquifer (%), LA is the surface area of LU ($m^2$), I is the infiltrated water volume from soil profile ($m^3$), E is the evaporated water volume from shallow aquifer ($m^3$), D is the water volume infiltrated to the deep aquifer ($m^3$). The calculation of I, E and D were kept as in SWAT model.

The altitude of the river bed in each subbasin was assumed to be the referenced value of the hydraulic head used to compute groundwater and surface water levels. HRUs were assumed to be homogeneous inside, with no additional differentiation in soil and material underneath, and lateral flow and the infiltration from soil profile was stopped when groundwater reach the soil profile.

Darcy's equation was applied to calculate groundwater flow between the LUs and water exchanges between the river and to calculate groundwater flow between the LUs and water exchanges between the river and the aquifer.

$$Q = K \times A \times \frac{\Delta H}{L}$$

where Q is water flow ($m^3.d^{-1}$), A is the cross-sectional area between two units ($m^2$), K is saturated hydraulic conductivity ($m.d^{-1}$), ΔH is hydraulic head difference between two units (m) and L is the distance between two units through which the water is routed (m).

As the river is filled by water, two implementations of Darcy's equation were required:

1) groundwater flow between two LUs:

$$K = \frac{(K_{lua} \times W_{lua}) + (K_{lub} \times W_{lub})}{(W_{lua} + W_{lub})}$$

$$W = (W_{lua} + W_{lub})/4$$

$$Q = 2 \times K \times A \times \frac{(H_{lua} - H_{lub})}{W}$$

where K represents the averaged hydraulic conductivity values of the two LUs ($K_{lua}$, $K_{lub}$) based on their widths ($m.d^{-1}$), $W_{lua}$ and $W_{lub}$ are the widths of the two LUs (m), $H_{lua}$ and $H_{lub}$ are the hydraulic heads of the two LUs (m), W is the distance between the centres of these two LUs on one side of channel. Since LUs located in two sides of the channel, each side got half of its width, W is a quarter of the total width of these two LUs (m). As groundwater flow occurs on both sides of the river, the flow was multiplied by two.

2) Groundwater flow between $LU_1$ and the river:

$$K = K_{lu}$$

$$W = (W_{lu})/4$$

$$Q = 2 \times K \times A \times \frac{(H_{lu} - H_{ch})}{W}$$

where K is the hydraulic conductivity value of $LU_1$ ($K_{lu}$) ($m.d^{-1}$); W is the quarter width of $LU_1$ ($W_{lu}$) (half of the width of one side of the channel) (m); and $H_{lu}$ and $H_{ch}$ are hydraulic heads of $LU_1$ and the river (m).

#### 3.2.2.7 Influence of flooding on surface water and groundwater level

The original algorithm for flooding events in the SWAT model only assumes that the flooded distance is five times the top channel width (Neitsch et al., 2009). The influence of floodplain geometry and the influence of flooded water on groundwater are not considered. The new algorithm was based on the water volume during a flood event:

$$U_f = (v - v_{max}) \times T$$

where $U_f$ is the flood volume ($m^3$), v is the discharge ($m^3s^{-1}$), $v_{max}$ is the maximum discharge value at which water could stay in the channel ($m^3s^{-1}$) and T is the travel time of water passing through the channel (s).

During a flood, the surface water level is the sum of the riverbank height and the water depth on the surface relative to the height of river bank:

$$A_f = L_{ch} * (W_{ch} + L_f)$$

$$H_{ch} = D_{ch} + \frac{U_f}{A_f}$$

where $A_f$ is the flooded area ($m^2$), $L_{ch}$ is the length of the channel (m), $W_{ch}$ is the width of the channel (m), $L_f$ is the flood distance on one side of the river bank (m), $H_{ch}$ is the surface water level and $D_{ch}$ is the height of the riverbank (m).

With regard to groundwater levels in the LUs during flood periods (if flood water arrives at a LU), the groundwater of this LU was assumed to be the same level as the surface water:

$$H_{luf} = H_{ch}$$

where $H_{luf}$ is the groundwater level of LU during the flood (m).

The infiltrated flood water was calculated as follows:

$$V_{in,f} = (H_{luf} - H_{lu}) \times A_{lu} \times p_{lu}$$

Where $V_{in,f}$ is the infiltrated flood water volume in LU ($m^3$), $A_{lu}$ is the surface area of the LU ($m^2$), $p_{lu}$ is the porosity of the LU (%).

The overbank flow would return back to the river the next day after flooding, and discharge of river water was recalculated:

$$IN = IN + U_f$$

$$v = IN/86400$$

Where $IN$ is the input water volume into the river ($m^3$).

#### 3.2.2.8 Transfer of dissolved elements

The transfer of dissolved elements between LUs and between LUs and surface water was calculated based on the water flow volume and concentration of the elements:

$$M_{lu} = M_{lu} + M_{in} - M_{out}$$

$$M_{in} = \sum(V_{in} * C_{in})$$

$$M_{out} = \sum(V_{out} * C_{lu})$$

$$C_{lu} = M_{lu}/V_{lu}$$

where $M_{lu}$ is the mass content of the element in LU (g), $M_{in}$ is the input mass (g), $M_{out}$ is the output mass (g). $V_{in}$ is input water volume ($m^3$), $C_{in}$ is the concentration of the elements in the input water ($mg \cdot l^{-1}$), $V_{out}$ is the output volume ($m^3$), $C_{lu}$ is the concentration of the element in calculated LU ($mg \cdot l^{-1}$) and $V_{lu}$ is the water volume storage in LU ($m^3$).

#### 3.2.2.9 Denitrification

The nitrate and organic carbon degradation equations of the saturated shallow aquifer zone in the study of Peyrard et al. (2011) were introduced into the SWAT-LUD model. The nitrate degradation is taken as denitrification, and the influences of both POC and DOC on denitrification were taken into account.

The denitrification rate was calculated as follows:

$$R_{NO_3} = -0.8(\rho \cdot (1-\varphi)/\varphi \cdot k_{POC}[POC] \cdot 10^6/M_c + k_{DOC}[DOC]) \cdot [NO_3]/(k_{NO_3} + [NO_3])$$

where $R_{NO_3}$ is the denitrification rate ($\mu mol \cdot l^{-1} \cdot d^{-1}$), $\rho$ is dry sediment density ($kg \cdot dm^{-3}$), $\varphi$ is sediment porosity, $k_{POC}$ is mineralisation rate constant of POC (particulate organic carbon) ($d^{-1}$), $POC$ is the POC content in the soil and aquifer sediment (‰), $M_c$ is carbon molar mass ($g \cdot mol^{-1}$), $DOC$ is the concentration of DOC in the aquifer water ($\mu mol \cdot l^{-1}$) $k_{DOC}$ is the mineralisation rate constant of DOC (dissolved organic carbon) ($d^{-1}$), $k_{NO_3}$ is half-saturation for nitrate limitation ($\mu mol \cdot l^{-1}$) and $NO_3$ is the nitrate concentration in the aquifer water ($\mu mol \cdot l^{-1}$).

#### 3.2.2.10 Nitrate leaching during flood period

On flood days, the portion of the nitrate storage in the soil profile was considered as having infiltrated into the aquifer along with infiltrated floodwater:

$$M_{NO_{3,i}} = M_{NO_{3,i-1}} + I_{NO_3,i}$$

$$I_{NO_{3,i}} = F_{NO_3} \times M_{NO_{3,soil,i}}$$

where $M_{NO_{3,i}}$ is the mass content of nitrate in the LU (g N-$NO_3^-$) on day i, $M_{NO_{3,i-1}}$ is the mass content of nitrate in the LU (g N-$NO_3^-$) on day i-1, $I_{NO_3}$ is the infiltrated nitrate from the soil profile into the aquifer during flood events on day i, $F_{NO_3}$ is the coefficient (%) and $M_{NO_{3,soil}}$ is the mass content of nitrate in the soil profile of LU (g N-$NO_3^-$) on day i.

#### 3.2.2.11 Organic carbon in SWAT-LUD

The flux and content of DOC was not simulated in the initial SWAT model. In the SWAT-LUD model, the flux of DOC in the shallow aquifer was included, which was simulated as a dissolved element such as nitrate. As the fluctuations of DOC were small in the aquifers of the region that far away from the river, the concentrations of DOC in $LU_2$ and $LU_3$ were assumed to be constant and the values were read as input values. DOC in the river water was assumed to be constant as well except during flood periods. As the concentration of DOC in the river water significantly increased during flooding days (Arango et al., 2007; Dalzell et al., 2005; Duan et al., 2007), a different value was given to the river water in flood periods. The DOC concentrations in $LU_1$ were calculated as the mixture of $LU_2$ and river water.

DOC could be consumed by denitrifying bacteria. The consumption rate was:

$$R_{DOC} = -k_{DOC}[DOC]$$

where $R_{DOC}$ is the DOC consumption rate ($\mu mol \cdot l^{-1} \cdot d^{-1}$).

In the SWAT model, the POC contents in the soil profiles were read as input values and were not simulated in the shallow aquifers. In the SWAT-LUD model, the POC contents in the top soil layers were considered higher than the others and the POC pools were separated into two parts: the top layer pool and the second layer pool. The POC content in the two pools was read as input values.

POC could be consumed by denitrifying bacteria as well. The consumption rate was:

$$R_{POC} = -k_{POC}[POC]$$

where $R_{POC}$ is the POC consumption rate ($‰ \cdot d^{-1}$)

## 3.3 Study site

### 3.3.1 The Garonne River

The Garonne River is the main river of the largest drainage basin in the southwest France, starting from Pyrenees mountains and flowing into the Atlantic Ocean. It is an eighth ordered river and the third longest river in France with the length of 525km and has a drainage area about 51500 $km^2$ at the last gauging station (Tonneins) (Figure 16). The basin includes most of the Aquitaine basin which is surrounded by the Massif Central mountain in the north-east, the Pyrenees mountains in the south and the Atlantic ocean in the west (Semhi et al., 2000).The climate of the Garonne watershed is impacted both by the Atlantic Ocean and Mediterranean sea. The average annual rainfall is about 900 mm (Caballero et al., 2007). The monthly temperatures ranged from 5°C in January to 20°C in July. The hydrology of the area is mainly influenced by the three places (Pyrenees Mountain, Massif Central and Atlantic ocean). The largest discharges occur twice a year, in the spring as a result of snow melt and in late autumn caused by intense rainfalls (Sánchez-Pérez et al., 2003). According to the data recorded at the Tonneins gauging station which is the last gauging station for the Garonne watershed, the mean annual discharge for the past 100 years (1913-2013) is around 600 $m^3 \cdot s^{-1}$. The highest is nearly 6000 $m^3 \cdot s^{-1}$ and the lowest around 80 $m^3 \cdot s^{-1}$. In a year, the mean higher discharge is in February (961 $m^3 \cdot s^{-1}$), and the lowest is found in August (176 $m^3 \cdot s^{-1}$) (Banque Hydro, http://www.hydro.eaufrance.fr/).

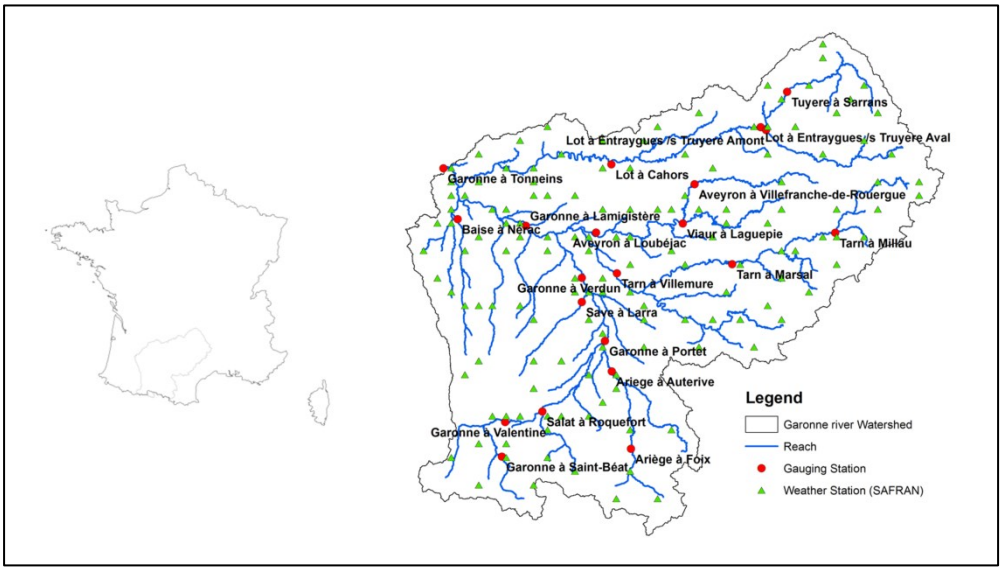


Figure 16. The location of the Garonne River and the gauging stations in the Garonne catchment

The main land use types in the Garonne watershed are pasture, agriculture and forest, which taken 34%, 31% and 19% of the total area respectively. The alluvial soil mainly exists in the Pyrenees area and Aquitaine basin, it occupied 5.8 % of the Garonne basin (Figure 15). The input data used to set up the SWAT model and the distribution of alluvial soil in the Garonne watershed are shown in Figure 17.

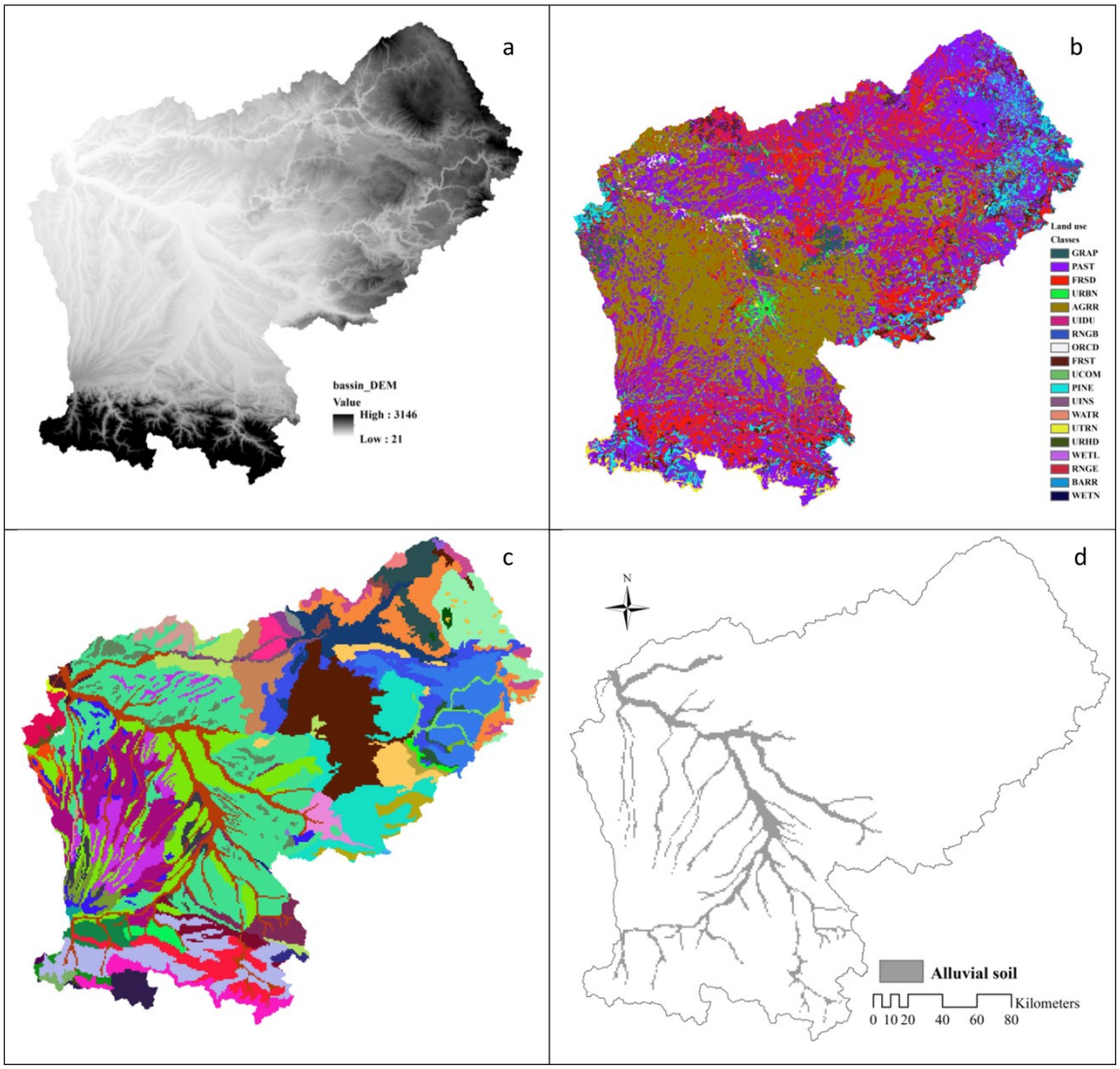


Figure 17. The input data of the SWAT model and the distribution of alluvial soil in the Garonne watershed, 'a' represents the DEM (Digital Elevation Model), 'b' represents the land use distribution, 'c' represents the soil type distribution (66 types of soil), and 'd' represents the location of alluvial soil in the Garonne watershed.

The sources of the input data are shown in Table 3.

Table 3. The sources of the input data of the SWAT Garonne project

| Data type | Data source | scale |
|---|---|---|
| DEM | NASA METI (ASTER, 2011) | Grid cell 90 m × 90m |
| Land use | Corine Land Cover (CLC, 2006) | 1:100 000 |
| Soil | European Soil Database (ESDB, 2006) | 1:1 000 000 |
| Climate | Météo-France | |

### 3.3.2 Floodplain area in the middle section of the Garonne River

The floodplain area in the middle Garonne River is locateed between Toulouse city and the confluence of the Tarn River (Figure 18). The floodplain widens up to 2 - 4 km. Between 4-7m of the coarse alluvium (sand and gravel) eroded from the Pyrenees Mountains during past glacial period deposited in the floodplain overlie impermeable molasse. The valley contains a classic flight of terraces that represent episodic bedrock valley deepening punctuated by lateral migration of deposition of sediments (Lancaster, 2005). A series of terraces exist in the floodplain, in which the high terrace delimited the floodplain. The middle terrace is cultivated and is rarely flooded (every 30–50 years), which has a width of about 2 km. The lower terrace with the width of a few hundred is devoted to poplar plantations, is flooded about every 5 years. The riparian zone has a width of 10-100m, and is flooded almost each year (Peyrard et al., 2008). The common natural riparian vegetation types found along this reach of the Garonne River include willow and ash (Pinay et al., 1998). The floodplain is heavily cultivated, high production of corn, sunflower and sorghum were sustained by fertilization and irrigation. Shallow aquifer has a common nitrate concentration of 50 - 100 $mg\cdot L^{-1}$ (Pinay et al., 1998; Sánchez-Pérez et al., 2003). The around region of the floodplain is heavily cultivated also, the agriculture land use occupied 72% of the floodplain watershed (Figure 19).

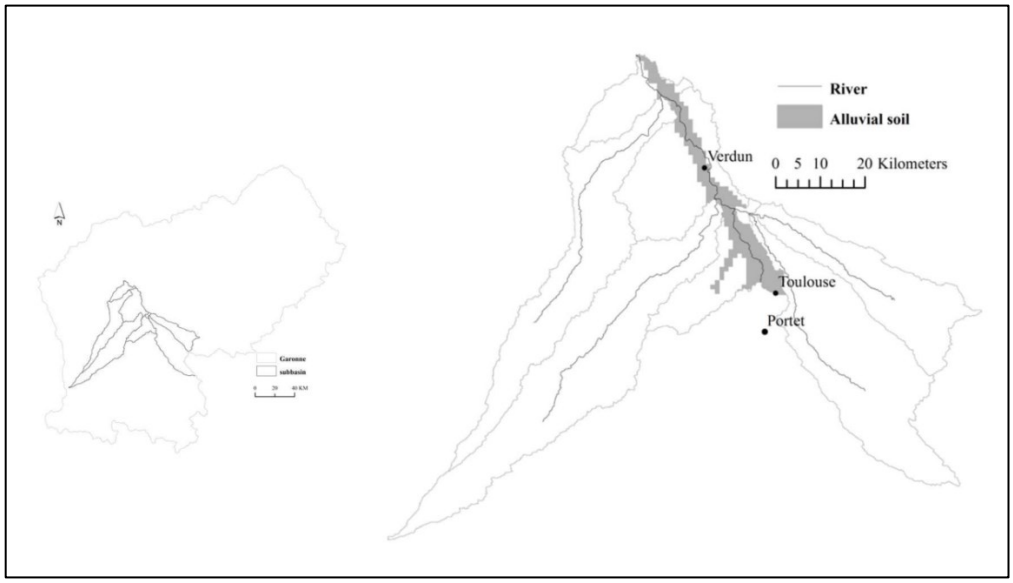


Figure 18. Location of the floodplain area of the middle section the Garonne River and the distribution of the alluvial soil along with the main channel

The channel is a meandering, single-thread channel, is around 85 km long. In the past, the Garonne River was incised as a result of mining of gravel and cobble from the riverbed (Beaudelin 1989). The longitudinal gradient is around 0.001 with a mean coefficient of sinuosity of 1.3. Portet gauging station located at about 10 km downstream of Toulouse city.

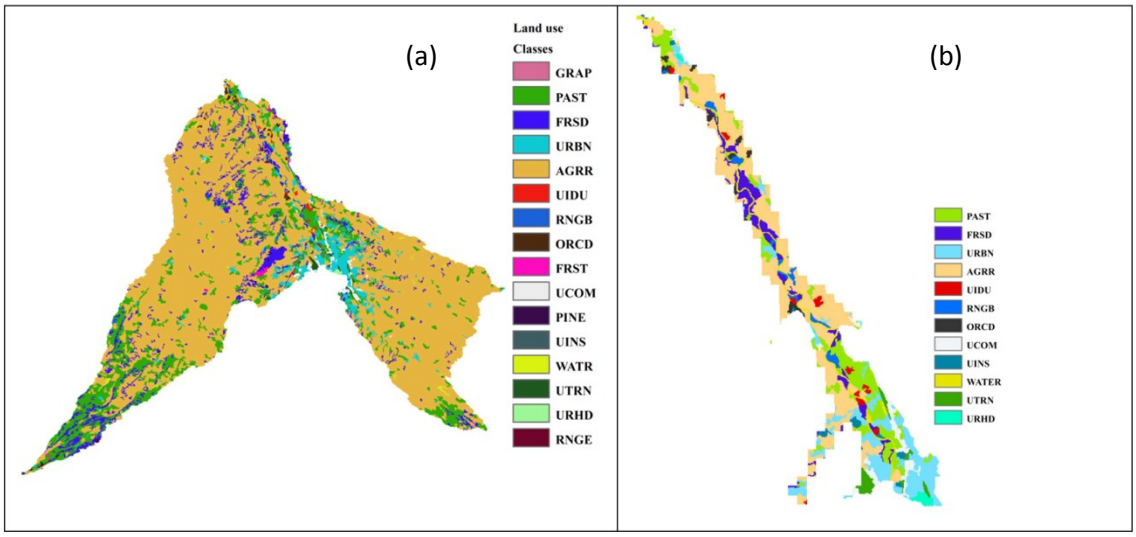


Figure 19. Land use types of the floodplain sub-watershed (a) and its alluvial soil region (b)

### 3.3.3 Monbéqui

The Monbéqui site is located in a meander of the alluvial plain of the Garonne River and the width of the floodplain in the area is about 4 km. The first 50 - 200 m of the riverbank is

covered by riparian forest and poplar plantations, surrounded by agricultural land. Several terraces exist in this area, generated by sediment deposition and washing out by flooding events. Artificial dykes have been constructed in the region to protect the agricultural land (Figure 20). The Verdun gauging station is located at about 4 km upstream of the study site-Monbéqui. It is the nearest gauging station to the study site at the Garonne River. At the Verdun gauging station, the Garonne has a watershed size of 13 730 $km^2$ and an annual average flow of about 200 $m^3 \cdot s^{-1}$. The monthly average flow ranges from about 75 $m^3 \cdot s^{-1}$ in August to about 340 $m^3 \cdot s^{-1}$ in May (Banque Hydro, http://www.hydro.eaufrance.fr/). The mean annual precipitation is about 690 mm in this area. Piezometers were installed in this site. The alluvium thickness ranges from 2.5 to 7.5 m, with an arithmetic mean of 5.7m (J. M. Sánchez-Pérez et al., 2003). The groundwater table varies from 2 to 5 m in low water periods and rise rapidly up to soil profile during floods (Weng et al., 2003).

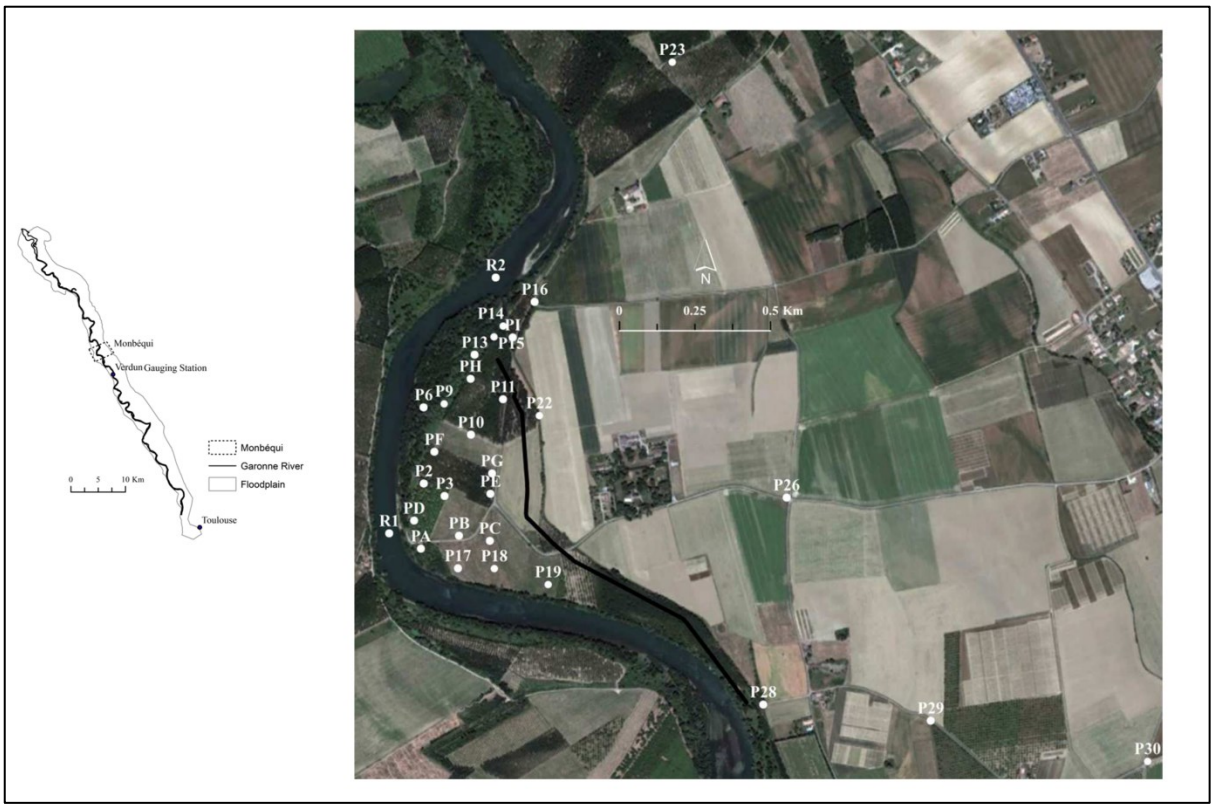


Figure 20. Location of Monbéqui study site and the distribution of piezometers and river sampling sites

### 3.3.3.1 Measurements

Groundwater, soil, and alluvial sediment samples were taken and analysed (Figure 21). Different piezometers were sampled in different period (Table 4). In which the field work in the 2013-2014 is the field sampling work of this thesis.

Table 4. Piezometers in different periods and measured parameters

| Period | Piezometers | Samples | Measured parameters |
|---|---|---|---|
| 1999-2000 | P9, P15, P19, P22, P23 and P30 | Continuous groundwater level record (Orphimedes, OTT) | Groundwater level |
| 2004-2005 | P6, P10, P13, P18 and P29 | Groundwater and alluvial sediment samples (monthly) | Groundwater level, physico-chemical parameters, AFDM |
| 2013-2014 | P2, P3, P6, P7, P9, P10, P11, P13, P14, P16, P17, P18, P22, P26, P28, P30, PA, PB, PC, PD, PE, PF, PG, PH, PI<br>R1, R2 | Continuous groundwater level record (CTD-Diver, Schlumberger, Germany)<br>Groundwater, river water and alluvial sediment samples (monthly) | Groundwater level, physico-chemical parameters, AFDM |

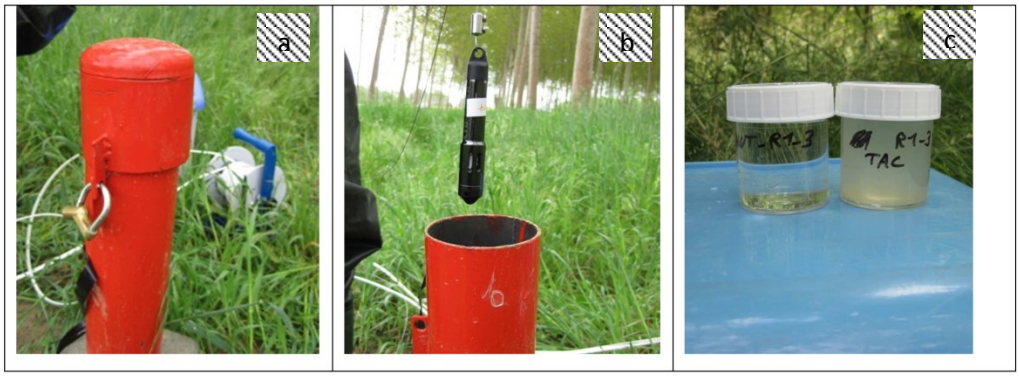


Figure 21. Installed piezometers in Monbéqui study site. 'a' shows the piezometer, 'b' shows the water level sensor installed in the piezometers, 'c' shows sampled groundwater.

Several piezometers were equipped with water-level sensors (Orphimedes, OTT (in 1999-2000) and CTD-Diver, Schlumberger, Germany (in 2013)) to record changes in groundwater level every ten minutes (Figure 19, b). In 1999-2000, the groundwater levels of 6 piezometers (P9, P15, P19, P22, P23 and P30) were recorded with water-level sensors while groundwater samples were not taken, therefore physico-chemical parameters were not analysed during this period. In 2004-2005, groundwater and alluvial sediment samples from five piezometers (P6, P10, P13, P18 and P29) were taken monthly with electric submersible pump. In 2013-2014, 25 piezometers and two river sites (R1, R2) were sampled monthly and groundwater-level sensors fitted in 5 piezometers (P7, P9, P14, P18 and P22), alluvial sediment were taken quarterly with electric submersible pump in this period.

Electrical conductivity (EC), pH, redox potential, oxygen content and temperature were measured in the field with the instrument WTW (pH/Cond 340i /SET), other parameters such as nitrate, dissolved organic carbon (DOC) ,chloride, AFDM were analysed in the laboratory. Nitrate and chloride were analysed with Alpkem Flow Solution IV Autoanalyser through spectrophotocolorimetric. DOC was analysed with TOC 2000A (Shimadzu) through thermal and infrared detection oxidation. For the AFDM, around 10g dry alluvial sediment was buried in the oven under 550°C during 4h. The AFDM content is the lost weight divided by the original alluvial sediment weight.

# Chapter 4. Improved simulation of river water and groundwater exchange in an alluvial plain using the SWAT model.

This chapter provides the description and definition of structure landscape unit (LU) in the floodplain area, the development of hydrologic module of SWAT-LUD (SWAT-Landscape Unit Darcy) and its application at Monbéqui site. Measured groundwater levels in period 1999-2000 are used to calibrate the model. Measured groundwater levels in period 2013, water exchange simulated with a 2D distributed model (2SWEM), measured concentrations of conservative tracer (chloride) and simulated concentrations of this same conservative tracer with 2SWEM are used to validate the simulated results. The SW-GW exchanged volume is quantified and the influence of river hydrologic conditions on SW-GW change is also analysed. This chapter presented the publication currently in a revising process of Hydrological processes.

# Improved simulation of river water and groundwater exchange in an alluvial plain using the SWAT model

*X Sun[a,b], L Bernard-Jannin[a,b], C Garneau [a,b] ,M Volk [c], JG Arnold[d], R Srinivasan[e],*

*S Sauvage[a,b], JM Sánchez-Pérez[a,b*]*

[a] *University of Toulouse; INPT, UPS; Laboratoire Ecologie Fonctionnelle et Environnement (EcoLab), Avenue de l'Agrobiopole, 31326 Castanet Tolosan Cedex, France*

[b] *CNRS, EcoLab, 31326 Castanet Tolosan Cedex, France*

[c] *UFZ Helmholtz Centre for Environmental Research, Department of Computational Landscape Ecology, Permoserstr. 15, D-04318 Leipzig, Germany*

[d] *Grassland, soil & water research laboratory USDA-ARS, Temple, TX 76502, USA*

[e] *Spatial Science Laboratory in the Department of Ecosystem Science and Management, Texas A&M University, College Station, TX 77845, USA*

*Corresponding author

E-mail: jose-miguel.sanchez-perez@univ-tlse3.fr

Tel. : 33 (0)5 34 32 39 20 Fax.: 33 (0)5 34 32 39 01

Address : Laboratoire d'Ecologie Fonctionnelle et Environnement (ECOLAB), UMR 5245 CNRS-UPS-INPT Ecole Nationale Supérieure Agronomique de Toulouse (ENSAT) Avenue de l'Agrobiopole BP 32607, Auzeville Tolosane 31326 CASTANET TOLOSAN Cedex FRANCE

**Abstract:** Hydrologic interaction between surface and subsurface water systems has a significant impact on water quality, ecosystems and biogeochemistry cycling of both systems. Distributed models have been developed to simulate this function, but they require detailed spatial inputs and extensive computation time. The SWAT model is a semi-distributed model that has been successfully applied around the world. However it has not been able to simulate the two way exchanges between surface water and groundwater. In this study, the SWAT-LU model – based on a catena method that routes flow across three landscape units (the divide, the hillslope and the valley) – was modified and applied in the floodplain of the Garonne River. The modified model was called SWAT-LUD. Darcy's equation was applied to simulate groundwater flow. The algorithm for surface water level simulation during flooding periods was modified and the influence of flooding on groundwater levels was added to the

model. Chloride was chosen as a conservative tracer to test simulated water exchanges. The simulated water exchange quantity from SWAT-LUD was compared with the output of a 2D distributed model, 2SWEM. The results showed that simulated groundwater levels in the LU adjoining the river matched the observed data very well. Additionally, SWAT-LUD model was able to reflect the actual water exchange between the river and the aquifer. It showed that river water discharge has a significant influence on the surface-groundwater exchanges. The main water flow direction in the river/groundwater interface was from groundwater to river, water flowed in this direction accounted for 65 % of the total exchanged water volume. The water mixing occurs mainly during high hydraulic periods. Flooded water was important for the SW-GW exchange process, it accounted for 69 % of total water flowed from the river to the aquifer. The new module also provides the option of simulating pollution transfer occurring at the river/groundwater interface at the catchment scale.

Keywords: SWAT model, Landscape Unit, water exchange, floodplain, Garonne River

## 4.1 Introduction

In recent decades, numerous studies have been carried out on the hydrological linkage between surface and subsurface (SW-GW) water systems (Grannemann and Sharp Jr., 1979; Harvey and Bencala, 1993; Wroblicky *et al.*, 1998b; Malard *et al.*, 2002). One of the most promising linkage concepts has been the development of what is known as the hyporheic zone. It was first presented by Orghidan (1959) as a special underground ecosystem, but numerous different definitions by ecologists, hydrologists and biogeochemists have since been proposed (Sophocleous, 2002; Hancock *et al.*, 2005). In all the definitions, the most important characteristic of hyporheic zones is the area of mixing between surface and subsurface water (White, 1993; Wondzell, 2011). As surface water contains rich oxygen and organic matter and groundwater contains abundant nutriment elements, the water mix between those two systems has a significant impact on water quality, ecosystems and biogeochemistry cycling (Brunke and Gonser, 1997; Boulton *et al.*, 1998; Sánchez-Pérez and Trémolières, 2003; Vervier *et al.*, 2009; Krause *et al.*, 2013; Marmonier *et al.*, 2012).

The processes occurring at the river/groundwater interface are particularly important for the alluvial plains. One of the important features of the alluvial plains is deposited sediment. Their depositional structure leads to higher hydraulic conductivity in the aquifer region than in adjacent upland (Woessner, 2000). As they support important agricultural

activities, groundwater in alluvial plains often suffer from nitrate pollution (Arrate *et al.*, 1997; Sánchez-Pérez *et al.*, 2003a; Liu *et al.*, 2005a; Almasri and Kaluarachchi, 2007). Several studies show that the surface-groundwater interface contributes to nitrogen retention and/or transformation of the land-surface water continuum (Sabater *et al.*, 2003; Weng *et al.*, 2003). This interface supports the purification of water by its ability to eliminate nitrates during their infiltration through the vegetation-soil system to groundwater, but also through diffusion from groundwater to surface water (Sanchez-Perez *et al.*, 1991a, 1991b; Takatert *et al.*, 1999) Hence, an understanding of the processes occurring in the surface-groundwater interface could offer considerable insight for the purposes of water management on a catchment scale.

SW-GW interactions are complex processes driven by geomorphology, hydrogeology and climate conditions (Sophocleous, 2002). In addition, it has been stated that overbank flow is a key hydrologic process affecting riparian water table dynamics and ecological processes (Naiman and Decamps, 1997; Rassam and Werner, 2008). Models have been developed to simulate the hydrological conditions of the surface water, groundwater and river/groundwater interface. Rassam and Werner (2008) reviewed models at different complex levels that represented the surface and subsurface processes that have influence on SW-GW exchange. The simulation of the SW-GW exchange is mainly carried out by using three types of models: i) models developed for subsurface water, ii) models developed for surface water and iii) models that integrated the interface of the two domains. To account for complex geometry, hydrological conditions and materials composition, most of the models developed for subsurface water are distributed models, such as MODFLOW (Storey *et al.*, 2003; Lautz and Siegel, 2006b) or HYDRUS (Langergraber and Šimůnek, 2005). These models usually require spatial inputs in high resolution and numerous parameters and are characterised by a significant computation time that inhibits their application on large scales. Models that are developed for surface water include QUAL2K (Park and Lee, 2002) and OTIS (Morrice *et al.*, 1997). In these models, the lateral floodplain operates as a storage pool to keep the upstream and downstream channel water balance. Loague and VanderKwaak (2004) and Kollet and Maxwell (2006) reviewed models that coupled surface and subsurface domains, FSTREAM (Hussein and Schwartz, 2003) and 2SWEM (Peyrard *et al.*, 2008) are examples for this type of model. Most of these models are still too complicate to apply at large scale.

Large-scale hydrological models have been developed to simulate hydrologic conditions at catchment or regional scale. Examples of such models include SWIM

(Krysanova *et al.*, 1998), TOPMODEL (Franchini *et al.*, 1996) and MODHYDROLOG (Chiew and McMahon, 1994). However, the river/groundwater interface is mostly not included in these models. To overcome this issue, the incorporation of conceptual and distributed models has been suggested, as in SWAT-MODFLOW (Sophocleous and Perkins, 2000; Kim *et al.*, 2008), WATLAC (Zhang and Li, 2009) and WASIM-ETH-I-MODFLOW (Krause and Bronstert, 2007). However these developments have still been unable to reflect the impacts of land use management on groundwater quantity or are not applicable in large watersheds. The Soil and Water Assessment Tool (SWAT) model is a deterministic, continuous, semi-distributed, watershed-scale simulation model that allows a number of different physical processes to be simulated in a watershed. SWAT can simulate a large watershed with readily available data and has been used successfully all over the world (Jayakrishnan *et al.*, 2005; Romanowicz *et al.*, 2005; Fohrer *et al.*, 2014). To reflect the hydrological connection between upslope and downslope parts of a landscape, a catena approach including divide, hillslope and floodplain landscape units has been developed and included in SWAT (Volk *et al.*, 2007; Arnold *et al.*, 2010, Rathjens *et al.*, 2015). The catena approach in the modified model (SWAT-LU) represents an effort to impose a systematic upscaling from a topographic position to a watershed scale. Within the catena, a more detailed downslope routing of surface runoff, lateral flow and groundwater can be accomplished, and the impact of upslope management on downslope landscape positions can be assessed (Arnold *et al.*, 2010; Bosch *et al.*, 2010). However, the hydrological processes are still single tracks in SWAT-LU and the function of SW-GW exchange in both directions is not included. Furthermore, the flooded distance during flooding events is fixed at five times the width of the top channel and the influence of flooding on groundwater levels is not taken into account.

In this study, a new module was developed to simulate the SW-GW exchange in the river/groundwater interface. The modified model was called SWAT-LUD. The SWAT-LUD model was tested on the example of the floodplain of the Garonne River, which has a typical alluvial plain starting from its middle section. Several distributed models (MODFLOW, MARTHE and 2SWEM) were applied to simulate the hydrological and biogeochemical processes in this area (Sánchez-Pérez *et al.*, 2003b; Weng *et al.*, 2003;Peyrard *et al.*, 2008). Groundwater levels and water exchanges between SW-GW were simulated in the present study. The simulated groundwater levels were then compared with the groundwater levels measured by the piezometers, and the simulated water exchanges verified by detecting the concentration of conservative tracer and undertaking a comparison with the simulated results of a 2D distributed model - 2SWEM model.

## 4.2 Methodology

### 4.2.1 SWAT model

The Soil and Water Assessment Tool (SWAT) model (Arnold *et al.*, 1998) is a semi-distributed, watershed-scale simulation model. It was developed to simulate the long-term impact of management on water, sediment and agricultural chemical yields in large river basins. It is a continuous time model that is operating on a daily time step. To represent the spatial heterogeneity, the watershed is first divided into subbasins. The subbasins are then subdivided into hydrologic response units (HRUs) which are particular combinations of land cover, soil type and slope. SWAT is a process-based model, the major components include hydrology, nutrients, erosion and pesticides. In the SWAT model, processes are simulated for each HRU and then aggregated in each subbasin by a weighted average (Arnold *et al.*, 1998; Neitsch *et al.*, 2009).

### 4.2.2 Model development

#### 4.2.2.1 Landscape Unit (LU) structure

In the HRU delineation method of the usual SWAT model, flow is summed at the subbasin scale and not routed across the landscape. For this application, the watershed was divided into three landscape units (LUs): the divide, the hillslope and the valley bottom. A representative catena was selected and flow routed across the catena as shown in Figure 1 (Volk *et al.*, 2007). Landscape Units (LU) represent additional units that take place between a subbasin and an HRU. Each subbasin is composed of three LUs, and HRUs are distributed across the different LUs (Volk *et al.*, 2007; Arnold *et al.*, 2010; Bosch *et al.*, 2010; Rathjens *et al.*, 2015). To represent the SW-GW exchanges occurring in the alluvial plain, a new type of subbasin called subbasin-LU was developed. Subbasin-LU corresponds to the subbasin delimited by the floodplain and the LU structure was applied in subbasin-LU. Processes in the upland area of floodplain were calculated according to the original SWAT model. Processes were simulated for each HRU and aggregated to the river. Upland and subbasin-LU were connected through the river. The definition of the widths of LUs was made according to the surface of floodplain covered by the flood return period: $LU_1$ represented the one-year return flood area, $LU_2$ represented the two to five-year return flood area and $LU_3$ corresponded to the ten or more years return flood area. LUs were located parallel to the channel and were defined by their widths and slopes. As LUs were located on both sides of the channel, the width of each side of LU was half its total width. All three LUs in one subbasin were

considered as being of the same length, which was the length of the channel. Processes in each HRU were still computed separately and then summed at LU scale. The length was defined based on the river's hydromorphological structure. Finally, the processes were computed between LUs. With the catena method, surface runoff and lateral flow from $LU_3$ (which was furthest from the channel) were routed through $LU_2$ to $LU_1$ (which was nearest to the channel) and then entered the channel (Figure 1). A detailed description of the catena method can be found in Volk *et al.* (2007) and Arnold *et al.* (2010).

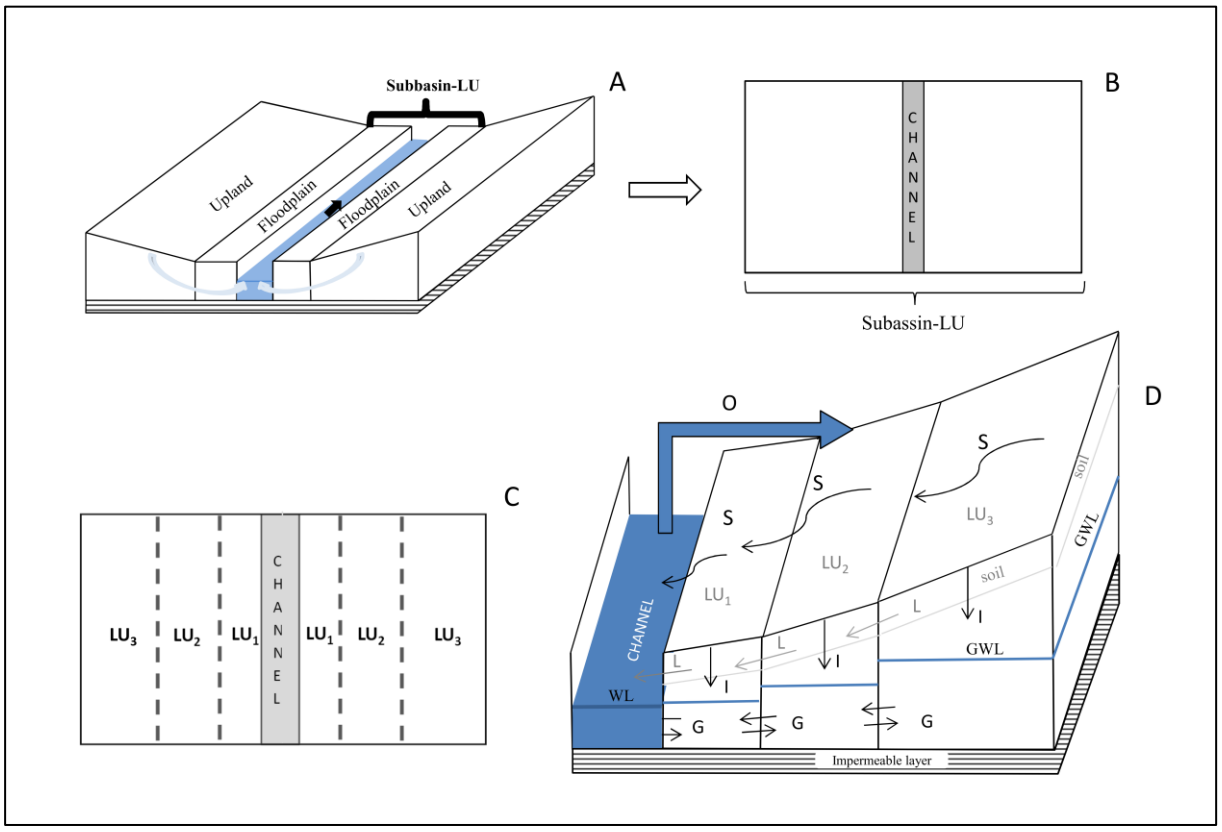


Figure 1. The Catena method and its landscape unit structure in the SWAT-LUD model. The figure shows the location of subbasin-LU ,the landscape unit (LU) structure in the SWAT-LUD model and the hydrologic processes: 'A' represents the location of subbasin-LU, 'B' represents subbasin-LU, 'C' represents the distribution of LUs in the subbasin-LU (plane), and 'D' represents the hydrologic processes in the landscape units where 'S' is surface flow, 'L' is lateral flow, 'I' is infiltration, 'G' is groundwater flow, 'O' is overbank flow, 'GWL' is groundwater level and 'WL' is river water level (according to Volk *et al.*, 2007 and Arnold *et al.*, 2010)

#### 4.2.2.2 SW-GW interaction with LU structure

Darcy's (1856) equation (equation 2.2.2.1) was applied to calculate groundwater flow between the LUs and water exchanges between the river and the aquifer. Each LU had a unique groundwater level. The altitude of the river bed in each subbasin was assumed to be

the referenced value of the hydraulic head used to compute groundwater and surface water levels. HRUs were assumed to be homogenous inside, with no additional differentiation in soil and material underneath, and lateral flow was not simulated:

$$Q = K \times A \times \frac{\Delta H}{L} \quad (2.2.2.1)$$

where Q is water flow ($m^3.d^{-1}$), A is the cross-sectional area between two units ($m^2$), K is saturated hydraulic conductivity ($m.d^{-1}$), ΔH is hydraulic head difference between two units (m) and L is the distance between two units through which the water is routed (m).

As the river is filled by water, two implementations of Darcy's equation were required:

3) groundwater flow between two LUs:

$$K = \frac{(K_{lua} \times W_{lua}) + (K_{lub} \times W_{lub})}{(W_{lua} + W_{lub})} \quad (2.2.2.2)$$

$$W = (W_{lua} + W_{lub})/4 \quad (2.2.2.3)$$

$$Q = 2 \times K \times A \times \frac{(H_{lua} - H_{lub})}{W} \quad (2.2.2.4)$$

where K represents the averaged hydraulic conductivity values of the two LUs ($K_{lua}$, $K_{lub}$) based on their widths ($m.d^{-1}$), $W_{lua}$ and $W_{lub}$ are the widths of the two LUs (m), $H_{lua}$ and $H_{lub}$ are the hydraulic heads of the two LUs (m), W is the distance between the centres of these two LUs on one side of channel. Since LUs located in two sides of the channel, each side got half of its width, W is a quarter of the total width of these two LUs (m). As groundwater flow occurs on both sides of the river, the flow was multiplied by two.

4) Groundwater flow between $LU_1$ and the river:

$$K = K_{lu} \quad (2.2.2.5)$$

$$W = (W_{lu})/4 \quad (2.2.2.6)$$

$$Q = 2 \times K \times A \times \frac{(H_{lu} - H_{ch})}{W} \quad (2.2.2.7)$$

where K is the hydraulic conductivity value of $LU_1$ ($K_{lu}$) ($m.d^{-1}$); W is the quarter width of $LU_1$ ($W_{lu}$) (half of the width of one side of the channel) (m); and $H_{lu}$ and $H_{ch}$ are hydraulic heads of $LU_1$ and the river (m).

#### 4.2.2.3 Influence of flooding to surface water and groundwater level

The original algorithm for flooding events in the SWAT model only assumes that the flooded distance is five times the top channel width (Neitsch *et al.*, 2009). The influence of floodplain geometry and the influence of flooded water on groundwater are not considered. The new algorithm was based on the water volume during a flood event:

$$U_f = (v - v_{max}) \times T \quad (2.2.3.1)$$

where $U_f$ is the flood volume ($m^3$), v is the discharge ($m^3s^{-1}$), $v_{max}$ is the maximum discharge value at which water could stay in the channel ($m^3s^{-1}$) and T is the travel time of water passing through the channel (s).

During a flood, the surface water level is the sum of the riverbank height and the water depth on the surface relative to the height of river bank:

$$A_f = L_{ch} * (W_{ch} + L_f) \quad (2.2.3.2)$$

$$H_{ch} = D_{ch} + \frac{U_f}{A_f} \quad (2.2.3.3)$$

where $A_f$ is the flooded area ($m^2$), $L_{ch}$ is the length of the channel (m), $W_{ch}$ is the width of the channel (m), $L_f$ is the flood distance on one side of the river bank (m), $H_{ch}$ is the surface water level and $D_{ch}$ is the height of the riverbank (m).

With regard to groundwater levels in the LUs during flood periods (if flood water arrives at a LU), the groundwater of this LU was assumed to be the same level as the surface water:

$$H_{luf} = H_{ch} \quad (2.2.3.4)$$

where $H_{luf}$ is the groundwater level of LU during the flood (m).

The infiltrated flood water was calculated as follows:

$$V_{in,f} = \left(H_{luf} - H_{lu}\right) \times A_{lu} \times p_{lu} \quad (2.2.3.5)$$

Where $V_{in,f}$ is the infiltrated flood water volume in LU ($m^3$), $A_{lu}$ is the surface area of the LU ($m^2$), $p_{lu}$ is the porosity of the LU (%).

The overbank flow would return back to the river the next day after flooding, and discharge of river water was recalculated:

$$IN = IN + U_f \quad (2.2.3.6)$$

$$v = IN/86400 \quad (2.2.3.7)$$

Where $IN$ is the input water volume ($m^3$)

#### 4.2.2.4 Transfer of dissolved elements

The transfer of dissolved elements between LUs and between LUs and surface water was calculated based on the water flow volume and concentration of the elements:

$$M_{lu} = M_{lu} + M_{in} - M_{out} \quad (2.2.4.1)$$

$$M_{in} = \sum(V_{in} * C_{in}) \quad (2.2.4.2)$$

$$M_{out} = \sum(V_{out} * C_{lu}) \quad (2.2.4.3)$$

$$C_{lu} = M_{lu}/V_{lu} \quad (2.2.4.4)$$

where $M_{lu}$ is the mass content of the element in LU (g), $M_{in}$ is the input mass (g), $M_{out}$ is the output mass (g). $V_{in}$ is input water volume ($m^3$), $C_{in}$ is the concentration of the elements in the input water ($mg \cdot l^{-1}$), $V_{out}$ is the output volume ($m^3$), $C_{lu}$ is the concentration of the element in calculated LU ($mg \cdot l^{-1}$) and $V_{lu}$ is the water volume storage in LU ($m^3$).

### 4.2.3 Study area

The Garonne River is the third longest river in France. Its hydrology is influenced by Mediterranean climate and melting snow from the mountainous areas. The typical alluvial plain starts from the middle section of the Garonne River. It contains between 4 and 7 m coarse deposits (quaternary sand and gravel) eroded from the Pyrenees Mountains during the past glacial periods that overlie the impermeable layer of molassic substratum (Lancaster, 2005). The Verdun gauging station is located at about 4 km upstream of the study site-Monbéqui. It is the nearest gauging station to the study site at the Garonne River. At the Verdun gauging station, the Garonne has a watershed size of 13 730 $km^2$ and an annual average flow of about 200 $m^3 \cdot s^{-1}$. The monthly average flow ranges from about 75 $m^3 \cdot s^{-1}$ in August to about 340 $m^3 \cdot s^{-1}$ in May (Banque Hydro, http://www.hydro.eaufrance.fr/). The greatest discharges occur twice a year, in the spring as a result of snow melt and in late autumn following intense rainfalls (Sánchez-Pérez *et al.*, 2003c). Previous studies in the Garonne river basin have shown that the river/groundwater interface play an important role at the reach scale, both in the retention of nitrogen and phosphorous (Vervier *et al.*, 2009) and in

controlling aquifer water quality (Iribar *et al.*, 2008). The study area is characterised by high nitrate pollution caused by agriculture (Jégo *et al.*, 2008, 2012a).

The study site is located in a meander of the alluvial plain of the Garonne River (Monbéqui) and the width of the floodplain in the area is about 4 km. The mean annual precipitation is about 690 mm in this area. The alluvium thickness ranges from 2.5 to 7.5 m, with an arithmetic mean of 5.7m (Sánchez-Pérez *et al.*, 2003c). The groundwater table varies from 2 to 5 m in low water periods and rise rapidly up to soil profile during floods (Weng *et al.*, 2003). The first 50 - 200 m of the riverbank is covered by riparian forest and poplar plantations, surrounded by agricultural land. Several terraces exist in this area, generated by sediment deposition and washing out by flooding events. Artificial dykes have been constructed in the region to protect the agricultural land (Figure 2).

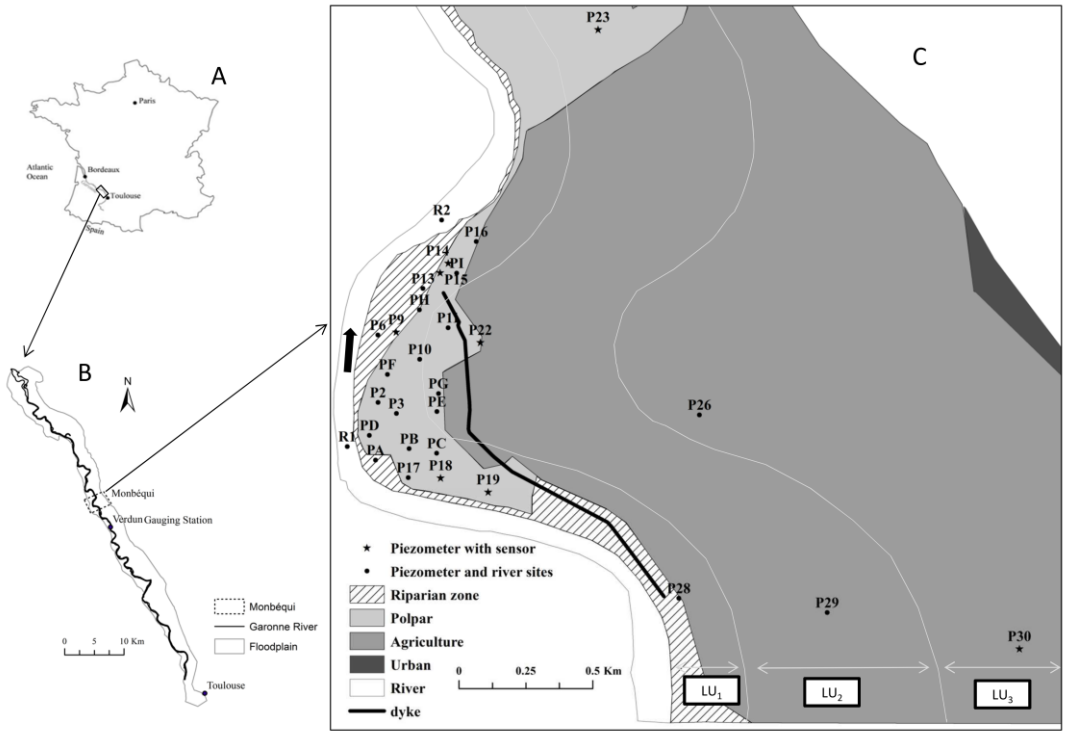


Figure 2. The Garonne River and the Monbéqui study site. 'A' represents the location of the Garonne River, 'B' represents the location of the alluvial plain and Monbéqui, and 'C' represents the piezometers in Monbéqui, the grid lines show the rough locations of LUs.

#### 4.2.3.1 Measurements

Twenty-nine piezometers were installed in the study area, nine of which were equipped with water-level sensors (Orphimedes, OTT (in 1999-2000) and CTD-Diver, Schlumberger,

Germany (in 2013)) to record changes in groundwater level every ten minutes. In addition, groundwater samples were taken monthly for analysis of physicochemical parameters. While pH, redox potential, electrical conductivity, oxygen content and temperature were measured in the field, other parameters such as nitrate, dissolved organic carbon and chloride were analysed in the laboratory.

In 1999-2000, the groundwater levels of 6 piezometers (P9, P15, P19, P22, P23 and P30) were recorded with water-level sensors while groundwater samples were not taken, therefore physicochemical parameters were not analysed during this period. In 2013, 25 piezometers (all the piezometers in Figure 2 except P15, P19, P23 and P29) and two river sites (R1, R2) were sampled monthly and groundwater-level sensors fitted in 5 piezometers (P7, P9, P14, P18 and P22). Piezometers were recorded in both periods are: P9, P22 and P30 (Figure 2).

### 4.2.4 Landscape Unit parameters

For the purposes of simplification, only one subbasin-LU was simulated in this study and each LU only contained one HRU. The daily discharge data of the Verdun gauging station were used as input data. Based on the flooded area of the Garonne River during different periods, the LU parameters are presented in Table 1, the values of porosity were given based on the study of Seltz (2001) and Weng *et al.* (2003). The distributions of piezometers with installed sensors in the three LUs were as follows: five piezometers were located in $LU_1$: P9, P14, P15, P18 and P19; two piezometers, P22 and P23, were located in $LU_2$; P30 located in $LU_3$.

Table 1. Parameters of LUs and channel

| | $LU_1$ | $LU_2$ | $LU_3$ | Channel |
|---|---|---|---|---|
| Width (km) | 0.4 | 0.8 | 3.0 | 0.22 |
| Length (km) | 6.374 | 6.374 | 6.374 | 6.347 |
| Slope (lateral) | 0.002 | 0.005 | 0.005 | -- |
| Slope (vertical) | -- | -- | -- | 0.001 |
| Porosity | 0.1 | 0.1 | 0.1 | -- |
| Depth (m) | -- | -- | -- | 4.0 |

In the model, each LU had one groundwater level value. With Darcy's equation, the altitude of the riverbed in each subbasin-LU was assumed to be the referenced hydraulic head. As the river sloped, the altitude of the riverbank was variable within one subbasin-LU. One referenced value had to be chosen for comparison with the measured groundwater levels in

each subbasin-LU. At the study site, P9 was the only piezometer with groundwater level sensors fitted during 1999-2000 and 2013 in $LU_1$. The groundwater level of $LU_1$ was more important to the calculation of the SW-GW exchange than that of the other two LUs. The altitude of the riverbed was set at 84.75 m NGF (National Geographique Français: the general levelling of France, with 'zero level' determined by the tide gauge in Marseille). It was calculated based on the altitude of the soil surface of P9 (88.95m NGF) minus 4 m, corresponding to the height of the riverbank minus 0.2 m and the slope of $LU_1$ which was 0.002.

### 4.2.5 Calibration and validation

#### 4.2.5.1 Groundwater levels

The calibration of the groundwater levels was performed manually. Since the flood that occurred in 2000 was the largest event in the recent 20 years, and the groundwater level sensors were installed in all the three LUs in the period of 1999-2000, the observed groundwater levels in this period were used as calibration data. The observed data from 2013 were taken as validation data. The simulated groundwater levels of the LUs (average value) were compared with corresponding piezometers (point value). To limit the error caused by the vertical slope, piezometers were chosen for comparison with the simulated groundwater levels in each LU based on their location relative to P9. In $LU_1$, P15 and P9 had similar observed values in the calibration period (1999-2000), but P15 had a longer available time series than P9. In $LU_2$, P22 was closer to P9 than P23. P30 was located upstream of P9, but was the only piezometer with a groundwater level sensor installed in $LU_3$. Therefore the observed groundwater levels of P15, P22, P30 during the calibration period (1999-2000) and P9, P22, P30 during the validation period (2013) were used for comparison with the simulated results of $LU_1$, $LU_2$ and $LU_3$ respectively.

#### 4.2.5.2 SW-GW exchanged water

Chloride as a well-known groundwater conservative tracer (Harvey *et al.*, 1989; Cox *et al.*, 2007) was chosen to verify the simulated water exchange between the river and $LU_1$. Since the concentrations of chloride were measured monthly, there is a lack of continuous observed data as input values of the model. However, the variations of the chloride concentrations in surface water and groundwater in $LU_2$ as well as in $LU_3$ were only slight, constant concentration values were given for the river, $LU_2$ and $LU_3$ during simulation. Concentration values were set based on the measured data in 2013 (Table 2), since this was

the only year in which surface water and groundwater samples were taken and analysed. The concentration values in $LU_1$ were simulated based on the mix of surface water and $LU_2$. The comparison of simulated and observed chloride concentrations in $LU_1$ could be used to verify the simulated SW-GW exchange in $LU_1$. Since the transport of chemistry elements was more complicated than water flow, it would be more difficult to match the simulated data for a LU with the observation from a certain piezometer. The chloride concentrations measured in all the 16 piezometers in $LU_1$ were compared with the simulated data.

Table 2. Detected values (in 2013) and constant values of chloride of river water and groundwater of $LU_3$ and $LU_2$

| Zone | | Chloride (Mean±SE) ($mg \cdot l^{-1}$) | Constant chloride ($mg \cdot l^{-1}$) |
|---|---|---|---|
| River | R1 | 8.97±1.05 | |
| | R2 | 9.38±1.14 | 9.00 |
| $LU_2$ | P22 | 78.22±3.60 | 75.00 |
| $LU_3$ | P26 | 54.88±2.67 | 50.00 |
| | P30 | 38.28±1.45 | |

2SWEM (Surface-Subsurface Water Exchange Model) is a 2D hydraulic model. Horizontal 2D Saint Venant equations for river flow and a 2D Dupuit equation for aquifer flow were coupled in the model to simulate the dynamic variation of aquifer water level. It was originally developed to simulate water exchange occurring in the river/groundwater interface (Peyrard *et al.*, 2008). Peyrard (2008) simulated surface water and groundwater exchange on the right side of the riverbank in the Monbéqui study area. The simulation was carried out for a 3.1 km length of the riverbank using the 2SWEM model at a daily time step. The result of the SWAT-LUD simulation was adjusted (total exchanged volume divided by the length of channel (6.374 km) then multiple by 3.1km) to match the distance of 3.1 km and then divided by two to compare it with the output of the 2SWEM model.

The coefficient of determination ($R^2$), Nash-Sutcliffe efficiency (NSE), Percent Bias (PBIAS) and RMSE observations standard deviation ratio (RSR) were chosen as evaluating parameters.

## 4.3 Results

### 4.3.1 Calibrated parameters

Hydraulic conductivities were determined by pumping tests and slug tests, varying from $10^{-2}$ to $10^{-5}$ $m \cdot s^{-1}$ (Weng *et al.*, 2003; Peyrard *et al.*, 2008). Since the simulations with the

SWAT-LUD model were carried out at a daily step, the converted daily hydraulic conductivities varied from 860 to 1 $m \cdot d^{-1}$. Calibrated parameters are given in Table 3.

Table 3. Manually-calibrated parameters

| Parameters | Default value | Calibrated values |
|---|---|---|
| Manning roughness coefficient | 0.014 | 0.070 |
| Hydraulic conductivity ($LU_1$) ($m \cdot d^{-1}$) | undefined | 300 |
| Hydraulic conductivity ($LU_2$) ($m \cdot d^{-1}$) | undefined | 200 |
| Hydraulic conductivity ($LU_3$) ($m \cdot d^{-1}$) | undefined | 100 |

### 4.3.2 Groundwater levels

Figure 3 shows the shallow water tables in the study site based on the measured data of all the piezometers in two periods in 2013.

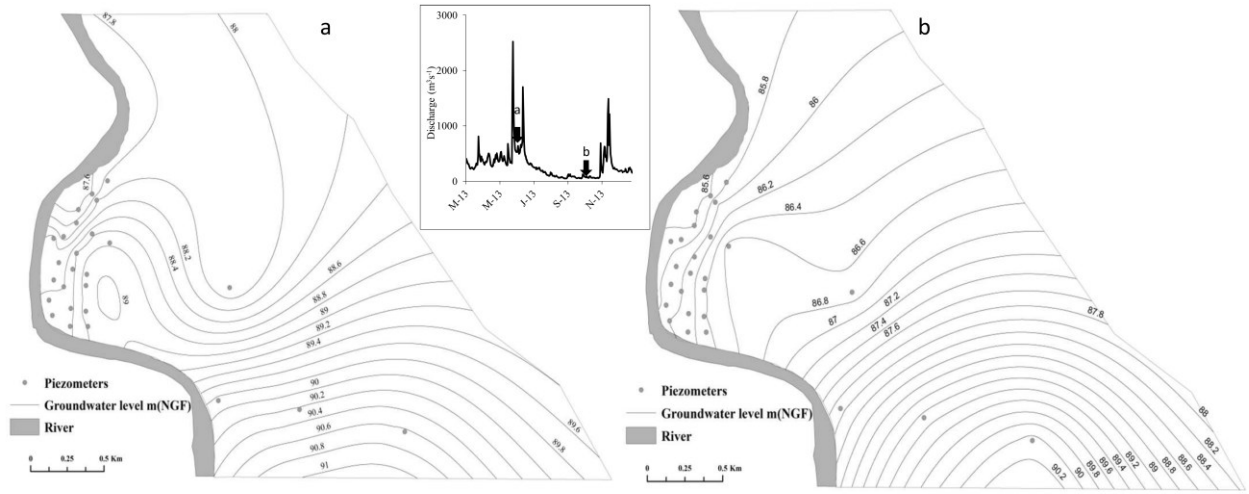


Figure 3. Contour maps of groundwater level in two periods. 'a' represents the groundwater levels in flood period and 'b' represents the groundwater levels in low hydraulic period.

It shows that in the period between two floods, the direction of groundwater flow in the meander is from river to floodplain and groundwater flowed from the floodplain to river in the stable low flow period.

The comparison of observed and simulated groundwater levels in the three LUs is shown in Figure 4.

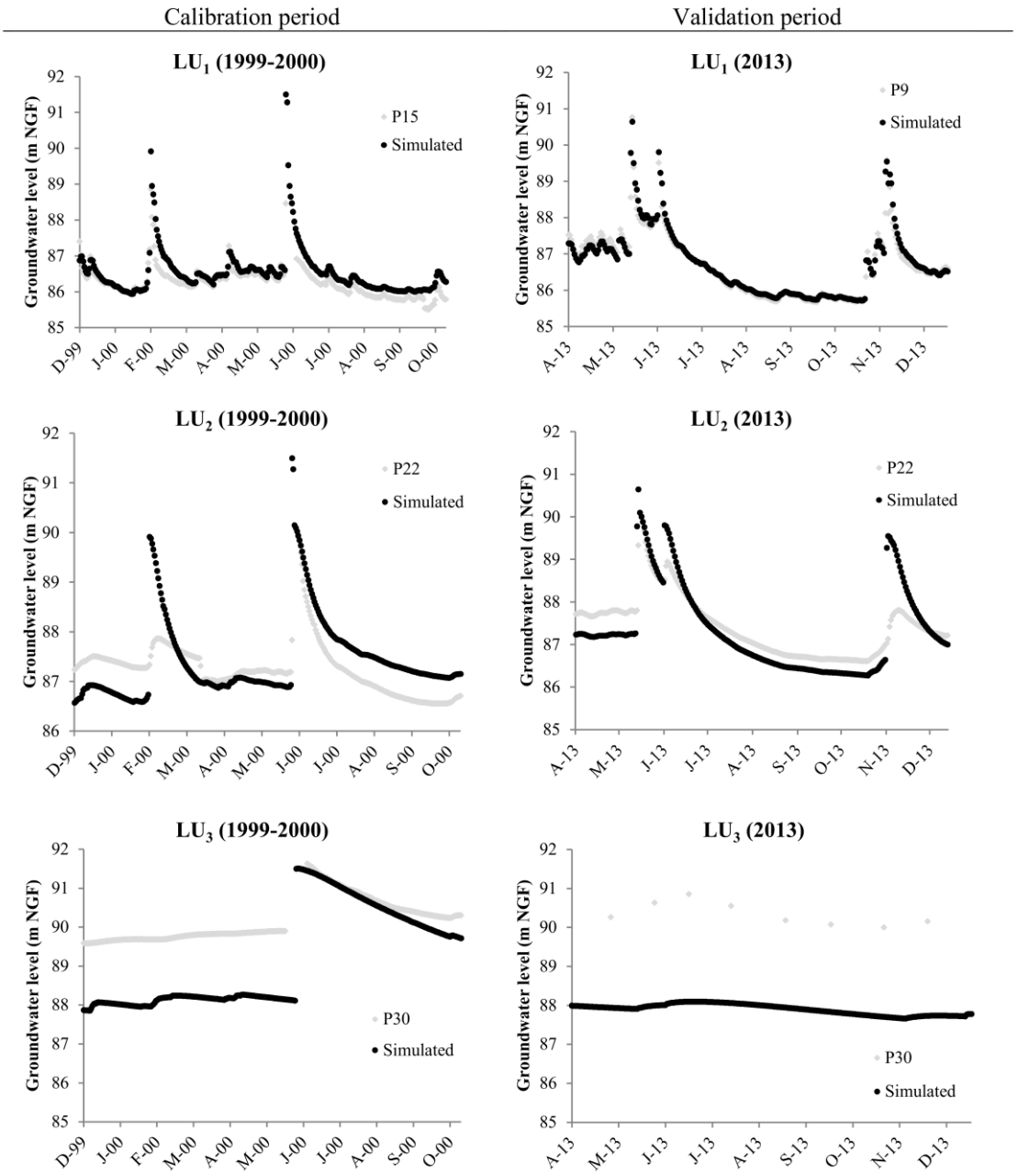


Figure 4. Observed and simulated groundwater levels in the calibration (1999-2000) and validation (2013) periods

The results demonstrated that observed and simulated values matched very well in $LU_1$, especially in 2013 when simulated and observed values almost overlapped ($R^2$ = 0.96, NSE = 0.95). There was considerable variation in the observed and simulated well heights in $LU_2$. The lower water level values of the simulations were under the observations and $LU_2$ was flooded too often compared to the observed data. For $LU_3$, the result showed that

simulated values were much lower than the observed data in $LU_3$, but the two curves had the same variation trend ($R^2$ = 0.94) (Table 4). The graph also showed that with an increase in distance from the river, there was a decrease in the fluctuation in groundwater.

Table 4. Parameters for evaluating the accuracy of groundwater levels simulated by the SWAT-LUD model

| | | $R^2$ | NSE | PBIAS | RSR |
|---|---|---|---|---|---|
| $LU_1$ | Calibration | 0.79 | 0.25 | -0.27 | 0.87 |
| | Validation | 0.96 | 0.95 | -0.05 | 0.22 |
| $LU_2$ | Calibration | 0.38 | -0.42 | -0.15 | 1.19 |
| | Validation | 0.78 | 0.48 | 0.09 | 0.72 |
| $LU_3$ | Calibration | 0.94 | -4.14 | 1.12 | 2.27 |
| | Validation | 0.75 | -72.3 | 2.68 | 8.56 |

### 4.3.3 Water exchange between surface water and groundwater

#### 4.3.3.1 Water exchange—verified with conservative elements

To verify simulated exchanged water, simulated concentration values of chloride ($Cl^-$) were compared with the mean values from the 16 piezometers. The simulated groundwater level in $LU_1$ was compared with P15 and P9, but only P9 was sampled in 2013. The detected values of $Cl^-$ of P9 were also compared with the simulated data (Figure. 5).

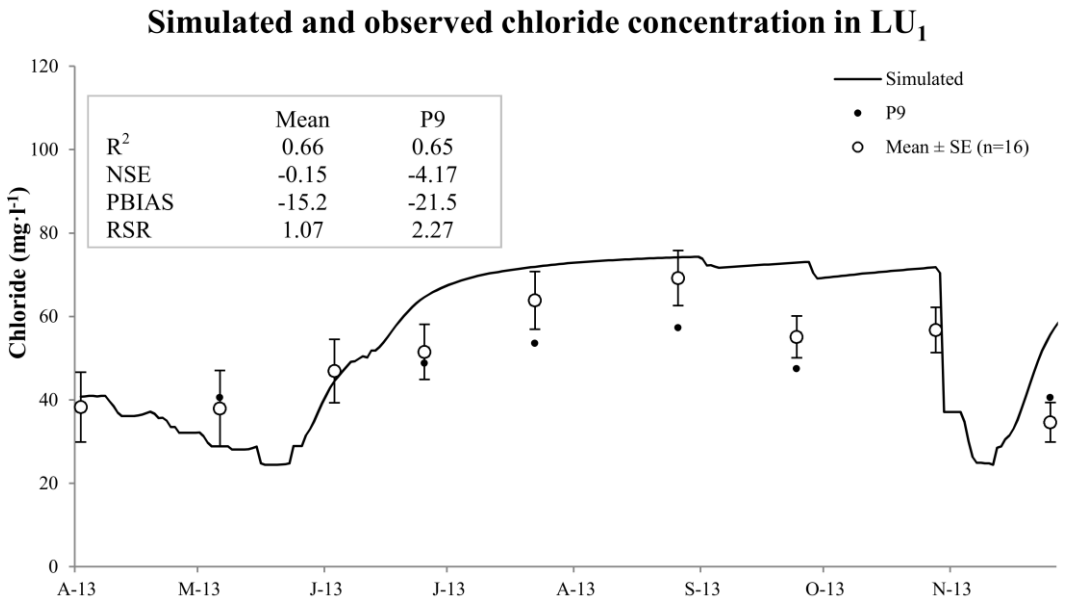


Figure 5. Comparison of concentration of chloride in $LU_1$ between the SWAT-LUD model's simulation and values detected from field sampling

Figure 5 shows large variations in observed values within $LU_1$, matching the mean values more closely than P9.

#### 4.3.3.2 Comparison with simulations by the 2SWEM model

Figure 6 shows the comparison between the results of the SWAT-LUD model and the results of the 2SWEM model. The models produced reasonably close results given the $R^2$ of 0.62 and NSE of 0.51 (Figure. 6). In the period before May 2005, SWAT-LUD predicted less surface water entering the aquifer than the 2SWEM model and the lag time of groundwater flow to the river was greater in 2SWEM than in SWAT-LUD. After a large peak in May 2005, the results of the two models were almost identical.

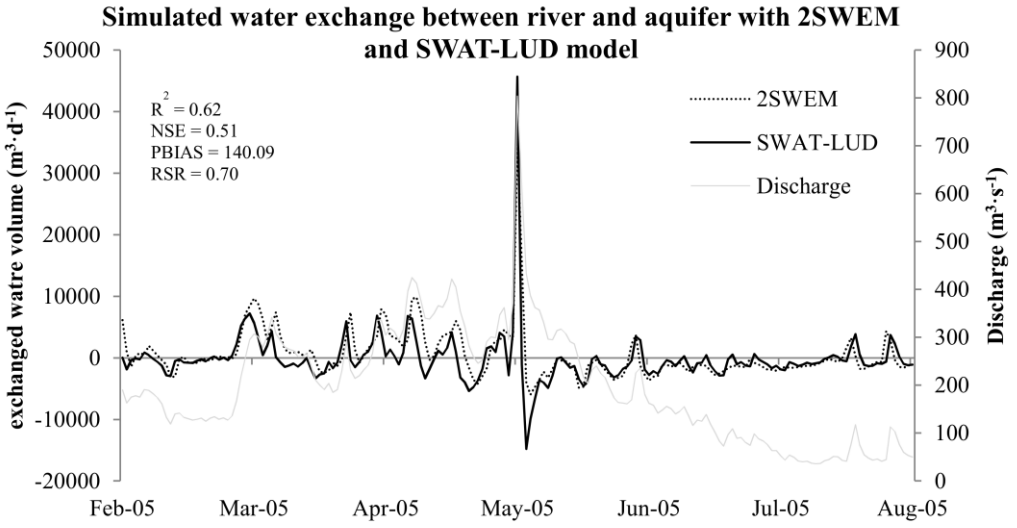


Figure 6. Comparison of the simulated water exchange between the SWAT-LUD model and the 2SWEM model

#### 4.3.3.3 Surface water and groundwater exchange

The water quantity exchanged annually between the river and the aquifer throughout the entire period simulated (1993-2013) is shown in Figure 7.

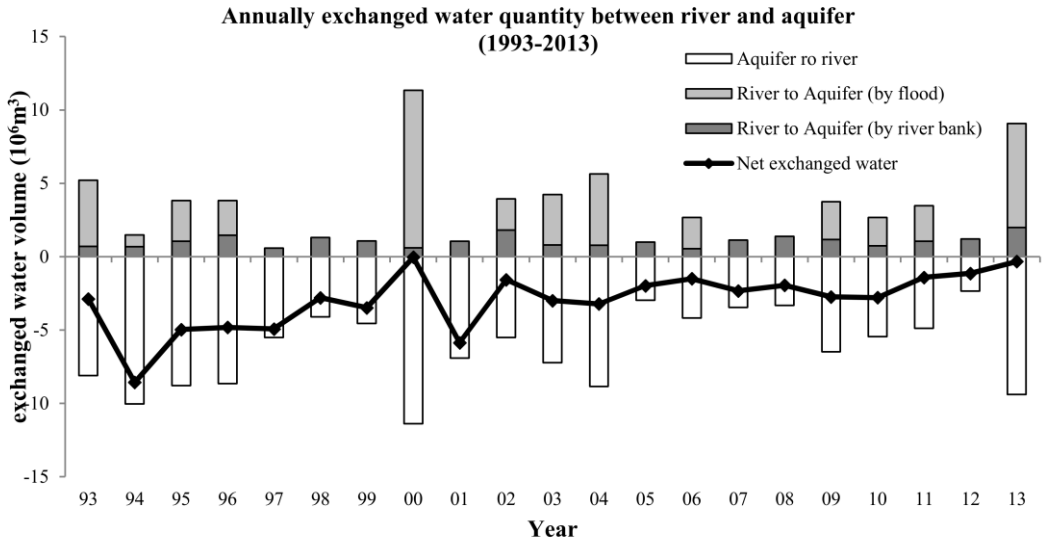


Figure 7. Annually exchanged water quantity between the river and the aquifer during the entire simulated period (1993-2013).

Water flow can occur in two directions: from the river to the aquifer and from the aquifer to the river. It was found that the dominant net flow direction was from the aquifer to the river and water exchange quantities varied annually. Water flowing from the river to the aquifer can be separated into two parts: (1) water infiltrating through the riverbank and (2) flooded water percolating through the surface of the LUs. Flooded water percolating through the soil surface accounted for 69 % of water flowed from the river to the aquifer. The annually flooded water volume and flooded days are shown in Figure 8.

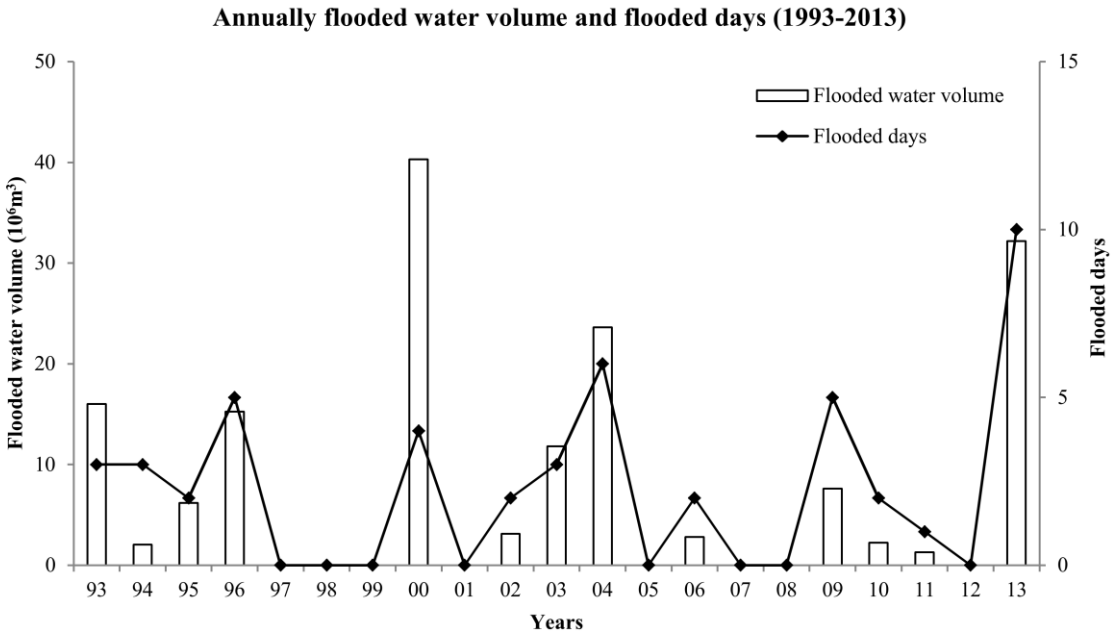


Figure 8. Annually flooded water volume and flooded days during the entire simulated period (1993-2013).

To understand the influence of river water discharge on the SW-GW exchanged water volumes, three river water discharge measurements were correlated with four simulated exchanged water volume components. The discharge measurements were annual mean discharge ($Q_m$), annual maximum discharge ($Q_{max}$) and annual discharge variation ($\Delta Q = \sqrt{\sum(Q - Q_m)^2}$ ). The exchanged water volumes were the annual absolute exchanged water volume flowing in two directions (from river to aquifer and from aquifer to river), net exchanged water volume and total absolute exchanged volume. Results are shown in Figure 9. This demonstrated that river water discharge had a significant impact on the exchanged water quantities between the river and the aquifer. Along with the increase of $Q_m$, $Q_{max}$ and $\Delta Q$, the water volumes flowing from the river to the aquifer and from the aquifer to the river also increased. Water flow from the aquifer to the river is better correlated with $\Delta Q$. $Q_{max}$ played the most significant role in water flowing from the river to the aquifer and total exchanged water volume. However, net exchanged water volumes were not significantly influenced by the discharge.

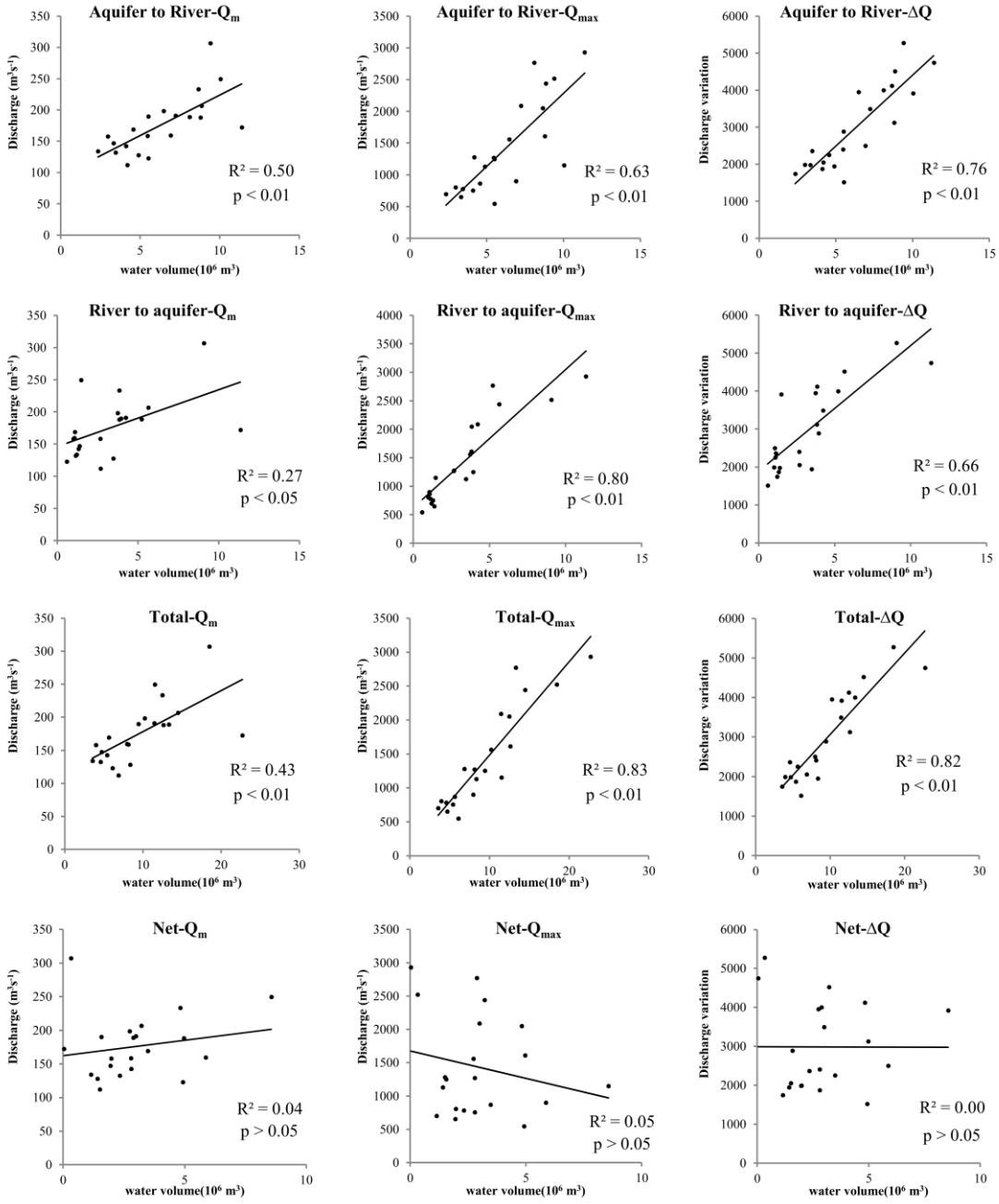


$Q_m$: Annual mean discharge; $Q_{max}$: Annual Maximum discharge; ΔQ: Annual variation of discharge ($\sqrt{\sum(Q - Q_m)^2}$)

Figure 9. Correspondence between river water discharge and exchanged water volume between the river and the aquifer

Based on the discharge values, simulated data were separated into two parts: low hydraulic period and high hydraulic period. The bound discharge value was set at 200 $m^3 \cdot s^{-1}$, which is the long-term mean discharge of the Verdun gauging station (http://www.hydro.eaufrance.fr/). The results are given in Table 5. During the entire

simulation period, the water that flowed from the aquifer to the river accounted for 65 % of the total exchanged water volume (exchanged water volume in two directions). The low hydraulic period contributed 57 % of the water that flowed from the aquifer to the river. The main water flow from the river to the aquifer occurred during the high hydraulic period, which amounted to 97 % of the total flow in this direction.

Table 5. Simulated exchanged water quantity between river and aquifer in two hydraulic periods (low water period and high water period) throughout the simulated period (1993-2013) (A to R means from aquifer to river, R to A means from river to aquifer)

| Discharge | All | | Low (< 200 $m^3 \cdot s^{-1}$) | | | High (> 200 $m^3 \cdot s^{-1}$) | | |
|---|---|---|---|---|---|---|---|---|
| | Value | % | Value | %(total) | %(period) | Value | %(total) | %(period) |
| Number of days | 7670 | | 5348 | 0.70 | | 2322 | 0.30 | |
| Exchanged water (A to R) ($10^7 m^3$) | 13.21 | 0.65 | 7.47 | 0.57 | 0.98 | 5.74 | 0.43 | 0.46 |
| Exchanged water (R to A) ($10^7 m^3$) | 6.98 | 0.35 | 0.18 | 0.03 | 0.02 | 6.80 | 0.97 | 0.54 |
| Total ($10^7 m^3$) | 20.19 | | 7.65 | 0.38 | | 12.54 | 0.62 | |
| Daily average ($10^4 m^3 \cdot d^{-1}$) | 2.63 | | 1.43 | | | 5.40 | | |

In the low hydraulic period, the main water flow direction was from the aquifer to the river, which was 98 % of the total water exchange in this period. The low flow period represented 70 % of the simulated days, but the amount of exchanged water was only 38 % of the total volume.

During the high hydraulic period, more water flowed from the river to the aquifer than from the aquifer to the river (54:46). However, the difference between those two flow directions was not as high as it was during the low flow period. The daily average flow in this period ($5.40 \times 10^4$ $m^3 \cdot d^{-1}$) was much greater than during the low water period ($1.43 \times 10^4$ $m^3 \cdot d^{-1}$).

## 4.4 Discussion

The SWAT-LU model was modified by adding in the floodplain area the module simulating SW-GW water exchange at the river/groundwater interface. The algorithms calculating surface water and groundwater levels during flooding were also modified in agreement with the module. The comparison of simulations and observations proved that the modified model was able to reflect accurately the actual hydrological dynamics in the aquifer of the floodplain of the Garonne River. Darcy's equation was used to calculate water exchanges caused by the difference in hydraulic heads between the channel water and groundwater levels in $LU_1$ - hydraulic conductivities are important parameters for calculating

the SW-GW interaction (Sophocleous, 2002). The comparison of simulations and observed groundwater levels confirmed that the model can accurately simulate groundwater levels. Moreover, the simulated SW-GW exchange was verified by comparing it with the detected values of tracer from field samples and the simulated water exchange with a 2D distributed model: the 2SWEM model. The results demonstrated that the SWAT-LUD model was able to simulate SW-GW water exchange accurately in terms of fluxes.

The model was able to reproduce the two-way interactions occurring in SW-GW exchanges. The contribution of surface water to subsurface flow is not considered in most of the existing catchment scale models such as SWIM (Krysanova *et al.*, 1998), TOPMODEL (Franchini *et al.*, 1996) or MODHYDROLOG (Chiew and McMahon, 1994). However the results from this study showed its importance, since it accounted for 35 % of total SW-GW exchanges over a long period. The two-way interaction controls water mixing in the river/groundwater interface is an important driver in biogeochemical reactions occurring in this area (Amoros and Bornette, 2002). The SWAT-LUD model presented here provides a solid basis for further model development aiming at the simulation of biogeochemical processes in floodplain areas at catchment scale.

Previous research and this study have proven that discharge in the channel is the main driving factor of the SW-GW exchange in the study site (Peyrard *et al.*, 2008). As the main water flow direction during low hydraulic periods is from the aquifer to the river, the water mixing in river/groundwater interface occurs mainly during high hydraulic periods. Flooding has been proven to influence the plant communities of wetlands, both in terms of soil nitrate reduction and groundwater flow (Hughes, 1990; Casanova and Brock, 2000; Brettar *et al.*, 2002; Alaoui-Sossé *et al.*, 2005). In the present study, flooded water was found to be important for the SW-GW exchange process, which needs further investigation in future. As a daily step model, SWAT-LUD could not reflect the detailed processes occurring during flooding events. In this study, during flood periods the groundwater levels of LUs reached by floodwater were considered to have the same value as the river water levels. The time lag of water infiltration was not taken into account and as the LU has a unique groundwater level, the risk of overestimating infiltrated flooded water increased along with the increase of the width of LUs. Since the surface area of $LU_3$ is much larger than the two other LUs, if flooded water arrives in $LU_3$, the infiltrated flooded water could be more easily overestimated. The large flood that occurred during the calibration period reached $LU_3$. This probably explained the high simulated groundwater levels in $LU_2$ and $LU_1$ after the flooding event. The algorithm

is still simple and the simulated exchanged water volume should be compared with the results of a distributed model or observed data in a future study.

The water loss caused by plant evapotranspiration especially in the riparian forest zones were stated in many studies (Boronina *et al.*, 2005; Butler *et al.*, 2007; Gribovszki *et al.*, 2008). However because the groundwater table is usually beneath the root zone in the study site except during flood period, water uptake by plants is negligible and was not stated in this study. The influences of pumping on groundwater and river water flow were stated also in some researches (Hunt, 1999; Cooper *et al.*, 2003; Rassam and Werner, 2008). This process was not included in the model yet, but it could be easily added to the model as an output source of groundwater in the future study. Due to the chosen model philosophy, the pumped water in each LU would be summed together and influence of pumping on groundwater level fluctuation would be simulated at LU scale (in contrast to more complex procedures in physically based models).

As a semi-distributed model, the SWAT-LUD model cannot consider detailed topographic information. In the model, each LU has a unique slope value, and mean hydraulic conductivity. Since the model was applied at floodplain scale, the impermeable layer was considered to be flat in the model, the complex topography of channel and adjacent floodplain was only considered to be mean slope for each LU. Channel processes and SW-GW water exchange were calculated at subbasin scale. Moreover, the groundwater was assumed to be flowing in a horizontal direction (perpendicular to the river flow). The vertical gradient of the groundwater hydraulic heads shown in Figure 10 was not considered. The existence of the vertical gradient was explained by the height difference between simulated groundwater levels and the observed values of P30 in $LU_3$. In $LU_2$, piezometer P22 was located just behind an artificial dyke, which was built to protect agricultural land from flooding. Flooded water has to move to the top of the dyke before it arrives at P22. As the model could not consider this local detailed information, $LU_2$ was oversaturated compared with the observation from P22. In addition, the simulated groundwater levels represented the average situations of all the LUs, so it would be difficult for the output of the model to match data from one piezometer closely. Moreover, hydraulic conductivity was a mean value in each LU. However, in reality, hydraulic conductivities are extremely heterogeneous (Weng *et al.*, 2003), so the uncertainties of water level simulations as a result of mean values linked to the mean values of hydraulic conductivities could be important when compared to local piezometers. To evaluate the uncertainties, a sensitivity analysis of hydraulic conductivity would be required.

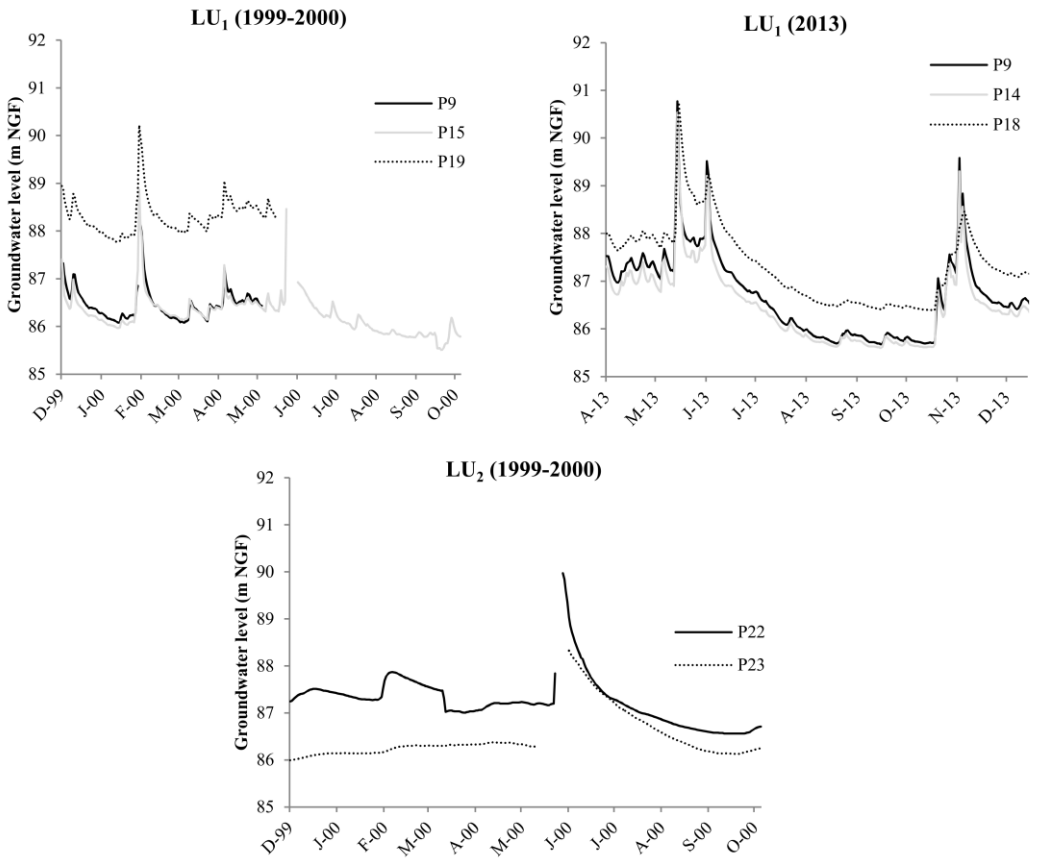


Figure 10. Observed groundwater levels in LUs with more than one piezometer equipped with a water level sensor.

The SWAT-LUD was not able to provide a detailed spatial distribution of hydraulic heads of the kind provided by physically-based models (MODFLOW(Sánchez-Pérez *et al.*, 2003b), MARTHE model (Weng *et al.*, 2003), 2SWEM (Peyrard *et al.*, 2008)). However, the objective of the study was not to provide accurate spatial representations of groundwater levels like the physically-based models, but to provide a good estimation of SW-GW interactions over a long timescale with a simple model. The model aimed to simulate large catchment sizes to support river basin water management. Therefore the complexity of physically-based models leading to long computation times for the simulation of small-scale areas (Lautz and Siegel, 2006b; Helton *et al.*, 2014) is not suitable. Moreover physically-based models need very detailed input information that can be difficult to collect, while this model needs only basic parameters. Nevertheless SWAT-LUD gave similar results for SW-GW interactions when compared with the physically-based 2SWEM model (Peyrard *et al.*,

2008). Although the shapes of the channels and LUs in the SWAT model were assumed to be straight and homogeneous, the values for exchanged water between river and aquifer simulated by the SWAT-LUD model were identical to the physically-based 2SWEM model. This showed that the SWAT-LUD model could accurately reflect the actual water exchange occurring at reach scale. SWAT-LUD was able to reproduce the spatial and temporal patterns of SW-GW exchanges at reach scale in a simple way, which means it can be used for large catchment simulation and to support river basin management studies.

## 4.5 Conclusions

This paper has described the new module of the SWAT-LUD model created to simulate surface water and floodplain groundwater. Darcy's equation was introduced to the model to simulate groundwater flow and SW-GW exchange occurring through the riverbank. The algorithms of river water and groundwater levels during flooding events were also modified. This new module was tested in a meander of the floodplain of the Garonne River in France. Comparisons between simulation results with observations from piezometers illustrated that the SWAT-LUD model could satisfactorily simulate groundwater levels near the area of the bank. Conservative tracer measured from field samples were used to validate the simulations, and SW-GW exchange modelling results with this approach corresponded well with the results obtained by a complex hydraulic model. This model was able to reflect accurately the actual water exchange between surface and subsurface systems of the alluvial plain of the Garonne River. River water discharge was found to have a great influence on the SW-GW exchange process. The main water flow direction was from groundwater to river, water flowed in this direction in the river/groundwater interface accounted for 65 % of the total exchanged water volume. The water mixing occurs mainly during high hydraulic periods. Flooded water was important for the SW-GW exchange process, it accounted for 69 % of total water flowed from the river to the aquifer. As a catchment-scale model, SWAT-LUD could easily be applied to a large catchment with basic available data. The SWAT-LUD model enabling simulation of GW-SW exchange processes at catchment scale would be a useful tool for evaluating the role of river buffer strips and wetlands in improving water quality. Future work should include: i) an application of the modified model in a larger catchment with multiple subbasins, and ii) the simulation of land management operations and biogeochemical processes in the river/groundwater interface.

Acknowledgements

We are grateful to N.B Sammons for her help with developing the module. This study was performed as part of the EU Interreg SUDOE IVB programme (ATTENAGUA - SOE3/P2/F558 project, http://www.attenagua-sudoe.eu) and funded by ERDF. This research has been carried out as a part of "ADAPT'EAU" (ANR-11-CEPL-008), a project supported by the French National Research Agency (ANR) within the framework of "The Global Environmental Changes and Societies (GEC&S) programme. X. Sun is supported by a grant from the China Scholarship Council (CSC).

References

Alaoui-Sossé B, Gérard B, Binet P, Toussaint M-L, Badot P-M. 2005. Influence of flooding on growth, nitrogen availability in soil, and nitrate reduction of young oak seedlings ( *Quercus robur* L.). *Annals of Forest Science* **62**: 593–600 DOI: 10.1051/forest:2005052

Almasri MN, Kaluarachchi JJ. 2007. Modeling nitrate contamination of groundwater in agricultural watersheds. *Journal of Hydrology* **343**: 211–229 DOI: 10.1016/j.jhydrol.2007.06.016

Amoros C, Bornette G. 2002. Connectivity and biocomplexity in waterbodies of riverine floodplains. *Freshwater Biology* **47**: 761–776 DOI: 10.1046/j.1365-2427.2002.00905.x

Arnold JG, Allen PM, Volk M, Williams JR, Bosch DD. 2010. Assessment of different representations of spatial variability on SWAT model performance. *Trans. ASABE* **53**: 1433–1443

Arnold JG, Srinivasan R, Muttiah RS, Williams JR. 1998. Large Area Hydrologic Modeling and Assessment Part I: Model Development1. *JAWRA Journal of the American Water Resources Association* **34**: 73–89 DOI: 10.1111/j.1752-1688.1998.tb05961.x

Arrate I, Sanchez-Perez JM, Antiguedad I, Vallecillo MA, Iribar V, Ruiz M. 1997. Groundwater pollution in Quaternary aquifer of Vitoria : Gasteiz (Basque Country, Spain): Influence of agricultural activities and water-resource management. *Environmental geology* **30**: 257–265 DOI: 10.1007/s002540050155

Boronina A, Golubev S, Balderer W. 2005. Estimation of actual evapotranspiration from an alluvial aquifer of the Kouris catchment (Cyprus) using continuous streamflow records. *Hydrological Processes* **19**: 4055–4068 DOI: 10.1002/hyp.5871

Bosch DD, Arnold JG, Volk M, Allen PM. 2010. Simulation of a low-gradient coastal plain watershed using the SWAT landscape model. *Trans. ASABE* **53**: 1445–1456

Boulton AJ, Findlay S, Marmonier P, Stanley EH, Valett HM. 1998. The Functional Significance of the Hyporheic Zone in Streams and Rivers. *Annual Review of Ecology and Systematics* **29**: 59–81 DOI: 10.1146/annurev.ecolsys.29.1.59

Brunke M, Gonser T. 1997. The ecological significance of exchange processes between rivers and groundwater. *Freshwater Biology* **37**: 1–33 DOI: 10.1046/j.1365-2427.1997.00143.x

Butler JJ, Kluitenberg GJ, Whittemore DO, Loheide SP, Jin W, Billinger MA, Zhan X. 2007. A field investigation of phreatophyte-induced fluctuations in the water table. *Water Resources Research* **43**: W02404 DOI: 10.1029/2005WR004627

Casanova MT, Brock MA. 2000. How do depth, duration and frequency of flooding influence the establishment of wetland plant communities? *Plant Ecology* **147**: 237–250 DOI: 10.1023/A:1009875226637

Chiew F, McMahon T. 1994. Application of the daily rainfall-runoff model MODHYDROLOG to 28 Australian catchments. *Journal of Hydrology* **153**: 383–416 DOI: 10.1016/0022-1694(94)90200-3

Cooper DJ, D'amico DR, Scott ML. 2003. Physiological and Morphological Response Patterns of Populus deltoides to Alluvial Groundwater Pumping. *Environmental Management* **31**: 0215–0226 DOI: 10.1007/s00267-002-2808-2

Cox MH, Su GW, Constantz J. 2007. Heat, Chloride, and Specific Conductance as Ground Water Tracers near Streams. *Ground Water* **45**: 187–195 DOI: 10.1111/j.1745-6584.2006.00276.x

Fohrer N, Dietrich A, Kolychalow O, Ulrich U. 2014. Assessment of the Environmental Fate of the Herbicides Flufenacet and Metazachlor with the SWAT Model. *Journal of Environment Quality* **43**: 75 DOI: 10.2134/jeq2011.0382

Franchini M, Wendling J, Obled C, Todini E. 1996. Physical interpretation and sensitivity analysis of the TOPMODEL. *Journal of Hydrology* **175**: 293–338 DOI: 10.1016/S0022-1694(96)80015-1

Grannemann NG, Sharp Jr. JM. 1979. Alluvial hydrogeology of the lower Missouri River valley. *Journal of Hydrology* **40**: 85–99 DOI: 10.1016/0022-1694(79)90089-1

Gribovszki Z, Kalicz P, Szilágyi J, Kucsara M. 2008. Riparian zone evapotranspiration estimation from diurnal groundwater level fluctuations. *Journal of Hydrology* **349**: 6–17 DOI: 10.1016/j.jhydrol.2007.10.049

Hancock PJ, Boulton AJ, Humphreys WF. 2005. Aquifers and hyporheic zones: Towards an ecological understanding of groundwater. *Hydrogeology Journal* **13**: 98–111 DOI: 10.1007/s10040-004-0421-6

Harvey JW, Bencala KE. 1993. The Effect of streambed topography on surface-subsurface water exchange in mountain catchments. *Water Resources Research* **29**: 89–98 DOI: 10.1029/92WR01960

Harvey RW, George LH, Smith RL, LeBlanc DR. 1989. Transport of microspheres and indigenous bacteria through a sandy aquifer: results of natural- and forced-gradient tracer experiments. *Environmental Science & Technology* **23**: 51–56 DOI: 10.1021/es00178a005

Helton AM, Poole GC, Payn RA, Izurieta C, Stanford JA. 2014. Relative influences of the river channel, floodplain surface, and alluvial aquifer on simulated hydrologic residence time in a montane river floodplain. *Geomorphology* **205**: 17–26 DOI: 10.1016/j.geomorph.2012.01.004

Hughes FMR. 1990. The Influence of Flooding Regimes on Forest Distribution and Composition in the Tana River Floodplain, Kenya. *The Journal of Applied Ecology* **27**: 475 DOI: 10.2307/2404295

Hunt B. 1999. Unsteady Stream Depletion from Ground Water Pumping. *Ground Water* **37**: 98–102 DOI: 10.1111/j.1745-6584.1999.tb00962.x

Hussein M, Schwartz FW. 2003. Modeling of flow and contaminant transport in coupled stream–aquifer systems. *Journal of Contaminant Hydrology* **65**: 41–64 DOI: 10.1016/S0169-7722(02)00229-2

Iribar A, Sánchez-Pérez JM, Lyautey E, Garabétian F. 2008. Differentiated free-living and sediment-attached bacterial community structure inside and outside denitrification hotspots in the river–groundwater interface. *Hydrobiologia* **598**: 109–121 DOI: 10.1007/s10750-007-9143-9

Jayakrishnan R, Srinivasan R, Santhi C, Arnold JG. 2005. Advances in the application of the SWAT model for water resources management. *Hydrological Processes* **19**: 749–762 DOI: 10.1002/hyp.5624

Jégo G, Martínez M, Antigüedad I, Launay M, Sanchez-Pérez JM, Justes E. 2008. Evaluation of the impact of various agricultural practices on nitrate leaching under the root zone of potato and sugar beet using the STICS soil-crop model. *The Science of the Total Environment* **394**: 207–221 DOI: 10.1016/j.scitotenv.2008.01.021

Jégo G, Sánchez-Pérez JM, Justes E. 2012. Predicting soil water and mineral nitrogen contents with the STICS model for estimating nitrate leaching under agricultural fields. *Agricultural Water Management* **107**: 54–65 DOI: 10.1016/j.agwat.2012.01.007

Kim NW, Chung IM, Won YS, Arnold JG. 2008. Development and application of the integrated SWAT–MODFLOW model. *Journal of Hydrology* **356**: 1–16 DOI: 10.1016/j.jhydrol.2008.02.024

Kollet SJ, Maxwell RM. 2006. Integrated surface–groundwater flow modeling: A free-surface overland flow boundary condition in a parallel groundwater flow model. *Advances in Water Resources* **29**: 945–958 DOI: 10.1016/j.advwatres.2005.08.006

Krause S, Bronstert A. 2007. The impact of groundwater–surface water interactions on the water balance of a mesoscale lowland river catchment in northeastern Germany. *Hydrological Processes* **21**: 169–184 DOI: 10.1002/hyp.6182

Krause S, Tecklenburg C, Munz M, Naden E. 2013. Streambed nitrogen cycling beyond the hyporheic zone: Flow controls on horizontal patterns and depth distribution of nitrate and dissolved oxygen in the upwelling groundwater of a lowland river. *Journal of Geophysical Research: Biogeosciences* **118**: 54–67 DOI: 10.1029/2012JG002122

Krysanova V, Müller-Wohlfeil D-I, Becker A. 1998. Development and test of a spatially distributed hydrological/water quality model for mesoscale watersheds. *Ecological Modelling* **106**: 261–289 DOI: 10.1016/S0304-3800(97)00204-4

Lam QD, Schmalz B, Fohrer N. 2010. Modelling point and diffuse source pollution of nitrate in a rural lowland catchment using the SWAT model. *Agricultural Water Management* **97**: 317–325 DOI: 10.1016/j.agwat.2009.10.004

Lancaster RR. 2005. Fluvial Evolution of the Garonne River, France: Integrating Field Data with Numerical Simulations Available at: http://etd.lsu.edu/docs/available/etd-11172005-131031/ [Accessed 30 June 2014]

Langergraber G, Šimůnek J. 2005. Modeling Variably Saturated Water Flow and Multicomponent Reactive Transport in Constructed Wetlands. *Vadose Zone Journal* **4**: 924 DOI: 10.2136/vzj2004.0166

Lautz LK, Siegel DI. 2006. Modeling surface and ground water mixing in the hyporheic zone using MODFLOW and MT3D. *Advances in Water Resources* **29**: 1618–1633 DOI: 10.1016/j.advwatres.2005.12.003

Liu A, Ming J, Ankumah RO. 2005. Nitrate contamination in private wells in rural Alabama, United States. *Science of The Total Environment* **346**: 112–120 DOI: 10.1016/j.scitotenv.2004.11.019

Loague K, VanderKwaak JE. 2004. Physics-based hydrologic response simulation: platinum bridge, 1958 Edsel, or useful tool. *Hydrological Processes* **18**: 2949–2956 DOI: 10.1002/hyp.5737

Malard F, Tockner K, Dole-Olivier M-J, Ward JV. 2002. A landscape perspective of surface–subsurface hydrological exchanges in river corridors. *Freshwater Biology* **47**: 621–640 DOI: 10.1046/j.1365-2427.2002.00906.x

Morrice JA, Valett HM, Dahm CN, Campana ME. 1997. Alluvial Characteristics, Groundwater–Surface Water Exchange and Hydrological Retention in Headwater Streams. *Hydrological Processes* **11**: 253–267 DOI: 10.1002/(SICI)1099-1085(19970315)11:3<253::AID-HYP439>3.0.CO;2-J

Naiman RJ, Decamps H. 1997. The Ecology of Interfaces: Riparian Zones. *Annual Review of Ecology and Systematics* **28**: 621–658

Neitsch SL, Arnold JG, Kiniry JR, Williams JR. 2009. Soil and Water Assessment Tool, Theoretical Documentation, Version 2009

Orghidan T. 1959. Ein neuer lebensraum des unterirdischen Wassers: Der hvporheische Biotop. *Archiv für Hydrobiologie*: 392–414

Park SS, Lee YS. 2002. A water quality modeling study of the Nakdong River, Korea. *Ecological Modelling* **152**: 65–75 DOI: 10.1016/S0304-3800(01)00489-6

Peyrard D. 2008. Un modèle hydrobiogéochimique pour décrire les échanges entre l'eau de surface et la zone hyporhéique de grandes plaines alluviales.phd, Université de Toulouse, Université Toulouse III - Paul Sabatier. Available at: http://thesesups.ups-tlse.fr/549/ [Accessed 28 February 2014]

Peyrard D, Sauvage S, Vervier P, Sanchez-Perez JM, Quintard M. 2008. A coupled vertically integrated model to describe lateral exchanges between surface and subsurface in large alluvial floodplains with a fully penetrating river. *Hydrological Processes* **22**: 4257–4273 DOI: 10.1002/hyp.7035

Rassam DW, Werner A. 2008. *Review of groundwater-surfacewater interaction modelling approaches and their suitability for Australian conditions*. eWater Cooperative Research Centre. Available at: http://www.ewater.com.au/uploads/files/Rassam_Werner-2008-Groundwater_Review.pdf [Accessed 16 March 2015]

Rathjens H, Oppelt N, Bosch DD, Arnold JG, Volk M. 2015. Development of a grid-based version of the SWAT landscape model. *Hydrological Processes* **29**(6): 900-914 DOI: 10.1002/hyp.10197

Romanowicz AA, Vanclooster M, Rounsevell M, La Junesse I. 2005. Sensitivity of the SWAT model to the soil and land use data parametrisation: a case study in the Thyle catchment, Belgium. *Ecological Modelling* **187**: 27–39 DOI: 10.1016/j.ecolmodel.2005.01.025

Sabater S, Butturini A, Clement J-C, Burt T, Dowrick D, Hefting M, Matre V, Pinay G, Postolache C, Rzepecki M, et al. 2003. Nitrogen Removal by Riparian Buffers along a European Climatic Gradient: Patterns and Factors of Variation. *Ecosystems* **6**: 0020–0030 DOI: 10.1007/s10021-002-0183-8

Sánchez-Pérez JM, Trémolières M. 2003. Change in groundwater chemistry as a consequence of suppression of floods: the case of the Rhine floodplain. *Journal of Hydrology* **270**: 89–104 DOI: 10.1016/S0022-1694(02)00293-7

Sánchez-Pérez JM, Antiguedad I, Arrate I, García-Linares C, Morell I. 2003a. The influence of nitrate leaching through unsaturated soil on groundwater pollution in an agricultural area of the Basque country: a case study. *Science of The Total Environment* **317**: 173–187 DOI: 10.1016/S0048-9697(03)00262-6

Sánchez-Pérez JM, Bouey C, Sauvage S, Teissier S, Antiguedad I, Vervier P. 2003b. A standardised method for measuring in situ denitrification in shallow aquifers: numerical validation and measurements in riparian wetlands. *Hydrology and Earth System Sciences* **7**: 87–96 DOI: 10.5194/hess-7-87-2003

Sanchez-Perez JM, Tremolieres M, Carbiener R. 1991a. Une station d'épuration naturelle des phosphates et nitrates apportés par les eaux de débordement du Rhin : la forêt alluviale à frêne et orme. *Comptes rendus de l'Académie des sciences. Série 3, Sciences de la vie* **312**: 395–402

Sanchez-Perez JM, Tremolieres M, Schnitzler A, Carbiener R. 1991b. Evolution de la qualité physico-chimique des eaux de la frange superficielle de la nappe phréatique en fonction du cycle saisonnier et des stades de succession des forêts alluviales rhénanes (Querco-Ulmetum minoris Issl. 24). *Acta oecologica : (1990)* **12**: 581–601

Sánchez-Pérez JM, Vervier P, Garabétian F, Sauvage S, Loubet M, Rols JL, Bariac T, Weng P. 2003c. Nitrogen dynamics in the shallow groundwater of a riparian wetland zone of the Garonne, SW France: nitrate inputs, bacterial densities, organic matter supply and denitrification measurements. *Hydrology and Earth System Sciences Discussions* **7**: 97–107

Seltz R. 2001. Analyse et modélisation d'une zone humide riveraine de la Garonne. l'Ecole de Physique du Globe de Strasbourg 1,81pp.

Sophocleous M. 2002. Interactions between groundwater and surface water: the state of the science. *Hydrogeology Journal* **10**: 52–67 DOI: 10.1007/s10040-001-0170-8

Sophocleous M, Perkins SP. 2000. Methodology and application of combined watershed and ground-water models in Kansas. *Journal of Hydrology* **236**: 185–201 DOI: 10.1016/S0022-1694(00)00293-6

Storey RG, Howard KWF, Williams DD. 2003. Factors controlling riffle-scale hyporheic exchange flows and their seasonal changes in a gaining stream: A three-dimensional groundwater flow model. *Water Resources Research* **39**: 1034 DOI: 10.1029/2002WR001367

Takatert N, Sanchez-Pérez JM, Trémolières M. 1999. Spatial and temporal variations of nutrient concentration in the groundwater of a floodplain: effect of hydrology, vegetation and substrate. *Hydrological Processes* **13**: 1511–1526 DOI: 10.1002/(SICI)1099-1085(199907)13:10<1511::AID-HYP828>3.0.CO;2-F

Vervier P, Bonvallet-Garay S, Sauvage S, Valett HM, Sanchez-Perez J-M. 2009. Influence of the hyporheic zone on the phosphorus dynamics of a large gravel-bed river, Garonne River, France. *Hydrological Processes* **23**: 1801–1812 DOI: 10.1002/hyp.7319

Volk M, Arnold JG, Bosch DD, Allen PM, Green CH. 2007. Watershed configuration and simulation of landscape processes with the SWAT model. In *MODSIM 2007 International Congress on Modelling and Simulation. Modelling and Simulation Society of Australia and New Zealand, Canberra, Australia*74–80. Available at: http://www.mssanz.org.au.previewdns.com/MODSIM07/papers/43_s47/Watersheds47_Volk_.pdf [Accessed 1 September 2014]

Weng P, Sánchez-Pérez JM, Sauvage S, Vervier P, Giraud F. 2003. Assessment of the quantitative and qualitative buffer function of an alluvial wetland: hydrological modelling of a large floodplain (Garonne River, France). *Hydrological Processes* **17**: 2375–2392 DOI: 10.1002/hyp.1248

White DS. 1993. Perspectives on Defining and Delineating Hyporheic Zones. *Journal of the North American Benthological Society* **12**: 61–69 DOI: 10.2307/1467686

Woessner WW. 2000. Stream and Fluvial Plain Ground Water Interactions: Rescaling Hydrogeologic Thought. *Ground Water* **38**: 423–429 DOI: 10.1111/j.1745-6584.2000.tb00228.x

Wondzell SM. 2011. The role of the hyporheic zone across stream networks. *Hydrological Processes* **25**: 3525–3532 DOI: 10.1002/hyp.8119

Wroblicky GJ, Campana ME, Valett HM, Dahm CN. 1998. Seasonal variation in surface-subsurface water exchange and lateral hyporheic area of two stream-aquifer systems. *Water Resources Research* **34**: 317–328 DOI: 10.1029/97WR03285

Zhang Q, Li L. 2009. Development and application of an integrated surface runoff and groundwater flow model for a catchment of Lake Taihu watershed, China. *Quaternary International* **208**: 102–108 DOI: 10.1016/j.quaint.2008.10.015

# Chapter 5. Assessment of the denitrification process in alluvial wetlands at floodplain scale using SWAT model.

This chapter describes the new module developed to represent the denitrification in the shallow aquifer of alluvial floodplains and its application in Monbéqui site based on the study of chapter 4. Nitrate exchanges in the shallow aquifer caused by the recharged river water through both lateral (river bank) and vertical (surface) infiltration and the influence of flooding on nitrate leaching were considered. The influences of both dissolved organic carbon (DOC) and particulate organic carbon (POC) on denitrification were evaluated. The measured groundwater nitrate concentration in 2005 and 2013 and the simulated infiltrated water and nitrate of STICS model were applied to calibrate the modified model. The nitrate flux and denitrification rate occurred in the shallow aquifer of Monbéqui site were quantified. This chapter written in the publication submitted to Ecological Engineering.

# Assessment of the denitrification process in alluvial wetlands at floodplain scale using SWAT model

**X. Sun[1,2], L. Bernard-Jannin[1,2], S. Sauvage[1,2], C. Garneau [1,2] , J.G. Arnold[3], R. Srinivasan[4],**

**JM Sánchez-Pérez[1,2*]**

*[1] University of Toulouse; INPT, UPS; Laboratoire Ecologie Fonctionnelle et Environnement (EcoLab), Avenue de l'Agrobiopole, 31326 Castanet Tolosan Cedex, France*

*[2] CNRS, EcoLab, 31326 Castanet Tolosan Cedex, France*

*[3] Grassland, Soil & Water Research Laboratory USDA-ARS, Temple, TX 76502, USA*

*[4] Spatial Science Laboratory in the Department of Ecosystem Science and Management, Texas A&M University, College Station, TX 77845, USA*

*Corresponding author

E-mail: jose-miguel.sanchez-perez@univ-tlse3.fr

Tel: 33 (0)5 34 32 39 20 Fax: 33 (0)5 34 32 39 01

Address: Laboratoire d'Ecologie Fonctionnelle et Environnement (ECOLAB), UMR 5245 CNRS-UPS-INPT Ecole Nationale Supérieure Agronomique de Toulouse (ENSAT) Avenue de l'Agrobiopole BP 32607, Auzeville Tolosane 31326 CASTANET TOLOSAN Cedex FRANCE

**Abstract:** As alluvial plains support intensive agricultural activities, they often suffer from groundwater nitrate pollution. Denitrification is recognised as an important process in nitrate pollution control in the riparian zone. In shallow aquifer zones influenced by recharged surface water, denitrification efficiently attenuates nitrate in groundwater as well, and the exchange between surface water and groundwater has a significant impact on the occurrence of denitrification. Denitrification is simulated in numerous models, however most models do not take account of the denitrification occurring in shallow aquifers or the influence of recharge surface water in the alluvial aquifer with organic carbon and bacteria. In this study, a new module was developed that represents the occurrence of denitrification in the shallow aquifer of alluvial floodplains. Nitrate exchanges in the shallow aquifer caused by the recharged river water through both lateral (river bank) and vertical (surface) infiltration and the influence of flooding on nitrate leaching were added to the SWAT-LUD model (SWAT-Landscape Unit Darcy). The influences of both dissolved organic carbon (DOC) and particulate organic carbon (POC) on denitrification were evaluated. The modified model was

applied on an experimental site located in the floodplain of the Garonne River (southwest France). Results showed that the modified SWAT-LUD model was able to simulate the aquifer nitrate concentration in the near bank zone (riparian zone) satisfactorily. The near bank zone in the floodplain played the most important role in attenuating nitrate through denitrification. The annual denitrification rate in the near bank zone was around 130 kg N-$NO_3^-$·$ha^{-1}$·$y^{-1}$, and around 40 % of the nitrate input to this zone was denitrified. POC is more important than DOC in the denitrification process, especially in the near bank zone, where 98 % of the nitrate was attenuated by POC. Relationships between denitrification rates, groundwater levels and total input nitrate masses in the near bank zone were determined. The results illustrated that groundwater levels were positively related to the denitrification rates in the near bank zone, the absolute denitrification rate increased along with the increase in nitrate content, and the relative consumption rate by denitrification decreased as the nitrate content increased.

**Keyword**s: SWAT-LUD model; denitrification; floodplain aquifer; Garonne River

## 5.1 Introduction

Nitrate pollution in surface water and groundwater systems has attracted worldwide attention (Bijay-Singh *et al.*, 1995; Carpenter *et al.*, 1998; Jalali, 2011). Excess nitrate in water bodies can cause eutrophication and impact aquatic ecosystems, also potentially causing health problems such as methaemoglobinaemia and cancer (McIsaac *et al.*, 2001; Camargo and Alonso, 2006). The European Union and the World Health Organization have set the standard for nitrate concentration at 50 mg·$l^{-1}$ for drinking water.

Agricultural activities are known to be a significant source of nitrate in groundwater (Hamilton and Helsel, 1995; Almasri and Kaluarachchi, 2004; Liu *et al.*, 2005b). As alluvial plains support intensive agricultural activities, they often suffer from groundwater nitrate pollution (Sánchez Pérez et al., 2003a; Liu et al., 2005; Arrate et al., 1997; Almasri and Kaluarachchi, 2007). Studies have shown that due to the rich content of oxygen and organic matter in surface water and abundant nutriment elements in groundwater, the water mix between those two systems contributes to nitrogen retention and/or transformation of the land-surface water continuum (Sabater *et al.*, 2003). The surface-groundwater interface supports the purification of water by eliminating nitrates during their infiltration through the vegetation-soil system to groundwater and through diffusion from groundwater to surface

water (Sanchez-Perez *et al.*, 1991a, 1991b; Takatert *et al.*, 1999). An understanding of nitrate attenuation processes occurring at the surface-groundwater interface would enhance understanding of nitrate cycling at catchment scale.

Riparian zones serve as interfaces between terrestrial and aquatic ecosystems and have proven to be efficient nitrate removal tools (Osborne and Kovacic, 1993; Lowrance *et al.*, 1997; Dosskey *et al.*, 2010). The dominant nitrate attenuation processes in riparian zones are plant uptake, denitrification and microbial immobilisation, of which denitrification has been recognised as the most important of these processes (Korom, 1992; Rivett *et al.*, 2008; Ranalli and Macalady, 2010; Vidon *et al.*, 2010). However, most of the studies have focused on riparian zones with shallow groundwater levels, with high moisture and high organic carbon storage in the soil profile triggering intense denitrification (Cooper, 1990; Hill, 1996; Burgin and Hamilton, 2007; Ranalli and Macalady, 2010). The hydrological conditions at the river/groundwater interfaces have been shown to have a significant impact on denitrifying processes in aquifers (Lamontagne *et al.*, 2005; Rassam *et al.*, 2008). In riparian zones where groundwater levels are lower than soil root zones, denitrification has been found to attenuate nitrate efficiently in groundwater. In these conditions, the recharged river water, rich in organic matter, has stimulated the occurrence of denitrification (Iribar, 2007; Sánchez-Pérez et al., 2003b).

Organic carbon is the 'energy' required to denitrify bacteria in the denitrification process. The complex composition of organic carbon in ecosystems makes it difficult to identify the effective carbon source (Hume *et al.*, 2002; Dodla *et al.*, 2008). Dissolved organic carbon (DOC) or bioavailable dissolved organic carbon (BDOC) have been taken as carbon sources of denitrification in most studies (Hill et al., 2000; Inwood et al., 2005; Peterson et al., 2013, Iribar et al., 2015). Furthermore, particulate organic carbon (POC) has been found to enhance the denitrification rate in aquatic and terrestrial ecosystems as well (Arango *et al.*, 2007; Stevenson *et al.*, 2011; Stelzer *et al.*, 2014). The DOC in groundwater is less bioavailable than DOC in rivers (Stutter *et al.*, 2013; Shen *et al.*, 2014), and DOC in recharged river water has been found to alter the composition and bioavailability of DOC in the groundwater mixing zone (Wong and Williams, 2010).

Since denitrification is highly variable spatially and temporally, modelling has proved to be an efficient tool for estimating the denitrification rate, especially on large spatial scales. Denitrification is simulated in numerous models. Heinen (2006) has introduced more than 50

models that include denitrification, such as the EPIC model (Marchetti *et al.*, 1997), the DAICY model (Hansen *et al.*, 1991) and the REMM model (Lowrance *et al.*, 2000). However, most of the models only simulate the denitrification process in the soil profile. Peyrard et al. (2011) has developed a 1D model to simulate denitrification in the hyporheic zone, but as a reach scale model, the influence of the surrounding landscape, such as agricultural activities, is not simulated in the model. The Soil and Water Assessment Tool (SWAT) is a physically-based, deterministic, continuous, watershed-scale simulation model allowing a number of different physical processes to be simulated in a watershed, which has been successfully applied all over the world (Jayakrishnan *et al.*, 2005; Romanowicz *et al.*, 2005; Fohrer *et al.*, 2013). Studies have been carried out to simulate nitrate pollution on a catchment scale with SWAT (Ferrant *et al.*, 2011, 2013; Boithias *et al.*, 2014; Cerro *et al.*, 2014). However, the simulation of the two-direction water exchange between river and groundwater occurring in the floodplain has not been simulated in the SWAT model. To solve this problem, a new structure called a landscape unit (LU) was developed and Darcy's equation was used to simulate the water exchange in the river/groundwater interface. The modified model was called SWAT-LUD (SWAT-Landscape Unit Darcy) (Sun et al., in press). Nevertheless, denitrification occurring at the river-groundwater interface was still not being taken into account.

The main objectives of this study were: i) to add the simulation of denitrification in the SWAT-LUD model, ii) to apply the modified SWAT-LUD to the alluvial floodplain of the Garonne River, iii) to quantify the dynamic nitrate removal rate through denitrification, iv) to quantify the nitrate circulation in the floodplain of the Garonne River, and v) to determine key parameters involved in denitrification processes.

## 5.2 Methodology

### 5.2.1 SWAT-LUD model

The Soil and Water Assessment Tool (SWAT) model is a semi-distributed, watershed-scale and continuous time model that operates on a daily time step (Arnold *et al.*, 1998). In SWAT, the watershed is divided into subbasins; subbasins are then separated into hydrologic response units (HRUs), which are the lumped area comprising the unique combination of land cover, soil type and slope. Processes have been simulated for each HRU and then aggregated into a subbasin by weighted average (Arnold *et al.*, 1998; Lam *et al.*, 2010).

With the traditional HRU delineation method, flow was not routed across the landscape. To represent the natural downward flow path, a new structure called a landscape unit (LU) was developed and the modified model called the SWAT-LU model. Each subbasin consisted of three LUs: the divide, the hillslope and the valley bottom. HRUs were distributed across the different LUs (Volk *et al.*, 2007; Arnold *et al.*, 2010; Bosch *et al.*, 2010; Rathjens *et al.*, 2014). Via this structure, processes in each HRU were still computed separately, but instead of being summed at the subbasin scale, they were summed at the LU scale. Surface runoff, lateral and groundwater flow from $LU_3$ (the divide) were routed through $LU_2$ (the hillslope) to $LU_1$ (the valley bottom) and then entered the river. However, the SWAT-LU model did not involve the surface water-groundwater (SW-GW) exchange function and the influence of flooding on groundwater. Since SW-GW exchange mainly occurs in the alluvial plain, a new type of subbasin called a subbasin-LU was developed to represent the floodplain area and the LU structure was applied to the subbasin-LU. Processes in the upland area were calculated using the original SWAT model, and upland and subbasin-LU were connected through the river. A new module was added to the SWAT-LU model to simulate the SW-GW exchange. In this module, Darcy's equation was applied to quantify exchanged water based on the LU structure. The influence of flooding on groundwater levels was simulated, and the transfer of dissolved elements between LUs and between LUs and surface water was also included in the model. Furthermore, the algorithm of the influence of flooding on river water level was modified. The modified model is called the SWAT-LUD model (Sun et al., in press). The location of LUs and the water flow path in a subbasin-LU are shown in Figure 1, and a detailed description can be found in Volk et al. (2007), Arnold et al. (2010) and Sun et al. (in press).

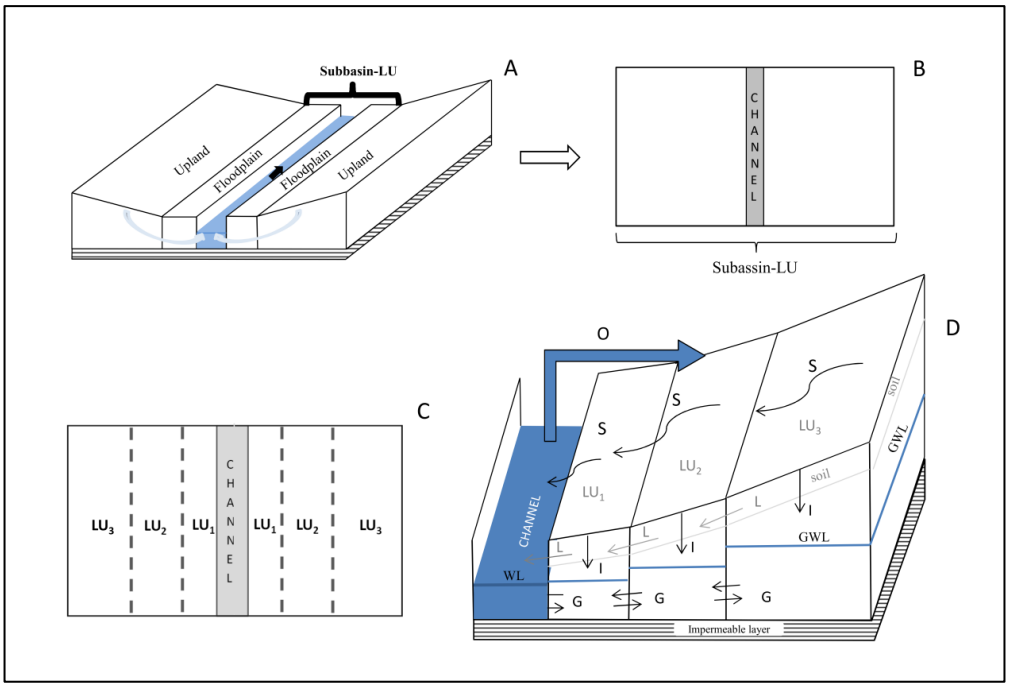


**Figure 1.** Location of subbasin-LU and the landscape unit (LU) structure in the SWAT-LUD model. The figure shows the hydrological processes: 'A' represents the location of subbasin-LU, 'B' represents subbasin-LU, 'C' represents the distribution of LUs in the subbasin-LU (plane), and 'D' represents the hydrologic processes in the landscape units where 'S' is surface flow, 'L' is lateral flow, 'I' is infiltration, 'G' is groundwater flow, 'O' is overbank flow, 'GWL' is groundwater level and 'WL' is river water level (according to Volk et al., 2007 and Arnold et al., 2010) (extracted from Sun et al. (in press))

### 5.2.2 Nitrogen cycle in the SWAT-LUD model

#### 5.2.2.1 Nitrogen cycle in soil profile

In the SWAT-LUD model, nitrogen cycles in the soil profile were kept as in the SWAT model except that the calculation of denitrification was replaced by equation 2.2.2.2. The nitrogen in the soil profile was separated into five pools. Two of the pools were inorganic forms, $NH_4^+$ and $NO_3^-$, while the other three were organic forms: fresh organic N, active humus and stable humus. The growth cycles of plants were simulated, which was a simplified version of the EPIC plant growth model (Williams et al., 1999). The management operations that control the plant growth cycle, such as planting, harvest, tillage, fertilisation application and pesticide application, were applied in each HRU (Neitsch *et al.*, 2009). All of these functions were retained in the SWAT-LUD model. The fluxes of nitrate in surface flow and lateral flow were modified in the SWAT-LUD model, such as water flow, and nitrate flowing from $LU_3$, passing through $LU_2$, entering $LU_1$ and then flowing into the river.

#### 5.2.2.2 Nitrate cycle in shallow aquifer

Nitrate cycling in the shallow aquifer was simulated in the SWAT model. The main processes were uptake by plants, percolation from the soil profile (equation 2.2.2.1), recharge to the deep aquifer, and flux into the main channel. A decay rate of nitrate in the shallow aquifer was also simulated (Neitsch *et al.*, 2009). In SWAT-LUD, the processes of percolation from soil profile, uptake by plant and the recharge to the deep aquifer remained as in the SWAT model. The decay of nitrate was replaced by denitrification, which was calculated with equation 2.2.2.2. The nitrate flow was calculated as a dissolved element in the shallow groundwater, flowing between LUs and between LUs and surface water, rather than flowing from each HRU into the main channel directly. The detailed description of the calculation of the transfer of dissolved elements can be found in Sun et al. (in press).

The recharge of nitrate from the soil profile to the aquifer layer was calculated as follows:

$$NO_{3_{rchrg,i}} = \left(1 - exp\left[-1/\sigma_{gw}\right]\right) \times NO_{3_{perc}} + exp\left[-1/\sigma_{gw}\right] \times NO_{3_{rchrg,i-1}} \quad 2.2.2.1$$

where $NO_{3_{rchrg,i}}$ is the amount of nitrate in recharge entering the aquifers on day i (kg N-$NO_3^-$·ha$^{-1}$), $\sigma_{gw}$is the delay time for aquifer recharge (days), $NO_{3_{perc}}$is the total amount of nitrate exiting the bottom of the soil profile on day i (kg N-$NO_3^-$·ha$^{-1}$), and $NO_{3_{rchrg,i-1}}$is the amount of nitrate in recharge entering the aquifers on the day i-1.

The nitrate and organic carbon degradation equations in the study of Peyrard et al. (2011) were introduced into the SWAT-LUD model. The nitrate degradation is taken as denitrification, and the influences of both POC and DOC on denitrification were taken into account.

The denitrification rate was calculated as follows:

$$R_{NO_3} = -0.8(\rho \cdot (1-\varphi)/\varphi \cdot k_{POC}[POC] \cdot 10^6/M_c + k_{DOC}[DOC]) \cdot [NO_3]/(k_{NO_3} + [NO_3]) \quad 2.2.2.2$$

where $R_{NO_3}$ is the denitrification rate (μmol·l$^{-1}$·d$^{-1}$), $\rho$ is dry sediment density (kg·dm$^{-3}$), $\varphi$ is sediment porosity, $k_{POC}$ is mineralisation rate constant of POC (particulate organic carbon) (d$^{-1}$), *POC* is the POC content in the soil and aquifer sediment (‰), $M_c$ is carbon molar mass (g·mol$^{-1}$), *DOC* is the concentration of DOC in the aquifer water (μmol·l$^{-1}$) $k_{DOC}$ is the mineralisation rate constant of DOC (dissolved organic carbon) (d$^{-1}$), $k_{NO_3}$is half-saturation for nitrate limitation (μmol·l$^{-1}$) and $NO_3$ is the nitrate concentration in the aquifer water (μmol·l$^{-1}$).

#### 5.2.2.3 Nitrate leaching during flood periods

On flood days, the portion of the nitrate storage in the soil profile was considered as having infiltrated into the aquifer along with infiltrated floodwater:

$$M_{NO_{3,i}} = M_{NO_{3,i-1}} + I_{NO_3,i} \qquad 2.2.3.1$$

$$I_{NO_{3,i}} = F_{NO_3} \times M_{NO_{3,soil,i}} \qquad 2.2.3.2$$

where $M_{NO_{3,i}}$ is the mass content of nitrate in the LU (g N-$NO_3^-$) on day i, $M_{NO_{3,i-1}}$ is the mass content of nitrate in the LU (g N-$NO_3^-$) on day i-1, $I_{NO_3}$ is the infiltrated nitrate from the soil profile into the aquifer during flood events on day i, $F_{NO_3}$ is the coefficient (%) and $M_{NO_{3,soil}}$ is the mass content of nitrate in the soil profile of LU (g N-$NO_3^-$) on day i.

### 5.2.3 Organic carbon in SWAT-LUD

The flux and content of DOC was not simulated in the SWAT model. In the SWAT-LUD model, the flux of DOC in the shallow aquifer was included, which was simulated as a dissolved element such as nitrate. As the fluctuations of DOC were small in the aquifers of the region that far away from the river, the concentrations of DOC in $LU_2$ and $LU_3$ were assumed to be constant and the values were read as input values. DOC in the river water was assumed to be constant as well except during flood periods. As the concentration of DOC in the river water significantly increased during flooding days (Dalzell *et al.*, 2005; Arango *et al.*, 2007; Duan *et al.*, 2007), a different value was given to the river water in flood periods. The DOC concentrations in $LU_1$ were calculated as the mixture of $LU_2$ and river water.

DOC could be consumed by denitrifying bacteria. The consumption rate was:

$$R_{DOC} = -k_{DOC}[DOC] \qquad 2.3.1$$

where $R_{DOC}$ is the DOC consumption rate ($\mu mol \cdot l^{-1} \cdot d^{-1}$).

In the SWAT model, the POC contents in the soil profiles were read as input values and were not simulated in the shallow aquifers. In the SWAT-LUD model, the POC contents in the top soil layers were considered higher than the others and the POC pools were separated into two parts: the top layer pool and the second layer pool. The POC content in the two pools was read as input values.

POC could be consumed by denitrifying bacteria as well. The consumption rate was:

$$R_{POC} = -k_{POC}[POC] \qquad 2.3.2$$

where $R_{POC}$ is the POC consumption rate ($‰ \cdot d^{-1}$)

### 5.2.4 Study site

The Garonne River is the largest river in southwest France. The typical alluvial plain starts from its middle section. The study site at Monbéqui is located in a meander of the floodplain, about 40 km north of the city of Toulouse. The mean annual precipitation is about 690 mm in this area. The nearest gauging station – the Verdun gauging station – is located about 4 km upstream of Monbéqui. In this area, the Garonne river has a watershed of 13,730 $km^2$ and an annual average flow of about 200 $m^3 \cdot s^{-1}$ which ranges from 10 $m^3 \cdot s^{-1}$ to 2900 $m^3 \cdot s^{-1}$ (Banque Hydro, http://www.hydro.eaufrance.fr/). The alluvial plain is about 4 km wide and contains a 4-7 m depth of deposited quaternary sand and gravel that overlie the molassic substratum impermeable layer (Lancaster, 2005, Sánchez-Pérez et al., 2003b).

The riparian forest and poplar plantations cover the first 50-200 m from the riverbank, beyond which lies agricultural land that accounts for 75 % of the total area. The main crops in the study area are corn and winter wheat; there is also sunflower, soybeans and rapeseed. Twenty-six piezometers were installed in the meander. Groundwater level sensors were installed in five piezometers to record the groundwater levels every 10 min. From April 2013 to March 2014, groundwater and sediment samples from all the piezometers and two river points except P29 were taken monthly for analysis of physicochemical parameters. To ensure the water sample corresponded to the aquifer and not to stagnant water accumulated in the piezometer, water samples were taken until conductivity of the extracted groundwater was constant (Sánchez-Pérez, 1992). Redox potential, pH, electrical conductivity, oxygen content and temperature were measured in the field. Other elements were analysed in the laboratory, such as nitrate, DOC, chloride and the AFDM (ash-free dry mass) contents of the sediment. In 2005 (January to July), groundwater samples from five piezometers (P6, P10, P13, P18 and P29) were taken monthly and elements such as nitrate, DOC and chloride were analysed.

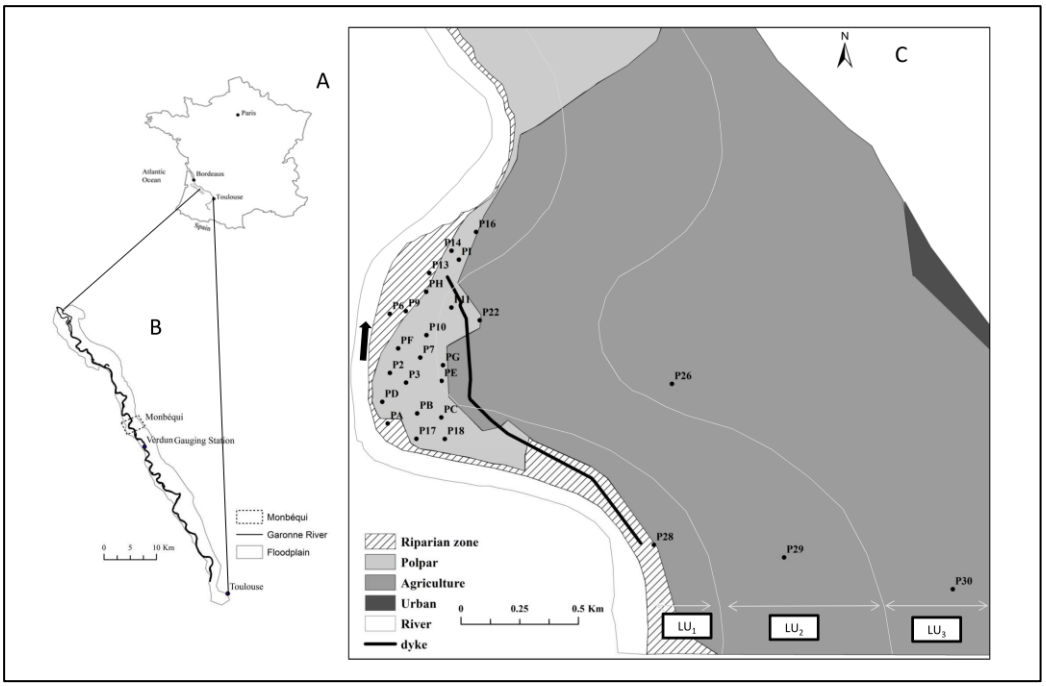


Fig 2. Locations of the piezometer in the Monbéqui study site. 'A' represents the location of the Garonne River, 'B' represents the location of the alluvial plain and Monbéqui, and 'C' represents the piezometers in Monbéqui, the grid lines show the rough locations of LUs.

### 5.2.5 LU parameters

The LUs in this study site were defined based on the flood return periods. $LU_1$ corresponded to the area that was flooded every year, which was mainly covered by riparian forest and poplar plantations, and 16 piezometers in 2013 and four piezometers in 2005 were located in this area. $LU_2$ represented the area that was flooded every two to five years, with two piezometers (P11 and P22) in 2013 and P29 in 2005 located in this zone. $LU_3$ corresponded to the area that was flooded every ten or more years, with P26 in 2013 located in this zone. $LU_2$ and $LU_3$ were mainly covered by agricultural land. The parameters of the LUs are given in Table 1.

Table 1. LU parameters

| | $LU_1$ | $LU_2$ | $LU_3$ |
|---|---|---|---|
| Width (km) | 0.4 | 0.8 | 3.0 |
| Length (km) | 6.374 | 6.374 | 6.374 |
| Slope (lateral) | 0.002 | 0.005 | 0.005 |
| Porosity | 0.1 | 0.1 | 0.1 |

The crop rotations applied in the LUs were based on data collected during 2005-2007 by Jégo (2008), which are shown in Table 2. In $LU_1$, the poplar plantation was considered to be deciduous forest.

Table 2. Land cover and crop rotation and management in the LUs

| | $LU_1$ | $LU_2$ | | | $LU_3$ | | |
|---|---|---|---|---|---|---|---|
| year | Land cover | Crops | Mineral fertilisation | Irrigation | Crops | Mineral fertilisation | Irrigation |
| 1 | Forest | Soybean | 0 | 0 | Winter wheat | 0 | 0 |
| 2 | Forest | Pea | 0 | 0 | Rapeseed | 150 | 0 |
| 3 | Forest | Corn | 150 | 175 | -- | -- | -- |

The concentration of nitrate in the river water was considered constant in this study and the value was determined based on the measured data in 2013, which was 2.26 ($N\text{-}NO_3^-$) $mg \cdot l^{-1}$. The DOC concentrations in the LUs and in the river water were determined based on the measured data in 2013. The topsoil layer was considered to be 0.5 m and the POC contents in this layer were given based on the measured data by Jégo (2008). The POC contents in lower layers, which were below the top 0.5 m, were given based on the measured AFDM values in 2013. The carbon content in AFDM was considered to be 50 % based on recent studies (Hauer and Lamberti, 2011; Wagner *et al.*, 2011; Griffiths *et al.*, 2012) (Table 3).

Table 3. Measured DOC and POC in the LUs and the river in 2013 and given constant values

| | | DOC ($mg \cdot l^{-1}$) (Measured) | DOC ($mg \cdot l^{-1}$) (Constant) | AFDM (%) (Measured) | POC (>50 cm) (%) (Constant) | POC (top 50cm) (%) (Constant) |
|---|---|---|---|---|---|---|
| $LU_1$ | | simulated | | 0.55±0.03 | 0.275 | 1.5 |
| $LU_2$ | P11 | 0.92±0.15 | 0.85 | 0.65±0.08 | 0.275 | 1.0 |
| | P22 | 0.83±0.09 | | 0.46±0.07 | | |
| $LU_3$ | P26 | 0.66±0.11 | 0.65 | 0.56±0.07 | 0.325 | 1.0 |
| | P30 | 0.65±0.13 | | 0.74±0.04 | | |
| River | R1 | 1.72±0.15 | 1.7 | | | |
| | R2 | 1.69±0.20 | 3 (During flooding) | | | |

### 5.2.6 Calibration and evaluation of the SWAT-LUD model

The simulation was carried out between 1993 and 2013. The calibration and validation of hydrological conditions can be found in Sun et al. (in press). In this study, nitrate concentrations in the shallow aquifer, measured in 2005 and 2013, and DOC concentrations in $LU_1$, measured in 2013, were used as calibration data. The simulated percolated water and leached nitrate from the soil profiles of the SWAT-LUD model in 2005-2007 were compared with the output of the STICS model to evaluate the simulated results. STICS is a dynamic soil-crop-atmosphere simulation model that has been successfully applied in the study site to simulate the water and nitrate content in the soil layers (Brisson et al., 2003). More details of the STICS model can be found in Brisson et al. (2003, 1998). Data obtained with SWAT were compared with the simulated results of Jégo et al. (2012) using the STIC model on the same study site. Percent bias (PBIAS) and root mean square error (RMSE) were chosen as evaluating parameters.

## 5.3 Results

### 5.3.1 Calibrated parameters

Manual calibration was performed to calibrate the daily simulated nitrate and DOC concentrations in the shallow aquifer. The calibrated parameters and values are shown in Table 4.

Table 4. Manually calibrated parameters

| | Description | Unit | Calibrated value |
|---|---|---|---|
| $k_{POC1}$ | $k_{POC}$ in $LU_1$ | $d^{-1}$ | $0.80\times10^{-5}$ |
| $k_{POC2}$ | $k_{POC}$ in $LU_2$ | $d^{-1}$ | $0.20\times10^{-6}$ |
| $k_{POC3}$ | $k_{POC}$ in $LU_3$ | $d^{-1}$ | $0.15\times10^{-6}$ |
| $k_{NO3}$ | half-saturation concentration of nitrate | $\mu mol\cdot l^{-1}$ | 30 |
| $k_{DOC1}$ | $k_{DOC}$ in $LU_1$ | $d^{-1}$ | 0.005 |
| $k_{DOC2}$ | $k_{DOC}$ in $LU_2$ | $d^{-1}$ | 0.002 |
| $k_{DOC3}$ | $k_{DOC}$ in $LU_3$ | $d^{-1}$ | 0.002 |
| $F_{NO3}$ | Percentage of leached nitrate from soil profile during flooding | % | 30 |

The results showed that the calibrated $k_{POC}$ and $k_{DOC}$ in $LU_1$ were much higher than in the other two LUs.

### 5.3.2 STICS and SWAT-LUD model comparison

A comparison of simulated percolated water and nitrate in the SWAT-LUD model and the STICS model in $LU_1$ and $LU_2$ is given in Figure 3.

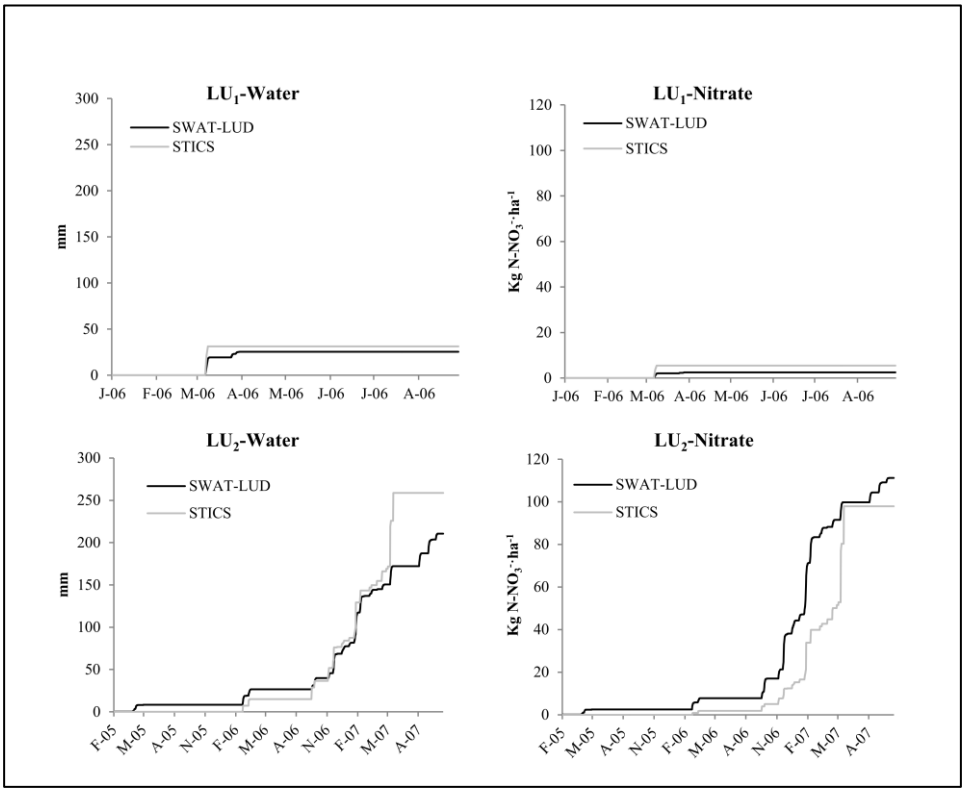


Figure 3. Simulated accumulated infiltrated water (in mm) and nitrate (kg $N\text{-}NO_3^-$ $ha^{-1}$) with SWAT-LUD and STICS models in $LU_1$ (deciduous forest) and $LU_2$ (crop system)

The results showed that the simulated results of these two models matched very well in both LUs. In $LU_2$, the main difference between the percolated water of the two models was in May 2007, while the STICS model simulated more infiltrated water. The comparison between those two LUs showed that infiltrated water and nitrate in $LU_1$ were much lower than in $LU_2$.

### 5.3.3 Nitrate concentrations in shallow aquifer

Figure 4 shows the comparison of simulated nitrate concentrations with observed values in the shallow aquifer over two periods (2005, 2013).

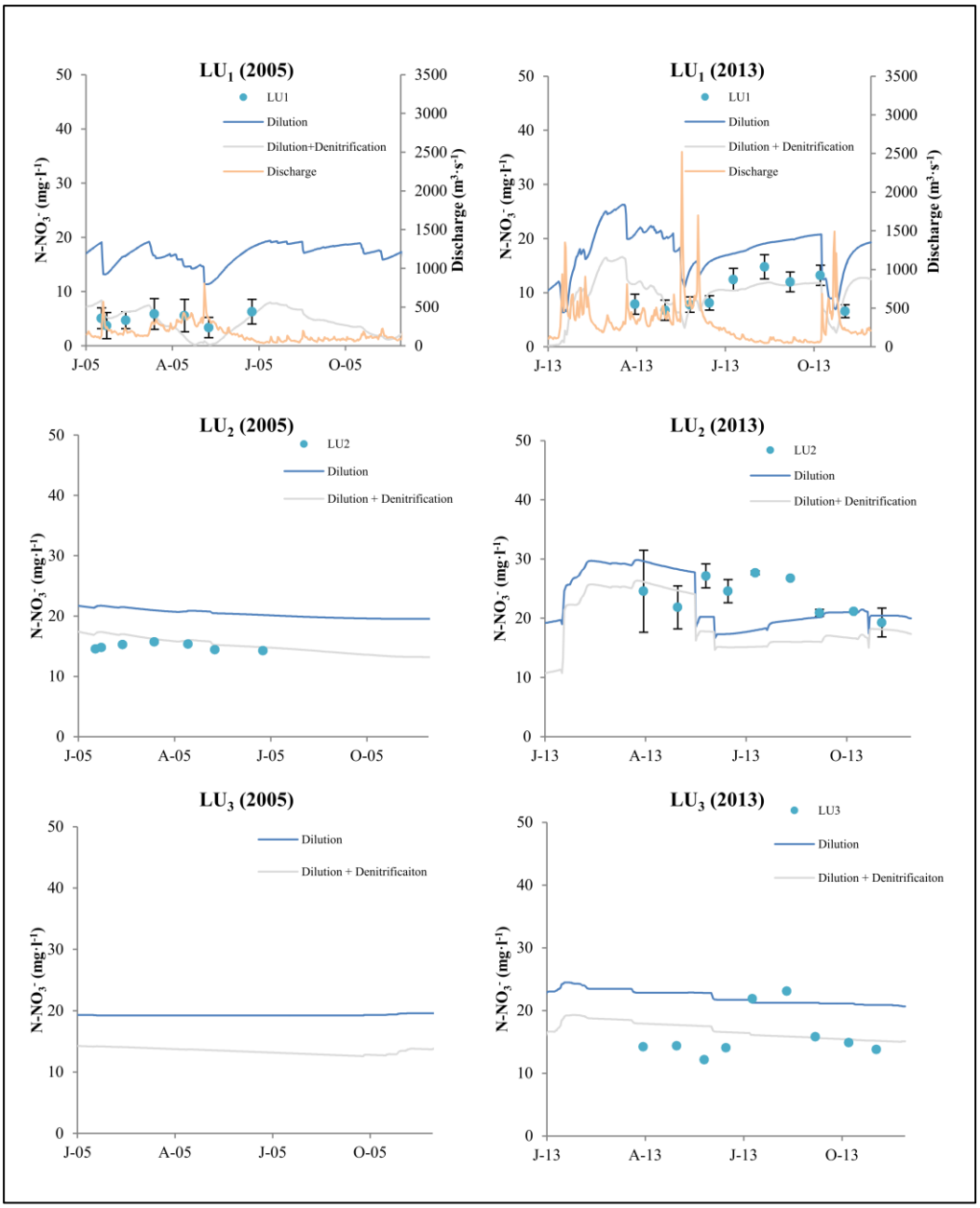


Figure 4. Simulated and observed nitrate concentrations in the aquifer of LUs during the years 2005 and 2013, where 'Dilution' is the simulated results with recharged river water and 'Dilution + Denitrification' is the simulated results with recharged river water and denitrification processes.

This showed that the observed values matched better with the simulated results with denitrification. The simulations that considered denitrification overestimated the groundwater nitrate concentration, but still were in good agreement with the observed data (Fig. 5).

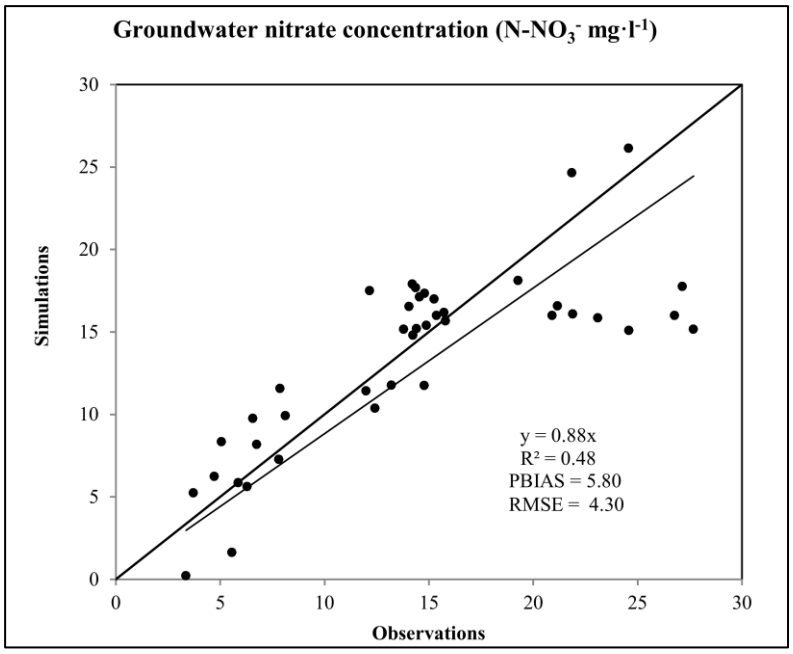


Figure 5. Observed and simulated (dilution plus denitrification) groundwater nitrate concentration in the two periods (2005, 2013)

The evaluated values between observed nitrate concentrations and simulated results with dilution plus denitrification in each LU for the two periods are shown in Table 4.

Table 4. Parameters for evaluating the accuracy of simulated nitrate concentrations in the shallow aquifer using the SWAT-LUD model

| | | PBIAS (%) | RMSE(mg $N\text{-}NO_3^-.L^{-1}$) |
|---|---|---|---|
| $LU_1$ | 2005 | 3.86 | 2.43 |
| | 2013 | -2.91 | 2.24 |
| $LU_2$ | 2005 | -8.99 | 1.60 |
| | 2013 | 22.60 | 7.50 |
| $LU_3$ | 2005 | -- | -- |
| | 2013 | -2.54 | 4.05 |

The observations and simulations matched well in $LU_1$ in both periods. The matching of $LU_2$ in 2013 was unsatisfactory. After the flooding (discharge $\geq$ 1008 $m^3/s$), the simulation decreased by the dilution of river water, however the observations in $LU_2$ kept the value high. As there was no observation of $LU_3$ in 2005, the comparison was only made in 2013. The measured nitrate concentration increased in August and September of 2013, however it was not reflected in the simulation. The results also illustrated that denitrification significantly decreased the nitration concentration in the floodplain aquifer.

### 5.3.4 DOC concentrations in the shallow aquifer

The simulated DOC concentrations were compared with the measured data of $LU_1$ in 2013 (Fig. 6).

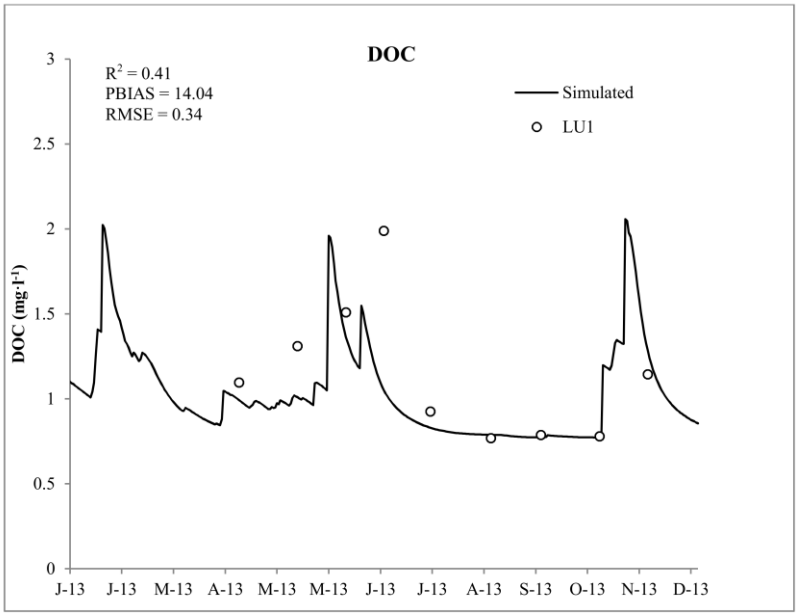


Figure 6. Simulated and observed DOC concentrations in 2013

The results showed that the simulated DOC concentration matched well with observations, except the observed data in July where just after the flooding the observation was higher than the simulations.

### 5.3.5 Denitrification rate

The simulated annual denitrification rate is shown in Figure 7. The denitrification rate in $LU_1$ was much higher than in the other two LUs, with average denitrification rates in $LU_1$, $LU_2$ and $LU_3$ for the entire simulation period (1993-2013) of 132.54±3.88, 6.13±0.25, 9.06±0.40 kg $N\text{-}NO_3^-\cdot ha^{-1}\cdot y^{-1}$ for the surface respectively. The groundwater depth in the three LUs are 1.62±0.06, 2.29±0.09, 3.97±0.19 m. And the denitrification rate for per unit of sediment in the three LUs are 8.09±0.18, 0.27, 0.23 g $N\text{-}NO_3^-\cdot m^{-3}\cdot y^{-1}$ respectively. For per kilometre length of the river, it turn to be 61.91±2.77 T $N\text{-}NO_3^-\cdot km^{-1}\cdot y^{-1}$.

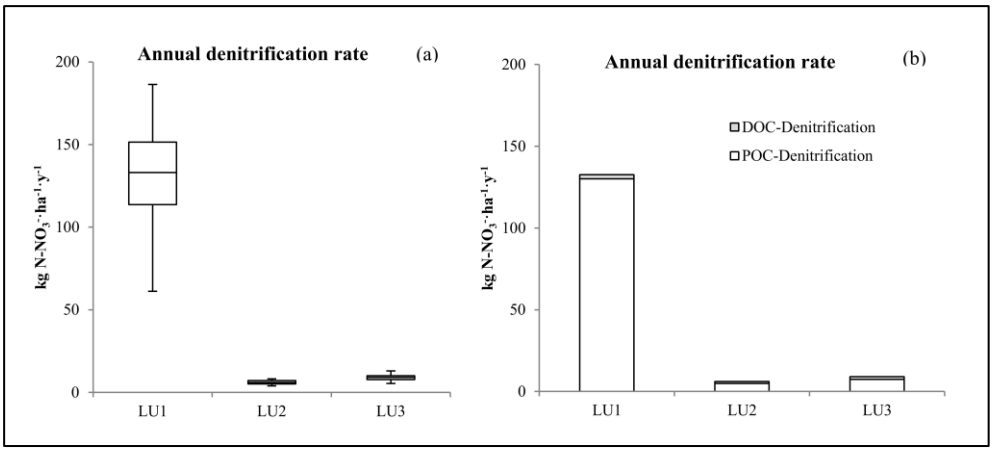


Figure 7. Simulated annual denitrification rates (a. annual total denitrification rates, b. annual denitrification rates triggered by DOC and POC) in the three LUs

Since two organic carbon sources were included in the model, the denitrification triggered by DOC and POC was separated and compared. The results are also shown in Figure 5. This revealed that POC played an extremely important role in the occurrence of denitrification. The nitrate consumption triggered by DOC was only 1.80 % of the total nitrate consumption in $LU_1$; in $LU_2$ and $LU_3$ the ratios were 20.93 % and 18.57 % respectively.

The annual flux of nitrate between LUs and between LUs and the river is shown in Figure 8. Since $LU_1$ was covered by forest, less nitrate leached into the shallow aquifer in $LU_1$ than in the other two LUs. $LU_2$ and $LU_3$ were the main sources of nitrate in the shallow aquifer. In $LU_1$, the quantity of nitrate recharged by river water (lateral flow and flooding) was almost the same as that infiltrated from soil. The nitrate consumption rates in $LU_3$, $LU_2$ and $LU_1$ were 31.37±2.35 %, 4.34±0.29 %, 43.92±2.31 % respectively, but around 52.6 T $N\text{-}NO_3^-$ still flowed to the river each year.

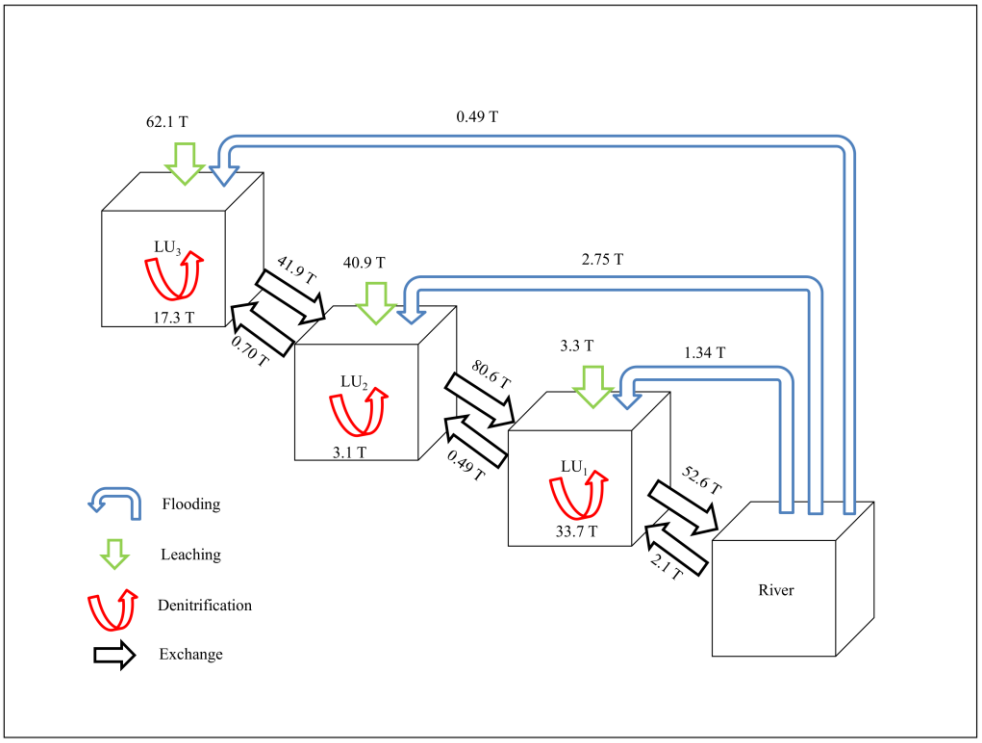


Figure 8. Simulated annual flux of nitrate ($N\text{-}NO_3^-$) in the floodplain area of Monbéqui

### 5.3.6 The influence of hydraulic conditions and nitrate content on denitrification

Since the denitrification rate of nitrate in $LU_1$ was much higher than in the other two LUs, the correspondence between denitrification rates and hydraulic conditions in $LU_1$ was analysed. Since river water discharge, recharged river water volume and groundwater flow corresponded positively to the groundwater level (Table 5).

Table 5. The coefficient of determinations between hydraulic elements in $LU_1$ based on the simulations of the entire simulated period (1993 to 2013)

| | Groundwater level (m) | River water discharge ($m^3 \cdot s^{-1}$) | Recharged river water volume ($m^3 \cdot d^{-1}$) | Groundwater flow ($m^3 \cdot d^{-1}$) |
|---|---|---|---|---|
| Groundwater level (m) | -- | -- | -- | -- |
| River water discharge ($m^3 \cdot s^{-1}$) | 0.88<br>$P < 0.01$, $n = 21$ | -- | -- | -- |
| Recharged river water volume ($m^3 \cdot d^{-1}$) | 0.31<br>$P < 0.01$, $n = 21$ | 0.30<br>$P < 0.01$, $n = 21$ | -- | -- |
| Groundwater flow ($m^3 \cdot d^{-1}$) | 0.77<br>$P < 0.01$, $n = 21$ | 0.44<br>$P < 0.01$, $n = 21$ | 0.24<br>$P < 0.05$, $n = 21$ | -- |

Since river water discharge, recharged rive water volume and groundwater are positivily related with groundwater level, an analysis of correspondence between groundwater levels and denitrification rate was performed (Fig. 9).

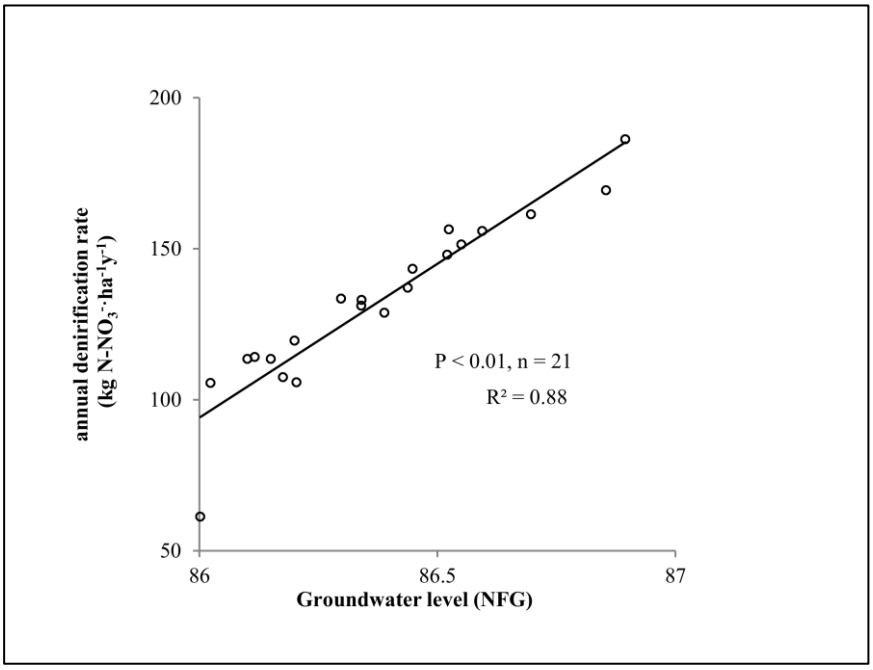


Figure 9. Correspondence between annual denitrification rate and groundwater level in the entire simulated period (1993-2013)

Results showed that denitrification rates were significantly positively correlated with groundwater level, with $R^2$ reaching 0.88 ($p<0.01$).

The relationship between nitrate input in $LU_1$ and denitrification rates in $LU_1$ were also examined. The absolute (denitrification rate) and relative (denitrification efficiency) denitrification abilities were compared with the total input nitrate mass in $LU_1$ (Fig. 10). It showed that the absolute consumption rate increased along with the increase in nitrate content, however the relative consumption rate decreased as the nitrate content increased, which meant that more nitrate entered $LU_1$ and more nitrate flowed into the river.

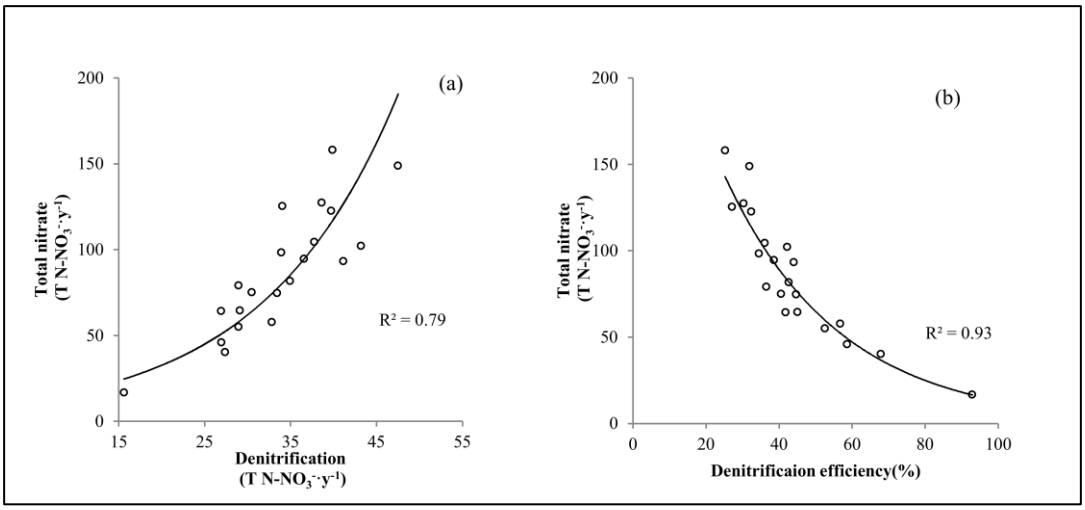


Figure 10. Relationship between denitrification (a. denitrification rate b. denitrification efficiency) and annual input nitrate in $LU_1$

## 5.4 Discussion

### 5.4.1 Denitrification

This study illustrated that the modified SWAT-LUD model could realistically simulate nitrate concentrations in groundwater while simulating the dilution of recharge from river flooding and denitrification in riparian areas at the alluvial floodplain scale. Models have previously been developed to simulate denitrification in aquifers (Kinzelbach *et al.*, 1991; Lee *et al.*, 2006, 2009; Bailey *et al.*, 2013), but the influence of recharged surface water has not been considered. The denitrification in the hyporheic zone has also been simulated, but these models are numerical models and cannot feasibly be applied on a large scale (Sheibley *et al.*, 2003; Zarnetske *et al.*, 2012). Compared with other denitrification models, SWAT-LUD simulated the two-direction SW-GW water exchange and denitrification that occurred in the shallow aquifer on a large spatial and temporal scale.

Denitrification was found to play an important role in nitrate pollution control at the study site, especially in the zone near the riverbank where river water and groundwater are well mixed, as it consumed about 40 % of the nitrate flowing through this zone. Denitrification is a complex process and the numbers of bacteria and enzymes were found to have an influence on this process (Philippot and Hallin, 2005; Bothe *et al.*, 2006; Wallenstein *et al.*, 2006). Several studies have demonstrated that the microenvironments play a significant role in the occurrence of denitrification, and hot moments and hotspots have been found to be crucial to the entire nitrate attenuation process (Groffman et al., 2009; Iribar et al., 2008, 2015; Vidon et al., 2010). However, the LUs in the SWAT-LUD model were assumed to be homogeneous;

denitrification occurred uniformly in each LU, making it difficult to match the simulated results with observed points. Since the SWAT-LUD model was developed for large river basins, the aim of the new module was to represent denitrification in the floodplain aquifer at catchment scale with relatively few input parameters and computational time, but not to represent detailed localised information.

### 5.4.2 Influence of hydraulic conditions on denitrification

Groundwater levels were found to have a significant influence on denitrification rates. As POC was found to be the main organic carbon source of denitrification in this study, the contact area between groundwater and POC increased with the rise in groundwater levels. The groundwater level increased with the rise of river water discharge too, so other than the DOC transported with the recharged river water, the enlarged groundwater levels also stimulated the occurrence of denitrification.

### 5.4.3 Nitrate dynamics

Since the STICS model has been shown to represent accurately the soil water content and nitrate at the study site (Jégo, 2008; Jégo et al., 2012), the comparison between SWAT and STICS illustrated that the SWAT model represented the leached water and nitrate correctly. The influence of flooding on the nitrate concentration in the aquifer was taken into account in this study. Wang et al. (2010) have found that the leached nitrate under heavy irrigation could contribute 60 % of the accumulated N in the soil profile. Since nitrate infiltration data was not collected during flooding at the study site, the parameter that represented this function was calibrated. The simulated nitrate concentrations in $LU_2$ matched more closely with the observations in 2005 than in 2013. There are several potential reasons for this. These include: 1) cropping systems may have changed between 2005 and 2013 and 2) flooding occurred in 2013 but not in 2005, making it more difficult to simulate the groundwater nitrate concentration with the influence of flooded water. After the flooding at the beginning of June 2013, the simulated results showed that the recharged river water diluted the nitrate concentration in $LU_2$, while the observed data maintained high values. Artificial dykes were built to protect agricultural land from flooding. Furthermore, as the simulated results represented the average condition of the LU, it was difficult to match the simulated results to the spatially observed points.

Corn is the common crop planted in the south of France, whose growth cycle is usually from May to October. However, the Mediterranean climate leads to dry summers in the

Garonne watershed. As corn needs more water than other crops, it is generally irrigated during the dry summer. The leached nitrate along with the irrigated water could explain the increase of nitrate in $LU_3$ in August and September 2013. The lack of continuously recorded and detailed crop rotation information also limited the ability of the SWAT-LUD model to represent the detailed localised nitrate concentration.

### 5.4.4 Influence of POC and DOC on denitrification

Among the two carbon sources, it was determined that POC played an extremely important role in the denitrifying process. The interior mechanisms of the influence of POC on denitrification are still not clear. It was generally considered that POC could stimulate denitrification directly and indirectly. The different quality and quantity of POC had a varying influence on nitrogen transformation. The decomposition of POC could release DOC and create the anaerobic environment, simultaneously increasing the denitrifying process (Arango *et al.*, 2007; Stelzer *et al.*, 2011, 2014). In the hyporheic zone, biofilm is an important component of POC and was found to have large impacts on the metabolism of river systems (Fischer *et al.*, 1996). Biofilm is regarded as an important organic matter storage site and absorption site for DOM owing to its large internal surface area (Koutný and Rulík, 2007).

A comparison of the influence of DOC and POC on denitrification in the aquifer had never been carried out before. Iribar (2007) measured the potential denitrification rate (DEA) in the groundwater and aquifer sediment, and DEA in the sediment was found to be 1000 times greater than in the groundwater. Bacteria have been found to be a medium of carbon storage (Ogawa *et al.*, 2001), however the contribution of bacteria-derived DOC in the groundwater has rarely been studied. A recent study found that around 20 % of the groundwater DOC is bacteria derived (Shen *et al.*, 2014). Since the riparian zone is most frequently recharged by river water, the bacteria of the biofilm attached to the aquifer sediment could be altered by the recharged DOC dissolved in the surface water. The riparian zone was flooded regularly, so buried POM could contribute to the denitrifying activity as well. Moreover, as this zone is mainly covered with riparian forest, more DOC infiltrated from the soil layer in the forest area than that from other land use types (Chantigny, 2003; Sanderman and Amundson, 2008).

The Garonne River is a poor organic carbon nutrient river, with a DOC concentration usually less than 3 mg/l in the river water and less than 1 mg/l in the groundwater. Considering that the content of BDOC is around 4-54 % of DOC in the surface water (Servais

*et al.*, 1989; Wiegner *et al.*, 2006; Wickland *et al.*, 2012) and only around 8 % in the groundwater (Shen *et al.*, 2014), there was not enough BDOC to support the decreased nitrate at the study site. $k_{DOC}$ is a highly variable parameter (it could range from 0.0001 to 1.22) depending on the organic carbon components and the specific biogeochemical environment (Rifai and Bedient, 1990; Hunter *et al.*, 1998; Boano *et al.*, 2007). In this study, the value $k_{DOC}$ was calibrated based on the observed DOC concentrations in $LU_1$, the nitrate concentration and the location of LUs. Since $LU_1$ is the LU nearest to the river, it has a higher value than other LUs. Tillman *et al*. (2003) studied the decay rate of leaves buried within the river sediment and the decay rate was considered to be $1.7\times10^{-3}$ and $9.7\times10^{-4}$ $d^{-1}$ in the downwelling and upwelling reach respectively. In the study of Peyrard et al. (2011), $k_{POC}$ was calibrated to be $1.1\times10^{-4}$ $d^{-1}$. Compared with these studies, the POC decay was low, but since it was applied in the shallow aquifer, the biogeochemical activity was lower in this area than the gravel bar and hyporheic zone under the river channel. In the present study, the $k_{POC}$ in $LU_1$ was much higher than in the other two LUs and $k_{POC1}$ was increased to match the simulated results with the low measured nitrate concentration in LU1. It was assumed that the organic carbon storage in the POC significantly stimulated the occurrence of denitrifying process. Anammox is another important anaerobic nitrogen attenuating process that produces dinitrogen gas with ammonium and nitrite directly. Anammox organisms have been identified in groundwater (Clark *et al.*, 2008; Humbert *et al.*, 2009). Moore et al. (2011) and Vetter et al. (2013) have both proved the importance of anammox in nitrogen assumption in the groundwater. However, the anammox process was not considered in this study and it was probably the 'dark zone' that explained the low nitrate in $LU_1$ which was represented by the higher $k_{POC1}$. Moreover, constant values of POC and DOC in LUs were given in the present study. However, POC and DOC are interactional and dynamically variable. The soil-derived DOC and POC were also not included in the SWAT-LUD model and the soil source may explain the difference between the simulated and observed DOC in June and July.

## 5.5 Conclusions

This paper describes the new module developed to simulate denitrification occurring in a floodplain aquifer. The denitrification equation that considered the influence of both POC and DOC was introduced to the model based on the new modules in SWAT-LUD described in Sun et al. (in press). The dilution of nitrate in the aquifer caused by the recharged river water through both lateral (river bank) and vertical (surface) infiltration was integrated into the model. The modified model was applied in the floodplain of the Garonne River. Simulated

leached water and nitrate from the soil profile were compared with the simulated results of the STICS model, which demonstrated that the SWAT-LUD model simulated the nitrate and water inputs from the soil profile correctly both spatially and temporally. The comparison with measured groundwater nitrate concentrations found that the modified SWAT-LUD model could correctly simulate the aquifer nitrate concentration in the near bank zone. The near bank zone in the floodplain played the most important role in attenuating nitrate through denitrification. The annual denitrification rate in the near bank zone was around 130 kg N-$NO_3^-$·$ha^{-1}$·$y^{-1}$, and around 40 % of the nitrate input to this zone was denitrified. POC was more important than DOC in the denitrifying process, especially in the near bank zone, and 98 % of the nitrate was attenuated by POC. The relationships between denitrification rates, groundwater levels and total input nitrate masses in the near bank zone were analysed. The results illustrated that groundwater levels were positively correlated to the denitrification rates in the near bank zone and the absolute consumption rate increased along with the increase in nitrate content. However, the relative consumption rate decreased as the nitrate content increased. The modified SWAT-LUD model was found to be a useful tool for quantifying the attenuation of nitrate pollution in the floodplain aquifer. Future work should include: i) an improvement to the module of carbon cycling in soil and river water in the model, ii) application of the modified model to a larger catchment with more subbasins and continuity on the river network.

**Acknowledgements**

We are grateful to N. B. Sammons for her help with developing the module. Dr. Samuel Teissier and Youen Grusson are also acknowledged for their help in the field and with laboratory work. This study was performed as part of the EU Interreg SUDOE IVB programme (ATTENAGUA - SOE3/P2/F558 project, http://www.attenagua-sudoe.eu) and funded by ERDF. This research has been carried out as a part of "ADAPT'EAU" (ANR-11-CEPL-008), a project supported by the French National Research Agency (ANR) as part of the Global Environmental Changes and Societies (GEC&S) programme. X. Sun is supported by a grant from the China Scholarship Council (CSC).

**References**

Almasri, M.N., Kaluarachchi, J.J., 2004. Assessment and management of long-term nitrate pollution of ground water in agriculture-dominated watersheds. J. Hydrol. 295, 225–245. doi:10.1016/j.jhydrol.2004.03.013

Almasri, M.N., Kaluarachchi, J.J., 2007. Modeling nitrate contamination of groundwater in agricultural watersheds. J. Hydrol. 343, 211–229. doi:10.1016/j.jhydrol.2007.06.016

Arango, C.P., Tank, J.L., Schaller, J.L., Royer, T.V., Bernot, M.J., David, M.B., 2007. Benthic organic carbon influences denitrification in streams with high nitrate concentration. Freshw. Biol. 52, 1210–1222. doi:10.1111/j.1365-2427.2007.01758.x

Arnold, J.G., Allen, P.M., Volk, M., Williams, J.R., Bosch, D.D., 2010. Assessment of different representations of spatial variability on SWAT model performance. Trans ASABE 53, 1433–1443.

Arnold, J.G., Srinivasan, R., Muttiah, R.S., Williams, J.R., 1998. Large Area Hydrologic Modeling and Assessment Part I: Model Development1. JAWRA J. Am. Water Resour. Assoc. 34, 73–89. doi:10.1111/j.1752-1688.1998.tb05961.x

Arrate, I., Sanchez-Perez, J.M., Antiguedad, I., Vallecillo, M.A., Iribar, V., Ruiz, M., 1997. Groundwater pollution in Quaternary aquifer of Vitoria : Gasteiz (Basque Country, Spain): Influence of agricultural activities and water-resource management. Environ. Geol. 30, 257–265. doi:10.1007/s002540050155

Bailey, R.T., Morway, E.D., Niswonger, R.G., Gates, T.K., 2013. Modeling Variably Saturated Multispecies Reactive Groundwater Solute Transport with MODFLOW-UZF and RT3D. Groundwater 51, 752–761. doi:10.1111/j.1745-6584.2012.01009.x

Bijay-Singh, Yadvinder-Singh, Sekhon, G.S., 1995. Fertilizer-N use efficiency and nitrate pollution of groundwater in developing countries. J. Contam. Hydrol. 20, 167–184. doi:10.1016/0169-7722(95)00067-4

Boano, F., Revelli, R., Ridolfi, L., 2007. Bedform-induced hyporheic exchange with unsteady flows. Adv. Water Resour. 30, 148–156. doi:10.1016/j.advwatres.2006.03.004

Boithias, L., Srinivasan, R., Sauvage, S., Macary, F., Sánchez-Pérez, J.M., 2014. Daily Nitrate Losses: Implication on Long-Term River Quality in an Intensive Agricultural Catchment of Southwestern France. J. Environ. Qual. 43, 46. doi:10.2134/jeq2011.0367

Bosch, D.D., Arnold, J.G., Volk, M., Allen, P.M., 2010. Simulation of a low-gradient coastal plain watershed using the SWAT landscape model. Trans ASABE 53, 1445–1456.

Bothe, H., Ferguson, S., Newton, W.E., 2006. Biology of the Nitrogen Cycle. Elsevier.

Brisson, N., Gary, C., Justes, E., Roche, R., Mary, B., Ripoche, D., Zimmer, D., Sierra, J., Bertuzzi, P., Burger, P., Bussière, F., Cabidoche, Y.M., Cellier, P., Debaeke, P., Gaudillère, J.P., Hénault, C., Maraux, F., Seguin, B., Sinoquet, H., 2003. An overview

of the crop model stics. Eur. J. Agron., Modelling Cropping Systems: Science, Software and Applications 18, 309–332. doi:10.1016/S1161-0301(02)00110-7

Brisson, N., Mary, B., Ripoche, D., Jeuffroy, M.H., Ruget, F., Nicoullaud, B., Gate, P., Devienne-Barret, F., Antonioletti, R., Durr, C., others, 1998. STICS: a generic model for the simulation of crops and their water and nitrogen balances. I. Theory and parameterization applied to wheat and corn. Agronomie 18, 311–346.

Burgin, A.J., Hamilton, S.K., 2007. Have we overemphasized the role of denitrification in aquatic ecosystems? A review of nitrate removal pathways. Front. Ecol. Environ. 5, 89–96. doi:10.1890/1540-9295(2007)5[89:HWOTRO]2.0.CO;2

Camargo, J.A., Alonso, Á., 2006. Ecological and toxicological effects of inorganic nitrogen pollution in aquatic ecosystems: A global assessment. Environ. Int. 32, 831–849. doi:10.1016/j.envint.2006.05.002

Carpenter, S.R., Caraco, N.F., Correll, D.L., Howarth, R.W., Sharpley, A.N., Smith, V.H., 1998. NONPOINT POLLUTION OF SURFACE WATERS WITH PHOSPHORUS AND NITROGEN. Ecol. Appl. 8, 559–568. doi:10.1890/1051-0761(1998)008[0559:NPOSWW]2.0.CO;2

Cerro, I., Antigüedad, I., Srinavasan, R., Sauvage, S., Volk, M., Sanchez-Perez, J.M., 2014. Simulating Land Management Options to Reduce Nitrate Pollution in an Agricultural Watershed Dominated by an Alluvial Aquifer. J. Environ. Qual. 43, 67. doi:10.2134/jeq2011.0393

Chantigny, M.H., 2003. Dissolved and water-extractable organic matter in soils: a review on the influence of land use and management practices. Geoderma, Ecological aspects of dissolved organic matter in soils 113, 357–380. doi:10.1016/S0016-7061(02)00370-1

Clark, I., Timlin, R., Bourbonnais, A., Jones, K., Lafleur, D., Wickens, K., 2008. Origin and Fate of Industrial Ammonium in Anoxic Ground Water—15N Evidence for Anaerobic Oxidation (Anammox). Ground Water Monit. Remediat. 28, 73–82. doi:10.1111/j.1745-6592.2008.00206.x

Cooper, A.B., 1990. Nitrate depletion in the riparian zone and stream channel of a small headwater catchment. Hydrobiologia 202, 13–26. doi:10.1007/BF02208124

Dalzell, B.J., Filley, T.R., Harbor, J.M., 2005. Flood pulse influences on terrestrial organic matter export from an agricultural watershed. J. Geophys. Res. Biogeosciences 2005–2012 110. doi:10.1029/2005jg000043

Dodla, S.K., Wang, J.J., DeLaune, R.D., Cook, R.L., 2008. Denitrification potential and its relation to organic carbon quality in three coastal wetland soils. Sci. Total Environ. 407, 471–480. doi:10.1016/j.scitotenv.2008.08.022

Dosskey, M.G., Vidon, P., Gurwick, N.P., Allan, C.J., Duval, T.P., Lowrance, R., 2010. The Role of Riparian Vegetation in Protecting and Improving Chemical Water Quality in Streams1. JAWRA J. Am. Water Resour. Assoc. 46, 261–277. doi:10.1111/j.1752-1688.2010.00419.x

Duan, S., Bianchi, T.S., Sampere, T.P., 2007. Temporal variability in the composition and abundance of terrestrially-derived dissolved organic matter in the lower Mississippi and Pearl Rivers. Mar. Chem. 103, 172–184. doi:10.1016/j.marchem.2006.07.003

Ferrant, S., Durand, P., Justes, E., Probst, J.-L., Sanchez-Perez, J.-M., 2013. Simulating the long term impact of nitrate mitigation scenarios in a pilot study basin. Agric. Water Manag. 124, 85–96. doi:10.1016/j.agwat.2013.03.023

Ferrant, S., Oehler, F., Durand, P., Ruiz, L., Salmon-Monviola, J., Justes, E., Dugast, P., Probst, A., Probst, J.-L., Sanchez-Perez, J.-M., 2011. Understanding nitrogen transfer dynamics in a small agricultural catchment: Comparison of a distributed (TNT2) and a semi distributed (SWAT) modeling approaches. J. Hydrol. 406, 1–15. doi:10.1016/j.jhydrol.2011.05.026

Fischer, H., Pusch, M., Schwoerbel, J., 1996. Spatial distribution and respiration of bacteria in stream-bed sediments. Arch. Für Hydrobiol. 137, 281–300.

Fohrer, N., Dietrich, A., Kolychalow, O., Ulrich, U., 2013. Assessment of the Environmental Fate of the Herbicides Flufenacet and Metazachlor with the SWAT Model. J. Environ. Qual. 0, 0. doi:10.2134/jeq2011.0382

Griffiths, N.A., Tank, J.L., Royer, T.V., Warrner, T.J., Frauendorf, T.C., Rosi-Marshall, E.J., Whiles, M.R., 2012. Temporal variation in organic carbon spiraling in Midwestern agricultural streams. Biogeochemistry 108, 149–169. doi:10.1007/s10533-011-9585-z

Groffman, P.M., Butterbach-Bahl, K., Fulweiler, R.W., Gold, A.J., Morse, J.L., Stander, E.K., Tague, C., Tonitto, C., Vidon, P., 2009. Challenges to incorporating spatially and temporally explicit phenomena (hotspots and hot moments) in denitrification models. Biogeochemistry 93, 49–77. doi:10.1007/s10533-008-9277-5

Hamilton, P.A., Helsel, D.R., 1995. Effects of Agriculture on Ground-Water Quality in Five Regions of the United States. Ground Water 33, 217–226. doi:10.1111/j.1745-6584.1995.tb00276.x

Hansen, S., Jensen, H.E., Nielsen, N.E., Svendsen, H., 1991. Simulation of nitrogen dynamics and biomass production in winter wheat using the Danish simulation model DAISY. Fertil. Res. 27, 245–259. doi:10.1007/BF01051131

Hauer, F.R., Lamberti, G.A., 2011. Methods in Stream Ecology. Academic Press.

Heinen, M., 2006. Simplified denitrification models: Overview and properties. Geoderma 133, 444–463. doi:10.1016/j.geoderma.2005.06.010

Hill, A.R., 1996. Nitrate Removal in Stream Riparian Zones. J. Environ. Qual. 25, 743. doi:10.2134/jeq1996.00472425002500040014x

Hill, A.R., Devito, K.J., Campagnolo, S., Sanmugadas, K., 2000. Subsurface denitrification in a forest riparianzone: Interactions between hydrology and supplies ofnitrate and organic carbon. Biogeochemistry 51, 193–223. doi:10.1023/A:1006476514038

Humbert, S., Tarnawski, S., Fromin, N., Mallet, M.-P., Aragno, M., Zopfi, J., 2009. Molecular detection of anammox bacteria in terrestrial ecosystems: distribution and diversity. ISME J. 4, 450–454. doi:10.1038/ismej.2009.125

Hume, N.P., Fleming, M.S., Horne, A.J., 2002. Denitrification Potential and Carbon Quality of Four Aquatic Plants in Wetland Microcosms. Soil Sci. Soc. Am. J. 66, 1706. doi:10.2136/sssaj2002.1706

Hunter, K.S., Wang, Y., Van Cappellen, P., 1998. Kinetic modeling of microbially-driven redox chemistry of subsurface environments: coupling transport, microbial metabolism and geochemistry. J. Hydrol. 209, 53–80. doi:10.1016/S0022-1694(98)00157-7

Inwood, S.E., Tank, J.L., Bernot, M.J., 2005. Patterns of denitrification associated with land use in 9 midwestern headwater streams. J. North Am. Benthol. Soc. 24, 227–245. doi:10.1899/04-032.1

Iribar, A., 2007. Composition des communautés bactériennes dénitrifiantes au sein d'un aquifère alluvial et facteurs contrôlant leur structuration : Relation entre structure des communautés et dénitrification (phd). Université de Toulouse, Université Toulouse III - Paul Sabatier.

Iribar, A., Sánchez-Pérez, J.M., Lyautey, E., Garabétian, F., 2008. Differentiated free-living and sediment-attached bacterial community structure inside and outside denitrification hotspots in the river–groundwater interface. Hydrobiologia 598, 109–121. doi:10.1007/s10750-007-9143-9

Iribar, A., Hallin, S., Sánchez-Pérez, J.M., Enwall, K., Poulet, N., Garabétian, F., 2015. Potential denitrification rates correlation with nosZ genotypes colonization pattern in an alluvial wetland. Ecol. Eng. (In press).

Jalali, M., 2011. Nitrate pollution of groundwater in Toyserkan, western Iran. Environ. Earth Sci. 62, 907–913. doi:10.1007/s12665-010-0576-5

Jayakrishnan, R., Srinivasan, R., Santhi, C., Arnold, J.G., 2005. Advances in the application of the SWAT model for water resources management. Hydrol. Process. 19, 749–762. doi:10.1002/hyp.5624

Jégo, G., 2008. Influence des activités agricoles sur la pollution nitrique des eaux souterraines. Analyse par modélisation des impacts des systèmes de grande culture sur les fuites de nitrate dans les plaines alluviales. Université de Toulouse, Université Toulouse III-Paul Sabatier.

Jégo, G., Sánchez-Pérez, J.M., Justes, E., 2012. Predicting soil water and mineral nitrogen contents with the STICS model for estimating nitrate leaching under agricultural fields. Agric. Water Manag. 107, 54–65. doi:10.1016/j.agwat.2012.01.007

Kinzelbach, W., Schäfer, W., Herzer, J., 1991. Numerical modeling of natural and enhanced denitrification processes in aquifers. Water Resour. Res. 27. doi:10.1029/91WR00474

Korom, S.F., 1992. Natural denitrification in the saturated zone: A review. Water Resour. Res. 28, 1657–1668. doi:10.1029/92WR00252

Koutný, J., Rulík, M., 2007. Hyporheic Biofilm Particulate Organic Carbon in a Small Lowland Stream (Sitka, Czech Republic): Structure and Distribution. Int. Rev. Hydrobiol. 92, 402–412. doi:10.1002/iroh.200610989

Lamontagne, S., Herczeg, A.L., Dighton, J.C., Jiwan, J.S., Pritchard, J.L., 2005. Patterns in groundwater nitrogen concentration in the floodplain of a subtropical stream (Wollombi Brook, New South Wales). Biogeochemistry 72, 169–190. doi:10.1007/s10533-004-0358-9

Lam, Q.D., Schmalz, B., Fohrer, N., 2010. Modelling point and diffuse source pollution of nitrate in a rural lowland catchment using the SWAT model. Agric. Water Manag. 97, 317–325. doi:10.1016/j.agwat.2009.10.004

Lancaster, R.R., 2005. Fluvial Evolution of the Garonne River, France: Integrating Field Data with Numerical Simulations [WWW Document]. URL http://etd.lsu.edu/docs/available/etd-11172005-131031/ (accessed 6.30.14).

Lee, E.J., Kim, M., Kim, Y., Lee, K.-K., 2009. Numerical and field investigation of enhanced in situ denitrification in a shallow-zone well-to-well recirculation system. Ecol. Model. 220, 2441–2449. doi:10.1016/j.ecolmodel.2009.06.014

Lee, M.-S., Lee, K.-K., Hyun, Y., Clement, T.P., Hamilton, D., 2006. Nitrogen transformation and transport modeling in groundwater aquifers. Ecol. Model. 192, 143–159. doi:10.1016/j.ecolmodel.2005.07.013

Liu, G.D., Wu, W.L., Zhang, J., 2005. Regional differentiation of non-point source pollution of agriculture-derived nitrate nitrogen in groundwater in northern China. Agric. Ecosyst. Environ. 107, 211–220. doi:10.1016/j.agee.2004.11.010

Lowrance, R., Altier, L.S., Newbold, J.D., Schnabel, R.R., Groffman, P.M., Denver, J.M., Correll, D.L., Gilliam, J.W., Robinson, J.L., Brinsfield, R.B., Staver, K.W., Lucas, W., Todd, A.H., 1997. Water Quality Functions of Riparian Forest Buffers in Chesapeake Bay Watersheds. Environ. Manage. 21, 687–712. doi:10.1007/s002679900060

Lowrance, R., Altier, L.S., Williams, R.G., Inamdar, S.P., Sheridan, J.M., Bosch, D.D., Hubbard, R.K., Thomas, D.L., 2000. REMM: The Riparian Ecosystem Management Model. J. Soil Water Conserv. 55, 27–34.

Marchetti, R., Donatelli, M., Spallacci, P., 1997. Testing Denitrification Functions of Dynamic Crop Models. J. Environ. Qual. 26, 394. doi:10.2134/jeq1997.00472425002600020009x

McIsaac, G.F., David, M.B., Gertner, G.Z., Goolsby, D.A., 2001. Eutrophication: Nitrate flux in the Mississippi River. Nature 414, 166–167. doi:10.1038/35102672

Moore, T.A., Xing, Y., Lazenby, B., Lynch, M.D.J., Schiff, S., Robertson, W.D., Timlin, R., Lanza, S., Ryan, M.C., Aravena, R., Fortin, D., Clark, I.D., Neufeld, J.D., 2011. Prevalence of Anaerobic Ammonium-Oxidizing Bacteria in Contaminated Groundwater. Environ. Sci. Technol. 45, 7217–7225. doi:10.1021/es201243t

Neitsch, S.L., Arnold, J.G., Kiniry, J.R., Williams, J.R., 2009. Soil and Water Assessment Tool, Theoretical Documentation, Version 2009.

Ogawa, H., Amagai, Y., Koike, I., Kaiser, K., Benner, R., 2001. Production of Refractory Dissolved Organic Matter by Bacteria. Science 292, 917–920. doi:10.1126/science.1057627

Osborne, L.L., Kovacic, D.A., 1993. Riparian vegetated buffer strips in water-quality restoration and stream management. Freshw. Biol. 29, 243–258. doi:10.1111/j.1365-2427.1993.tb00761.x

Peterson, M.E., Curtin, D., Thomas, S., Clough, T.J., Meenken, E.D., 2013. Denitrification in vadose zone material amended with dissolved organic matter from topsoil and subsoil. Soil Biol. Biochem. 61, 96–104. doi:10.1016/j.soilbio.2013.02.010

Peyrard, D., Delmotte, S., Sauvage, S., Namour, P., Gerino, M., Vervier, P., Sanchez-Perez, J.M., 2011. Longitudinal transformation of nitrogen and carbon in the hyporheic zone of an N-rich stream: A combined modelling and field study. Phys. Chem. Earth Parts ABC, Man and River Systems: From pressures to physical, chemical and ecological status 36, 599–611. doi:10.1016/j.pce.2011.05.003

Philippot, L., Hallin, S., 2005. Finding the missing link between diversity and activity using denitrifying bacteria as a model functional community. Curr. Opin. Microbiol., Ecology and industrial microbiology/Edited by Sergio Sánchez and Betty Olson · Techniques/Edited by Peter J Peters and Joel Swanson 8, 234–239. doi:10.1016/j.mib.2005.04.003

Ranalli, A.J., Macalady, D.L., 2010. The importance of the riparian zone and in-stream processes in nitrate attenuation in undisturbed and agricultural watersheds – A review of the scientific literature. J. Hydrol. 389, 406–415. doi:10.1016/j.jhydrol.2010.05.045

Rassam, D.W., Pagendam, D.E., Hunter, H.M., 2008. Conceptualisation and application of models for groundwater–surface water interactions and nitrate attenuation potential in riparian zones. Environ. Model. Softw. 23, 859–875. doi:10.1016/j.envsoft.2007.11.003

Rathjens, H., Oppelt, N., Bosch, D.D., Arnold, J.G., Volk, M., 2014. Development of a grid-based version of the SWAT landscape model. Hydrol. Process. n/a–n/a. doi:10.1002/hyp.10197

Rifai, H.S., Bedient, P.B., 1990. Comparison of biodegradation kinetics with an instantaneous reaction model for groundwater. Water Resour. Res. 26, 637–645. doi:10.1029/WR026i004p00637

Rivett, M.O., Buss, S.R., Morgan, P., Smith, J.W.N., Bemment, C.D., 2008. Nitrate attenuation in groundwater: A review of biogeochemical controlling processes. Water Res. 42, 4215–4232. doi:10.1016/j.watres.2008.07.020

Romanowicz, A.A., Vanclooster, M., Rounsevell, M., La Junesse, I., 2005. Sensitivity of the SWAT model to the soil and land use data parametrisation: a case study in the Thyle catchment, Belgium. Ecol. Model. 187, 27–39. doi:10.1016/j.ecolmodel.2005.01.025

Sabater, S., Butturini, A., Clement, J.-C., Burt, T., Dowrick, D., Hefting, M., Matre, V., Pinay, G., Postolache, C., Rzepecki, M., Sabater, F., 2003. Nitrogen Removal by

Riparian Buffers along a European Climatic Gradient: Patterns and Factors of Variation. Ecosystems 6, 0020–0030. doi:10.1007/s10021-002-0183-8

Sanchez-Perez, J.M., Tremolieres, M., Carbiener, R., 1991a. Une station d'épuration naturelle des phosphates et nitrates apportés par les eaux de débordement du Rhin : la forêt alluviale à frêne et orme. Comptes Rendus Académie Sci. Sér. 3 Sci. Vie 312, 395–402.

Sanchez-Perez, J.M., Tremolieres, M., Schnitzler, A., Carbiener, R., 1991b. Evolution de la qualité physico-chimique des eaux de la frange superficielle de la nappe phréatique en fonction du cycle saisonnier et des stades de succession des forêts alluviales rhénanes (Querco-Ulmetum minoris Issl. 24). Acta Oecologica 1990 12, 581–601.

Sánchez-Pérez, J.M., 1992. Fonctionnement hydrochimique d'un Ecosysteme forestier inondable de la plaine du Rhin. La foret alluviale du secteur de l'île de Rhinau en Alsace (France). PhD, Universite Louis Pasteur, Strasbourg, 176 pp.

Sánchez-Pérez, J.M., Antiguedad, I., Arrate, I., García-Linares, C., Morell, I., 2003a. The influence of nitrate leaching through unsaturated soil on groundwater pollution in an agricultural area of the Basque country: a case study. Sci. Total Environ. 317, 173–187. doi:10.1016/S0048-9697(03)00262-6

Sánchez-Pérez, J.M., Vervier, P., Garabétian, F., Sauvage, S., Loubet, M., Rols, J.L., Bariac, T., Weng, P., 2003b. Nitrogen dynamics in the shallow groundwater of a riparian wetland zone of the Garonne, SW France: nitrate inputs, bacterial densities, organic matter supply and denitrification measurements. Hydrol. Earth Syst. Sci. Discuss. 7, 97–107.

Sanderman, J., Amundson, R., 2008. A comparative study of dissolved organic carbon transport and stabilization in California forest and grassland soils. Biogeochemistry 92, 41–59. doi:10.1007/s10533-008-9249-9

Servais, P., Anzil, A., Ventresque, C., 1989. Simple method for determination of biodegradable dissolved organic carbon in water. Appl. Environ. Microbiol. 55, 2732–2734.

Sheibley, R.W., Jackman, A.P., Duff, J.H., Triska, F.J., 2003. Numerical modeling of coupled nitrification–denitrification in sediment perfusion cores from the hyporheic zone of the Shingobee River, MN. Adv. Water Resour., Modeling Hyporheic Zone Processes 26, 977–987. doi:10.1016/S0309-1708(03)00088-5

Shen, Y., Chapelle, F.H., Strom, E.W., Benner, R., 2014. Origins and bioavailability of dissolved organic matter in groundwater. Biogeochemistry 1–18. doi:10.1007/s10533-014-0029-4

Stelzer, R.S., Bartsch, L.A., Richardson, W.B., Strauss, E.A., 2011. The dark side of the hyporheic zone: depth profiles of nitrogen and its processing in stream sediments. Freshw. Biol. 56, 2021–2033. doi:10.1111/j.1365-2427.2011.02632.x

Stelzer, R.S., Scott, J.T., Bartsch, L.A., Parr, T.B., 2014. Particulate organic matter quality influences nitrate retention and denitrification in stream sediments: evidence from a carbon burial experiment. Biogeochemistry 119, 387–402. doi:10.1007/s10533-014-9975-0

Stevenson, B.A., Schipper, L.A., McGill, A., Clark, D., 2011. Denitrification and Availability of Carbon and Nitrogen in a Well-drained Pasture Soil Amended with Particulate Organic Carbon. J. Environ. Qual. 40, 923. doi:10.2134/jeq2010.0463

Stutter, M.I., Richards, S., Dawson, J.J.C., 2013. Biodegradability of natural dissolved organic matter collected from a UK moorland stream. Water Res. 47, 1169–1180. doi:10.1016/j.watres.2012.11.035

Sun, X., Bernard-Jannin, L, Garneau, C., Arnold, J.G., Srinivasan, R., Sauvage, S., Sánchez-Pérez, J.M., 2015. Improved simulation of river water and groundwater exchange in an alluvial plain using the SWAT model. Hydrol. Process.(In press)

Takatert, N., Sanchez-Pérez, J.M., Trémolières, M., 1999. Spatial and temporal variations of nutrient concentration in the groundwater of a floodplain: effect of hydrology, vegetation and substrate. Hydrol. Process. 13, 1511–1526. doi:10.1002/(SICI)1099-1085(199907)13:10<1511::AID-HYP828>3.0.CO;2-F

Tillman, D.C., Moerke, A.H., Ziehl, C.L., Lamberti, G.A., 2003. Subsurface hydrology and degree of burial affect mass loss and invertebrate colonisation of leaves in a woodland stream. Freshw. Biol. 48, 98–107.

Vetter, R., 2013. Assessing the role of anammox in a nitrogen contaminated aquifer. University of North Carolina Wilmington.

Vidon, P., Allan, C., Burns, D., Duval, T.P., Gurwick, N., Inamdar, S., Lowrance, R., Okay, J., Scott, D., Sebestyen, S., 2010. Hot Spots and Hot Moments in Riparian Zones: Potential for Improved Water Quality Management1. JAWRA J. Am. Water Resour. Assoc. 46, 278–298. doi:10.1111/j.1752-1688.2010.00420.x

Volk, M., Arnold, J.G., Bosch, D.D., Allen, P.M., Green, C.H., 2007. Watershed configuration and simulation of landscape processes with the SWAT model, in:

MODSIM 2007 International Congress on Modelling and Simulation. Modelling and Simulation Society of Australia and New Zealand, Canberra, Australia. pp. 74–80.

Wagner, R., Marxsen, J., Zwick, P., Cox, E.J., 2011. Central European Stream Ecosystems: The Long Term Study of the Breitenbach. John Wiley & Sons.

Wallenstein, M.D., Myrold, D.D., Firestone, M., Voytek, M., 2006. Environmental controls on denitrifying communities and denitrification rates: insights from molecular methods. Ecol. Appl. 16, 2143–2152. doi:10.1890/1051-0761(2006)016[2143:ECODCA]2.0.CO;2

Wang, H., Ju, X., Wei, Y., Li, B., Zhao, L., Hu, K., 2010. Simulation of bromide and nitrate leaching under heavy rainfall and high-intensity irrigation rates in North China Plain. Agric. Water Manag. 97, 1646–1654. doi:10.1016/j.agwat.2010.05.022

Wiegner, T.N., Seitzinger, S.P., Glibert, P.M., Bronk, D.A., 2006. Bioavailability of dissolved organic nitrogen and carbon from nine rivers in the eastern United States. Aquat. Microb. Ecol. 43, 277–287.

Wickland, K.P., Aiken, G.R., Butler, K., Dornblaser, M.M., Spencer, R.G.M., Striegl, R.G., 2012. Biodegradability of dissolved organic carbon in the Yukon River and its tributaries: Seasonality and importance of inorganic nitrogen. Glob. Biogeochem. Cycles 26, GB0E03. doi:10.1029/2012GB004342

Williams, J.R., 1995. The EPIC model. 909–1000.

Wong, J.C.Y., Williams, D.D., 2010. Sources and seasonal patterns of dissolved organic matter (DOM) in the hyporheic zone. Hydrobiologia 647, 99–111. doi:10.1007/s10750-009-9950-2

Zarnetske, J.P., Haggerty, R., Wondzell, S.M., Bokil, V.A., González-Pinzón, R., 2012. Coupled transport and reaction kinetics control the nitrate source-sink function of hyporheic zones. Water Resour. Res. 48, W11508. doi:10.1029/2012WR011894

# Chapter 6. Assessment of the surface water - groundwater exchange and shallow aquifer denitrification in the floodplain area using the SWAT-LUD model.

This chapter describes the application of SWAT-LUD in the middle floodplain of the Garonne basin. Multiple classic subbasins and subbasin-LUs were included in the study area, the connection between classic subbasin and subbasin-LU was carried out. The floodplain water storage function was presented and the influence of denitrification in the floodplain shallow aquifer on river nitrate flux was quantified. This chapter is written in the publication prepared to be submitted to Sustainability of water quality and ecology.

# Assessment of the surface water - groundwater exchange and shallow aquifer denitrification in the floodplain area using the SWAT-LUD model

X. Sun[1,2], L. Bernard-Jannin[1,2], Y. Grusson[1,3], J.G. Arnold[4], R. Srinivasan[5], S. Sauvage[1,2], J.M. Sanchez Perez[1,2*]

[1] *University of Toulouse; INPT, UPS; Laboratoire Ecologie Fonctionnelle et Environnement (EcoLab), Avenue de l'Agrobiopole, 31326 Castanet Tolosan Cedex, France*

[2] *CNRS, EcoLab, 31326 Castanet Tolosan Cedex, France*

[3] *Chaire de recherche EDS en previsions et actions hydrologiques, Department of Civil and Water Engineering, Université Laval, Québec, G1V 0A6, Canada*

[4] *Grassland, Soil & Water Research Laboratory USDA-ARS, Temple, TX 76502, USA*

[5] *Spatial Science Laboratory in the Department of Ecosystem Science and Management, Texas A&M University, College Station, TX 77845, USA*

*Corresponding author

E-mail: jose-miguel.sanchez-perez@univ-tlse3.fr

Tel: 33 (0)5 34 32 39 20 Fax: 33 (0)5 34 32 39 01

Address: Laboratoire d'Ecologie Fonctionnelle et Environnement (ECOLAB), UMR 5245 CNRS-UPS-INPT Ecole Nationale Supérieure Agronomique de Toulouse (ENSAT) Avenue de l'Agrobiopole BP 32607, Auzeville Tolosane 31326 CASTANET TOLOSAN Cedex FRANCE

Abstract: Floodplains support intensive agricultural activities, since recharged groundwater in cultivated fields is an important source of the nitrate contamination of surface water, the nitrate level in groundwater can have a significant influence on the quality of surface water. As surface water contains rich oxygen and organic matter and groundwater contains abundant nutriment elements, numerous studies indicated the importance of interactions between groundwater and surface water (SW-GW). Denitrification is known as an important process that decreases the nitrate load of groundwater discharging into streams. However, rare of the large scale models included floodplain shallow aquifer denitrification functions. The SWAT-LUD model is developed based on the SWAT model. Modules that represented SW-GW exchange and shallow aquifer denitrification in the floodplain area were involved in the model. In this study, the SWAT-LUD model was applied in the middle floodplain area of the Garonne catchment. Observed river water discharges, groundwater levels and shallow aquifer nitrate concentrations were used for calibration. Results proved that SWAT-LUD model could represent the SW-GW exchange and shallow aquifer denitrification appropriately. The

simulated results illustrated that the main water flow direction at this interface is from aquifer to river, which taken 66% of the total exchanged water volume. The denitrification in the shallow aquifer reduced groundwater nitrate concentration obviously, it consumed almost 50% of nitrate originated from the simulate area flow to the channel. POC played an extremely important role in the occurrence of denitrification. More than 90% of the denitrification is triggered by POC. In the studied river section, the nitrate main come from the upstream river water. The channel nitrate concentration was recuded around 0.13 mg· $L^{-1}$ with the shallow aquifer denitrification function in the alluvial plain area.

**Keyword**s: SWAT-LUD model; denitrification; floodplain aquifer; Garonne River

## 6.1 Introduction

The excessive chemical N fertilization during the past century caused environmental and health problems, like more greenhouse gases - nitrous oxide and ammonia released to the atmosphere, soil and water body acidification and eutrophication caused by the excessive inorganic nitrogen in aquatic ecosystem (Gruber and Galloway, 2008). Nitrate pollution that enter aquatic ecosystems via point and nonpoint sources had drawn worldwide attention for a long time (Bijay-Singh et al., 1995; Carpenter et al., 1998; Jalali, 2011). Floodplains support intensive agricultural activities, in Europe and North America, up to 90% of floodplains are cultivated (Tockner and Stanford, 2002). Recharged groundwater in cultivated fields is an important source of the nitrate contamination of surface water, and the nitrate level in groundwater can have a significant influence on the quality of surface water (Cey et al., 1999).

The hydrologic connectivity links floodplains and rivers into integrated ecosystems. Particulate and dissolved matter exchanged between those two systems via both surface flow and groundwater flow (Tockner et al., 1999). As surface water contains rich oxygen and organic matter and groundwater contains abundant nutriment elements, numerous studies indicated the importance of interactions between groundwater and surface water as they have significant influence on the biotic communities and ecosystem process on both river and shallow aquifer ecosystems (Bayley, 1995; Thomaz et al., 2007).

Riparian zones are known as the buffer zones that located between the terrestrial and the aquatic ecosystems (Gregory et al., 1991). Numerous studies have proposed that denitrification in riparian areas is an important process that reduces the nitrate load of

groundwater discharging into streams (Hill, 1996; Maître et al., 2003; Martin et al., 1999). Since organic carbon is usually identified as the major factor that limiting denitrification rate in shallow aquifer system, the rich content of organic carbon in riparian soil was identified support the high rate of denitrification (Hill, 1996). The importance of riparian hydrologic condition on denitrification was recognized (Lamontagne et al., 2005; Rassam et al., 2008) and it was suggest that the denitrification may be strongly influenced by the riparian zone hydrogeological setting and hydraulic properties of the underlying geological deposits (Vidon and Hill, 2005). The shallow depth of groundwater increases the interaction of groundwater with organic rich surface soils which favors denitrification (Gold et al., 2001; Roulet, 1990). Compared with the study of denitrification in the riparian soil, the denitrification occurs in the groundwater was paid much less attention. Studies proved that the denitrification in the shallow aquifer played an important role in nitrate depletion also (Iribar, 2007; Sánchez-Pérez et al., 2003) and Sun et al (submitted) found that around 40% of upland nitrate entered into the riparian zone was consumed through denitrification.

SW-GW interaction is a complex process that driven by geomorphology, hydrogeology and climate conditions (Sophocleous, 2002). Most of the models involved this function are distributed models, such as MODFLOW (Lautz and Siegel, 2006; Storey et al., 2003), MOHID (Bernard-Jannin et al. submitted), HYDRUS (Langergraber and Šimůnek, 2005) or 2SWEM (Peyrard *et al.*, 2008). This type of model usually requires spatial inputs in high resolution, numerous parameters and are characterised by a significant computation time that inhibit their application on large scales. The river/groundwater interface is mostly not included in large scale conceptual hydrological models. To overcome this issue, conceptual and distributed models have been incorporated, such as SWAT-MODFLOW (Kim et al., 2008; Sophocleous and Perkins, 2000), WATLAC (Zhang and Li, 2009) and WASIM-ETH-I-MODFLOW (Krause and Bronstert, 2007), but the limitation of distributed model still exist in the incorporated model.

Denitrification occurs in the soil profile is contained in numerous models. Heinen (2006) has reviewed more than 50 models that include simplified denitrification process in the soil layers. The riparian ecosystem management model (REMM) is the model developed to help make decisions on management of riparian buffers to control nonpoint source pollution (Lowrance et al., 2000). Denitrification function was included in the REMM model, but like other model, it was considered only occur in soil profile, the shallow groundwater processes were not included, and the exchange between surface water and subsurface water wasn't taken into account. Moreover, REMM model is a field scale model, the upland process should

be simulated by other models, and the carbon cycling in the model is complicate, it would be difficult to be applied at catchment scale. The influences of riparian zones on biogeochemical cycling at catchment scale were involved in several model, like RNM (riparian nitrogen model) model, SWIM (soil and water integrated model) model and SWAT (The Soil and Water Assessment Tool) model. RNM model was developed to simulate nitrate removal from groundwater and surface water through denitrification as they interact with riparian zone soil at catchment scale (Rassam et al., 2005, 2008), the groundwater levels are simulated in this model. Hattermann *et al.* (2006) added the wetland function in SWIM model, in which the influence of plant uptake and denitrification in the riparian zone on nitrogen cycling were included into the model. In SWIM model, a decay rate was applied to represent the denitrification occurs in the shallow aquifer. In SWAT model, a decay coefficient of shallow aquifer nitrate was introduced also, but instead of depending on the actual nitrate concentration in SWIM model, the decay rate depends on the initial nitrate concentration in the shallow aquifer in SWAT model. The SW-GW exchange and denitrification occurred in the shallow aquifer are not simulated by these models.

To represent the SW-GW exchange, a new type of subbasin called subbasin-LU was developed in SWAT model and the landscape unit (LU) structure was introduced into the subbasin-LU, the modified model is called SWAT-LUD (Sun et al. revised). The shallow aquifer denitrification function was added to SWAT-LUD model, the influence of SW-GW exchange and flooding on nitrate cycling were involved in the model also. The modified model was applied only in one subbasin-LU and the impact of shallow aquifer denitrification on channel nitrate content was not carried out. The objectives of this study are test the applicability of the SWAT-LUD model at larger scale and quantify the influence of SW-GW exchange and shallow aquifer denitrification on nitrate transport both in the river and shallow aquifer.

## 6.2 Method

### 6.2.1 SWAT-LUD

The SWAT model is a process-based, semi-distributed and watershed-scale model (Arnold et al., 1998). To represent the spatial heterogeneity, the SWAT model includes three main constructions: basin, subbasin and hydrologic response unit (HRU). The basin is separated into subbasins; subbasins are divided into HRUs, which are particular combinations of land cover, soil type and slope. In the SWAT model, processes are simulated for each HRU

and then aggregated in each subbasin by a weighted average (Arnold et al., 1998; Lam et al., 2010). With the traditional HRU delineation method, flow is summed at the subbasin scale, the natural downward flow that routed across the landscape is not represented. For this application, an additional unit called Landscape Units (LU) that take place between a subbasin and an HRU was developed and added to the model (Volk *et al.,* 2007). Each subbasin is composed of three LUs (the divide ($LU_3$), the hillslope ($LU_2$) and the valley bottom ($LU_1$)), and HRUs are distributed across the different LUs, the modified model was called SWAT-LU. In SWAT-LU, the hydrologic processes are still single tracks (flow from $LU_3$ routed through $LU_2$ to $LU_1$ and then entered the river), the function of two direction SW-GW exchanges and the influence of flooding on groundwater are not included. To represent the SW-GW exchanges occur in the alluvial plain, the subbasin that holds alluvial soil was separated into two subbasins: subbasin-LU and classic subbasin. Subbasin-LU corresponds to the subbasin delimited by the floodplain and the LU structure was applied in it. In subbasin-LU, Darcy's equation was applied to calculate water exchanges between LUs and between $LU_1$ and the river based on the LU structure. The recharged flood water volume during flooding and the transfer of dissolved elements between LUs and between $LU_1$ and river water were also involved in the model. In the upland classic model, the processes were kept as in initial SWAT model, processes were simulated for each HRU and aggregated to the river. The subbasin-LU and classic subbasin were linked through the river, and the modified model was called SWAT-LUD (Sun et al, revised). The evolution of SWAT model and the main modifications were shown in Figure 1.

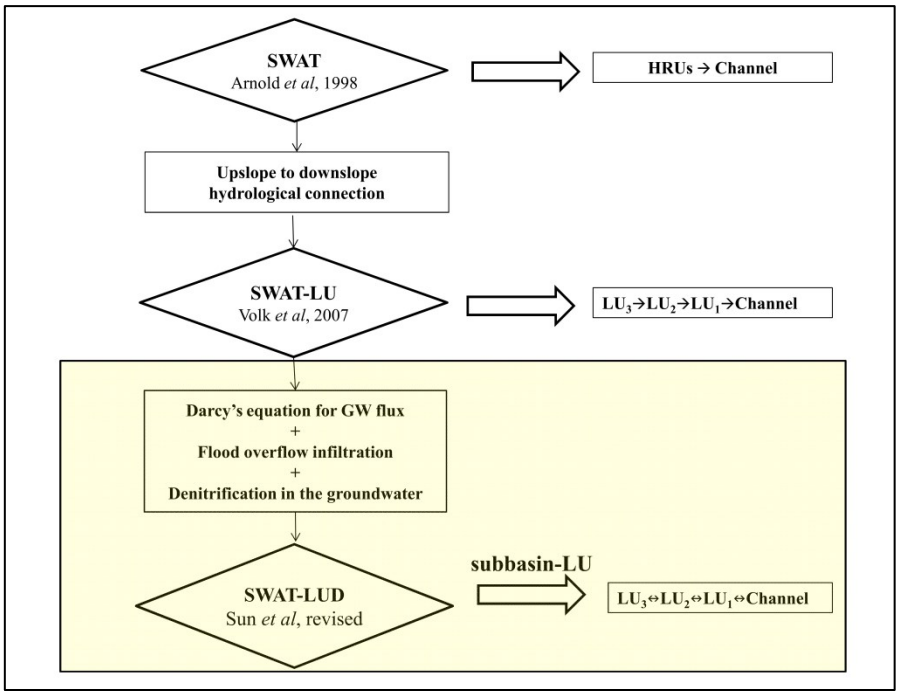


Figure 1. Evolution of the SWAT model and the main modifications

The hydrologic processes in SWAT-LUD model were shown in Figure 2. The denitrification occuring in the shallow aquifer that triggered by both dissolved organic carbon (DOC) and particulate organic carbon (POC) was added to the model, and the recharged soil nitrate along with infiltrated floodwater was considered also by the model (Sun et al., submitted). In this study, the denitrification occurs in the soil profile was kept as in SWAT model except when groundwater arrive soil profile, in that case, the denitrification was calculated with the equation that applied for shallow aquifer. The detailed description of the modification in the model could be found in Sun et al (revised) and Sun et al (submitted).

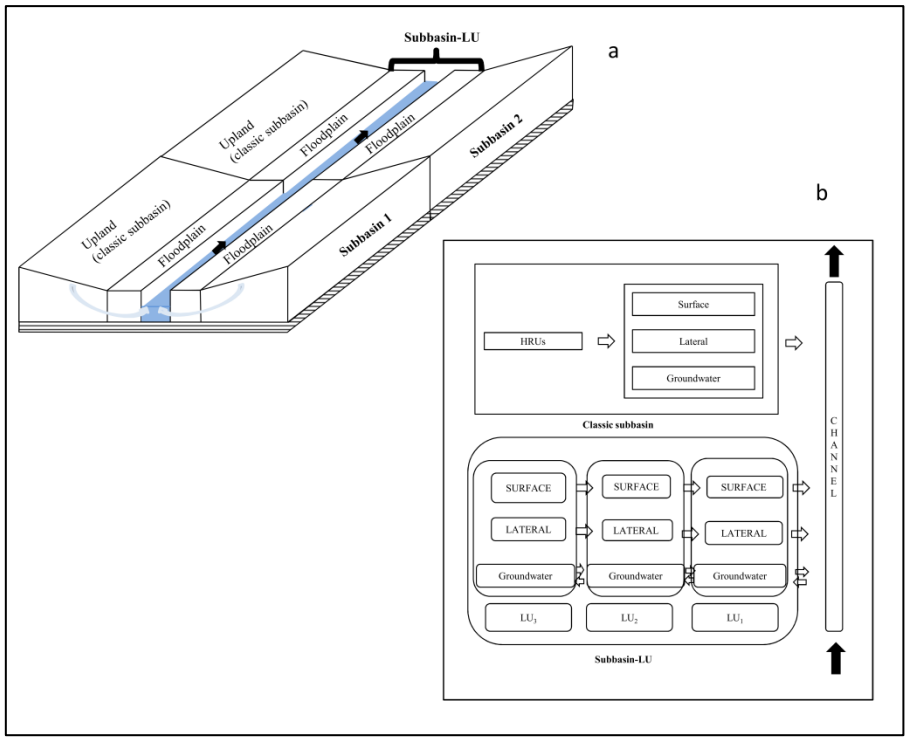


Figure 2. The hydrologic process of SWAT-LUD 'a' represents the location of subbasin-LU and the connection between subbasins, 'b' represents the hydrologic processes in subbasin-LU and classic subbasin and their connection through the river.

### 6.2.2 Definition of LUs and distribution of HRUs

In the previous studies, only one subbasin-LU was simulated and each LU contained only one HRU. The definition of the widths of LUs was made according to the surface of floodplain covered by the flood return period: $LU_1$ represented the one-year return flood area, $LU_2$ represented the two to five-year return flood area and $LU_3$ corresponded to the ten or more years return flood area (Sun et al, revised, Sun et al., submitted). With multiple subbains, the boundary of floodplain and return flooded areas are more difficult to be definited. Since alluvial soils are generally associated with floodplains, the distribution of floodplain was considered to be the same as the alluvial soil. The surface area of $LU_1$, $LU_2$ and $LU_3$ were considered to be 10%, 20% and 70% of the alluvial soil area respectively which correspondence to the flood return periods (1 year, 2-5 years and 10 or more years respectively).

#### 6.2.2.1 Distribution of HRUs in LUs

Alluvial HRUs (except urban alluvial HRUs) in the subbasin-LU were simplified into three groups based on their land use type: forest alluvial HRU (F-HRU), pasture alluvial HRU

(P-HRU) and Agricultural alluvial HRU (A-HRU). The alluvial HRUs with land cover of all types of forest were integrated to be an F-HRU. The characters of the F-HRU were considered to be the same as the largest forest alluvial HRU before the integration. The alluvial HRUs with pasture land cover or land types similar to the characters of pasture (like orchard or vineyard) were integrated to be a P-HRU, and the alluvial HRUs with agriculture land use were integrated to be an A-HRU. The characters of these two HRUs were chosen with the same method for the F-HRU, taken the characters of the largest HRU before the integration.

Since the general natural distribution of land use in alluvial area is characterized by the succession of riparian forest, pasture and agriculture as the increase of the distance from the river. Based on this succession of land use, the distribution of HRUs into LUs was as follows: Firstly, F-HRU was assigned into $LU_1$. If the area of the F-HRU is larger than $LU_1$, the F-HRU was separated into two HRUs, one corresponding to the area of $LU_1$ and another to the remaining area. If the area of the F-HRU is smaller than $LU_1$, then all F-HRU was assigned into $LU_1$, and the empty area in $LU_1$ was completed by P-HRU. In this case, if the P-HRU area is bigger than the empty area in $LU_1$, the P-HRU was then separated into two HRUs, one corresponding to the area of the empty area in $LU_1$, another one to the remaining area. If P-HRU is smaller than the empty area in $LU_1$, then all the P-HRU was assigned into $LU_1$ and the empty area in $LU_1$ was completed by A-HRU. In this condition, A-HRU was divided into 2 HRUs. The same method was applied to distribute HRUs into $LU_2$ and $LU_3$. All the HRUs of the same type have the same characters.

### 6.2.3 Study site

The Garonne River is the main river of the largest drainage basin in the southwest France, starting from Pyrenees mountains and flowing into the Atlantic Ocean. It is an eighth ordered river and the third longest river in France with the length of 525 km and has a drainage area about 51 500 $km^2$ at the last gauging station (Tonneins). The basin includes most of the Aquitaine basin which is surrounded by the Massif Central in the north-east, the Pyrenees mountains in the south and the Atlantic ocean in the west (Semhi et al., 2000).The climate of the Garonne watershed is impacted by the Atlantic Ocean and Mediterranean sea. The average annual rainfall is about 900mm (Caballero et al., 2007). The monthly temperature ranged from 5°C in January to 20°C in July. The hydrology of the area is mainly influenced by the three places (Pyrenees Mountain, Massif Central and Atlantic Ocean). The largest discharges

occur twice a year, in the spring as a result of snow melt and in late autumn caused by intense rainfalls (Sánchez-Pérez et al., 2003).

The studied floodplain area is located in the middle Garonne River, between Toulouse city and the confluence of the Tarn River. The floodplain widens up to 2-4 km. Between 4-7m of the coarse alluvium (sand and gravel) eroded from the Pyrenees Mountains during past glacial periods deposited in the floodplain overlie impermeable molasse. The valley contains a classic flight of terraces that represent episodic bedrock valley deepening punctuated by lateral migration of deposition of sediments (Lancaster, 2005). A series of terraces exist in the floodplain, in which the high terrace delimited the floodplain. The middle terrace is cultivated and is rarely flooded (every 30–50 years), which has a width of about 2 km. The lower terrace with the width of a few hundred is devoted to poplar plantations, is flooded about every 5 years. The riparian zone has a width of 10-100m, and is flooded almost each year (Peyrard et al., 2008). The common natural riparian vegetation types found along this reach of the Garonne River include willow and ash (Pinay et al., 1998). The floodplain is heavily cultivated, high production of corn, sunflower and sorghum were sustained by fertilization and irrigation. Shallow aquifer has a common nitrate concentration of 50 - 100 mg $L^{-1}$(Pinay et al., 1998; Sánchez-Pérez et al., 2003) (Figure 4).

The channel is a meandering, single-thread channel, is around 85 km long with a mean coefficient of sinuosity of 1.3. In the past, the Garonne River was incised as a result of mining of gravel and cobble from the riverbed (Beaudelin 1989). The longitudinal gradient is around 0.001in this section, the river bed altitude along with the main channel is shown in Figure 5. Portet gauging station located at about 10 km downstream of Toulouse city. The average daily flow is around 200 $m^3 \cdot s^{-1}$, but it ranges from about 20 $m^3 \cdot s^{-1}$ to about 4300 $m^3 \cdot s^{-1}$ (Banque Hydro, http://www.hydro.eaufrance.fr/). Four piezometers with continuous record of groundwater levels documented by BRGM (Bureau de Recherches Géologiques et Minières) located in the study site (Figure 3).

Monbéqui is located in a meander of the alluvial plain. In Monbéqui, the first 50 - 200 m of the riverbank is covered by riparian forest and poplar plantations, surrounded by agricultural land. Several terraces exist in this area, generated by sediment deposition and washing out by flooding events. Artificial dykes have been constructed in the region to protect the agricultural land. Piezometers were installed in this site. The alluvium thickness ranges from 2.5 to 7.5 m, with an arithmetic mean of 5.7m (Sánchez-Pérez et al., 2003). The

groundwater table varies from 2 to 5 m in low water periods and rise rapidly up to soil profile during floods (Weng et al., 2003).

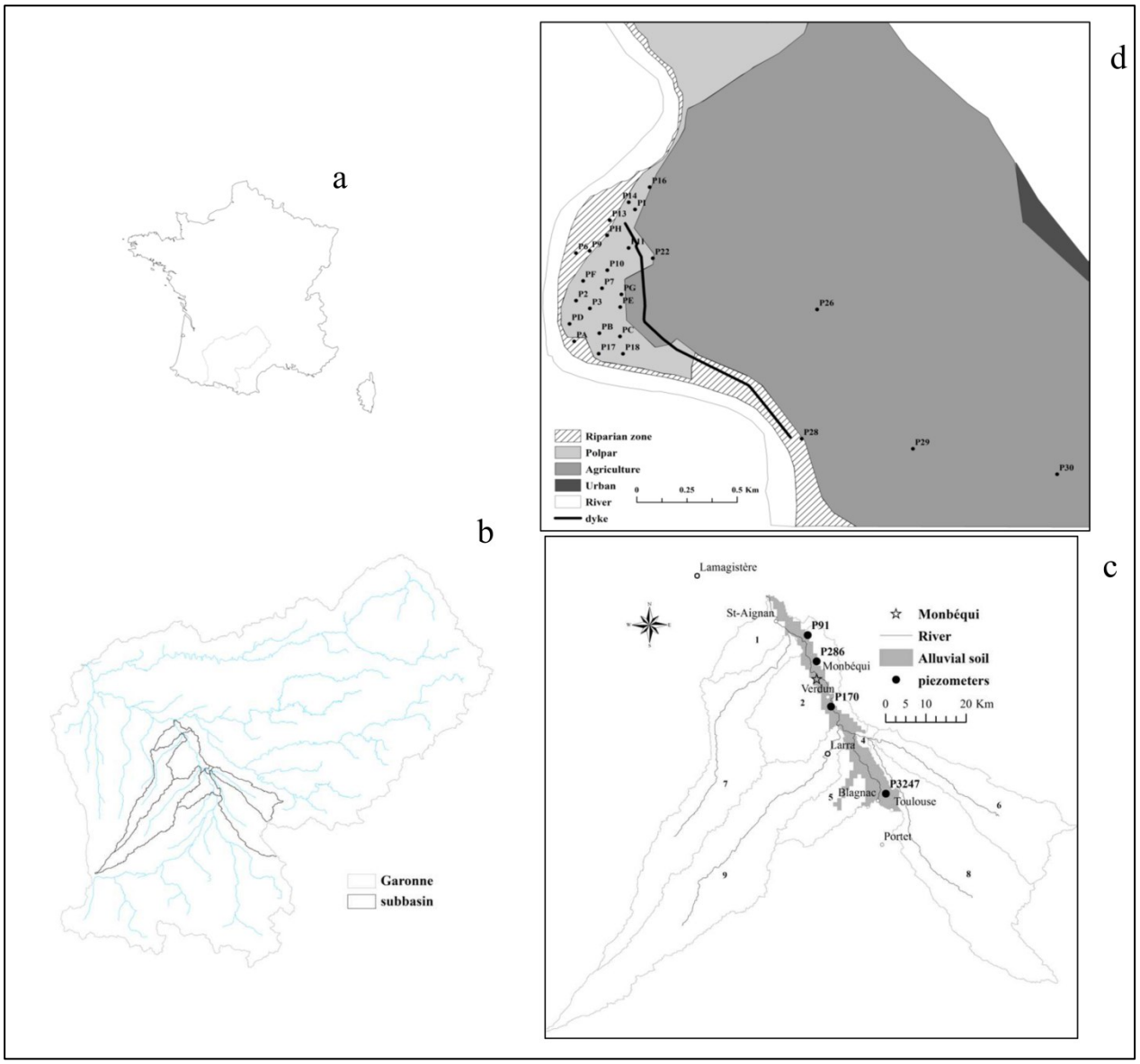


Figure 3. Location of the study site. 'a' represents the location of the Garonne River, 'b' represents the location of studied floodplain, 'c' represents the location of piezometers in the three subbasin-LUs and 'd' represents the distribution of piezometers in Monbéqui.

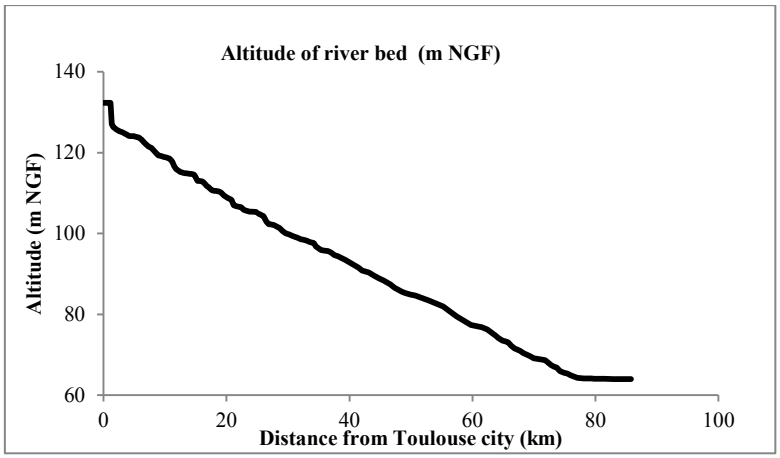


Figure 4. Altitude of the river bed in the studied floodplain (according to Sauvage et al., 2003).

### 6.2.4 Subbasins and LUs parameters

The subbasin-LU and LU parameters are presented in Table 1. Subbasin-LU (1) is the subbasin-LU near to the Portet gauging station, and subbasin-LU (3) is the subbasin-LU farthest from the Portet gauging station. The values of porosity were given based on the study of Seltz (2001) and Weng et al. (2003).

Table 1. The parameters of the three subbasin-LUs and the LUs.

| | Area (km2) | Channel | | | LUs | | | | | |
|---|---|---|---|---|---|---|---|---|---|---|
| | | | | | | | | | HRUs | |
| | | Long (km) | Width (m) | Slope (m/m) | | Slope (m/m) | porosity | Area ($km^2$) | Land use | Fraction of LU (%) |
| Subbasin-LU (1) | 57.27 | 22.11 | 200 | 0.00063 | $LU_1$ | 0.002 | 0.1 | 5.73 | PAST | 0.1 |
| | | | | | | | | | FRSD | 0.9 |
| | | | | | $LU_2$ | 0.005 | 0.1 | 11.45 | PAST | 1.0 |
| | | | | | $LU_3$ | 0.005 | 0.1 | 40.09 | PAST | 0.36 |
| | | | | | | | | | AGRR | 0.64 |
| Subbaisn-LU (2) | 87.95 | 40.53 | 200 | 0.00078 | $LU_1$ | 0.002 | 0.1 | 8.79 | FRSD | 1.0 |
| | | | | | $LU_2$ | 0.005 | 0.1 | 17.59 | PAST | 0.5 |
| | | | | | | | | | FRSD | 0.35 |
| | | | | | | | | | AGRR | 0.15 |
| | | | | | $LU_3$ | 0.005 | 0.1 | 61.56 | AGRR | 1.0 |
| Subbasin-LU (3) | 22.26 | 13.04 | 200 | 0.00069 | $LU_1$ | 0.002 | 0.1 | 2.23 | PAST | 0.7 |
| | | | | | | | | | FRSD | 0.3 |
| | | | | | $LU_2$ | 0.005 | 0.1 | 4.45 | PAST | 1.0 |
| | | | | | $LU_3$ | 0.005 | 0.1 | 15.58 | PAST | 0.1 |
| | | | | | | | | | AGRR | 0.9 |

The crop rotations applied in the agricultural area was given based on the study of the Save River (Boithias, 2012; Boithias et al., 2014) (Table 2).

Table 2. Crop rotations applied in the agriculture area

| Year | Month | Day | Operation | Crop | Type | Quantity | Unit |
|---|---|---|---|---|---|---|---|
| 1 | 7 | 25 | Tillage | | Generic Conservation Tillage | | |
| 1 | 10 | 1 | Tillage | | Generic Conservation Tillage | | |
| 2 | 1 | 31 | Tillage | | Harrow 10 Bar Tine 36 Ft | | |
| 2 | 4 | 1 | Plant | Corn | | | |
| 2 | 4 | 1 | Fertilization | | 18-46-00 | 150 | $kg \cdot ha^{-1}$ |
| 2 | 6 | 7 | Fertilization | | 46-00-00 | 435 | $kg \cdot ha^{-1}$ |
| 2 | 7 | 1 | Irrigation | | | 30 | mm |
| 2 | 7 | 10 | Irrigation | | | 30 | mm |
| 2 | 7 | 20 | Irrigation | | | 30 | mm |
| 2 | 8 | 1 | Irrigation | | | 30 | mm |
| 2 | 8 | 20 | Irrigation | | | 30 | mm |
| 2 | 9 | 1 | Irrigation | | | 30 | mm |
| 2 | 9 | 10 | Irrigation | | | 30 | mm |
| 2 | 10 | 15 | Harvest and kill | | | | |
| 2 | 11 | 1 | Plant | Wheat | | | |
| 3 | 1 | 25 | Fertilization | | 15-15-00 | 200 | $kg \cdot ha^{-1}$ |
| 3 | 3 | 10 | Fertilization | | 33-00-00 | 200 | $kg \cdot ha^{-1}$ |
| 3 | 7 | 10 | Harvest and kill | | | | |
| 3 | 9 | 8 | Tillage | | Generic Fall Plowing Operation | | |
| 4 | 4 | 1 | Tillage | | Harrow 10 Bar Tine 36 Ft | | |
| 4 | 4 | 15 | Plant | Sunflower | | | |
| 4 | 4 | 15 | Fertilization | | 15-15-00 | 300 | $kg \cdot ha^{-1}$ |
| 4 | 8 | 25 | Harvest and kill | | | | |
| 4 | 11 | 1 | Plant | Wheat | | | |
| 5 | 1 | 25 | Fertilization | | 15-15-00 | 200 | $kg \cdot ha^{-1}$ |
| 5 | 3 | 10 | Fertilization | | 33-00-00 | 200 | $kg \cdot ha^{-1}$ |
| 5 | 7 | 10 | Harvest and kill | | | | |

The daily discharge data of the Portet gauging station were used as input data. The concentration of nitrate in the input river water was considered to be constant in this study. The value was determined based on the measured data in Blagnac station (exit of Toulouse city) to take into account the influence of Toulouse city (www.eaufrance.fr ), which is 1.13 ($N\text{-}NO_3^-$) $mg \cdot L^{-1}$. The constant DOC concentrations in the shallow aquifers of LUs were

given based on the measured data in 2013, the DOC concentrations in the river water were given based on the measured data in Blagnac, Verdun and St-Aignan stations (www.eaufrance.fr ).

The topsoil layer was determined to be 0.5 m. The POC contents in the topsoil layers and lower layers were given based on the measured values by Jego (2008) and the measured AFDM (Ash Free Dry Mass) values of the alluvial sediment in 2013 respectively. The POC content in AFDM was considered to be 50 % based on recent studies (Griffiths et al., 2012; Hauer and Lamberti, 2011; Wagner et al., 2011). (Table 3)

Table 3. The given constant values of DOC in shallow aquifer and river water and POC in soil and shallow aquifer sediment

| | DOC ($mg \cdot l^{-1}$) (Constant) | POC (>50 cm) (%) (Constant) | POC (top 50cm) (%) (Constant) |
|---|---|---|---|
| $LU_1$ | simulated | 0.275 | 1.5 |
| $LU_2$ | 0.85 | 0.275 | 1.0 |
| $LU_3$ | 0.65 | 0.325 | 1.0 |
| River | 2.3<br>4.5 (During flooding) | | |

### 6.2.5 Calibration and evaluation

The simulation was carried out between 1997 and 2013. The calibration was performed automatically and manually. The observed discharges from the Larra, Verdun and Lamagistère gauging stations were used for the automatically calibration with SWAT-Cup. The observed groundwater levels of the four piezometers (P91, P170, P286 and P3247) were used for annually calibration. Since there is no piezometer located in subbasin-LU (3), observed groundwater levels in P91 were used to calibrate the simulated groundwater level in subbasin-LU (3). The shallow aquifer nitrate concentration observation is located only in the Monbéqui site, the measured nitrate concentration in 2004-2005 and 2013 in Monbéqui were used for manually calibration. The distributions of piezometers in the three LUs of the two periods in Monbéqui are shown in Table 4. Percent bias (PBIAS) and root mean square error (RMSE) were chosen as evaluating parameters.

Table 4. The distributions of piezometers in the three LUs for the calibration of shallow aquifer nitrate

| | LU1 | LU2 | LU3 |
|---|---|---|---|
| 2004-2005 | P6, P18 | P10 | P29 |
| 2013 | P6, P18, P17, P16, P2, PA, PD | P2, P3, P7, P9, P10, P13, P14, PB, PC, PF, PH, PI, PE, PG | P26, P22, P11 |

## 6.3 Results

### 6.3.1 Calibrated parameters

The automatically calibrated parameters are shown in Table 5.

Table 5. Automatically calibrated parameters

| | Description | File | Type | Verdun | Larra | Lamagistère |
|---|---|---|---|---|---|---|
| | | | | Subbasin Numbers | | |
| | | | | 9 | 5,4,6,8 | 1,2,7 |
| CN2 | SCS runoff curve number | .mgt | r | -0.014 | -0.040 | -0.048 |
| ALPHA_BF | Baseflow recession constant (1/days) | .gw | v | 0.44 | 0.89 | 0.35 |
| GW_DELAY | Groundwater delay time (days) | .gw | a | -27.33 | 59.49 | -23.19 |
| GWQMN | Threshold depth of water in the shallow aquifer required for return flow to occur (mm $H_2O$) | .gw | a | -43.67 | -77.67 | 181.67 |
| ESCO | Soil evaporation compensation factor | .hru | v | 0.72 | 0.72 | 0.93 |
| GW_REVAP | Groundwater “revap” coefficient | .gw | v | 0.062 | 0.028 | 0.072 |
| RCHRG_DP | Deep aquifer percolation fraction | .gw | a | 0.033 | 0.013 | 0.0073 |
| SOL_AWC | Avaiable water capacity of the soil layer (mm $H_2O$/mm soil) | .sol | r | 0.0087 | 0.046 | -0.019 |
| REVAPMN | Threshold depth of shallow aquifer revap or percolation to the deep aquifer to occur (mm $H_2O$) | .gw | c | -303.67 | 449.67 | -443.00 |
| CANMX | Maximum canopy storage (mm $H_2O$) | .hru | v | 22.65 | 28.25 | 13.65 |
| CH_K1 | Effetive hydraulic conductivity in tributary channel alluvium (mm/hr) | .sub | r | 3.63 | 7.25 | 36.77 |
| CH_S1 | Average slope of tributary channels (m/m) | .sub | r | -0.012 | -- | -- |
| SHALLST | Initial depth of water in the shallow aquifer (mm $H_2O$) | .gw | v | 595 | -- | 958.33 |
| DEEPST | Initial depth of water in the deep aquifer (mm $H_2O$) | .gw | v | 3241.67 | -- | 1865.00 |

| | | | | | | |
|---|---|---|---|---|---|---|
| GW_SPYLD | Specific yield of the shallow aquifer ($m^3/m^3$) | .gw | r | 0.17 | -- | -- |
| GWHT | Initial groundwater height (m) | .gw | r | 0.31 | 7.91 | -- |
| CH_W1 | Average width of tributary channels (m) | .sub | r | -- | -0.02 | 0.045 |
| CH_N1 | Manning's N value for the tributary channels | .sub | r | -- | -0.011 | -- |

Types of the parameters: r, relative (means the existing parameter value is multiplied by (1+a given value)); a, absolute (means the given value is added to the existing parameter value); v, replace (means the existing parameter value is to be replaced by the given value).

The manually calibrated parameters are shown in Table 6. The manually calibrated parameters were considered have the same values in the three subbasin-LUs.

Table 6. Manually calibrated parameters

| | Description | Unit | Calibrated values |
|---|---|---|---|
| | | | Subbasin-LU |
| CHD | Depth of the channel | m | 5 |
| CH_N | Manning n | -- | 0.06 |
| $K_{LU1}$ | Hydraulic conductivity of $LU_1$ | m/d | 100 |
| $K_{LU2}$ | Hydraulic conductivity of $LU_2$ | m/d | 50 |
| $K_{LU3}$ | Hydraulic conductivity of $LU_2$ | m/d | 50 |
| $K_{NO3}$ | half-saturation concentration of nitrate | $\mu mol \cdot l^{-1}$ | 30 |
| $k_{POC1}$ | Kpoc of $LU_1$ | $d^{-1}$ | 0.8e-5 |
| $k_{POC2}$ | Kpoc of $LU_2$ | $d^{-1}$ | 1.5e-6 |
| $k_{POC3}$ | Kpoc of $LU_3$ | $d^{-1}$ | 0.4e-6 |
| $k_{DOC1}$ | Kdoc of $LU_1$ | $d^{-1}$ | 0.005 |
| $k_{DOC2}$ | Kdoc of $LU_2$ | $d^{-1}$ | 0.002 |
| $k_{DOC3}$ | Kdoc of $LU_3$ | $d^{-1}$ | 0.002 |
| $F_{NO3}$ | Percentage of leached nitrate from soil profile during flooding | % | 30 |

### 6.3.2 Surface water - groundwater exchange

#### 6.3.2.1 Groundwater levels

The comparison of simulated and observed groundwater levels in the three subbasin-LUs are shown in Figure 5.

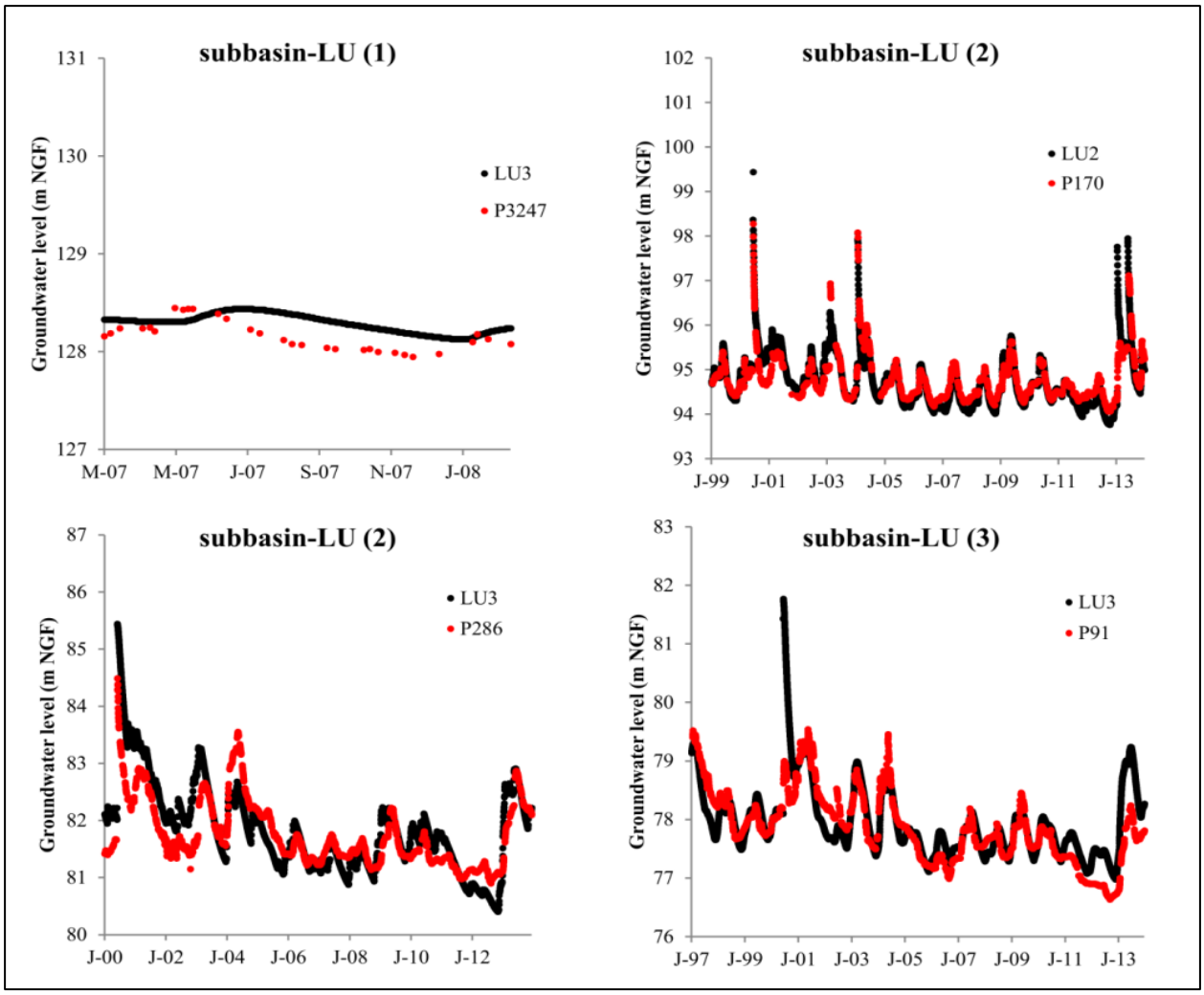


Figure 5. Simulated and observed groundwater levels in the three subbasin-LUs

The results showed that simulations and observations matched very well in the three subbasin-LUs in the long simulated period (Table 7).

Table 7. Parameters for evaluating the accuracy of simulated groundwater levels of the shallow aquifer using the SWAT-LUD model

| | LU | RMSE | PBIAS |
|---|---|---|---|
| Subbasin-LU(1) | $LU_3$ | 0.19 | -0.10 |
| Subbasin-LU(2) | $LU_2$ | 0.27 | 0.01 |
| | $LU_3$ | 0.47 | -0.13 |
| Subbasin-LU(3) | $LU_3$ | 0.57 | -0.02 |

### 5.1.1.1 Flood peak

The floodplain water storage function added in the model is shown in Figure 6, which appearances the flood peak of the largest flood event in the simulated period. It was proved that the flood peak decreased significantly (from 3040 to 1970 $m^3/s$) after flooded path the floodplain and the flooded water rested three days on the floodplain before totally return back to the channel.

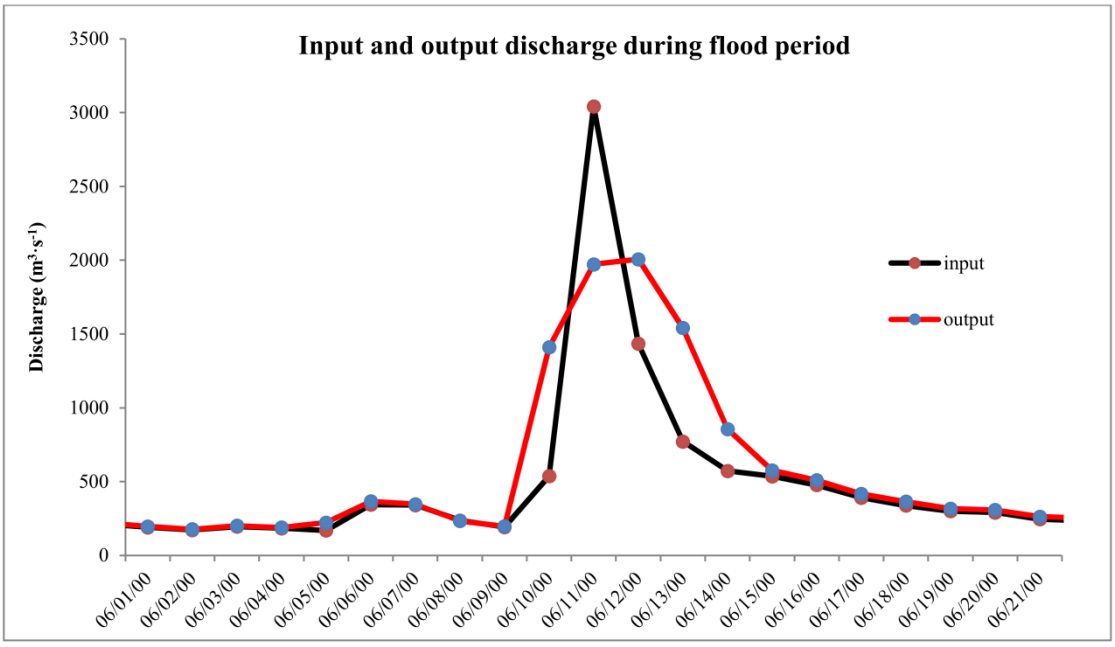


Figure 6. Simulated output of discharge during the flood peak (in which, input is the input water discharge of subbasin-LU (1), output is the output discharge of subbasin-LU (3)).

### 5.1.1.2 Exchanged water

The annually exchanged water quantity between the river and the aquifer in the three subbasin-LUs throughout the entire period simulated (1997-2013) is shown in Figure 8.

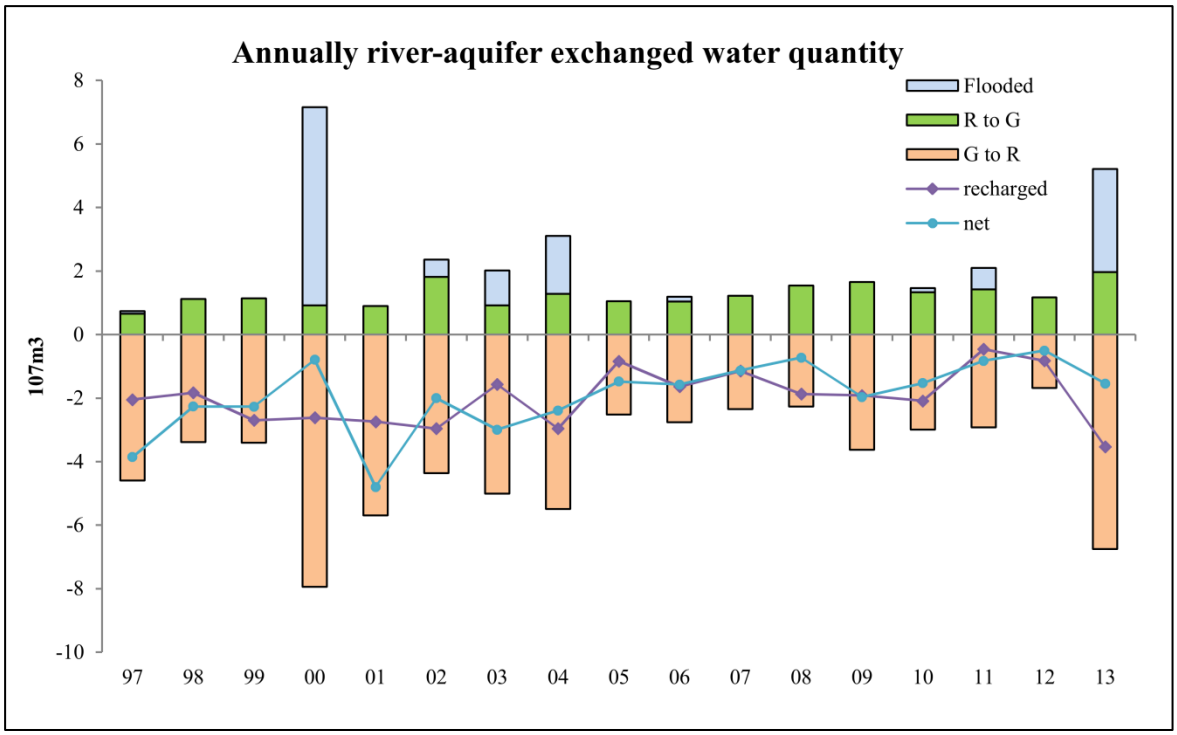


Figure 8. Annually exchanged water quantity between the river and the aquifer during the entire simulated period (1997-2013). Flooded means infiltrated flooded river water, R to G means infiltration of river water enter into aquifer through river bank, G to R means groundwater flow to the river, recharged means infiltrated soil water, net means the difference between the two direction flow.

It was found that the main water flow direction is from aquifer to river, which taken 66% of the total exchanged water volume. The water recharged from soil profile played an important role in SW-GW exchanged (33% of the total exchange). The over bank infiltration taken around 14% of the total exchanged water volume in the entire simulated period.

### 6.3.3 Denitrification

#### 6.3.3.1 Groundwater nitrate concentration

The simulated groundwater nitrate concentrations were compared with the observed data in Monbéqui (Figure 8).

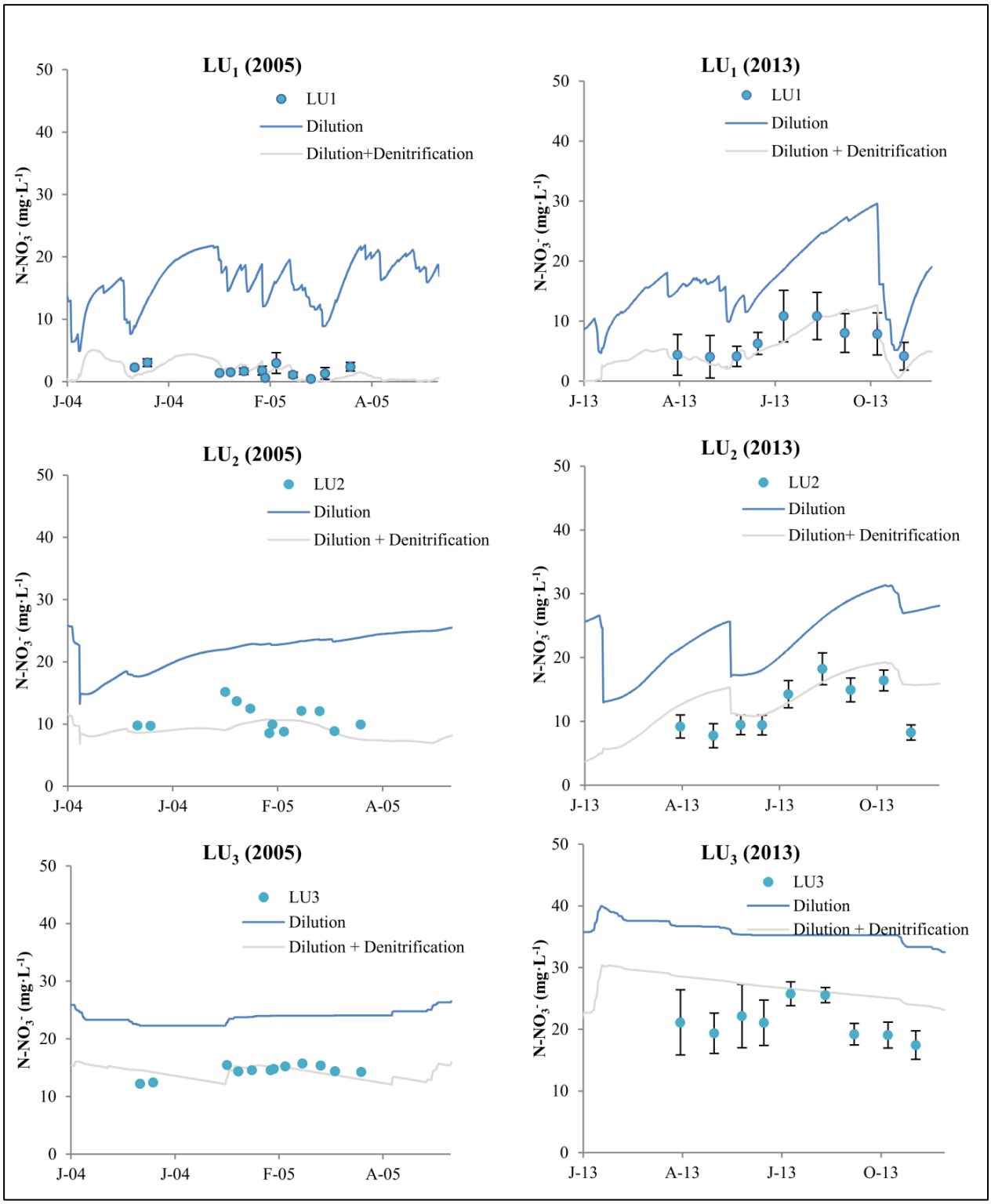


Figure 8. Simulated and observed nitrate concentrations in the aquifer of LUs during the years 2005 and 2013, where 'Dilution' is the simulated results with recharged river water and 'Dilution + Denitrification' is the simulated results with recharged river water and denitrification processes.

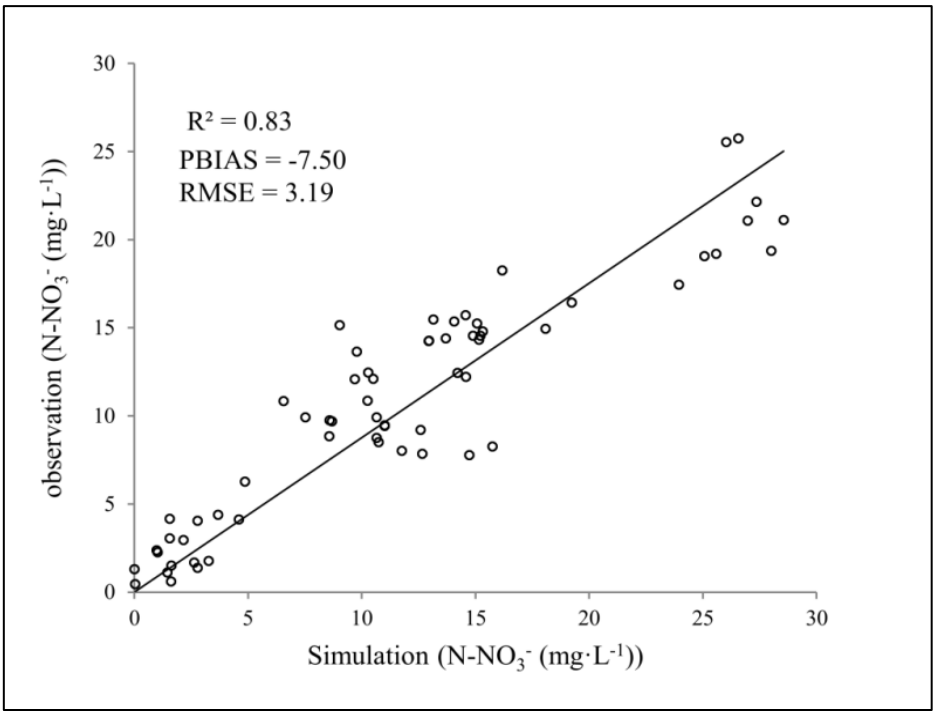


Figure 9. Observed and simulated (dilution plus denitrification) groundwater nitrate concentration in the two periods (2005, 2013)

It showed that the denitrification reduced groundwater nitrate concentration obviously. The simulated groundwater nitrate concentration with the consideration of denitrification matched well with the observed data (Figure 9).

### 6.3.3.2 Denitrification rate

The simulated annual denitrification rates are shown in Figure 10.

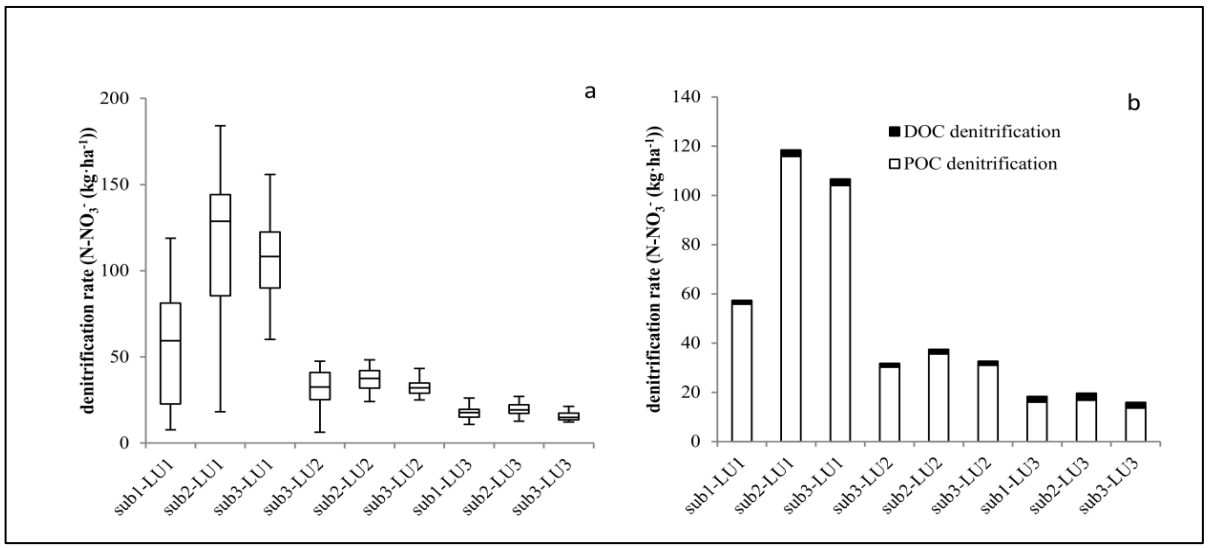

Figure 10. Simulated annual denitrification rates (a. annual total denitrification rates, b. annual denitrification rates triggered by DOC and POC) in the three subbasin-LUs

It was found that the denitrification rates occurred in $LU_1$s were more important than other two LUs in all the three subbasin-LUs. The average annual denitrification rates in the $LU_1$s of the three subbasin-LUs range from 55-120 Kg $N\text{-}NO_3^-\cdot ha^{-1}$, which is 26-38 T $N\text{-}NO_3^-\cdot km^{-1}$ for per kilometre length of the river. POC played an extremely important role in the occurrence of denitrification, more than 90% of the denitrification in the three subbasin-LUs is triggered by POC.

### 6.3.4 The influence of hydraulic conditions and nitrate content on denitrification

An analysis of correspondence between groundwater levels, groundwater nitrate concentrations and denitrification rate in $LU_1$s were performed (Fig. 11, 12).

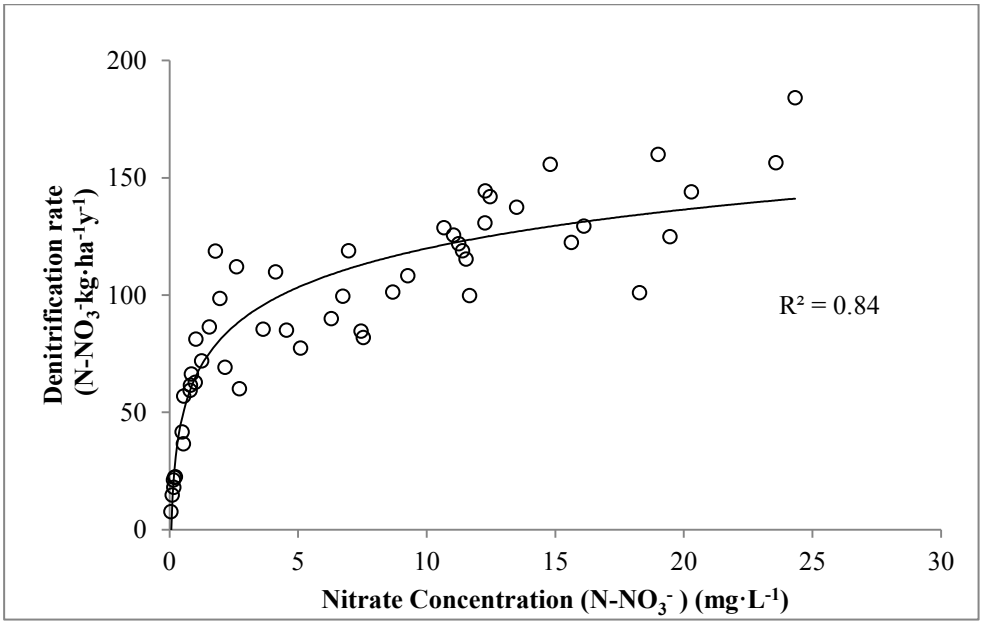


Figure 11. Correspondence between annual denitrification rates and nitrate concentrations in the entire simulated period (1997-2013)

It was proved that shallow aquifer denitrification rates highly related with the groundwater nitrate concentrations. The denitrification rate increase rapidly along with the rise of nitrate concentration during low nitrate content period. It became relatively stable after groundwater nitrate concentration was higher than 5 $mg\cdot L^{-1}$.

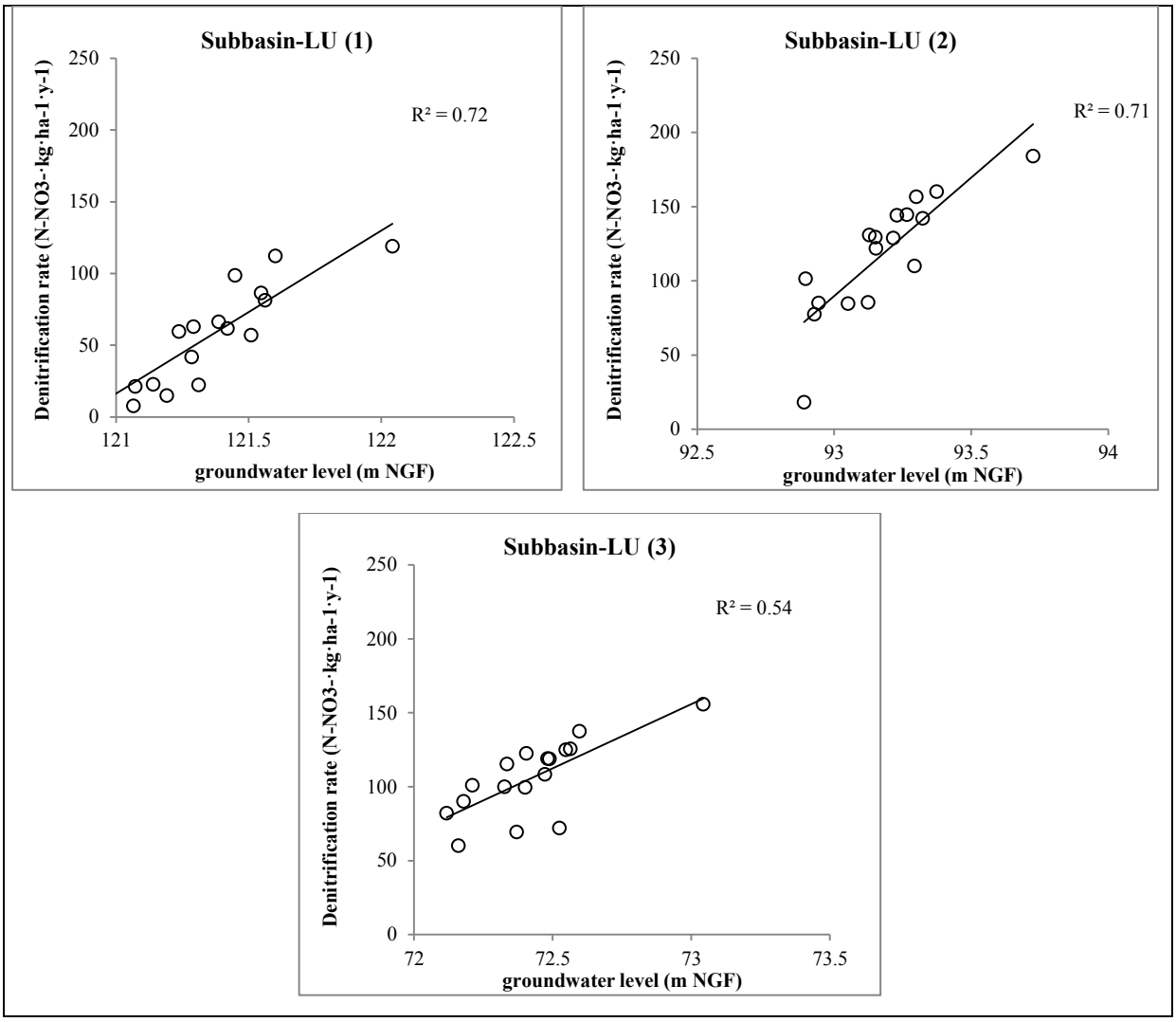


Figure 12. Correspondence between annual denitrification rates and relative groundwater levels in the entire simulated period (1997-2013)

The correspondence between groundwater levels and shallow aquifer denitrification rates showed that denitrification rate positively related with relative groundwater level in the three subbasin-LUs.

### 6.3.5 Channel nitrate balance

The comparison between simulated and observed nitrate contents that flow out of the simulated area is shown in Figure 13. It showed the simulations corresponding well with the observations, the nitrate output contents were simulated appropriately.

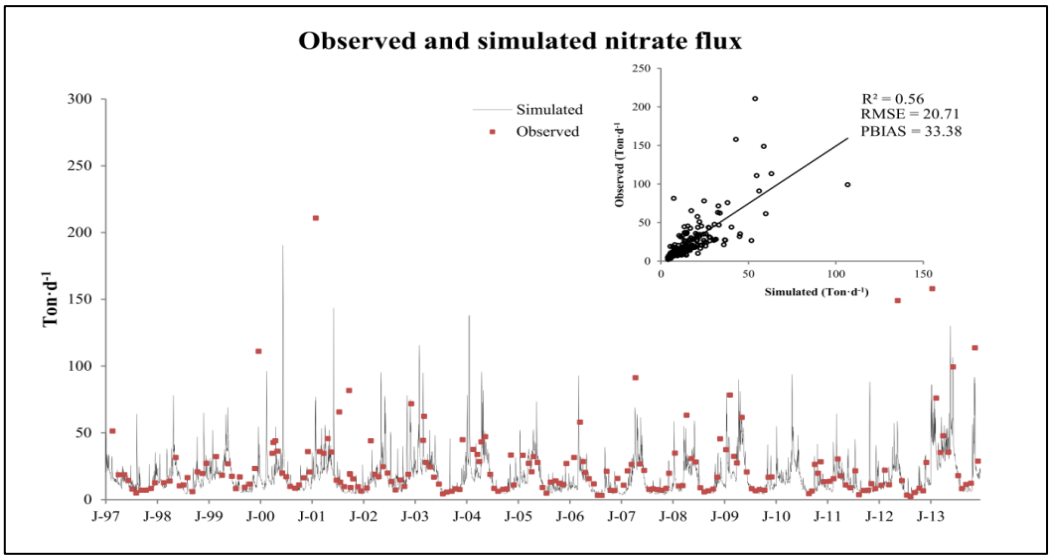


Figure 13. Simulated and observed nitrate content in the output of the study area

The average annual nitrate balance in the studied area is shown in Figure 14.

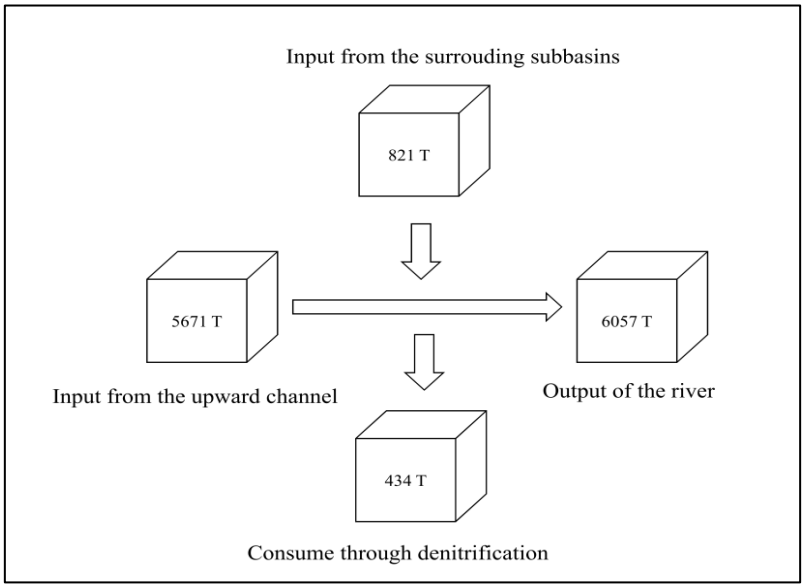


Figure 14. Average annual nitrate ($N\text{-}NO_3^-$) balance ($ton \cdot y^{-1}$) in the study area in the entire simulated period (1997-2013)

It indicated that the main nitrate source is the upstream river (87% of the total nitrate input), and denitrification in the floodplain consumed almost 50% of nitrate flow to the river originated from the studied area.

The annual reduced nitrate output discharges and nitrate concentration in the output of simulated area (output of subbaisn-LU (3)) caused by added shallow aquifer denitrification are shown in Figure 15.

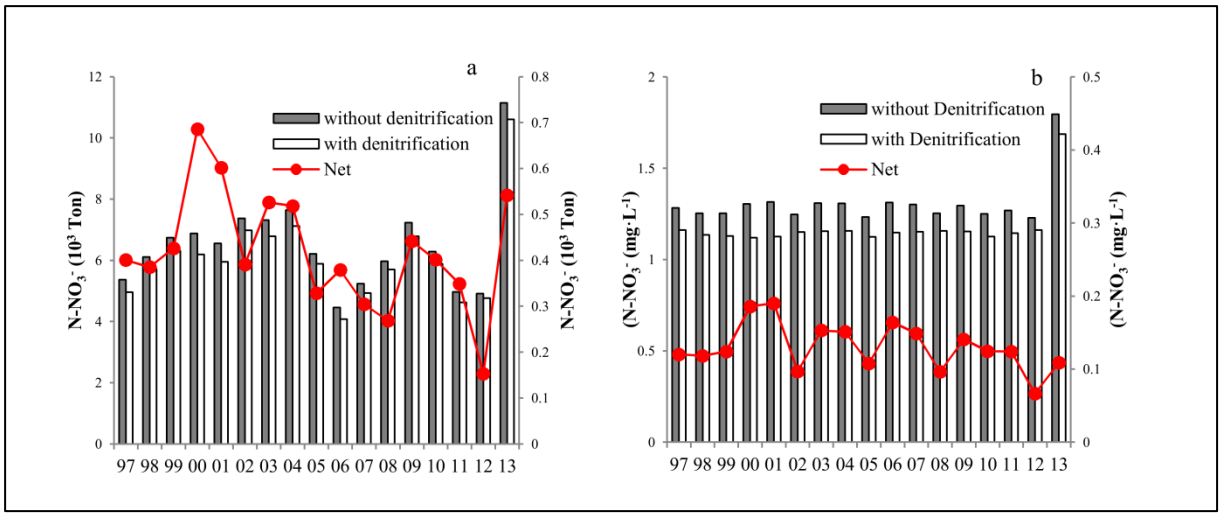


Figure 15. Annually reduced nitrate output content (a) and concentration (b) through denitrification

The annual $N\text{-}NO_3^-$ total nitrate discharge in the output of simulated area was reduced 150-680 Ton with the consideration of denitrification in the shallow aquifers of the subbasin-LUs. The reductions of $N\text{-}NO_3^-$ concentration range from 0.07 to 0.19 mg· $L^{-1}$.

## 6.4 Discussion

SWAT-LUD was applied in the middle Garonne floodplain area, numerous classic subbasins and subbasin-LUs were involved in the study area. The comparison between simulated and observed groundwater levels in the three subbasin-LUs proved that SWAT-LUD could represent the SW-GW exchange process occurred in floodplain region at large scale appropriately. The denitrification occurred in the shallow aquifer underneath the root zone was rarely paid attention. Gomez *et al.* (2012) simulated the biogeochemical zonation patterns with the concept of biogeochemical timescales. Denitrifying process in the hyporheic zones were simulated also. Zarnetske *et al.* (2012) integrated residence time model with a multiple Monod kinetics model that simulate the concentrations of oxygen ($O_2$), ammonium ($NH_4^+$), nitrate ($NO_3^-$) and dissolved organic carbon (DOC). Sheibley *et al.* (2003) simulated nitrification and denitrification process in sediment perfusion cores from the hyporheic zone. In 2SWEM model, the model NEMIS was coupled into the model to simulate the denitrification process in the floodplain hyporheic zone (Peyrard, 2008). However most of these models could only be applied at local scale, the model that simulated the nitrate attenuation process at river-floodplain interface at catchment scale still does not exist. The added modules in SWAT-LUD model provided the possible to simulate the SW-GW exchange and shallow aquifer denitrification in the floodplain area at the catchment scale. It

supplemented the modelling method of hydrologic and biogeochemical cycling that developed for the large scale application.

Most of the catchment scale hydrological models did not involve the contribution of surface water to subsurface flow, such as SWIM (Krysanova et al., 1998), TOPMODEL (Franchini et al., 1996) or MODHYDROLOG (Chiew and McMahon, 1994). The results from this study showed that it accounted for 34 % of total SW-GW exchanges over a long period in the floodplain area, which is almost the same as infiltrated rainfall (33%). Infiltrated flooded water was proved played an important role on the SW-GW exchange (Sophocleous, 2002; Wett *et al.*, 2002; Sun et al, revised; Bernard-Jannin et al, submitted). In this study, the infiltrated flooded river water taken 13.60% of the total exchanged water volume. Except the influence on groundwater, the floodplain played water storage function also during flood period that reduced the river water discharge (Frappart et al., 2005). The topographies of the channel and the connected floodplain have important influence of floodplain water storage capacity during flooding events (Roni et al., 2005). SWAT-LUD is a daily time step model, and the parameters that represented the topography of floodplain in SWAT-LUD are simple, each LU was defined with only unique width and slope. It limited the precise simulation of the water storage. As a semi-distributed model, the objective of the SWAT-LUD is to represent hydrologic condition the at large spatial and long temporal scale, it restricted the ability of detail representation.

The comparison of denitrification rate triggered by POC and DOC illustrated that compared with DOC, POC played an extremely important role. Since denitrification is a biological process, the identification of sources and bioavailability of POC in the shallow aquifer would be key factors of the understanding of shallow aquifer denitrification. The possible sources of POC in the shallow aquifer are: 1) buried organic material; 2) transported along with infiltrated river water; 3) transferred by bacterial from DOC; 4) infiltrated from soil. The POC content in the shallow aquifer of $LU_1$ is the same as in $LU_2$ and lesser than in $LU_3$, Kpoc in $LU_1$ was increased to match the simulated groundwater nitrate concentration with the observed low nitrate concentration. It suggested that the POC in $LU_1$ is more bioavailable than other two LUs. Since $LU_1$ is the most active zone interacts with river water, the POC and DOC in the river water would have more important influence on this zone than other two farther zones. Since POC and DOC of river water are more bioavailable than shallow aquifer, it could improve the denitrification rate in $LU_1$. Moreover, $LU_1$ is mainly covered with riparian forest, the POC content in the top layer of $LU_1$ is higher than other two

LUs also (Jego, 2008). The riparian forest root probably provided more bioavailable POC. Anammox is another important anaerobic nitrogen attenuating process in the shallow aquifer (Moore et al., 2011; Vetter, 2013). The anammox process was not considered in this study, and it probably could explain the low nitrate in $LU_1$ which was represented by the higher $k_{POC1}$.

The shallow aquifer nitrate concentration is significantly reduced through denitrification. The shallow aquifer denitrification consumed almost 50% of nitrate originated from the simulate area flow to the channel. It suggested the importance of the addition of shallow aquifer denitrification.

## 6.5 Conclusion

SWAT-LUD model was applied in the middle floodplain of Garonne River, several classic subbain and subbasin-LUs are involved in the simulated area. The SW-GW exchange at the river floodplain interface and denitrification occurs in the shallow aquifer were simulated and quantified. The influence of over bank water infiltration on groundwater level and dilution of groundwater nitrate pollution are considered and the floodplain water storage function during flooding is taken into account also. Simulate results were compared with the measured groundwater levels in the three subbasin-LUs and groundwater nitrate concentrations measured from the Monbéqui site. Results proved that SWAT-LUD could represent the SW-GW exchange and shallow aquifer denitrification appropriately. The main water flow direction at this interface is from aquifer to river, which taken 66% of the total exchanged water volume. The denitrification in the shallow aquifer obviously decreased groundwater nitrate concentration, it consumed almost 50% of nitrate originated from the simulate area flow to the channel. POC played an extremely important role in the occurrence of denitrification. The nitrate main comes from the upstream river water. The channel nitrate concentration was recuded around 0.13 mg· $L^{-1}$ with the shallow aquifer denitrification function in the alluvial plain area.

**Acknowledgements**

We are grateful to Dr. Samuel Teissier for his help in the field and with laboratory work. This study was performed as part of the EU Interreg SUDOE IVB programme (ATTENAGUA - SOE3/P2/F558 project, http://www.attenagua-sudoe.eu) and funded by ERDF. This research has been carried out as a part of "ADAPT'EAU" (ANR-11-CEPL-008),

a project supported by the French National Research Agency (ANR) as part of the Global Environmental Changes and Societies (GEC&S) programme. X. Sun is supported by a grant from the China Scholarship Council (CSC).

**References**

Arnold, J.G., Srinivasan, R., Muttiah, R.S., Williams, J.R., 1998. Large Area Hydrologic Modeling and Assessment Part I: Model Development1. JAWRA J. Am. Water Resour. Assoc. 34, 73–89. doi:10.1111/j.1752-1688.1998.tb05961.x

Bayley, P.B., 1995. Understanding Large River: Floodplain Ecosystems. BioScience 45, 153–158. doi:10.2307/1312554

Bijay-Singh, Yadvinder-Singh, Sekhon, G.S., 1995. Fertilizer-N use efficiency and nitrate pollution of groundwater in developing countries. J. Contam. Hydrol. 20, 167–184. doi:10.1016/0169-7722(95)00067-4

Boithias, L., 2012. Modélisation des transferts de pesticides à l'échelle des bassins versants en période de crue.

Boithias, L., Srinivasan, R., Sauvage, S., Macary, F., Sánchez-Pérez, J.M., 2014. Daily Nitrate Losses: Implication on Long-Term River Quality in an Intensive Agricultural Catchment of Southwestern France. J. Environ. Qual. 43, 46. doi:10.2134/jeq2011.0367

Caballero, Y., Voirin-Morel, S., Habets, F., Noilhan, J., LeMoigne, P., Lehenaff, A., Boone, A., 2007. Hydrological sensitivity of the Adour-Garonne river basin to climate change. Water Resour. Res. 43, W07448. doi:10.1029/2005WR004192

Carpenter, S.R., Caraco, N.F., Correll, D.L., Howarth, R.W., Sharpley, A.N., Smith, V.H., 1998. NONPOINT POLLUTION OF SURFACE WATERS WITH PHOSPHORUS AND NITROGEN. Ecol. Appl. 8, 559–568. doi:10.1890/1051-0761(1998)008[0559:NPOSWW]2.0.CO;2

Cey, E.E., Rudolph, D.L., Aravena, R., Parkin, G., 1999. Role of the riparian zone in controlling the distribution and fate of agricultural nitrogen near a small stream in southern Ontario. J. Contam. Hydrol. 37, 45–67. doi:10.1016/S0169-7722(98)00162-4

Chiew, F., McMahon, T., 1994. Application of the daily rainfall-runoff model MODHYDROLOG to 28 Australian catchments. J. Hydrol. 153, 383–416. doi:10.1016/0022-1694(94)90200-3

Franchini, M., Wendling, J., Obled, C., Todini, E., 1996. Physical interpretation and sensitivity analysis of the TOPMODEL. J. Hydrol. 175, 293–338. doi:10.1016/S0022-1694(96)80015-1

Frappart, F., Seyler, F., Martinez, J.-M., León, J.G., Cazenave, A., 2005. Floodplain water storage in the Negro River basin estimated from microwave remote sensing of inundation area and water levels. Remote Sens. Environ. 99, 387–399. doi:10.1016/j.rse.2005.08.016

Gold, A.J., Groffman, P.M., Addy, K., Kellogg, D.Q., Stolt, M., Rosenblatt, A.E., 2001. Landscape Attributes as Controls on Groithd Water Nitrate Removal Capacity of Riparian Zones1. JAWRA J. Am. Water Resour. Assoc. 37, 1457–1464. doi:10.1111/j.1752-1688.2001.tb03652.x

Gomez, J.D., Wilson, J.L., Cardenas, M.B., 2012. Residence time distributions in sinuosity-driven hyporheic zones and their biogeochemical effects. Water Resour. Res. 48, W09533. doi:10.1029/2012WR012180

Gregory, S.V., Swanson, F.J., McKee, W.A., Cummins, K.W., 1991. An Ecosystem Perspective of Riparian Zones. BioScience 41, 540–551. doi:10.2307/1311607

Griffiths, N.A., Tank, J.L., Royer, T.V., Warrner, T.J., Frauendorf, T.C., Rosi-Marshall, E.J., Whiles, M.R., 2012. Temporal variation in organic carbon spiraling in Midwestern agricultural streams. Biogeochemistry 108, 149–169. doi:10.1007/s10533-011-9585-z

Gruber, N., Galloway, J.N., 2008. An Earth-system perspective of the global nitrogen cycle. Nature 451, 293–296. doi:10.1038/nature06592

Hattermann, F.F., Krysanova, V., Habeck, A., Bronstert, A., 2006. Integrating wetlands and riparian zones in river basin modelling. Ecol. Model., Pattern and Processes of Dynamic Mosaic Landscapes -- Modelling, Simulation, and Implications 199, 379–392. doi:10.1016/j.ecolmodel.2005.06.012

Hauer, F.R., Lamberti, G.A., 2011. Methods in Stream Ecology. Academic Press.

Heinen, M., 2006. Simplified denitrification models: Overview and properties. Geoderma 133, 444–463. doi:10.1016/j.geoderma.2005.06.010

Hill, A.R., 1996. Nitrate Removal in Stream Riparian Zones. J. Environ. Qual. 25, 743. doi:10.2134/jeq1996.00472425002500040014x

Iribar, A., 2007. Composition des communautés bactériennes dénitrifiantes au sein d'un aquifère alluvial et facteurs contrôlant leur structuration : Relation entre structure des communautés et dénitrification (phd). Université de Toulouse, Université Toulouse III - Paul Sabatier.

Jalali, M., 2011. Nitrate pollution of groundwater in Toyserkan, western Iran. Environ. Earth Sci. 62, 907–913. doi:10.1007/s12665-010-0576-5

Jego, G., 2008. Influence des activités agricoles sur la pollution nitrique des eaux souterraines. Analyse par modélisation des impacts des systèmes de grande culture sur les fuites de nitrate dans les plaines alluviales. Université de Toulouse, Université Toulouse III-Paul Sabatier.

Kim, N.W., Chung, I.M., Won, Y.S., Arnold, J.G., 2008. Development and application of the integrated SWAT–MODFLOW model. J. Hydrol. 356, 1–16. doi:10.1016/j.jhydrol.2008.02.024

Krause, S., Bronstert, A., 2007. The impact of groundwater–surface water interactions on the water balance of a mesoscale lowland river catchment in northeastern Germany. Hydrol. Process. 21, 169–184. doi:10.1002/hyp.6182

Krysanova, V., Müller-Wohlfeil, D.-I., Becker, A., 1998. Development and test of a spatially distributed hydrological/water quality model for mesoscale watersheds. Ecol. Model. 106, 261–289. doi:10.1016/S0304-3800(97)00204-4

Lamontagne, S., Herczeg, A.L., Dighton, J.C., Jiwan, J.S., Pritchard, J.L., 2005. Patterns in groundwater nitrogen concentration in the floodplain of a subtropical stream (Wollombi Brook, New South Wales). Biogeochemistry 72, 169–190. doi:10.1007/s10533-004-0358-9

Lam, Q.D., Schmalz, B., Fohrer, N., 2010. Modelling point and diffuse source pollution of nitrate in a rural lowland catchment using the SWAT model. Agric. Water Manag. 97, 317–325. doi:10.1016/j.agwat.2009.10.004

Langergraber, G., Šimůnek, J., 2005. Modeling Variably Saturated Water Flow and Multicomponent Reactive Transport in Constructed Wetlands. Vadose Zone J. 4, 924. doi:10.2136/vzj2004.0166

Lautz, L.K., Siegel, D.I., 2006. Modeling surface and ground water mixing in the hyporheic zone using MODFLOW and MT3D. Adv. Water Resour. 29, 1618–1633. doi:10.1016/j.advwatres.2005.12.003

Lowrance, R., Altier, L.S., Williams, R.G., Inamdar, S.P., Sheridan, J.M., Bosch, D.D., Hubbard, R.K., Thomas, D.L., 2000. REMM: The Riparian Ecosystem Management Model. J. Soil Water Conserv. 55, 27–34.

Maître, V., Cosandey, A.-C., Desagher, E., Parriaux, A., 2003. Effectiveness of groundwater nitrate removal in a river riparian area: the importance of hydrogeological conditions. J. Hydrol. 278, 76–93. doi:10.1016/S0022-1694(03)00134-3

Martin, T.L., Kaushik, N.K., Trevors, J.T., Whiteley, H.R., 1999. Review: Denitrification in temperate climate riparian zones. Water. Air. Soil Pollut. 111, 171–186. doi:10.1023/A:1005015400607

Moore, T.A., Xing, Y., Lazenby, B., Lynch, M.D.J., Schiff, S., Robertson, W.D., Timlin, R., Lanza, S., Ryan, M.C., Aravena, R., Fortin, D., Clark, I.D., Neufeld, J.D., 2011. Prevalence of Anaerobic Ammonium-Oxidizing Bacteria in Contaminated Groundwater. Environ. Sci. Technol. 45, 7217–7225. doi:10.1021/es201243t

Peyrard, D., 2008. Un modèle hydrobiogéochimique pour décrire les échanges entre l'eau de surface et la zone hyporhéique de grandes plaines alluviales (phd). Université de Toulouse, Université Toulouse III - Paul Sabatier.

Peyrard, D., Sauvage, S., Vervier, P., Sanchez-Perez, J.M., Quintard, M., 2008. A coupled vertically integrated model to describe lateral exchanges between surface and subsurface in large alluvial floodplains with a fully penetrating river. Hydrol. Process. 22, 4257–4273. doi:10.1002/hyp.7035

Pinay, G., Ruffinoni, C., Wondzell, S., Gazelle, F., 1998. Change in Groundwater Nitrate Concentration in a Large River Floodplain: Denitrification, Uptake, or Mixing? J. North Am. Benthol. Soc. 17, 179–189. doi:10.2307/1467961

Rassam, D., Hunter, H.M., Pagendam, D., Cooperative Research Centre for Catchment Hydrology, 2005. The Riparian Nitrogen Model (RNM): basic theory and conceptualisation. CRC for Catchment Hydrology, Monash University, Clayton, Vic.

Rassam, D.W., Pagendam, D.E., Hunter, H.M., 2008. Conceptualisation and application of models for groundwater–surface water interactions and nitrate attenuation potential in riparian zones. Environ. Model. Softw. 23, 859–875. doi:10.1016/j.envsoft.2007.11.003

Roni, P., Quimby, E., Society, A.F., 2005. Monitoring Stream and Watershed Restoration. CABI.

Roulet, N.T., 1990. Hydrology of a headwater basin wetland: Groundwater discharge and wetland maintenance. Hydrol. Process. 4, 387–400. doi:10.1002/hyp.3360040408

Sánchez-Pérez, J.M., Vervier, P., Garabétian, F., Sauvage, S., Loubet, M., Rols, J.L., Bariac, T., Weng, P., 2003. Nitrogen dynamics in the shallow groundwater of a riparian wetland zone of the Garonne, SW France: nitrate inputs, bacterial densities, organic matter supply and denitrification measurements. Hydrol. Earth Syst. Sci. Discuss. 7, 97–107.

Sauvage, S., Teissier, S., Vervier, P., Améziane, T., Garabétian, F., Delmas, F., Caussade, B., 2003. A numerical tool to integrate biophysical diversity of a large regulated river: hydrobiogeochemical bases. The case of the Garonne River (France). River Res. Appl. 19, 181–198. doi:10.1002/rra.698

Seltz, R., 2001. Analyse et modélisation d'une zone humide riveraine de la Garonne. l'Ecole de Physique du Globe de Strasbourg 1.

Semhi, K., Amiotte Suchet, P., Clauer, N., Probst, J.-L., 2000. Impact of nitrogen fertilizers on the natural weathering-erosion processes and fluvial transport in the Garonne basin. Appl. Geochem. 15, 865–878. doi:10.1016/S0883-2927(99)00076-1

Sheibley, R.W., Jackman, A.P., Duff, J.H., Triska, F.J., 2003. Numerical modeling of coupled nitrification–denitrification in sediment perfusion cores from the hyporheic zone of the Shingobee River, MN. Adv. Water Resour., Modeling Hyporheic Zone Processes 26, 977–987. doi:10.1016/S0309-1708(03)00088-5

Sophocleous, M., 2002. Interactions between groundwater and surface water: the state of the science. Hydrogeol. J. 10, 52–67. doi:10.1007/s10040-001-0170-8

Sophocleous, M., Perkins, S.P., 2000. Methodology and application of combined watershed and ground-water models in Kansas. J. Hydrol. 236, 185–201. doi:10.1016/S0022-1694(00)00293-6

Storey, R.G., Howard, K.W.F., Williams, D.D., 2003. Factors controlling riffle-scale hyporheic exchange flows and their seasonal changes in a gaining stream: A three-dimensional groundwater flow model. Water Resour. Res. 39, 1034. doi:10.1029/2002WR001367

Thomaz, S.M., Bini, L.M., Bozelli, R.L., 2007. Floods increase similarity among aquatic habitats in river-floodplain systems. Hydrobiologia 579, 1–13. doi:10.1007/s10750-006-0285-y

Tockner, K., Pennetzdorfer, D., Reiner, N., Schiemer, F., Ward, J.V., 1999. Hydrological connectivity, and the exchange of organic matter and nutrients in a dynamic river–floodplain system (Danube, Austria). Freshw. Biol. 41, 521–535. doi:10.1046/j.1365-2427.1999.00399.x

Tockner, K., Stanford, J.A., 2002. Riverine flood plains: present state and future trends. Environ. Conserv. null, 308–330. doi:10.1017/S037689290200022X

Vetter, R., 2013. ASSESSING THE ROLE OF ANAMMOX IN A NITROGEN CONTAMINATED AQUIFER. University of North Carolina Wilmington.

Vidon, P., Hill, A.R., 2005. Denitrification and patterns of electron donors and acceptors in eight riparian zones with contrasting hydrogeology. Biogeochemistry 71, 259–283. doi:10.1007/s10533-005-0684-6

Vitousek, P.M., Aber, J.D., Howarth, R.W., Likens, G.E., Matson, P.A., Schindler, D.W., Schlesinger, W.H., Tilman, D.G., 1997. Human alteration of the global nitrogen cycle: sources and consequences. Ecol. Appl. 7, 737–750. doi:10.1890/1051-0761(1997)007[0737:HAOTGN]2.0.CO;2

Volk, M., Arnold, J.G., Bosch, D.D., Allen, P.M., Green, C.H., 2007. Watershed configuration and simulation of landscape processes with the SWAT model, in: MODSIM 2007 International Congress on Modelling and Simulation. Modelling and Simulation Society of Australia and New Zealand, Canberra, Australia. pp. 74–80.

Wagner, R., Marxsen, J., Zwick, P., Cox, E.J., 2011. Central European Stream Ecosystems: The Long Term Study of the Breitenbach. John Wiley & Sons.

Weng, P., Sánchez-Pérez, J.M., Sauvage, S., Vervier, P., Giraud, F., 2003. Assessment of the quantitative and qualitative buffer function of an alluvial wetland: hydrological modelling of a large floodplain (Garonne River, France). Hydrol. Process. 17, 2375–2392. doi:10.1002/hyp.1248

Wett, B., Jarosch, H., Ingerle, K., 2002. Flood induced infiltration affecting a bank filtrate well at the River Enns, Austria. J. Hydrol., Attenuation of Groundwater Pollution by Bank Filtration 266, 222–234. doi:10.1016/S0022-1694(02)00167-1

Zarnetske, J.P., Haggerty, R., Wondzell, S.M., Bokil, V.A., González-Pinzón, R., 2012. Coupled transport and reaction kinetics control the nitrate source-sink function of hyporheic zones. Water Resour. Res. 48, W11508. doi:10.1029/2012WR011894

Zhang, Q., Li, L., 2009. Development and application of an integrated surface runoff and groundwater flow model for a catchment of Lake Taihu watershed, China. Quat. Int., Larger Asian Rivers: Climate Change, River Flow and Sediment Flux 208, 102–108. doi:10.1016/j.quaint.2008.10.015

## 6.6 Assessment of surface water-groundwater exchanges in alluvial floodplain at the catchment scale using SWAT model

### 6.6.1 Introduction

The hydrologic connectivity links floodplains and rivers into integrated ecosystems (Tockner *et al.*, 1999). This connection has significant influence on the biotic communities and ecosystem process on both river and floodplain ecosystems (Bayley, 1995; Thomaz *et al.*, 2007). Large floodplains have an important role in the hydrologic cycle of watershed. In the flooding period, the water storage function of the floodplain could modify the river water and sediment transport (Frappart *et al.*, 2005).

The SWAT model is a process-based, semi-distributed and watershed-scale model (Arnold et al., 1998). However the surface water and groundwater exchange process was not included in the SWAT model. Modules represented exchanges between the river and its accompanying alluvial aquifer and biogeochemical processes in shallow aquifer of alluvial plain were developed. They were added to the SWAT model and the modified model was called SWAT-LUD. The SWAT-LUD model was applied at the small basin area (Monbéqui site in chapter 4 and floodplain area in chapter 6. The results proved that the SWAT-LUD model could represent the water exchange and shallow aquifer denitrification processes occurred at the floodplain satisfactory. In this study, a tool was developed to generate input files for the SWAT-LUD model and the SWAT-LUD model was applied at the Garonne catchment.

### 6.6.2 Method

#### 6.6.2.1 Create-LU tool

A Fortran subroutine called Create-LU was developed to separate classic subbaisn and subbasin-LU, the parameters of LUs in the subbasin-LUs and the distribution of alluvial HURs into LUs were done with this tool also. The algorithm includes different steps which are: 1) Reading output files from SWAT initial project; 2) Defining LUs according to flooded area for different return periods; 3) distributing alluvial HRUs into LUs based on their land use and slope.

#### 6.6.2.2 Garonne Catchment

The Garonne River is an eighth ordered river and the main river of the largest drainage basin in the southwest France. It is the third longest river in France with the length of 525km and has a drainage area about 51500 $km^2$ at the last gauging station (Tonneins). The main

land use types in the Garonne watershed are pasture, agriculture and forest, which taken 34%, 31% and 19% of the total area respectively. The alluvial soil occupied 5.8 % of the Garonne basin. The distribution of alluvial soil in the Garonne Catchment is shown in Figure 22. The detailed discription of the Garonne catchment could be find in section 3.3.1.

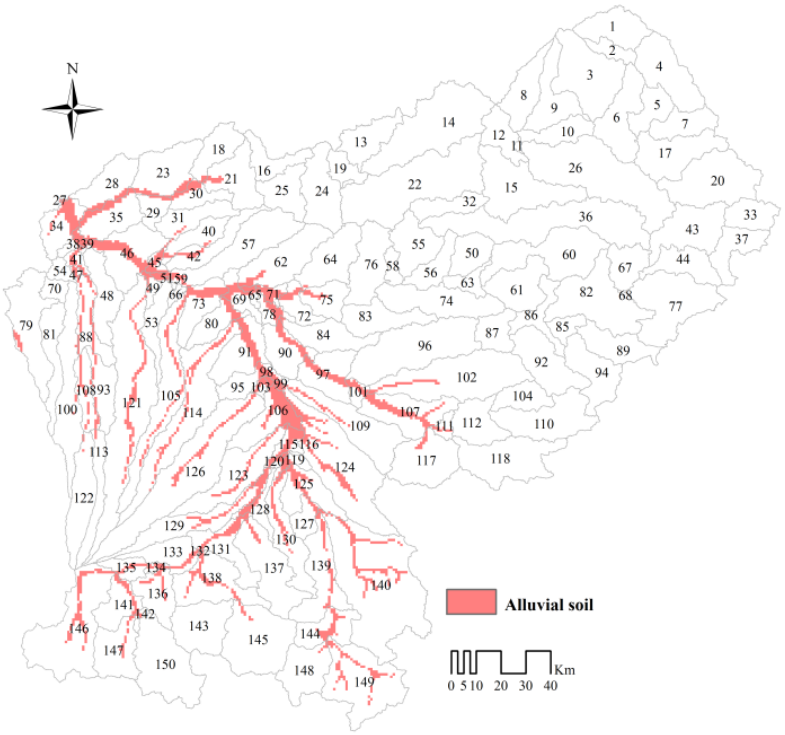


Figure 22. The location of alluvial soil in the Garonne watershed and the distribution of subbasins in the initial SWAT project

### *6.6.2.3 Distribution of subbasin and LUs in the Garonne Catchment*

The initial subbasin number of the SWAT project is 150, and 64 of them content alluvial soil. After the separation of classic subbasin and subbasin-LU, the total subbasin number (classic subbasin and subbasin-LU) is 213 (one of the initial subbasin is consisted with only alluvial soil) (Table 5).

Table 5. Numbers of subbasin and reach of the SWAT-LUD project

| | subbasin | Subbasin-LU | Classic subbasin | Reach |
|---|---|---|---|---|
| Number | 213 | 64 | 149 | 150 |

The area of $LU_1$, $LU_2$, $LU_3$ in the subbasin-LUs are considered to be 10%, 20% and 70% of the total area of the subbasin-LUs respectively according to the covered area in the floosplain with different flood return periods (1 year, 2-5 years and more than 10 years). The

saturated hydrologic conductivity are consider to be the same in different subbasin-LUs, which are 300, 200 and 100 $m \cdot d^{-1}$ in the three LUs according to the study in Monbéqui site (Table 6). The lengths of the three LUs are the same as the length of channel, the width of each LU are calculated based on the area and length.

Table 6. The character of LUs in each subbasin-LU

| | $LU_1$ | $LU_2$ | $LU_3$ |
|---|---|---|---|
| Area (% of the area of subbasin-LU) | 10 | 20 | 70 |
| K (Hydraulic conductivity) | 300 | 200 | 100 |

### 6.6.3 Main results and discussion

The comparisons between simulations of SWAT-LUD and SWAT with the observed river water discharges at Tonneins gauging station are shown in Figure xx and Figure 23 and it showed that simulations of SWAT-LUD model matched better with observations than simulation of SWAT model. The main difference between the two simulated results is the discharge peaks of the flood events, the simulations of SWAT-LUD are significantly lower than the simulations of SWAT model.

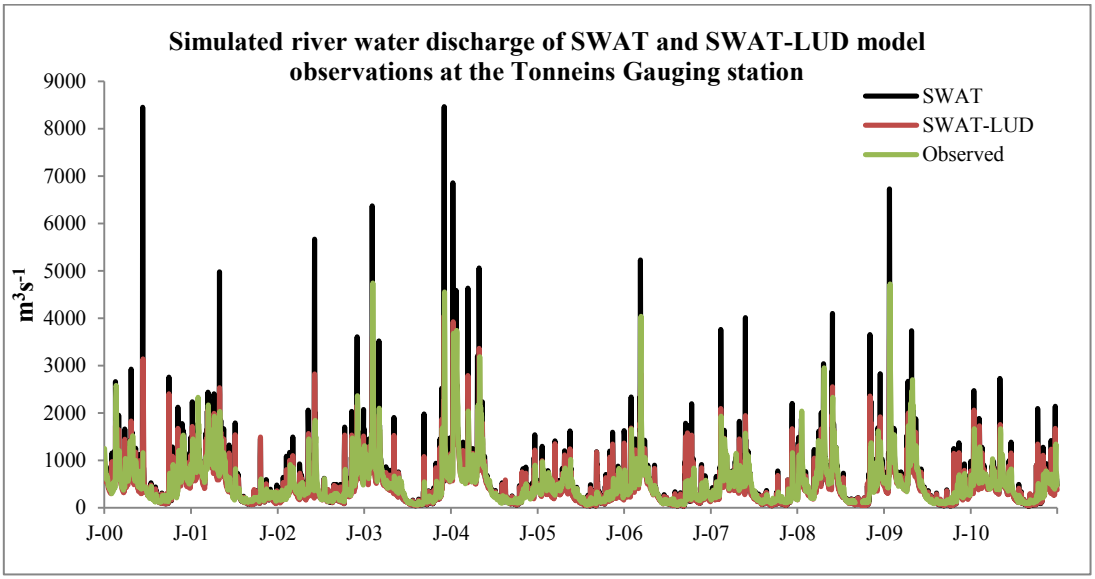


Figure 23. The comparison of simulated river water discharge of SWAT and SWAT-LUD model with observations at the Tonneins Gauging station

The different response of the SWAT and SWAT-LUD model for the flooding event is shown in Figure 24. The comparison of simulations and observation showed that the large discharge arrived two days before the observation and the simulated peak of SWAT-LUD

model are closer to the observed data. It illustrated that the flooding function added in SWAT-LUD model decreased the flood peak significantly. Since the simulated peak arrived two days before the observation, it suggested that lag of surface flow is underestimated in the study region.

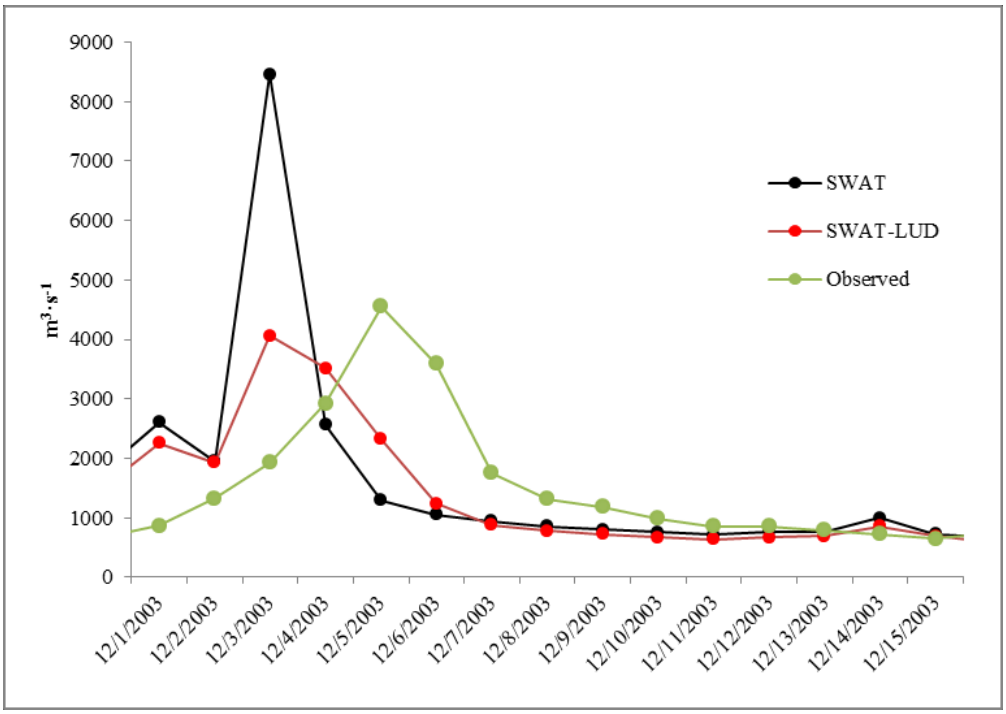


Figure 24. The comparison of simulations of SWAT and SWAT-LUD model with observations during a flood period at the Tonneins Gauging station

The total exchanged water volume in all the Garonne catchment is shown in Figure 25. The water storage on the surface of floodplain during flooding was not included in the exchanged volume.

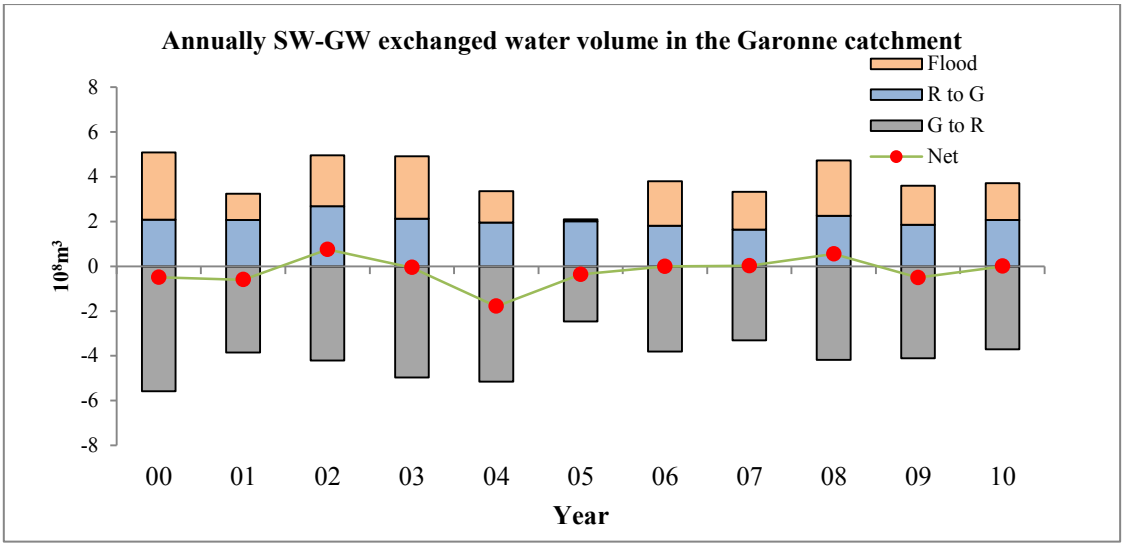

Figure 25. Annually SW-GW exchanged water volume in the Garonne catchment (2000-2010). In which Flood means infiltrated flooded river water, R to G means infiltration of river water enter into aquifer through river bank, G to R means groundwater flow to the river, net means the difference between the two direction flow

The results showed that the exchanged water volumes through the two directions are equilibrium at the catchment area. The infiltrated flooded river water taken almost 50% of the total water volume flowed from river to aquifer.

The relative importance of annual SW-GW exchanged volume is shown in Figure 26.

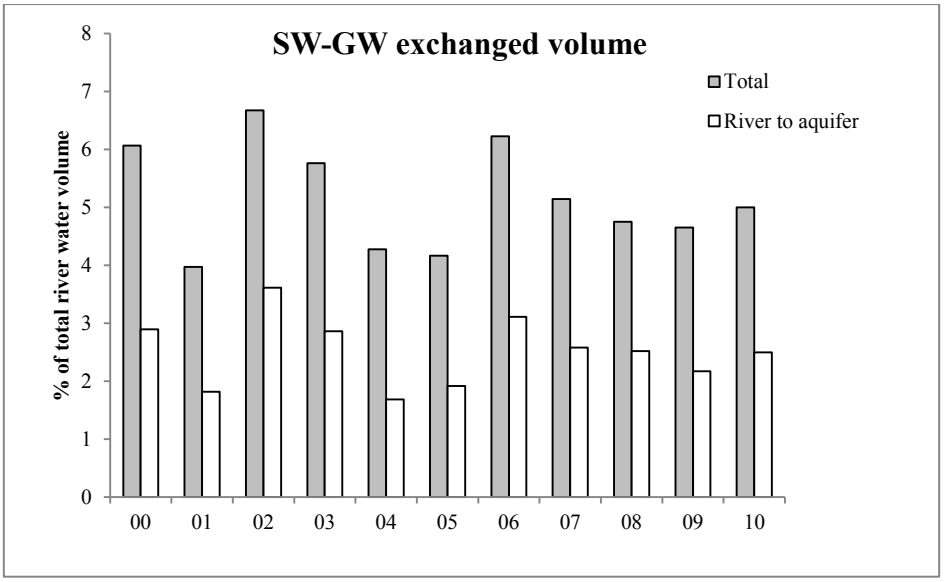


Figure 26. Relative importance of surface water – groundwater exchange compared with the river water discharge at catchment scale

The total exchanged water volume and the water volume flowed from river to shallow aquifer taken around 5% and 2% respectively of output discharge at catchment scale.

### 6.6.4 Conclusion

A tool called Create-LU was developed to generate input files for the SWAT-LUD model and the SWAT-LUD model was applied at the Garonne catchment. The results showed that simulated river water discharge of SWAT-LUD model matched better with observations than simulation of SWAT model at Tonneins gauging station. The main difference between the two simulated results is the discharge peaks of the flood events, the simulations of SWAT-LUD are significantly lower than the simulations of SWAT model. The analyse of the total exchanged water volume in the catchment scale showed that the infiltrated flooded river water

taken almost 50% of the total water volume flowed from river to aquifer. The total exchanged water volume and the water volume flowed from river to shallow aquifer taken around 5% and 2% of output discharge. In this study, the SW-GW exchange was analyzed at the catchment scale only, the different response at different section should be analyzed. Moreover, the simulation and quantification of denitrification rate in the shallow aquifer of floodplain at the catchment scale should be carried out in the future study.

# 7. Conclusions and perspectives

## 7.1 Conclusions

The objective of this thesis was to quantify SW-GW exchanged water volume and the shallow aquifer denitrification function in the floodplain area at the catchment scale based on modelling approach. The SWAT model is a semi-distributed operating at the watershed scale. It can simulate a large watershed with readily available data and has been used successfully all over the world. The SWAT model was chosen to simulate the hydrologic processes and nitrogen cycling in this study. However, the processes that represented the two direction water exchanges between river and groundwater and the denitrification processes occurring in the floodplain shallow aquifer has not been included in the SWAT model. To achieve the objective, modules representing the SW-GW exchange processes, the floodplain water storage function during the flood period, the transfer of dissolved elements along with the SW-GW exchange and the denitrification processes taking place in the shallow aquifer of floodplain area were developed and added into the SWAT model. The modified model was applied at different spatial scales to quantify the exchanged water volume and the mitigation of nitrate pollution in groundwater and river systems. The different steps carried out in this thesis were: i) development of the hydrologic module to simulate SW-GW exchange and application of the modified model to a meander of the floodplain-Monbéqui; ii) development of the shallow aquifer denitrification module to evaluate the influence of shallow aquifer denitrification, and validation of the module at the meander of Monbéqui; iii) application of the modified model at the catchment scale.

1) Hydrologic module

Since dissolved elements are transported along with the water flow, the module that represented SW-GW exchanges was firstly developed and tested. In the module, Darcy's equation was introduced to simulate groundwater flow and SW-GW exchange occurring through the riverbank based on the Landscape Unit structure at the floodplain area. The algorithms calculating the river water and groundwater levels during flooding events were also modified. The new levels were calculated based on the flooded water volume. The module was integrated to the SWAT model, and the modified model was called SWAT-LUD.

The developed module was tested at different spatial scales. Firstly in chapter 4, the new developed module was applied to a floodplain meander of the Garonne river (around 25 $km^2$). Then in chapter 6, the module was applied to the middle floodplain section of the Garonne

catchment (around 4 600 $km^2$) and finally to the entire Garonne catchment (around 51 500 $km^2$). The results showed that the modified hydrologic module have the ability to satisfactorily represent SW-GW exchange at different scales.

The exchanged SW-GW water volume was quantified. It was found that the river water discharge has a great influence on the SW-GW exchanges processes. The water mixing occurs mainly during high hydraulic periods and flooded water was important for the SW-GW exchange process. At the meander and middle floodplain scale, the main water flow direction is from groundwater to river, and water flowing in this direction accounted for around 65 % of the total exchanged water volume. At the catchment scale, the exchanged water volumes flowing through the two directions are almost at equilibrium. The annual total exchanged water volume represented around 5% of the total river discharge. The application of new algorithm representing the floodplain water storage function proved that the flood peak decreased significantly and the simulated results matched better with the observed data when considering this function.

2) Shallow aquifer denitrification module

The module representing the transport of dissolved elements and shallow aquifer denitrification processes occurring in a floodplain aquifer was developed. The transport is calculated according to the exchanged water volume and the concentration of the elements, and the influence of flooding on nitrate leaching was also taken into account. The influences of both dissolved organic carbon (DOC) and particulate organic carbon (POC) on denitrification were evaluated.

The developed module was applied at the meander and at the middle floodplain section of the Garonne catchment as shown in chapter 5 and 6 respectively. The comparison with measured groundwater nitrate concentrations proved that the added module could correctly represent the aquifer nitrate concentration in the near bank zone. In the meander, the annual simulated denitrification rate in the near bank zone was around 130 kg $N\text{-}NO_3^- \cdot ha^{-1} \cdot y^{-1}$, and around 40 % of the nitrate input to this zone was denitrified. In the middle floodplain section, the annual denitrification rate in the near bank zone of three subbasin-LUs ranged from 55 to 120 kg $N\text{-}NO_3^- \cdot ha^{-1} \cdot y^{-1}$. The shallow aquifer denitrification consumed almost 50% of nitrate originating from the surrounding area and flowing to the channel. Compared with DOC, POC played an extremely important role in the occurrence of denitrification. In the near bank zone, 98 % of the nitrate was attenuated through POC consumption.

The correspondence between denitrification rates, groundwater levels and total input nitrate masses in the near bank zone were analysed at the meander scale. The results illustrated that groundwater levels were positively correlated to the denitrification rates in the near bank zone ($R^2$ = 0.88) and the absolute consumption rate increased along with the increase in nitrate content ($R^2$ = 0.79). However, the relative consumption rate decreased as the nitrate content increased ($R^2$ = 0.93). In the middle floodplain section, the influence of shallow aquifer denitrification on river nitrate flux was analysed. It was found that the nitrate mainly come from the upstream river water. The nitrate concentration in the output of the simulated area was decreased around 0.13 $mg \cdot L^{-1}$ due to the influence of the floodplain shallow aquifer denitrification function.

## 7.2 Perspectives

1) Organic carbon

The quantification of the influence of floodplain shallow aquifer denitrification at catchment scale should be simulated and analyzed. Organic carbon is a necessary element in the occurrence of denitrification. In the studies at the meander and at the middle floodplain section scales, constant values of DOC concentration were set to the river water and shallow groundwater. At the large catchment scale, the DOC concentration should be different for different subbasins. However since the cycle of DOC was not simulated in the SWAT and SWAT-LUD model, the new module that represented the DOC cycle in river water and groundwater should be developed and added to the model. The simulation of DOC concentration at the river water with the SWAT model was tested at Save River by Uhart (2013). The equation based on the study of Ludwig et al. (1996) was introduced in the model, which is as follows:

$$F_{DOC} = 0.0040Q - 8.76Slope + 0.095SoilC$$

Where $F_{DOC}$ is the DOC flowing out of the basin ($T \cdot km^{-2} \cdot y^{-1}$); Q is the output discharge of the catchment (mm); slope is the average slope of the basin (radian); and SoilC is the soil organic carbon content ($kg \cdot m^{-3}$).

This equation could be applied to the Garonne catchment to simulate the river water DOC flux.

The DOC dynamic in the shallow groundwater is rarely studied, and most of the models that take into account the shallow aquifer DOC cycle are physically based model,

likein the study of Chapelle et al. (2014). As SWAT model is a semi-distributed model, a simplified equation should be chosen and tested in the SWAT model.

The POC content in the soil profile could be simulated or read in as input data in the SWAT model, but the POC content in the shallow aquifer sediment was not simulated. Moreover, the results in the Garonne catchment suggested that POC played an extremely important role, the measurement and simulation of this value would be important. In this study, the measured AFDM content in the shallow aquifer sediment was used to evaluate POC content. The simulation and definition of POC content in the shallow aquifer would be a challenge in the future study.

2) Linkage of upland and floodplain

In the SWAT-LUD model, the upland classic subbasin and floodplain subbasin-LU are connected through the river and the influence of the upland area on the floodplain was not represented. As in the SWAT-LUD model, the output water flowing out of the upland classic subbasin is summed together before flowing into the river. To improve the connection the surface, lateral and groundwater flow in the upland should be separately summed and then routed to the downward subbasin-LU, instead of having all subbasin and subbasin-LU water flows being summed together.

3) Underneath hyporheic zone

In the SWAT-LUD model, the altitude of the river bed in each subbasin was assumed to be the reference value for the hydraulic head used to compute groundwater and surface water levels. The storage water volume in the shallow aquifer is calculated based on the average height of LU (the height in the middle of each LU) and the porosity of shallow aquifer. Moreover, the height of LU is calculated based on the height of river bank and slopes of LUs. The water storage beneath hyporheic zone (beneath the river bed) is not taken into account. In the Garonne catchment, the deposited sediment in the floodplain overlies impermeable molasses and rare water exists beneath the hyporheic zone. However in many other catchments, the water storage beneath the hyporheic zone can have a great influence on the biogeochemical cycles also. To apply the SWAT-LUD model in the river with deep hyporheic zone, the storage groundwater in the zone below the river bed should be included in the model. To solve this problem, another water pool should be added to represent the water

storage in the underneath sediment. The transfer between the top layer shallow aquifer and this pool and the denitrification processes occurred in this zone should also be considered.

4) SW-GW exchange

Since Darcy's equation is used to calculate the SW-GW exchange, the exchanged water volume is based on the difference of water levels in the two domains. The simulation of river water level would have a great influence on the accuracy of simulated SW-GW exchange. The river water height is greatly influenced by the width and slope of the channel (section 3.1.1.2). The infiltrated flooded water was found to play an important role on the SW-GW exchange. Finally the maximum river channel water flow storage capacity is also influenced by the channel shape. The definition of the channel section is calculated only based on the drainage area in the SWAT-LUD model, the correspondence between simulated and actual channel widths and depths should be carried out.

5) Sensitivity analyse and application in other catchments

The sensitivity analyse should be carried out with the new added parameters and the parameters in the initial SWAT model that are connected with the new modules. This would help to understand the importance of the different parameters and improve calibration procedure in the future studies. The modified SWAT-LUD model should also be applied to other catchments, especially in larger catchment than the Garonne catchment with wide riparian zone and floodplain area such as the Amazon River and the Yangtze River.

6) User manual preparation

In order to help other researchers to apply the SWAT-LUD model in other basins, a user manual should be prepared to explain the details of the new developed modules and to list the necessary input data files and format.

# CONCLUSIONS

L'objectif principal de cette thèse était de quantifier les volumes d'eau échangés entre la nappe et la rivière ainsi que l'importance des processus de dénitrification dans les aquifères alluviaux à l'échelle du bassin versant en s'appuyant sur un travail de modélisation. Le modèle SWAT est un modèle semi-distribué, opérant à l'échelle du bassin versant. Il permet de simuler des bassins versants de grandes tailles avec des données facilement disponibles et a été appliqué avec succès dans de nombreuses études à travers le monde. Le modèle SWAT a été choisi pour simuler les processus hydrologiques et le cycle de l'azote dans cette étude. Cependant, la simulation des échanges nappe-rivière dans les deux directions ainsi que les processus de dénitrification qui se produisent dans les aquifères peu profonds de la plaine alluviale ne sont pas pris en compte dans la version originale de SWAT. Afin d'atteindre l'objectif, des modules représentant les échanges nappe-rivière, la rétention de l'eau dans la plaine alluviale pendant les crues débordantes, le transport des éléments dissous via les échanges nappe-rivière et les processus de dénitrification se produisant dans les aquifères alluviaux ont été développés et ajoutés dans le modèle SWAT. Le modèle modifié a ensuite été appliqué à différentes échelles spatiales pour quantifier les volumes d'eau échangés ainsi que l'atténuation de la contamination par les nitrates des eaux souterraines et de la rivière. Les différentes étapes accomplies dans cette thèse ont été : i) le développement d'un module hydrologique pour simuler les échanges nappe-rivière et son application à l'échelle d'un méandre de la plaine alluviale, Monbéqui ; ii) le développement d'un module pour simuler les processus de dénitrification dans les aquifères alluviaux et son application au site de Monbéqui et iii) l'application du modèle modifié à l'échelle de la plaine alluviale de la Garonne dans son cours moyen puis à l'échelle de tout son bassin versant.

1) Module hydrologique

Comme les éléments dissous sont transportés par les flux hydrologiques, le module simulant les échanges nappe-rivière a été développé et testé en premier. Dans ce module, l'équation de Darcy a été introduite pour simuler les écoulements souterrains et les échanges nappe-rivière localisés au niveau des berges du fleuve, sur la base de la structure *Lanscape Unit*, au niveau de la plaine alluviale. L'algorithme calculant les niveaux d'eau de la rivière et de la nappe pendant les épisodes de crues a également été modifié pour ajuster les niveaux d'eau en

fonction du volume d'eau inondant la plaine. Ce module a été intégré au modèle SWAT et la version modifiée du modèle a été appelée SWAT-LUD.

Le nouveau module a été testé à différentes échelles spatiales. Tout d'abord, dans le chapitre 4, le module a été appliqué à un méandre de la Garonne (25 km²). Ensuite, dans le chapitre 6, le module a été appliqué à l'échelle de la plaine alluviale de la Garonne (4 600 km²) et finalement à tout le bassin versant de la Garonne (51 500 km²). Les résultats ont montré que le module hydrologique a la capacité de représenter les échanges nappe-rivière de façon réaliste à différentes échelles.

Le volume d'eau échangé entre la nappe et la rivière a été quantifié. Il est apparu que le débit de la rivière a une grande influence sur les échanges nappe-rivière. Le mélange entre les eaux de nappe et la rivière se produit surtout pendant les périodes de hautes eaux et les volumes d'eau débordante jouent un rôle important dans les échanges nappe-rivière. À l'échelle du méandre et de la moyenne section de la plaine alluviale, l'eau s'écoule principalement de la nappe vers la rivière contribuant pour près de 65% des échanges totaux. À l'échelle du bassin versant, le volume d'eau échangé est quasiment identique selon les deux directions. Le volume annuel d'eau échangé entre la nappe et la rivière représente environ 5% du débit annuel de la Garonne. L'application du nouvel algorithme représentant le stockage de l'eau de débordement dans la plaine alluviale a montré que les pics de crues diminuent significativement et que les résultats simulés correspondent mieux à la réalité en prenant en compte cette fonction.

2) Module de dénitrification dans les aquifères alluviaux

Un module représentant le transport des éléments dissous et les processus de dénitrification dans les aquifères alluviaux a été développé. Le transport des éléments est calculé en fonction du volume d'eau échangé et de la concentration de l'élément considéré. Le lessivage des nitrates via l'infiltration de l'eau débordante a également été intégré dans le module. Le rôle du carbone organique dissous (COD) et du carbone organique particulaire (COP) sur la dénitrification ont également été évalués.

Ce module a été appliqué à l'échelle du méandre et de la plaine alluviale de la Garonne dans son cours moyen. Les résultats sont présentés respectivement dans les chapitres 5 et 6. La

comparaison avec les concentrations de chlorure mesurées dans la nappe a montré que le module pouvait représenter correctement les concentrations en nitrates de l'aquifère dans la zone riparienne. À l'échelle du méandre, le taux annuel de dénitrification simulé est d'environ 130 kg $N\text{-}NO3^{-}.ha^{-1}.an^{-1}$ et environ 40% des nitrates arrivant dans cette zone ont été dégradés à travers la dénitrification. À l'échelle de la plaine alluviale de la Garonne, le taux annuel de dénitrification simulé pour la zone riparienne varie entre 55 et 120 $N\text{-}NO3^{-}.ha^{-1}.an^{-1}$. Environ 50 % des nitrates provenant des zones voisines ont été dégradés via les processus de dénitrification au lieu de rejoindre la rivière. En comparaison avec le COD, le POC joue un rôle prépondérant dans le déroulement des processus de dénitrification. Dans la zone riparienne, 98% des nitrates atténués l'ont été via la consommation de POC par les bactéries responsables de la dénitrification.

Les correspondances entre les taux de dénitrification, les niveaux de nappe et les apports de nitrates dans la zone riparienne ont été analysées à l'échelle du méandre. Les résultats ont montré que les taux de dénitrification sont positivement corrélés avec les niveaux de la nappe ($R^2$=0.88) et avec les concentrations en nitrates ($R^2$=0.79). Cependant les taux de dénitrification relatifs à la concentration en nitrates sont négativement corrélés avec les concentrations en nitrates ($R^2$=0.93). À l'échelle de la plaine alluviale, l'influence de la dénitrification dans l'aquifère alluvial sur les flux de nitrates dans la rivière a été analysée. Il a été montré que les nitrates sont majoritairement apportés par la rivière en amont du domaine simulé. La concentration en nitrate en aval du domaine simulé a diminué de 0.13 $mg.L^{-1}$ due à la dénitrification se produisant dans les aquifères alluviaux.

# Bibliographie

Almasri, M.N., Kaluarachchi, J.J., 2007. Modeling nitrate contamination of groundwater in agricultural watersheds. J. Hydrol. 343, 211–229. doi:10.1016/j.jhydrol.2007.06.016

Almasri, M.N., Kaluarachchi, J.J., 2004. Assessment and management of long-term nitrate pollution of ground water in agriculture-dominated watersheds. J. Hydrol. 295, 225–245. doi:10.1016/j.jhydrol.2004.03.013

Altier, L., Lowrance, R., Williams, R., Inamdar, S., Bosch, D., Sheridan, J., Hubbard, R., Thomas, D., 2005. Riparian Ecosystem Management Model.

Alvarez, L., Bricio, C., Blesa, A., Hidalgo, A., Berenguer, J., 2014. Transferable Denitrification Capability of Thermus thermophilus. Appl. Environ. Microbiol. 80, 19–28. doi:10.1128/AEM.02594-13

Arango, C.P., Tank, J.L., Schaller, J.L., Royer, T.V., Bernot, M.J., David, M.B., 2007. Benthic organic carbon influences denitrification in streams with high nitrate concentration. Freshw. Biol. 52, 1210–1222. doi:10.1111/j.1365-2427.2007.01758.x

Arnold, J.G., Allen, P.M., Volk, M., Williams, J.R., Bosch, D.D., 2010. Assessment of different representations of spatial variability on SWAT model performance. Trans ASABE 53, 1433–1443.

Arnold, J.G., Srinivasan, R., Muttiah, R.S., Williams, J.R., 1998. Large Area Hydrologic Modeling and Assessment Part I: Model Development1. JAWRA J. Am. Water Resour. Assoc. 34, 73–89. doi:10.1111/j.1752-1688.1998.tb05961.x

Arrate, I., Sanchez-Perez, J.M., Antiguedad, I., Vallecillo, M.A., Iribar, V., Ruiz, M., 1997. Groundwater pollution in Quaternary aquifer of Vitoria : Gasteiz (Basque Country, Spain): Influence of agricultural activities and water-resource management. Environ. Geol. 30, 257–265. doi:10.1007/s002540050155

Bailey, R.T., Morway, E.D., Niswonger, R.G., Gates, T.K., 2013. Modeling Variably Saturated Multispecies Reactive Groundwater Solute Transport with MODFLOW-UZF and RT3D. Groundwater 51, 752–761. doi:10.1111/j.1745-6584.2012.01009.x

Bainbridge, Z.T., Brodie, J.E., Faithful, J.W., Sydes, D.A., Lewis, S.E., 2009. Identifying the land-based sources of suspended sediments, nutrients and pesticides discharged to the Great Barrier Reef from the Tully–Murray Basin, Queensland, Australia. Mar. Freshw. Res. 60, 1081–1090.

Baldwin, D. s., Mitchell, A. m., 2000. The effects of drying and re-flooding on the sediment and soil nutrient dynamics of lowland river–floodplain systems: a synthesis. Regul.

Rivers Res. Manag. 16, 457–467. doi:10.1002/1099-1646(200009/10)16:5<457::AID-RRR597>3.0.CO;2-B

Banach, A.M., Banach, K., Visser, E.J.W., Stępniewska, Z., Smits, A.J.M., Roelofs, J.G.M., Lamers, L.P.M., 2009. Effects of summer flooding on floodplain biogeochemistry in Poland; implications for increased flooding frequency. Biogeochemistry 92, 247–262. doi:10.1007/s10533-009-9291-2

Bardini, L., 2013. Impact of hyporheic zones on nutrient dynamics. Politecnico di Torino.

Bates, H.K., Spalding, R.F., 1998. Aquifer Denitrification as Interpreted from In Situ Microcosm Experiments. J. Environ. Qual. 27, 174. doi:10.2134/jeq1998.00472425002700010025x

Bates, P.D., Wilson, M.D., Horritt, M.S., Mason, D.C., Holden, N., Currie, A., 2006. Reach scale floodplain inundation dynamics observed using airborne synthetic aperture radar imagery: Data analysis and modelling. J. Hydrol., Measurement and Parameterization of Rainfall Microstructure 328, 306–318. doi:10.1016/j.jhydrol.2005.12.028

Bayley, P.B., 1995. Understanding Large River: Floodplain Ecosystems. BioScience 45, 153–158. doi:10.2307/1312554

Beaudoin, N., Saad, J.K., Van Laethem, C., Machet, J.M., Maucorps, J., Mary, B., 2005. Nitrate leaching in intensive agriculture in Northern France: Effect of farming practices, soils and crop rotations. Agric. Ecosyst. Environ. 111, 292–310. doi:10.1016/j.agee.2005.06.006

Bending, G.D., Turner, M.K., Jones, J.E., 2002. Interactions between crop residue and soil organic matter quality and the functional diversity of soil microbial communities. Soil Biol. Biochem. 34, 1073–1082. doi:10.1016/S0038-0717(02)00040-8

Bijay-Singh, Yadvinder-Singh, Sekhon, G.S., 1995. Fertilizer-N use efficiency and nitrate pollution of groundwater in developing countries. J. Contam. Hydrol. 20, 167–184. doi:10.1016/0169-7722(95)00067-4

Boano, F., Demaria, A., Revelli, R., Ridolfi, L., 2010. Biogeochemical zonation due to intrameander hyporheic flow. Water Resour. Res. 46, W02511. doi:10.1029/2008WR007583

Boano, F., Revelli, R., Ridolfi, L., 2007. Bedform-induced hyporheic exchange with unsteady flows. Adv. Water Resour. 30, 148–156. doi:10.1016/j.advwatres.2006.03.004

Böhlke, J.K., Denver, J.M., 1995. Combined Use of Groundwater Dating, Chemical, and Isotopic Analyses to Resolve the History and Fate of Nitrate Contamination in Two

Agricultural Watersheds, Atlantic Coastal Plain, Maryland. Water Resour. Res. 31, 2319–2339. doi:10.1029/95WR01584

Böhlke, J.K., Wanty, R., Tuttle, M., Delin, G., Landon, M., 2002. Denitrification in the recharge area and discharge area of a transient agricultural nitrate plume in a glacial outwash sand aquifer, Minnesota. Water Resour. Res. 38, 10–1. doi:10.1029/2001WR000663

Boithias, L., Srinivasan, R., Sauvage, S., Macary, F., Sánchez-Pérez, J.M., 2014. Daily Nitrate Losses: Implication on Long-Term River Quality in an Intensive Agricultural Catchment of Southwestern France. J. Environ. Qual. 43, 46. doi:10.2134/jeq2011.0367

Bosch, D.D., Arnold, J.G., Volk, M., Allen, P.M., 2010. Simulation of a low-gradient coastal plain watershed using the SWAT landscape model. Trans ASABE 53, 1445–1456.

Bothe, H., Ferguson, S., Newton, W.E., 2006. Biology of the Nitrogen Cycle. Elsevier.

Boulton, A.J., Datry, T., Kasahara, T., Mutz, M., Stanford, J.A., 2010. Ecology and management of the hyporheic zone: stream–groundwater interactions of running waters and their floodplains. J. North Am. Benthol. Soc. 29, 26–40. doi:10.1899/08-017.1

Boulton, A.J., Findlay, S., Marmonier, P., Stanley, E.H., Valett, H.M., 1998. The Functional Significance of the Hyporheic Zone in Streams and Rivers. Annu. Rev. Ecol. Syst. 29, 59–81. doi:10.1146/annurev.ecolsys.29.1.59

Braunschweig, F., Leitao, P.C., Fernandes, L., Pina, P., Neves, R.J.J., 2004. The object-oriented design of the integrated water modelling system MOHID, in: Science, C.T.M. and G.F.P.B.T.-D. in W. (Ed.), Computational Methods in Water Resources: Volume 2 Proceedings of the XVth International Conference on Computational Methods in Water Resources. Elsevier, pp. 1079–1090. doi:http://dx.doi.org/10.1016/S0167-5648(04)80126-6

Brown, A.G., 1997. Alluvial Geoarchaeology: Floodplain Archaeology and Environmental Change. Cambridge University Press.

Brunke, M., Gonser, T., 1997a. The ecological significance of exchange processes between rivers and groundwater. Freshw. Biol. 37, 1–33. doi:10.1046/j.1365-2427.1997.00143.x

Brunke, M., Gonser, T., 1997b. The ecological significance of exchange processes between rivers and groundwater. Freshw. Biol. 37, 1–33. doi:10.1046/j.1365-2427.1997.00143.x

Burt, T.P., Pinay, G., Matheson, F.E., Haycock, N.E., Butturini, A., Clement, J.C., Danielescu, S., Dowrick, D.J., Hefting, M.M., Hillbricht-Ilkowska, A., Maitre, V., 2002. Water table fluctuations in the riparian zone: comparative results from a pan-European experiment. J. Hydrol. 265, 129–148. doi:10.1016/S0022-1694(02)00102-6

Caballero, Y., Voirin-Morel, S., Habets, F., Noilhan, J., LeMoigne, P., Lehenaff, A., Boone, A., 2007. Hydrological sensitivity of the Adour-Garonne river basin to climate change. Water Resour. Res. 43, W07448. doi:10.1029/2005WR004192

Camargo, J.A., Alonso, Á., 2006. Ecological and toxicological effects of inorganic nitrogen pollution in aquatic ecosystems: A global assessment. Environ. Int. 32, 831–849. doi:10.1016/j.envint.2006.05.002

Canter, L.W., 1996. Nitrates in Groundwater. CRC Press.

Cardenas, M.B., Wilson, J.L., 2007a. Effects of current–bed form induced fluid flow on the thermal regime of sediments. Water Resour. Res. 43, W08431. doi:10.1029/2006WR005343

Cardenas, M.B., Wilson, J.L., 2007b. Dunes, turbulent eddies, and interfacial exchange with permeable sediments. Water Resour. Res. 43, W08412. doi:10.1029/2006WR005787

Cardenas, M.B., Wilson, J.L., Zlotnik, V.A., 2004. Impact of heterogeneity, bed forms, and stream curvature on subchannel hyporheic exchange. Water Resour. Res. 40, W08307. doi:10.1029/2004WR003008

Carpenter, S.R., Caraco, N.F., Correll, D.L., Howarth, R.W., Sharpley, A.N., Smith, V.H., 1998. NONPOINT POLLUTION OF SURFACE WATERS WITH PHOSPHORUS AND NITROGEN. Ecol. Appl. 8, 559–568. doi:10.1890/1051-0761(1998)008[0559:NPOSWW]2.0.CO;2

Cerro, I., Antigüedad, I., Srinavasan, R., Sauvage, S., Volk, M., Sanchez-Perez, J.M., 2014. Simulating Land Management Options to Reduce Nitrate Pollution in an Agricultural Watershed Dominated by an Alluvial Aquifer. J. Environ. Qual. 43, 67. doi:10.2134/jeq2011.0393

Cey, E.E., Rudolph, D.L., Aravena, R., Parkin, G., 1999. Role of the riparian zone in controlling the distribution and fate of agricultural nitrogen near a small stream in southern Ontario. J. Contam. Hydrol. 37, 45–67. doi:10.1016/S0169-7722(98)00162-4

Chapelle, F.H., Kauffman, L.J., Widdowson, M.A., 2014. Modeling the effects of naturally occurring organic carbon on chlorinated ethene transport to a public supply well. Ground Water 52 Suppl 1, 76–89. doi:10.1111/gwat.12152

Chen, D.J.Z., MacQuarrie, K.T.B., 2004. Numerical simulation of organic carbon, nitrate, and nitrogen isotope behavior during denitrification in a riparian zone. J. Hydrol. 293, 235–254. doi:10.1016/j.jhydrol.2004.02.002

Chiew, F., McMahon, T., 1994. Application of the daily rainfall-runoff model MODHYDROLOG to 28 Australian catchments. J. Hydrol. 153, 383–416. doi:10.1016/0022-1694(94)90200-3

Christensen, T.H., Bjerg, P.L., Banwart, S.A., Jakobsen, R., Heron, G., Albrechtsen, H.-J., 2000. Characterization of redox conditions in groundwater contaminant plumes. J. Contam. Hydrol. 45, 165–241. doi:10.1016/S0169-7722(00)00109-1

Cooper, J.R., Gilliam, J.W., Daniels, R.B., Robarge, W.P., 1987. Riparian Areas as Filters for Agricultural Sediment1. Soil Sci. Soc. Am. J. 51, 416. doi:10.2136/sssaj1987.03615995005100020029x

Curie, F., Ducharne, A., Sebilo, M., Bendjoudi, H., 2009. Denitrification in a hyporheic riparian zone controlled by river regulation in the Seine river basin (France). Hydrol. Process. 23, 655–664. doi:10.1002/hyp.7161

Dalzell, B.J., Filley, T.R., Harbor, J.M., 2005. Flood pulse influences on terrestrial organic matter export from an agricultural watershed. J. Geophys. Res. Biogeosciences 2005–2012 110. doi:10.1029/2005jg000043

DeSimone, L.A., Howes, B.L., 1998. Nitrogen transport and transformations in a shallow aquifer receiving wastewater discharge: A mass balance approach. Water Resour. Res. 34, 271–285. doi:10.1029/97WR03040

Dodla, S.K., Wang, J.J., DeLaune, R.D., Cook, R.L., 2008. Denitrification potential and its relation to organic carbon quality in three coastal wetland soils. Sci. Total Environ. 407, 471–480. doi:10.1016/j.scitotenv.2008.08.022

Dosskey, M.G., Vidon, P., Gurwick, N.P., Allan, C.J., Duval, T.P., Lowrance, R., 2010. The Role of Riparian Vegetation in Protecting and Improving Chemical Water Quality in Streams1. JAWRA J. Am. Water Resour. Assoc. 46, 261–277. doi:10.1111/j.1752-1688.2010.00419.x

Duan, S., Bianchi, T.S., Sampere, T.P., 2007. Temporal variability in the composition and abundance of terrestrially-derived dissolved organic matter in the lower Mississippi and Pearl Rivers. Mar. Chem. 103, 172–184. doi:10.1016/j.marchem.2006.07.003

Dutta, D., Herath, S., Musiake, K., 2000. Flood inundation simulation in a river basin using a physically based distributed hydrologic model. Hydrol. Process. 14, 497–519. doi:10.1002/(SICI)1099-1085(20000228)14:3<497::AID-HYP951>3.0.CO;2-U

Ferrant, S., Durand, P., Justes, E., Probst, J.-L., Sanchez-Perez, J.-M., 2013. Simulating the long term impact of nitrate mitigation scenarios in a pilot study basin. Agric. Water Manag. 124, 85–96. doi:10.1016/j.agwat.2013.03.023

Ferrant, S., Oehler, F., Durand, P., Ruiz, L., Salmon-Monviola, J., Justes, E., Dugast, P., Probst, A., Probst, J.-L., Sanchez-Perez, J.-M., 2011. Understanding nitrogen transfer dynamics in a small agricultural catchment: Comparison of a distributed (TNT2) and a semi distributed (SWAT) modeling approaches. J. Hydrol. 406, 1–15. doi:10.1016/j.jhydrol.2011.05.026

Findlay, S., Strayer, D., Goumbala, C., Gould, K., 1993. Metabolism of streamwater dissolved organic carbon in the shallow hyporheic zone. Limnol. Oceanogr. 38, 1493–1499.

Fischer, H., Pusch, M., Schwoerbel, J., 1996. Spatial distribution and respiration of bacteria in stream-bed sediments. Arch. Für Hydrobiol. 137, 281–300.

Fohrer, N., Dietrich, A., Kolychalow, O., Ulrich, U., 2013. Assessment of the Environmental Fate of the Herbicides Flufenacet and Metazachlor with the SWAT Model. J. Environ. Qual. 0, 0. doi:10.2134/jeq2011.0382

Franchini, M., Wendling, J., Obled, C., Todini, E., 1996. Physical interpretation and sensitivity analysis of the TOPMODEL. J. Hydrol. 175, 293–338. doi:10.1016/S0022-1694(96)80015-1

Frappart, F., Seyler, F., Martinez, J.-M., León, J.G., Cazenave, A., 2005. Floodplain water storage in the Negro River basin estimated from microwave remote sensing of inundation area and water levels. Remote Sens. Environ. 99, 387–399. doi:10.1016/j.rse.2005.08.016

Freeze, R.A., Cherry, J.A., 1979. Groundwater. Prentice-Hall.

Frigg, R., Hartmann, S., 2012. Models in Science, in: Zalta, E.N. (Ed.), The Stanford Encyclopedia of Philosophy.

Gerrard, A.J., 1992. Soil Geomorphology. Springer Science & Business Media.

Gillham, R.W., 1991. Nitrate Contamination of Ground Water in Southern Ontario and the Evidence for Denitrification, in: Bogárdi, I., Kuzelka, R.D., Ennenga, W.G. (Eds.), Nitrate Contamination, NATO ASI Series. Springer Berlin Heidelberg, pp. 181–198.

Gold, A.J., Groffman, P.M., Addy, K., Kellogg, D.Q., Stolt, M., Rosenblatt, A.E., 2001. Landscape Attributes as Controls on Groithd Water Nitrate Removal Capacity of Riparian Zones1. JAWRA J. Am. Water Resour. Assoc. 37, 1457–1464. doi:10.1111/j.1752-1688.2001.tb03652.x

Gomez, J.D., Wilson, J.L., Cardenas, M.B., 2012. Residence time distributions in sinuosity-driven hyporheic zones and their biogeochemical effects. Water Resour. Res. 48, W09533. doi:10.1029/2012WR012180

Gregory, S.V., Swanson, F.J., McKee, W.A., Cummins, K.W., 1991. An Ecosystem Perspective of Riparian Zones. BioScience 41, 540–551. doi:10.2307/1311607

Groffman, P.M., Gold, A.J., Simmons, R.C., 1992. Nitrate Dynamics in Riparian Forests: Microbial Studies. J. Environ. Qual. 21, 666. doi:10.2134/jeq1992.00472425002100040022x

Gruber, N., Galloway, J.N., 2008. An Earth-system perspective of the global nitrogen cycle. Nature 451, 293–296. doi:10.1038/nature06592

Hamilton, P.A., Helsel, D.R., 1995. Effects of Agriculture on Ground-Water Quality in Five Regions of the United States. Ground Water 33, 217–226. doi:10.1111/j.1745-6584.1995.tb00276.x

Hancock, P.J., Boulton, A.J., Humphreys, W.F., 2005. Aquifers and hyporheic zones: Towards an ecological understanding of groundwater. Hydrogeol. J. 13, 98–111. doi:10.1007/s10040-004-0421-6

Hansen, S., Jensen, H.E., Nielsen, N.E., Svendsen, H., 1991. Simulation of nitrogen dynamics and biomass production in winter wheat using the Danish simulation model DAISY. Fertil. Res. 27, 245–259. doi:10.1007/BF01051131

Harvey, J.W., Böhlke, J.K., Voytek, M.A., Scott, D., Tobias, C.R., 2013. Hyporheic zone denitrification: Controls on effective reaction depth and contribution to whole-stream mass balance. Water Resour. Res. 49, 6298–6316. doi:10.1002/wrcr.20492

Hattermann, F.F., Krysanova, V., Habeck, A., Bronstert, A., 2006. Integrating wetlands and riparian zones in river basin modelling. Ecol. Model., Pattern and Processes of Dynamic Mosaic Landscapes -- Modelling, Simulation, and Implications 199, 379–392. doi:10.1016/j.ecolmodel.2005.06.012

Heathwaite, A.L., 2005. Dynamics and Biogeochemistry of River Corridors and Wetlands. IAHS.

Heinen, M., 2006. Simplified denitrification models: Overview and properties. Geoderma 133, 444–463. doi:10.1016/j.geoderma.2005.06.010

Helton, A.M., Poole, G.C., Meyer, J.L., Wollheim, W.M., Peterson, B.J., Mulholland, P.J., Bernhardt, E.S., Stanford, J.A., Arango, C., Ashkenas, L.R., Cooper, L.W., Dodds, W.K., Gregory, S.V., Hall, R.O., Hamilton, S.K., Johnson, S.L., McDowell, W.H., Potter, J.D., Tank, J.L., Thomas, S.M., Valett, H.M., Webster, J.R., Zeglin, L., 2010.

Thinking outside the channel: modeling nitrogen cycling in networked river ecosystems. Front. Ecol. Environ. 9, 229–238. doi:10.1890/080211

Helton, A.M., Poole, G.C., Payn, R.A., Izurieta, C., Stanford, J.A., 2012. Scaling flow path processes to fluvial landscapes: An integrated field and model assessment of temperature and dissolved oxygen dynamics in a river-floodplain-aquifer system. J. Geophys. Res. Biogeosciences 117, G00N14. doi:10.1029/2012JG002025

Hill, A.R., 1996. Nitrate Removal in Stream Riparian Zones. J. Environ. Qual. 25, 743. doi:10.2134/jeq1996.00472425002500040014x

Hill, A.R., Devito, K.J., Campagnolo, S., Sanmugadas, K., 2000. Subsurface denitrification in a forest riparianzone: Interactions between hydrology and supplies ofnitrate and organic carbon. Biogeochemistry 51, 193–223. doi:10.1023/A:1006476514038

Hoffmann, C.C., Kjaergaard, C., Uusi-Kämppä, J., Hansen, H.C.B., Kronvang, B., 2009. Phosphorus Retention in Riparian Buffers: Review of Their Efficiency. J. Environ. Qual. 38, 1942. doi:10.2134/jeq2008.0087

Hume, N.P., Fleming, M.S., Horne, A.J., 2002. Denitrification Potential and Carbon Quality of Four Aquatic Plants in Wetland Microcosms. Soil Sci. Soc. Am. J. 66, 1706. doi:10.2136/sssaj2002.1706

Hussein, M., Schwartz, F.W., 2003. Modeling of flow and contaminant transport in coupled stream–aquifer systems. J. Contam. Hydrol. 65, 41–64. doi:10.1016/S0169-7722(02)00229-2

Ice, G., 2004. History of Innovative Best Management Practice Development and its Role in Addressing Water Quality Limited Waterbodies. J. Environ. Eng. 130, 684–689. doi:10.1061/(ASCE)0733-9372(2004)130:6(684)

Inwood, S.E., Tank, J.L., Bernot, M.J., 2005. Patterns of denitrification associated with land use in 9 midwestern headwater streams. J. North Am. Benthol. Soc. 24, 227–245. doi:10.1899/04-032.1

Iribar, A., 2007. Composition des communautés bactériennes dénitrifiantes au sein d'un aquifère alluvial et facteurs contrôlant leur structuration : Relation entre structure des communautés et dénitrification (phd). Université de Toulouse, Université Toulouse III - Paul Sabatier.

Jalali, M., 2011. Nitrate pollution of groundwater in Toyserkan, western Iran. Environ. Earth Sci. 62, 907–913. doi:10.1007/s12665-010-0576-5

Jardine, T.D., Kidd, K.A., Rasmussen, J.B., 2011. Aquatic and terrestrial organic matter in the diet of stream consumers: implications for mercury bioaccumulation. Ecol. Appl. 22, 843–855. doi:10.1890/11-0874.1

Jayakrishnan, R., Srinivasan, R., Santhi, C., Arnold, J.G., 2005. Advances in the application of the SWAT model for water resources management. Hydrol. Process. 19, 749–762. doi:10.1002/hyp.5624

Johnson, P. a., Shepherd, M. a., Hatley, D. j., Smith, P. n., 2002. Nitrate leaching from a shallow limestone soil growing a five course combinable crop rotation: the effects of crop husbandry and nitrogen fertilizer rate on losses from the second complete rotation. Soil Use Manag. 18, 68–76. doi:10.1111/j.1475-2743.2002.tb00052.x

Jones, J.B., Mulholland, P.J., 1999. Streams and Ground Waters. Academic Press.

Jung, H.C., Jasinski, M., Kim, J.-W., Shum, C.K., Bates, P., Neal, J., Lee, H., Alsdorf, D., 2012. Calibration of two-dimensional floodplain modeling in the central Atchafalaya Basin Floodway System using SAR interferometry. Water Resour. Res. 48, W07511. doi:10.1029/2012WR011951

Junk, W., 1989. The flood concept in River-Floodplain systems.

Justes, E., Mary, B., Nicolardot, B., 1999. Comparing the effectiveness of radish cover crop, oilseed rape volunteers and oilseed rape residues incorporation for reducing nitrate leaching. Nutr. Cycl. Agroecosystems 55, 207–220. doi:10.1023/A:1009870401779

Kinzelbach, W., Schäfer, W., Herzer, J., 1991. Numerical modeling of natural and enhanced denitrification processes in aquifers. Water Resour. Res. 27. doi:10.1029/91WR00474

Kollet, S.J., Maxwell, R.M., 2006. Integrated surface–groundwater flow modeling: A free-surface overland flow boundary condition in a parallel groundwater flow model. Adv. Water Resour. 29, 945–958. doi:10.1016/j.advwatres.2005.08.006

Körner, H., Zumft, W.G., 1989. Expression of denitrification enzymes in response to the dissolved oxygen level and respiratory substrate in continuous culture of Pseudomonas stutzeri. Appl. Environ. Microbiol. 55, 1670–1676.

Koutný, J., Rulík, M., 2007. Hyporheic Biofilm Particulate Organic Carbon in a Small Lowland Stream (Sitka, Czech Republic): Structure and Distribution. Int. Rev. Hydrobiol. 92, 402–412. doi:10.1002/iroh.200610989

Krause, S., Heathwaite, L., Binley, A., Keenan, P., 2009. Nitrate concentration changes at the groundwater-surface water interface of a small Cumbrian river. Hydrol. Process. 23, 2195–2211. doi:10.1002/hyp.7213

Krause, S., Tecklenburg, C., Munz, M., Naden, E., 2013. Streambed nitrogen cycling beyond the hyporheic zone: Flow controls on horizontal patterns and depth distribution of nitrate and dissolved oxygen in the upwelling groundwater of a lowland river. J. Geophys. Res. Biogeosciences 118, 54–67. doi:10.1029/2012JG002122

Krysanova, V., Müller-Wohlfeil, D.-I., Becker, A., 1998. Development and test of a spatially distributed hydrological/water quality model for mesoscale watersheds. Ecol. Model. 106, 261–289. doi:10.1016/S0304-3800(97)00204-4

Lancaster, R.R., 2005. Fluvial Evolution of the Garonne River, France: Integrating Field Data with Numerical Simulations [WWW Document]. URL http://etd.lsu.edu/docs/available/etd-11172005-131031/ (accessed 6.30.14).

Langhans, S.D., Tockner, K., 2006. The role of timing, duration, and frequency of inundation in controlling leaf litter decomposition in a river-floodplain ecosystem (Tagliamento, northeastern Italy). Oecologia 147, 501–509. doi:10.1007/s00442-005-0282-2

Lautz, L.K., Siegel, D.I., 2006. Modeling surface and ground water mixing in the hyporheic zone using MODFLOW and MT3D. Adv. Water Resour. 29, 1618–1633. doi:10.1016/j.advwatres.2005.12.003

Lee, E.J., Kim, M., Kim, Y., Lee, K.-K., 2009. Numerical and field investigation of enhanced in situ denitrification in a shallow-zone well-to-well recirculation system. Ecol. Model. 220, 2441–2449. doi:10.1016/j.ecolmodel.2009.06.014

Lee, M.-S., Lee, K.-K., Hyun, Y., Clement, T.P., Hamilton, D., 2006. Nitrogen transformation and transport modeling in groundwater aquifers. Ecol. Model. 192, 143–159. doi:10.1016/j.ecolmodel.2005.07.013

Lee, P., Smyth, C., Boutin, S., 2004. Quantitative review of riparian buffer width guidelines from Canada and the United States. J. Environ. Manage. 70, 165–180. doi:10.1016/j.jenvman.2003.11.009

Liu, G.D., Wu, W.L., Zhang, J., 2005. Regional differentiation of non-point source pollution of agriculture-derived nitrate nitrogen in groundwater in northern China. Agric. Ecosyst. Environ. 107, 211–220. doi:10.1016/j.agee.2004.11.010

Liu, X., Zhang, X., Zhang, M., 2008. Major Factors Influencing the Efficacy of Vegetated Buffers on Sediment Trapping: A Review and Analysis. J. Environ. Qual. 37, 1667. doi:10.2134/jeq2007.0437

Liu, Y., Yang, W., Wang, X., 2008. Development of a SWAT extension module to simulate riparian wetland hydrologic processes at a watershed scale. Hydrol. Process. 22, 2901–2915. doi:10.1002/hyp.6874

Loague, K., VanderKwaak, J.E., 2004. Physics-based hydrologic response simulation: platinum bridge, 1958 Edsel, or useful tool. Hydrol. Process. 18, 2949–2956. doi:10.1002/hyp.5737

Lowrance, R., Altier, L.S., Newbold, J.D., Schnabel, R.R., Groffman, P.M., Denver, J.M., Correll, D.L., Gilliam, J.W., Robinson, J.L., Brinsfield, R.B., Staver, K.W., Lucas, W., Todd, A.H., 1997. Water Quality Functions of Riparian Forest Buffers in Chesapeake Bay Watersheds. Environ. Manage. 21, 687–712. doi:10.1007/s002679900060

Lowrance, R., Altier, L.S., Williams, R.G., Inamdar, S.P., Sheridan, J.M., Bosch, D.D., Hubbard, R.K., Thomas, D.L., 2000. REMM: The Riparian Ecosystem Management Model. J. Soil Water Conserv. 55, 27–34.

Ludwig, W., Probst, J.-L., Kempe, S., 1996. Predicting the oceanic input of organic carbon by continental erosion. Glob. Biogeochem. Cycles 10, 23–41. doi:10.1029/95GB02925

Maître, V., Cosandey, A.-C., Desagher, E., Parriaux, A., 2003. Effectiveness of groundwater nitrate removal in a river riparian area: the importance of hydrogeological conditions. J. Hydrol. 278, 76–93. doi:10.1016/S0022-1694(03)00134-3

Malanson, G.P., 1993. Riparian Landscapes. Cambridge University Press.

Malcolm, I.A., Soulsby, C., Youngson, A.F., Hannah, D.M., 2005. Catchment-scale controls on groundwater–surface water interactions in the hyporheic zone: implications for salmon embryo survival. River Res. Appl. 21, 977–989. doi:10.1002/rra.861

Marchetti, R., Donatelli, M., Spallacci, P., 1997. Testing Denitrification Functions of Dynamic Crop Models. J. Environ. Qual. 26, 394. doi:10.2134/jeq1997.00472425002600020009x

Martin, T.L., Kaushik, N.K., Trevors, J.T., Whiteley, H.R., 1999. Review: Denitrification in temperate climate riparian zones. Water. Air. Soil Pollut. 111, 171–186. doi:10.1023/A:1005015400607

Maskey, S., 2004. Modelling Uncertainty in Flood Forecasting Systems. CRC Press.

Matteo, M., Randhir, T., Bloniarz, D., 2006. Watershed-Scale Impacts of Forest Buffers on Water Quality and Runoff in Urbanizing Environment. J. Water Resour. Plan. Manag. 132, 144–152. doi:10.1061/(ASCE)0733-9496(2006)132:3(144)

McClain, M.E., Boyer, E.W., Dent, C.L., Gergel, S.E., Grimm, N.B., Groffman, P.M., Hart, S.C., Harvey, J.W., Johnston, C.A., Mayorga, E., McDowell, W.H., Pinay, G., 2003. Biogeochemical Hot Spots and Hot Moments at the Interface of Terrestrial and Aquatic. Ecosystems 6, 301–312. doi:10.1007/s10021-003-0161-9

McIsaac, G.F., David, M.B., Gertner, G.Z., Goolsby, D.A., 2001. Eutrophication: Nitrate flux in the Mississippi River. Nature 414, 166–167. doi:10.1038/35102672

Meisinger, J.J., Delgado, J.A., 2002. Principles for managing nitrogen leaching. J. Soil Water Conserv. 57, 485–498.

Mishima, Y., Takada, M., Kitagawa, R., 2010. Evaluation of intrinsic vulnerability to nitrate contamination of groundwater: appropriate fertilizer application management. Environ. Earth Sci. 63, 571–580. doi:10.1007/s12665-010-0725-x

Moreira-Turcq, P., Bonnet, M.-P., Amorim, M., Bernardes, M., Lagane, C., Maurice, L., Perez, M., Seyler, P., 2013. Seasonal variability in concentration, composition, age, and fluxes of particulate organic carbon exchanged between the floodplain and Amazon River. Glob. Biogeochem. Cycles 27, 119–130. doi:10.1002/gbc.20022

Morrice, J.A., Valett, H.M., Dahm, C.N., Campana, M.E., 1997. Alluvial Characteristics, Groundwater–Surface Water Exchange and Hydrological Retention in Headwater Streams. Hydrol. Process. 11, 253–267. doi:10.1002/(SICI)1099-1085(19970315)11:3<253::AID-HYP439>3.0.CO;2-J

Mulholland, P.J., Helton, A.M., Poole, G.C., Hall, R.O., Hamilton, S.K., Peterson, B.J., Tank, J.L., Ashkenas, L.R., Cooper, L.W., Dahm, C.N., Dodds, W.K., Findlay, S.E.G., Gregory, S.V., Grimm, N.B., Johnson, S.L., McDowell, W.H., Meyer, J.L., Valett, H.M., Webster, J.R., Arango, C.P., Beaulieu, J.J., Bernot, M.J., Burgin, A.J., Crenshaw, C.L., Johnson, L.T., Niederlehner, B.R., O'Brien, J.M., Potter, J.D., Sheibley, R.W., Sobota, D.J., Thomas, S.M., 2008. Stream denitrification across biomes and its response to anthropogenic nitrate loading. Nature 452, 202–205. doi:10.1038/nature06686

Naiman, R.J., Decamps, H., 1997. The Ecology of Interfaces: Riparian Zones. Annu. Rev. Ecol. Syst. 28, 621–658.

Neitsch, S.L., Arnold, J.G., Kiniry, J.R., Williams, J.R., 2009. Soil and Water Assessment Tool, Theoretical Documentation, Version 2009.

Nguyen, K.L.H., Technische Universiteit Delft, Unesco-IHE Institute for Water Education, 2013. The effect of riparian zones on nitrate removal by denitrification at the river basin scale.

Noe, G.B., Hupp, C.R., 2005. Carbon, nitrogen, and phosphorus accumulation in floodplains of atlantic coastal plain rivers, usa. Ecol. Appl. 15, 1178–1190. doi:10.1890/04-1677

Orghidan, T., 1959. Ein neuer lebensraum des unterirdischen Wassers: Der hvporheische Biotop. Arch. Für Hydrobiol. 392–414.

Osborne, L.L., Kovacic, D.A., 1993. Riparian vegetated buffer strips in water-quality restoration and stream management. Freshw. Biol. 29, 243–258. doi:10.1111/j.1365-2427.1993.tb00761.x

Park, S.S., Lee, Y.S., 2002. A water quality modeling study of the Nakdong River, Korea. Ecol. Model. 152, 65–75. doi:10.1016/S0304-3800(01)00489-6

Peterjohn, W.T., Correll, D.L., 1984. Nutrient Dynamics in an Agricultural Watershed: Observations on the Role of A Riparian Forest. Ecology 65, 1466–1475. doi:10.2307/1939127

Peterson, M.E., Curtin, D., Thomas, S., Clough, T.J., Meenken, E.D., 2013. Denitrification in vadose zone material amended with dissolved organic matter from topsoil and subsoil. Soil Biol. Biochem. 61, 96–104. doi:10.1016/j.soilbio.2013.02.010

Peyrard, D., 2008. Un modèle hydrobiogéochimique pour décrire les échanges entre l'eau de surface et la zone hyporhéique de grandes plaines alluviales (phd). Université de Toulouse, Université Toulouse III - Paul Sabatier.

Peyrard, D., Delmotte, S., Sauvage, S., Namour, P., Gerino, M., Vervier, P., Sanchez-Perez, J.M., 2011. Longitudinal transformation of nitrogen and carbon in the hyporheic zone of an N-rich stream: A combined modelling and field study. Phys. Chem. Earth Parts ABC, Man and River Systems: From pressures to physical, chemical and ecological status 36, 599–611. doi:10.1016/j.pce.2011.05.003

Peyrard, D., Sauvage, S., Vervier, P., Sanchez-Perez, J.M., Quintard, M., 2008. A coupled vertically integrated model to describe lateral exchanges between surface and subsurface in large alluvial floodplains with a fully penetrating river. Hydrol. Process. 22, 4257–4273. doi:10.1002/hyp.7035

Piégay, H., Pautou, G., Ruffinoni, C., 2003. Les forêts riveraines des cours d'eau: écologie, fonctions et gestion. Forêt privée française.

Pinay, G., Decamps, H., 1988. The role of riparian woods in regulating nitrogen fluxes between the alluvial aquifer and surface water: A conceptual model. Regul. Rivers Res. Manag. 2, 507–516. doi:10.1002/rrr.3450020404

Pinay, G., Ruffinoni, C., Wondzell, S., Gazelle, F., 1998. Change in Groundwater Nitrate Concentration in a Large River Floodplain: Denitrification, Uptake, or Mixing? J. North Am. Benthol. Soc. 17, 179–189. doi:10.2307/1467961

Rassam, D., Hunter, H.M., Pagendam, D., Cooperative Research Centre for Catchment Hydrology, 2005. The Riparian Nitrogen Model (RNM): basic theory and conceptualisation. CRC for Catchment Hydrology, Monash University, Clayton, Vic.

Rassam, D.W., Pagendam, D.E., Hunter, H.M., 2008. Conceptualisation and application of models for groundwater–surface water interactions and nitrate attenuation potential in riparian zones. Environ. Model. Softw. 23, 859–875. doi:10.1016/j.envsoft.2007.11.003

Rivett, M.O., Buss, S.R., Morgan, P., Smith, J.W.N., Bemment, C.D., 2008. Nitrate attenuation in groundwater: A review of biogeochemical controlling processes. Water Res. 42, 4215–4232. doi:10.1016/j.watres.2008.07.020

Rivett, M.O., Smith, J.W.N., Buss, S.R., Morgan, P., 2007. Nitrate occurrence and attenuation in the major aquifers of England and Wales. Q. J. Eng. Geol. Hydrogeol. 40, 335–352. doi:10.1144/1470-9236/07-032

Robertson, A.I., Bunn, S.E., Boon, P.I., Walker, K.F., 1999. Sources, sinks and transformations of organic carbon in Australian floodplain rivers. Mar. Freshw. Res. 50, 813–829.

Romanowicz, A.A., Vanclooster, M., Rounsevell, M., La Junesse, I., 2005. Sensitivity of the SWAT model to the soil and land use data parametrisation: a case study in the Thyle catchment, Belgium. Ecol. Model. 187, 27–39. doi:10.1016/j.ecolmodel.2005.01.025

Roulet, N.T., 1990. Hydrology of a headwater basin wetland: Groundwater discharge and wetland maintenance. Hydrol. Process. 4, 387–400. doi:10.1002/hyp.3360040408

Sabo, J.L., Sponseller, R., Dixon, M., Gade, K., Harms, T., Heffernan, J., Jani, A., Katz, G., Soykan, C., Watts, J., Welter, J., 2005. Riparian zones increase regional species richness by harboring different, not more, species. Ecology 86, 56–62. doi:10.1890/04-0668

Sánchez-Pérez, J.M., Antiguedad, I., Arrate, I., García-Linares, C., Morell, I., 2003. The influence of nitrate leaching through unsaturated soil on groundwater pollution in an agricultural area of the Basque country: a case study. Sci. Total Environ. 317, 173–187. doi:10.1016/S0048-9697(03)00262-6

Sánchez-Pérez, J.M., Trémolières, M., 2003. Change in groundwater chemistry as a consequence of suppression of floods: the case of the Rhine floodplain. J. Hydrol. 270, 89–104. doi:10.1016/S0022-1694(02)00293-7

Sánchez-Pérez, J.M., Vervier, P., Garabétian, F., Sauvage, S., Loubet, M., Rols, J.L., Bariac, T., Weng, P., 2003. Nitrogen dynamics in the shallow groundwater of a riparian wetland zone of the Garonne, SW France: nitrate inputs, bacterial densities, organic matter supply and denitrification measurements. Hydrol. Earth Syst. Sci. Discuss. 7, 97–107.

Schindler, J.E., Krabbenhoft, D.P., 1998. The hyporheic zone as a source of dissolved organic carbon and carbon gases to a temperate forested stream. Biogeochemistry 43, 157–174. doi:10.1023/A:1006005311257

Seitzinger, S., Harrison, J.A., Böhlke, J.K., Bouwman, A.F., Lowrance, R., Peterson, B., Tobias, C., Drecht, G.V., 2006. Denitrification across landscapes and waterscapes: a synthesis. Ecol. Appl. 16, 2064–2090. doi:10.1890/1051-0761(2006)016[2064:DALAWA]2.0.CO;2

Semhi, K., Amiotte Suchet, P., Clauer, N., Probst, J.-L., 2000. Impact of nitrogen fertilizers on the natural weathering-erosion processes and fluvial transport in the Garonne basin. Appl. Geochem. 15, 865–878. doi:10.1016/S0883-2927(99)00076-1

Servais, P., Anzil, A., Ventresque, C., 1989. Simple method for determination of biodegradable dissolved organic carbon in water. Appl. Environ. Microbiol. 55, 2732–2734.

Sheibley, R.W., Jackman, A.P., Duff, J.H., Triska, F.J., 2003. Numerical modeling of coupled nitrification–denitrification in sediment perfusion cores from the hyporheic zone of the Shingobee River, MN. Adv. Water Resour., Modeling Hyporheic Zone Processes 26, 977–987. doi:10.1016/S0309-1708(03)00088-5

Shen, Y., Chapelle, F.H., Strom, E.W., Benner, R., 2014. Origins and bioavailability of dissolved organic matter in groundwater. Biogeochemistry 1–18. doi:10.1007/s10533-014-0029-4

ŠImek, M., Cooper, J.E., 2002. The influence of soil pH on denitrification: progress towards the understanding of this interaction over the last 50 years. Eur. J. Soil Sci. 53, 345–354. doi:10.1046/j.1365-2389.2002.00461.x

Simmelsgaard, S.E., 1998. The effect of crop, N-level, soil type and drainage on nitrate leaching from Danish soil. Soil Use Manag. 14, 30–36. doi:10.1111/j.1475-2743.1998.tb00607.x

Singh, P., Singh, V.P., 2001. Snow and Glacier Hydrology. Springer Science & Business Media.

Sloan, P.G., Moore, I.D., 1984. Modeling subsurface stormflow on steeply sloping forested watersheds. Water Resour. Res. 20, 1815–1822. doi:10.1029/WR020i012p01815

Smart, R.P., Soulsby, C., Cresser, M.S., Wade, A.J., Townend, J., Billett, M.F., Langan, S., 2001. Riparian zone influence on stream water chemistry at different spatial scales: a GIS-based modelling approach, an example for the Dee, NE Scotland. Sci. Total Environ. 280, 173–193. doi:10.1016/S0048-9697(01)00824-5

Sophocleous, M., 2002. Interactions between groundwater and surface water: the state of the science. Hydrogeol. J. 10, 52–67. doi:10.1007/s10040-001-0170-8

Starr, R.C., Gillham, R.W., 1993. Denitrification and Organic Carbon Availability in Two Aquifers. Ground Water 31, 934–947. doi:10.1111/j.1745-6584.1993.tb00867.x

Stelzer, R.S., Bartsch, L.A., Richardson, W.B., Strauss, E.A., 2011. The dark side of the hyporheic zone: depth profiles of nitrogen and its processing in stream sediments. Freshw. Biol. 56, 2021–2033. doi:10.1111/j.1365-2427.2011.02632.x

Stelzer, R.S., Scott, J.T., Bartsch, L.A., Parr, T.B., 2014. Particulate organic matter quality influences nitrate retention and denitrification in stream sediments: evidence from a carbon burial experiment. Biogeochemistry 119, 387–402. doi:10.1007/s10533-014-9975-0

Stevenson, B.A., Schipper, L.A., McGill, A., Clark, D., 2011. Denitrification and Availability of Carbon and Nitrogen in a Well-drained Pasture Soil Amended with Particulate Organic Carbon. J. Environ. Qual. 40, 923. doi:10.2134/jeq2010.0463

Storey, R.G., Howard, K.W.F., Williams, D.D., 2003. Factors controlling riffle-scale hyporheic exchange flows and their seasonal changes in a gaining stream: A three-dimensional groundwater flow model. Water Resour. Res. 39, 1034. doi:10.1029/2002WR001367

Stuart, M.E., Gooddy, D.C., Bloomfield, J.P., Williams, A.T., 2011. A review of the impact of climate change on future nitrate concentrations in groundwater of the UK. Sci. Total Environ. 409, 2859–2873. doi:10.1016/j.scitotenv.2011.04.016

Surridge, B.W.J., Heathwaite, A.L., Baird, A.J., 2007. The Release of Phosphorus to Porewater and Surface Water from River Riparian Sediments. J. Environ. Qual. 36, 1534. doi:10.2134/jeq2006.0490

Tabacchi, E., Lambs, L., Guilloy, H., Planty-Tabacchi, A.-M., Muller, E., Dcamps, H., 2000. Impacts of riparian vegetation on hydrological processes. Hydrol. Process. 14, 2959–2976. doi:10.1002/1099-1085(200011/12)14:16/17<2959::AID-HYP129>3.0.CO;2-B

Thomaz, S.M., Bini, L.M., Bozelli, R.L., 2007. Floods increase similarity among aquatic habitats in river-floodplain systems. Hydrobiologia 579, 1–13. doi:10.1007/s10750-006-0285-y

Tockner, K., Pennetzdorfer, D., Reiner, N., Schiemer, F., Ward, J.V., 1999. Hydrological connectivity, and the exchange of organic matter and nutrients in a dynamic river–

floodplain system (Danube, Austria). Freshw. Biol. 41, 521–535. doi:10.1046/j.1365-2427.1999.00399.x

Tockner, K., Stanford, J.A., 2002. Riverine flood plains: present state and future trends. Environ. Conserv. null, 308–330. doi:10.1017/S037689290200022X

Townsend, P.A., Walsh, S.J., 1998. Modeling floodplain inundation using an integrated GIS with radar and optical remote sensing. Geomorphology, Application of remote sensing and GIS in geomorphology 21, 295–312. doi:10.1016/S0169-555X(97)00069-X

Trancoso, A.R., Braunschweig, F., Chambel Leitão, P., Obermann, M., Neves, R., 2009. An advanced modelling tool for simulating complex river systems. Sci. Total Environ. 407, 3004–3016. doi:http://dx.doi.org/10.1016/j.scitotenv.2009.01.015

Triska, F.J., Duff, J.H., Avanzino, R.J., 1993. The role of water exchange between a stream channel and its hyporheic zone in nitrogen cycling at the terrestrial—aquatic interface, in: Hillbricht-Ilkowska, A., Pieczyńska, E. (Eds.), Nutrient Dynamics and Retention in Land/Water Ecotones of Lowland, Temperate Lakes and Rivers, Developments in Hydrobiology. Springer Netherlands, pp. 167–184.

Trudell, M.R., Gillham, R.W., Cherry, J.A., 1986. An in-situ study of the occurrence and rate of denitrification in a shallow unconfined sand aquifer. J. Hydrol. 83, 251–268. doi:10.1016/0022-1694(86)90155-1

Uhart, A., 2013. Modélisation des transferts de carbone organique dans le bassin versant Garonne.

Vervier, P., Bonvallet-Garay, S., Sauvage, S., Valett, H.M., Sanchez-Perez, J.-M., 2009. Influence of the hyporheic zone on the phosphorus dynamics of a large gravel-bed river, Garonne River, France. Hydrol. Process. 23, 1801–1812. doi:10.1002/hyp.7319

Vidon, P.G.F., Hill, A.R., 2004. Landscape controls on the hydrology of stream riparian zones. J. Hydrol. 292, 210–228. doi:10.1016/j.jhydrol.2004.01.005

Vidon, P., Hill, A.R., 2005. Denitrification and patterns of electron donors and acceptors in eight riparian zones with contrasting hydrogeology. Biogeochemistry 71, 259–283. doi:10.1007/s10533-005-0684-6

Vitousek, P.M., Aber, J.D., Howarth, R.W., Likens, G.E., Matson, P.A., Schindler, D.W., Schlesinger, W.H., Tilman, D.G., 1997. Human alteration of the global nitrogen cycle: sources and consequences. Ecol. Appl. 7, 737–750. doi:10.1890/1051-0761(1997)007[0737:HAOTGN]2.0.CO;2

Vogel, J.C., Talma, A.S., Heaton, T.H.E., 1981. Gaseous nitrogen as evidence for denitrification in groundwater. J. Hydrol. 50, 191–200. doi:10.1016/0022-1694(81)90069-X

Volk, M., Arnold, J.G., Bosch, D.D., Allen, P.M., Green, C.H., 2007. Watershed configuration and simulation of landscape processes with the SWAT model, in: MODSIM 2007 International Congress on Modelling and Simulation. Modelling and Simulation Society of Australia and New Zealand, Canberra, Australia. pp. 74–80.

Vuksanovic, V., De Smedt, F., Van Meerbeeck, S., 1996. Transport of polychlorinated biphenyls (PCB) in the Scheldt Estuary simulated with the water quality model WASP. J. Hydrol. 174, 1–18. doi:10.1016/0022-1694(95)02759-9

Wang, H., Ju, X., Wei, Y., Li, B., Zhao, L., Hu, K., 2010. Simulation of bromide and nitrate leaching under heavy rainfall and high-intensity irrigation rates in North China Plain. Agric. Water Manag. 97, 1646–1654. doi:10.1016/j.agwat.2010.05.022

Weng, P., Sánchez-Pérez, J.M., Sauvage, S., Vervier, P., Giraud, F., 2003. Assessment of the quantitative and qualitative buffer function of an alluvial wetland: hydrological modelling of a large floodplain (Garonne River, France). Hydrol. Process. 17, 2375–2392. doi:10.1002/hyp.1248

Westerman, R.L., Boman, R.K., Raun, W.R., Johnson, G.V., 1994. Ammonium and Nitrate Nitrogen in Soil Profiles of Long-Term Winter Wheat Fertilization Experiments. Agron. J. 86, 94. doi:10.2134/agronj1994.00021962008600010018x

Wickland, K.P., Aiken, G.R., Butler, K., Dornblaser, M.M., Spencer, R.G.M., Striegl, R.G., 2012. Biodegradability of dissolved organic carbon in the Yukon River and its tributaries: Seasonality and importance of inorganic nitrogen. Glob. Biogeochem. Cycles 26, GB0E03. doi:10.1029/2012GB004342

Wiegner, T.N., Seitzinger, S.P., Glibert, P.M., Bronk, D.A., 2006. Bioavailability of dissolved organic nitrogen and carbon from nine rivers in the eastern United States. Aquat. Microb. Ecol. 43, 277–287.

Wondzell, S.M., 2011. The role of the hyporheic zone across stream networks. Hydrol. Process. 25, 3525–3532. doi:10.1002/hyp.8119

Wong, J.C.Y., Williams, D.D., 2010. Sources and seasonal patterns of dissolved organic matter (DOM) in the hyporheic zone. Hydrobiologia 647, 99–111. doi:10.1007/s10750-009-9950-2

Wroblicky, G.J., Campana, M.E., Valett, H.M., Dahm, C.N., 1998. Seasonal variation in surface-subsurface water exchange and lateral hyporheic area of two stream-aquifer systems. Water Resour. Res. 34, 317–328. doi:10.1029/97WR03285

Yamazaki, D., Kanae, S., Kim, H., Oki, T., 2011. A physically based description of floodplain inundation dynamics in a global river routing model. Water Resour. Res. 47, W04501. doi:10.1029/2010WR009726

Zarnetske, J.P., Haggerty, R., Wondzell, S.M., Baker, M.A., 2011. Dynamics of nitrate production and removal as a function of residence time in the hyporheic zone. J. Geophys. Res. Biogeosciences 116, G01025. doi:10.1029/2010JG001356

Zarnetske, J.P., Haggerty, R., Wondzell, S.M., Bokil, V.A., González-Pinzón, R., 2012. Coupled transport and reaction kinetics control the nitrate source-sink function of hyporheic zones. Water Resour. Res. 48, W11508. doi:10.1029/2012WR011894

Zhao, R.-F., Chen, X.-P., Zhang, F.-S., Zhang, H., Schroder, J., Römheld, V., 2006. Fertilization and Nitrogen Balance in a Wheat–Maize Rotation System in North China. Agron. J. 98, 938. doi:10.2134/agronj2005.0157

Zumft, W.G., 1997. Cell biology and molecular basis of denitrification. Microbiol. Mol. Biol. Rev. 61, 533–616.